

“Synthesis of Novel Liquid Crystalline Compounds
with Varied Molecular Structures and Their
Mesomorphic Characterization”

A Thesis submitted to

The Maharaja Sayajirao University of Baroda

For the degree of
Doctor of Philosophy
in
Applied Chemistry

by

Purvang D. Patel

Applied Chemistry Department
Faculty of Technology and Engineering
The M.S.University of Baroda
Vadodara-390 001

January - 2013

Dedicated
To My
Beloved
Grand Parents

Tel: 2434188



APPLIED CHEMISTRY DEPARTMENT
Faculty of Technology & Engineering,
The Maharaja Sayajirao University of Baroda,
POST BOX NO. 51, KALABHAVAN
VADODARA-390001 (India)

DST-FIST Sponsored Department

Date: 04-01-2013

Certificate

This is to certify that the thesis entitled “Synthesis of novel liquid crystalline compounds with varied molecular structures and their mesomorphic characterization” submitted for Ph.D. degree in Applied Chemistry by Mr. Purvang D. Patel incorporates the original research work carried out by him under my supervision.

Prof. Jayrang S. Dave
Research Guide

Prof. P. T. Deota
Head
Applied Chemistry Department

Prof. A. N. Misra
Dean
Faculty of Technology and Engineering

Acknowledgements

At the outset, I wish to pay my humble obeisance to the almighty God for giving me the energy, inspiration and wisdom to take up this task; I have been his guiding hand that has brought this task to a successful completion.

I take this opportunity to extend my sincere thanks to my mentor and guide Professor Jayrang S. Dave, who not only suggested problem, but also took an active and keen interest in my work and helped me tide over some occasions of frustration and disappointment by his, kind inspiration, encouragement and invaluable guidance throughout the investigation.

I am thankful to Prof. A. N. Misra, The Dean, Faculty of Technology & Engineering and Prof. P. T. Deota, The Head, Applied Chemistry Department, for having provided me the laboratory facilities.

I am also thankful to Dr. C. B. Upasani, Director, M/s. Jyoti Om Chemical Research Centre Pvt. Ltd., G.I.D.C., Ankleshwar, for his valuable discussion.

Award of Research Scholar under the University Research Scholarship 2011-2012 is acknowledged greatly.

I express my thanks to all my colleagues for their various help. I express my thanks to my juniors for their pleasant company.

I also express my thanks to teaching and non-teaching staff of the department for their co-operation and help.

I am short in words to express to my inner sentiments towards my family members for their support and pushing throughout the hard time, which has made it possible for me to reach end of this voyage. My vocabulary fails to convey depth of my sentiments for my grandparents and my family for their persistent encouragement. I cannot forget my grandmother for her most supportive role in my life. My heartily thanks to my wife for her valuable support and encouragement.

(Purvang D. Patel)

Contents

Abbreviations of Mesomorphic terms	i
Chapter 1. Introduction	
1.1 History of Liquid Crystals	2
1.2 Classification of Liquid Crystals	2
1.3 Thermotropic of Liquid Crystals	3
1.3.1 Smectic Liquid Crystals	5
1.3.2 Nematic Liquid Crystals	7
1.3.3 Cholesteric Liquid Crystals	8
1.3.4 Blue Phases	9
1.3.5 Twist grain boundary [TGB] phases	9
1.3.6 Ferroelectric and Anti-ferroelectric Liquid Crystals	9
1.3.7 Discotic Liquid Crystals	10
1.3.8 Sanidic Liquid Crystals	11
1.4 Lyotropic Liquid Crystals	12
1.5 Influence of molecular structure on mesomorphism	12
1.5.1 Effect of terminal substituents on mesomorphism	13
1.5.2 Effect of lateral substituents on mesomorphism	14
1.6 Mesomorphism in homologous series	15
1.7 Banana Shaped Liquid Crystals	16
1.8 Mesogenic oligomers having flexible spacers	17
1.8.1 Mesogenic Dimers	18
1.8.2 Mesogenic Trimers	18
1.8.3 Mesogenic Tetramers	18
1.9 Polymer Liquid Crystals	18
1.9.1 Main Chain Polymer Liquid Crystals (MC-PLCs)	19
1.9.2 Side Chain Polymer Liquid Crystal (SC-PLCs)	20
1.10 Metallomesogens	20
1.11 Mixed mesomorphism	21
1.12 Physical properties of Liquid Crystals	22
1.13 Biological System	22
1.14 Applications of Liquid Crystals	23
1.14.1 Display applications of Liquid Crystals	23
1.14.2 Non Display applications of Liquid Crystals	24
1.15 Polarizing Optical Microscopy	27
1.16 Differential Scanning Calorimetry	28
Chapter 2. Aims and Objectives	29

Chapter 3. Mesogenic homologous series having terminal fluoro group	31
3.1 Introduction	31
3.2 Experimental	32
3.3 Results and Discussion	81
Chapter 4. Mesogens having heterocyclic furfural moiety and chalcone as one of the central linkages	91
4.1 Introduction	91
4.2 Experimental	92
4.3 Results and Discussion	126
Chapter 5. Mesogenic homologous series having ester and ethylideneamino central linkages	133
5.1 Introduction	133
5.2 Experimental	133
5.3 Results and Discussion	159
Chapter 6. Bent- shaped mesogens derived from Diphenylether moiety	166
6.1 Introduction	166
6.2 Experimental	167
6.3 Results and Discussion	184
Chapter 7. Mixed Mesomorphism	190
7.1 Introduction	190
7.2 Experimental	191
7.3 Type I	194
7.4 Type II	203
7.5 Type III	206
Chapter 8. References	212
Summary	235
List of Presentation	242
Research Publications	243

Abbreviations of Mesomorphic terms

Cr	Crystalline (Solid)
M	Mesomorphic (Liquid Crystalline)
I	Isotropic (Liquid)
N	Nematic
Ch	Cholesteric
S	Smectic
Sc	Smectic C
Sc*	Chiral Smectic C
S _A	Smectic A
PLC	Polymer Liquid Crystals
MC-PLC	Main Chain Polymer Liquid Crystals
SC-PLC	Side Chain Polymer Liquid Crystals

It has been recognized that, under appropriate conditions of temperature and pressure, matter may exist in three possible states of aggregation—the solid, the isotropic liquid and the gas. The molecule in a solid possesses positional order. The liquid state is quite different in that the molecules neither occupy a specific average position nor remain oriented in a particular way. When a solid melts to isotropic liquid, both types of order are lost completely; the molecules move and tumble randomly. However, in certain compounds while the thermal energy received at a definite stage is able to cause flow, making the domain structure loosened to an extent, yet it is not enough to shatter the order of crystallinity completely. A sort of residual orderly orientation of molecules persists until another temperature is reached which totally eliminates regularity of structure altogether. Between these two transitions, both being definite, the properties displayed are unique indeed. This state of existence is independent within the definite temperature range and is neither totally crystalline nor completely liquid, but has properties of both. The state is known as “mesophase” or “mesomorphic state”. This term, derived from the Greek, *mesos*, between or intermediate and *phasis*, a state or phase, does stress the intermediate nature of these states of matter. The phenomenon is known as “mesomorphism”; the compounds that exhibit this unique property are called “Liquid Crystals” or “mesomorphs” or “mesogens”. Liquid crystals, as their name suggests, are a phase of matter that is intermediate between an isotropic liquid and a crystalline solid. Schematic representation of solids, liquid crystals and liquid is given in figure 1.1.

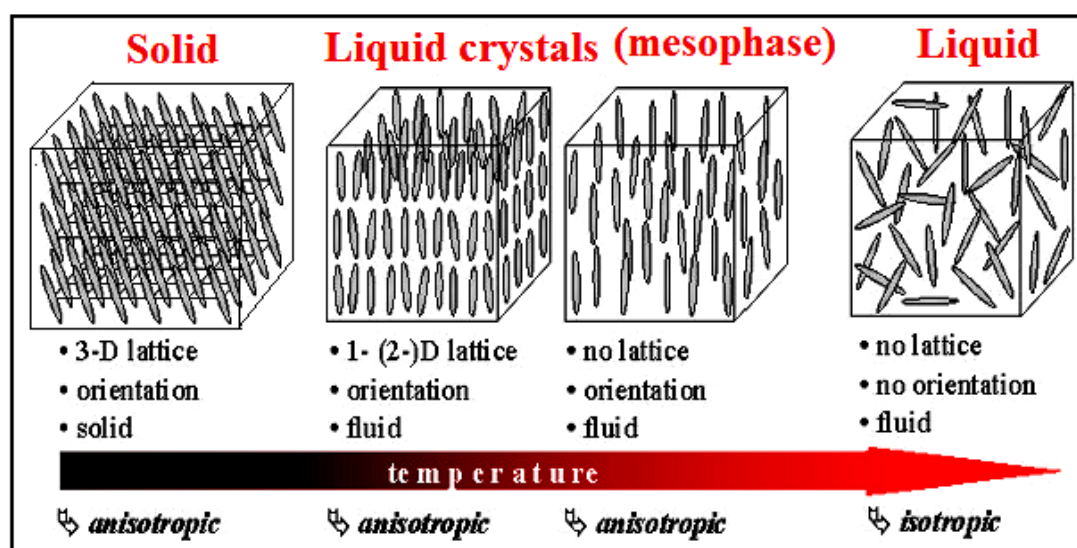


Figure 1.1 Schematic representation of solid, liquid crystals and liquid

The molecules in the liquid crystal phase are free to move about in much the same fashion as in a liquid, but as they do so they tend to remain oriented in a certain direction. Liquid crystals are self-organizing anisotropic fluids whose properties can be changed by the application of electric or magnetic fields. This allows them to be used in display devices such as laptop computer screens. The liquid crystalline state can be divided into a number of mesophases (or sub-phases) and many liquid crystals have a number of phase transitions between these mesophases.

1.1 History of Liquid Crystals

The person generally given credit for “discovering” liquid crystals is an Austrian botanist named Friedrich Reinitzer [1]; in 1888, when Reinitzer observed the melting behavior of cholesteryl benzoate, found a phenomenon of double melting. On heating these esters, the solid first melted to an opaque liquid exhibiting vivid colour, which, on further heating transformed to an optically clear liquid. It is followed by Lehmann [2] who coined the word ‘Liquid crystals’ to describe the phenomenon. Soon after, Gatterman and Ritchke [3] and Vorlander [4] investigated several liquid crystalline compounds. The culmination of all these efforts is the classification scheme by Friedel in 1922 [5]. Friedel and Friedel [6] proposed the term ‘mesomorphic state’ as the phase is an intermediate of a crystalline solid and an isotropic liquid. Brown and Shaw [7] have used the term ‘mesomorphism’ for the title of their first review. Studies on the physical properties of liquid crystals are carried out in 1930’s; after which work on this field slowed down. Shortly before 1960, it once again gained momentum and then the progress is swift and substantial.

1.2 Classification of Liquid Crystals

Liquid crystals are classified into two main categories according to the manner in which they are obtained.

- (1) Thermotropic liquid crystals (2) Lyotropic liquid crystals

Gray and Winsor [8] classified lyotropic and thermotropic liquid crystals as amphiphilic and non-amphiphilic mesogens, respectively.

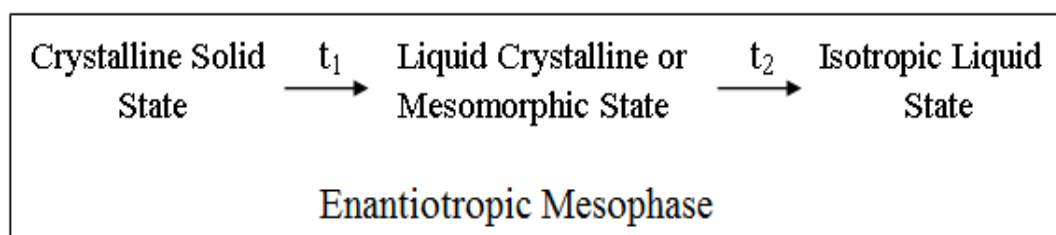
1.3 Thermotropic Liquid Crystals

Mesophases are most commonly observed when a suitable compound is heated to a temperature above that at which the crystal lattice is stable. This type of mesomorphism is termed thermotropic.

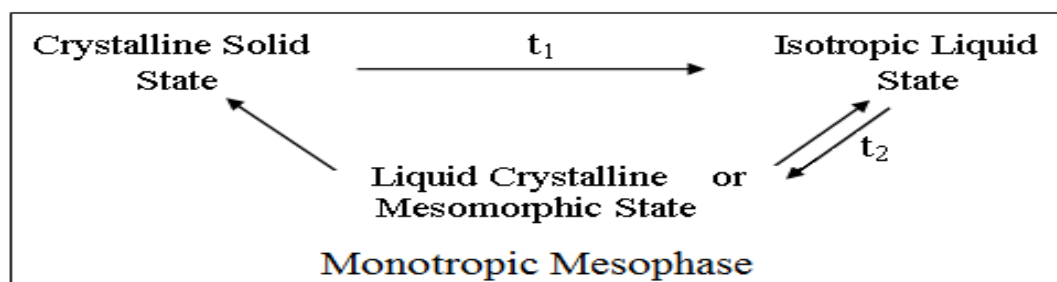
The thermal motions of the molecules within the lattice increase and eventually the vibrations become so intense on heating a fully ordered molecular crystal, which broken down the regular arrangement with the loss of long range of orientational and positional order to give disorganized isotropic liquid. However for many compounds, this process occurs by way of one or more intermediate phases as the temperature is increased; form anisotropic fluids these phases are known as mesophases.

On heating, liquid crystals exhibit first mesophase and than change into an isotropic liquid on further heating, which is reversible. On cooling, isotropic liquid changes to liquid crystalline phase and on further cooling solidifies, however many times super cooling takes place. The mesomorphic transitions which occur on heating the sample and reverse in opposite order on cooling is termed as enantiotropic mesomorphic state.

The sequence of changes of state for a compound which exhibits enantiotropic mesophases may be illustrated as below.



However, such a crystalline compound melts normally to give the isotropic liquid on heating, but on cooling the isotropic liquid exhibit a mesophase, before crystallization. This kind of mesophases is termed as monotropic mesomorphic state. The sequence of changes of state for a compound which exhibits monotropic mesophases may be illustrated as below.



Most of liquid crystals fall into the category of thermotropic liquid crystals. The vast majority of thermotropic liquid crystals are composed of rod-like molecules and according to a modern proposal [9] may also be called ‘calamitic liquid crystals’, (In Greek – calamos means rod). They are classified broadly into three types: Smectic, Nematic and Cholesteric. Liquid crystalline compounds may either exclusively be smectic or nematic or smectic and nematic or smectic and cholesteric. They may exhibit polymesomorphism. The transition temperatures are always definite and define the stability of different mesophases. Schematic representation of phase sequence for liquid crystals is given in figure 1.2. The change with increasing temperature may be represented as;

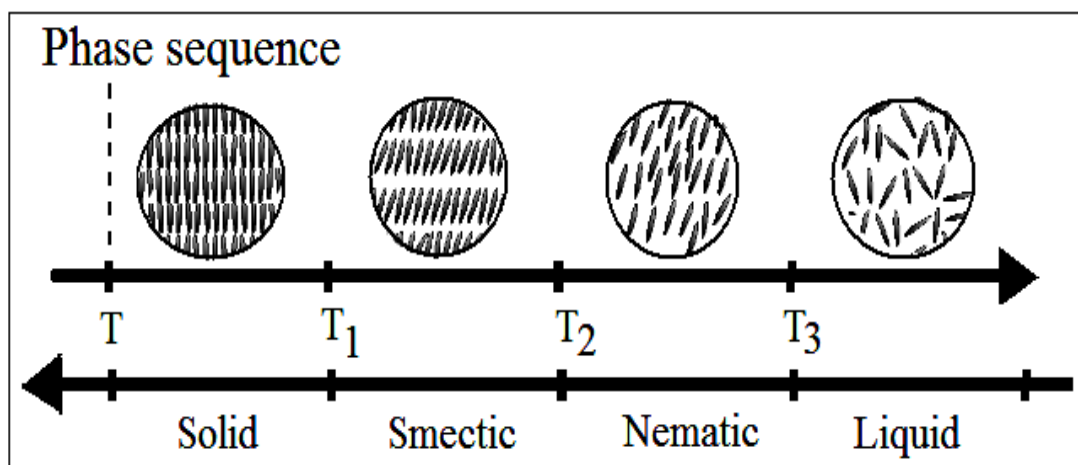
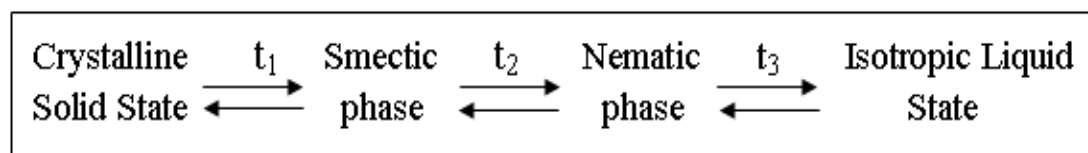


Figure 1.2 Schematic representation of phase sequence for liquid crystals

1.3.1 Smectic Liquid Crystals

It is a turbid, viscous state, with certain properties reminiscent of those found for soaps. The term smectic is in fact derived from the Greek word ‘smectose’-soap like. Smectic mesophase is the most ordered one. The smectic state is another distinct mesophase of liquid crystal substances. Molecules in this phase show a degree of translation order not present in the nematic. In the smectic state, the molecules maintain the general orientational order of nematic, but also tend to align themselves in layers or planes. Motion is restricted to within these planes, and separate planes are observed to flow past each other. The increased order means that the smectic state is more “solid-like” than the nematic. Many compounds are observed to form more than one type of smectic phase; as many as 12 of these variations have been identified.

Hermann [10] and Saupe [11] have classified the smectic phases into two classes; smectic phases with unstructured layers and smectic phases with structured layers. The extensive work of Sackmann and Demus [12] has revealed some of the detailed arrangements of these phases and classified smectic phases according to the texture observed in the mesophase. (Table 1.1)

Moreover, de Vries [13, 14] has classified smectic into three main classes on the basis of X-ray studies. The class first contains smectic A,C,F and D, the class second contains smectic E, G and H, the class third contains the smectic B. Levelut et al [15] have designated smectic O phase in 1-(methyl)-heptyl-terephthalidene-bis-amino cinnamate. Bennemann et al [16] have reported some mesogenic chiral compounds, which show a smectic Q phase just below the clearing point. Bennemann, Bepke and Lo'tzsch [17] have carried out structural investigation of smectic Q phase. Schematic representation of different smectic phases is given in figure 1.3.

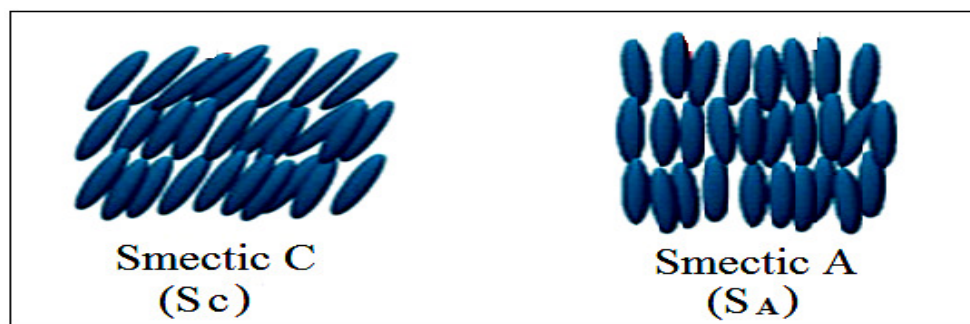


Figure 1.3 Schematic representation of smectic phases

Table1.1: Texture classification of smectic phases

Type of smectic phase	Structure	Texture
Smectic A	Planar	1. Stepped drops 2. Oily streaks 3. Homeotropic
	Non-Planar	1. Simple dygonal 2. Simple fan shaped 3. Focal conic fan shaped 4. Batonnets 5. Bubble textures
	Cylinders	1. Myelinic textures
Smectic C	Planar	1. Homogeneous 2. Stepped drops 3. Schlieren
	Non-Planar	1. Broken polygonal 2. Broken fan shaped 3. Batonnets
	Twisted	1. Planar 2. Schlieren 3. Straited fan shaped
Smectic F	Planar	1. Schlieren 2. Stepped drops
	Non-Planar Dupin cyclides	1. Stripped broken fan
Smectic B	Hexagonal	1. Mosaic 2. Homeotropic 3. Stepped drops 4. Batonnets 5. Ovals 6. Lancets
	Non-Planar Dupin cyclides	1. Focal conic fan shaped
	Tilted	1. Mosaic 2. Planar
Smectic E	Planar	1. Mosaic 2. Stepped
	Non-Planar	1. Straited 2. Stripped fan shaped
Smectic G	Planar	1. Mosaic 2. Stepped drops
Smectic D	Cubic bands	1. Isotropic mosaic

1.3.2 Nematic Liquid Crystals

The nematic liquid crystal phase is characterized by molecules that have no positional order but tend to point in the same direction. The word “Nematic” is derived from a Greek word ‘Nema’ meaning threads as the phase exhibits threaded schlieren texture. The molecules in nematic phase are arranged with their long axis parallel to each other but they are not separated in layers.

De Vries [18] proposed classification of nematic phases based on X-ray diffraction pattern as follows;

1. Skewed cybotactic Nematic
2. Normal cybotactic Nematic
3. Classical Nematic.

Schematic representation of nematic phase is given in figure 1.4, which shows that the molecules point vertically but are arranged with no particular order.

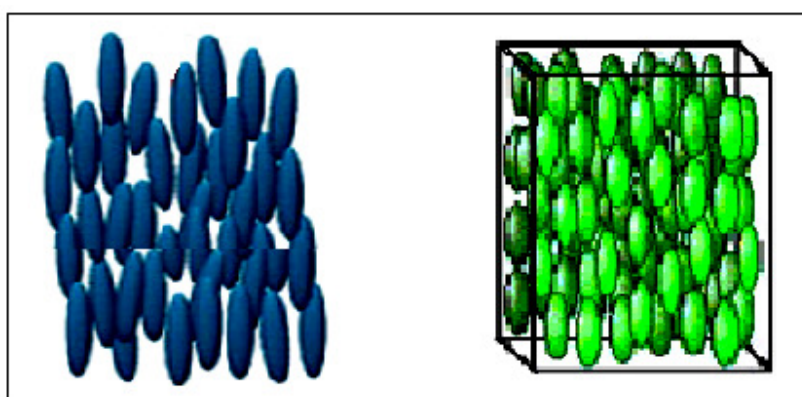


Figure 1.4 Schematic representation of Nematic phase

The molecules in the nematic phase exist in the form of groups, each group consisting about 1,00,000 parallel molecules. These groups are referred to as swarms. The ‘Swarm Theory’ is first proposed by E. Bose [19] in 1990, to explain the molecular arrangement and order in the nematic phase.

Nematic liquid crystals are optically positive and can be formed by compounds which are optically inactive or by racemic modification. A new type of mesophase is obtained by Zimmer and White [20], during the process of carbonisation and is termed as Gasparoux [21]. Numbers of workers have reported re-entrant nematic phase below the smectic phase [22, 23], which is generally exhibited by a few compounds possessing a nitro or cyano end group with positive dielectric anisotropy.

1.3.3 Cholesteric Liquid Crystals

The phase which, in most regards, is similar to the nematic phase but with chiral structure is known as the cholesteric phase. This phase is exhibited by compounds composed of chiral molecules or if chiral dopants [24-26] are added to a non-chiral (regular) nematic. The name is based on the fact that derivatives of the infamous cholesteryl benzoate [1] are initially found to exhibit this phase. In this phase molecules arranged themselves in a helical structure. The phase can be described as being made up of nematic planes helically piled over one another so that the director is rotating uniformly about the director normal. Certain cholesteric compounds can selectively scatter light into different colours. The colours of the reflected light can be determined by (a) a pitch of helix (b) by temperature (c) the angle of incident beams. These unique optical properties are the basis behind the commercially successful use of chiral nematics in thermotropic devices. Schematic representation of Cholesteric phase and helical structure is shown in figure 1.5.

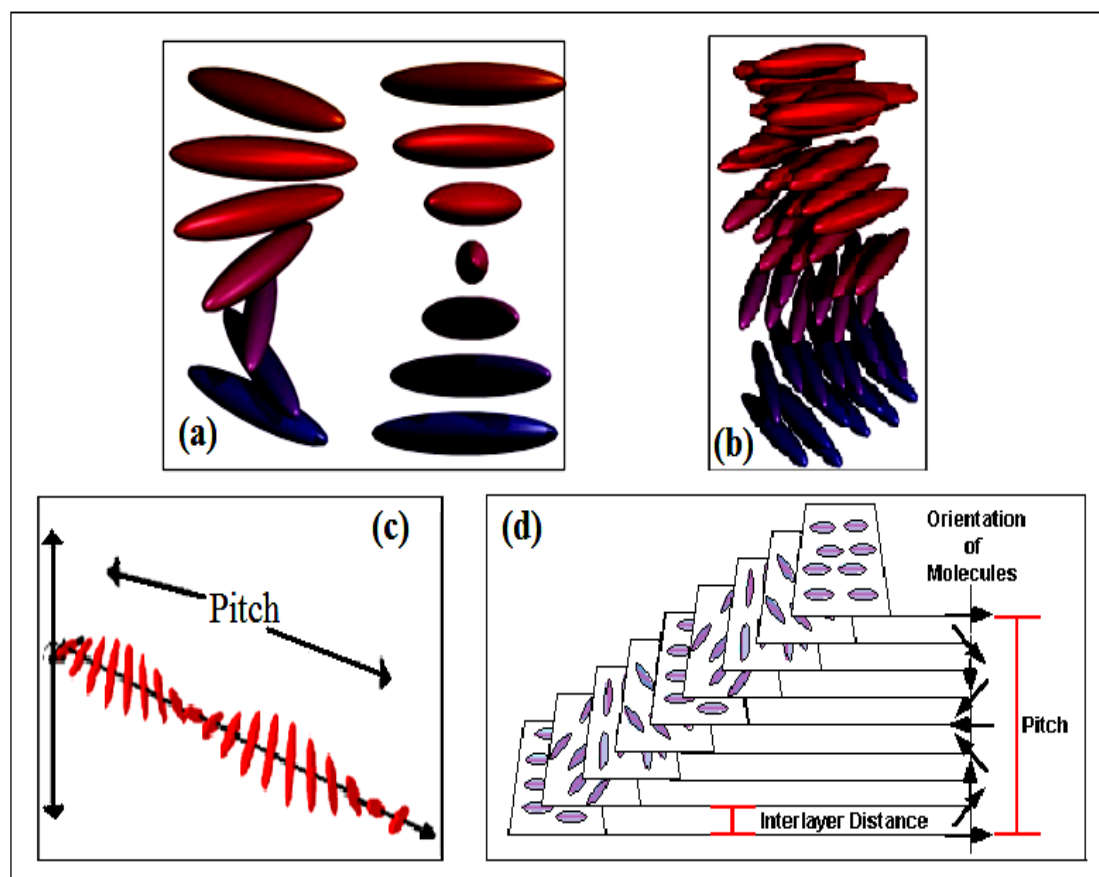


Figure 1.5 (a) and (b) Schematic representation of Cholesteric phase
(c) and (d) Schematic representation of helical structure

1.3.4 Blue Phases

Blue phases appear over a narrow temperature range between the chiral nematic phase (N^*), which has a relatively short helical pitch, and the isotropic phase [27, 28]. The defect phase may have simple cubic, body centered cubic, and amorphous structures [29, 30]. Blue Phases are considered to consist of a double-twist-cylinder (DTC) structure and are classified into three categories depending on the assembly structure of the DTC: BP I, BP II and BP III, listed in the order of increasing temperature [31, 32]. M. Lee et al [33] investigated blue phases of a nematogenic achiral bent-core molecule doped with chiral additive.

1.3.5 Twist grain boundary [TGB] phases

Chiral liquid crystals have the tendency to form cholesteric- like helical director field; on the other hand, the molecular interactions may favor a smectic layer structure. The competition between these two structural features can result in frustrated structures containing a regular lattice of grain boundaries, which in turn consist of a lattice of screw dislocations. This phase is known as the twist grain boundary phase (TGB). In 1988 Renn and Lubensky [34] developed a specific model of this structure of TGB phase. A short time later, in 1989, Goodby et al. [35] reported the discovery of the TGBA phase existing between the SmA^* and the isotropic phases. X-ray studies performed by Srajer et al. [36] confirmed that the essential features and the physical properties of the TGBA phase are very well described by the Renn-Lubensky model. Nagappa et al. have observed the TGB-A phase in mixtures of cholesteric with nematic [37] and with smectic [38] compounds. Some interesting research work for TGB phases are reported [39-42].

1.3.6 Ferroelectric and Anti-ferroelectric Liquid Crystals

If a compound made up of chiral molecule exhibits smectic C phase or a smectic C phase of nonchiral molecules is doped with a chiral dopants then that phase is called as chiral smectic C phase. The tilted molecule presses from one layer to another giving rise to a helical structure similar to the cholesteric liquid crystals. The helical structure of the chiral smectic C phase had been recognized in the early 1970s [43-44]. The tilted director rotates from layer to layer forming a helical structure (Fig. a). Various

ferroelectric liquid crystalline materials are developed by Goodby et al [45-46]. The ferroelectric phase has an alternating tilted structure. The alternation is not symmetrical and more layers are tilted in one direction (Fig. d). In antiferroelectric arrangement the adjacent layers of the molecules are oppositely tilted (Fig. e) and alternation of molecules is symmetrical. Some compounds having antiferroelectric liquid crystalline properties are reported [47-50]

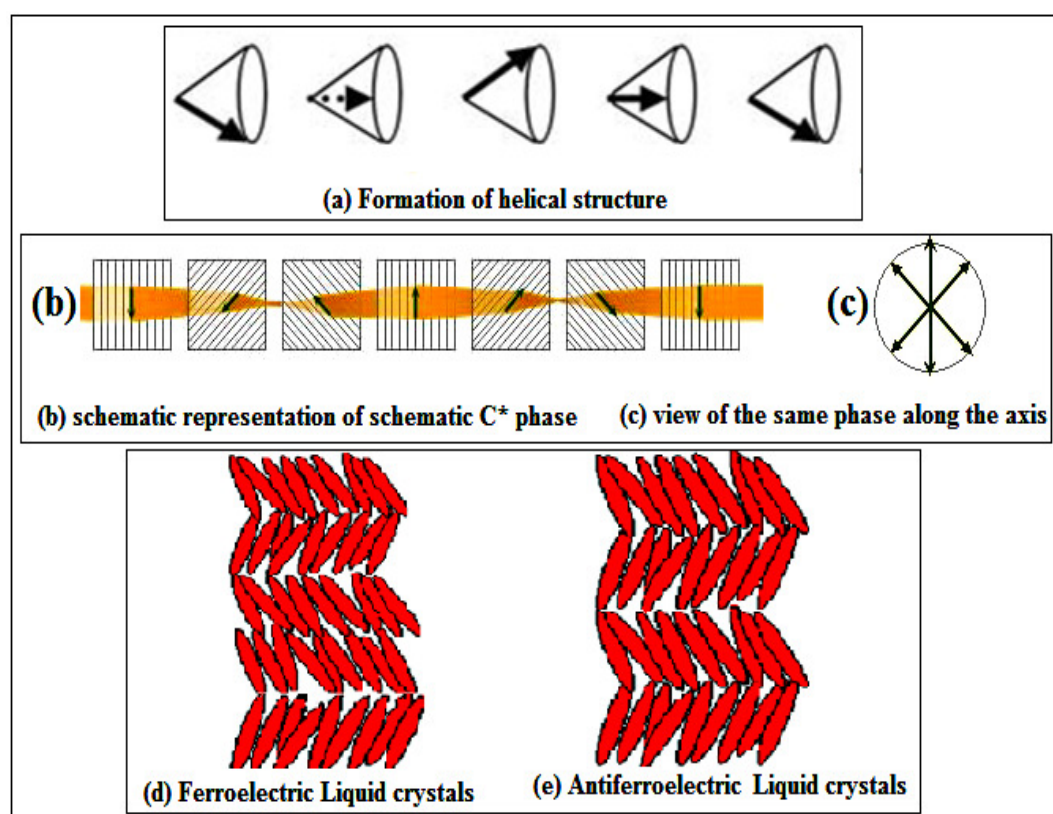


Figure 1.6 Formation of ferroelectric and antiferroelectric liquid crystals

1.3.7 Discotic Liquid Crystals

The mesophases exhibited by compounds composed of disc like molecules are known as discotic liquid crystals. The first discotic liquid crystal is synthesized and identified by Chandrasakher et al in 1977 [51]. Discotic phase may be classified into two fundamental types: columnar and nematic. In columnar phases, the molecules are stacked one upon another to form columns which may be arranged in hexagonal, tetragonal, rectangular or tilted arrays. Schematic representation of columnar discotic liquid crystals is given in figure 1.7.

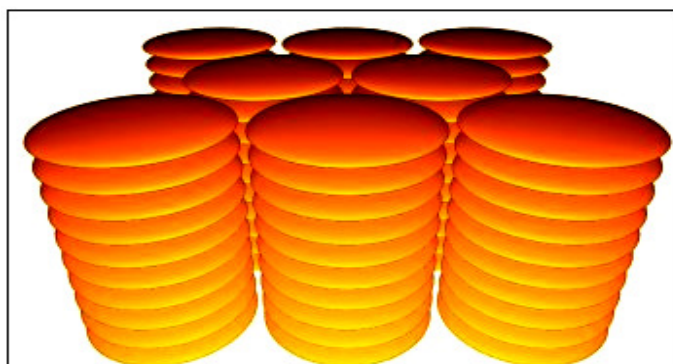


Figure 1.7 Schematic representation of columnar discotic liquid crystals

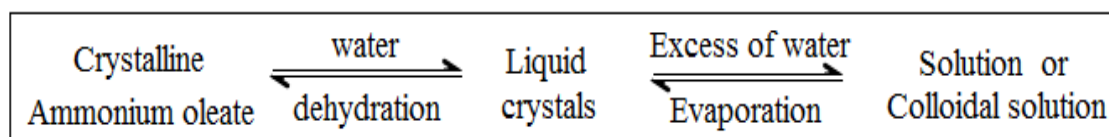
The nematic phases are anisotropic fluids with a single order parameter with a tendency to align the disc-shaped molecules parallel to each other. Triphenylene based compounds showing columnar phase developed by Boden et al [52]. Room temperature columnar phase is observed in polyalkynyl benzene based disc shaped molecules by Varshney et al [53]. Swen Mahlstedt et al, have reported a novel donor acceptor mesogen [54]. Discotic liquid crystals having crown ethers as central units are synthesized by M. Kaller et al [55] and C. Zhang et al [56]. Banana shaped discotic liquid crystals are reported by S. Kumar et al [57]. Recently, K. C. Majumdar et al [58] observed columnar phases from non disk-shaped mesogens. Some interesting discotic liquid crystals are reported by various researchers [59-62].

1.3.8 Sanidic Liquid Crystals

Compounds between the rod like and disc like molecules are the lath like species. They are generally fused or twin compounds derived from Greek word 'sanidic' means broad. These phases are called sanidic and are first found in polymeric liquid crystals reported by Ringsdorf et al. in 1986 [63]. The board like molecule of this compound can form a nematic phase, however contrary to the behavior in "normal" nematic phases; the rotation around the molecular long axis is strongly hindered. Therefore the structure of these phases is characterized by translational period in accordance with length, breadth, thickness of scattering maximum. Sanidics can be considered as a class of liquid crystals intermediate between discotic columnar and calamatic liquid crystals. Photoconductive behavior is found in a series of sanidic liquid crystal materials by D. Haristoy et al [64].

1.4 Lyotropic Liquid Crystals

This class of mesophase is induced by the effect of solvent on amphiphilic molecules; the solvent generally being water. At a critical concentration the solution exhibits liquid crystalline properties. Lehmann [65] is the first to recognize the mesomorphic state of ammonium oleate in aqueous solution. Lyotropic substances are strongly birefringent. Mesophase in binary systems of amphiphiles and water may be classified as (a) the neat phase (b) the middle phase (c) the viscous isotropic phase (d) the isotropic phase and (e) the inverse phase [66]. Lyotropic substances with other solvents are also studied [67-69]. Lyotropic liquid crystals are also affected by temperature changes. Hysteresis is observed in the properties of a ternary lyotropic liquid crystal system [70]. Lyotropic liquid crystals of hydrated phospholipids are studied [71] as model medium for studies of antimicrobial agent activity. The gradual breakdown of the crystal lattice by addition of water or in general solvent may be represented as



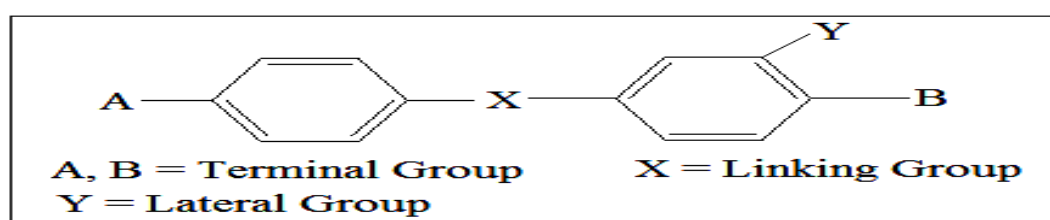
1.5 Influence of molecular structure on mesomorphism

The association between molecular structure and the mesomorphic properties of calamatic liquid crystals has been rigorously studied by Gray [72, 73]. Demus et al. [74-77] have given quite a detailed account of effect of chemical constitution on mesomorphism. The majority of thermotropic liquid crystals are aromatic in nature consisting of polarizable planer benzene rings linked with one another and having terminal alkyl or alkoxy group. Merely suitable structural geometry may not turn the compound to behave as a liquid crystal; intermolecular forces also play a very important role. These intermolecular forces are of three types.

1. Dipole- dipole attractions the direct interaction between permanent dipoles in the molecules.
2. Induced dipole attractions arising from the mutual polarization of the molecules by their permanent dipole moments.

3. Dispersion forces-the interaction between instantaneous dipoles produced by spontaneous oscillations of the electron clouds of the molecules.

The majority of thermotropic liquid crystals are aromatic in nature consisting of polarisable and planar rigid aromatic rings linked with one another through linking groups like -N=N-, -CH=N-, -COO-, -CH₂-COO-, -COO-CH₂-CH₂-O-, -CH=CH- etc. [167]. The increase in number of benzene rings increases the stability of the mesophases. The general structure can be represented as follows.



1.5.1 Effect of terminal substituents on mesomorphism

Terminal groups present in the molecules have their own importance because of their polarity. It has been found that terminal substituted compounds exhibit more stable mesophases compared to unsubstituted mesogenic compounds. However, for smectic liquid crystals certain terminal groups reduce the thermal stability. As the carbon chain of alkoxy or alkyl group is lengthened the tendency of depressing the melting point is increased. Liquid crystals of moderate chain lengths are normally purely nematic, increasing the length of the carbon chain gives both smectic and nematic mesophases and of very long chain length usually exhibits only smectic phases. Gray [78] has discussed in detail, the effect of increase in alkyl chain in a mesogenic homologous series. Demus et al. [79] have synthesized terminally swallowtail type of compounds and established that by selecting proper geometry of molecules the liquid crystalline property can be maintained in such system.

Branching in terminal chain often reduces liquid crystal phase stability [80] but is known to introduce tilted smectic phases in the system [81]. Branching at any point appears to have greater effect on the nematic than on the smectic thermal stability [82]. Chain branching also provide the opportunity to use a chiral alkyl chain and thereby produce a chiral smectic C phase (Sc*) [81].

The terminal group efficiency order which has been compiled [83] for smectic phase in rod-like aromatic system is

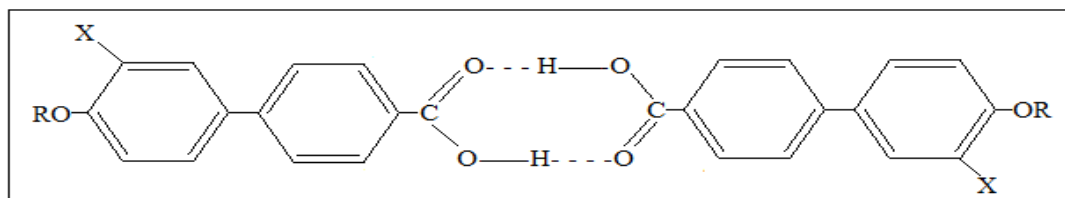


The nematic group efficiency order is



1.5.2 Effects of lateral substituents on mesomorphism

The effects of introducing lateral substituents into the elongated molecules of mesogenic compounds are considered. This type of structural change has been made systematically for a few types of compound by introducing a range of lateral substituents into the aromatic ring of core parts of the molecules [84].



The substituent X will have two effects;

- (1) The long molecular axes may be forced apart by the substituent, reducing intermolecular forces of attraction and thus lowering liquid crystal thermal stability. Since lateral interactions will be most effected, the thermal stability of the smectic mesophase should decrease more than that of the nematic mesophase.
- (2) The change from a ring-H to a ring-X bond will increase the molecular polarizability and possibly also the molecular dipolarity. This should increase lateral intermolecular attractions, enhancing liquid crystal thermal stability, particularly that of the smectic mesophase.

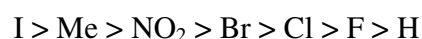
Lateral substituents may force apart the molecules and may thus reduce the intermolecular lateral cohesions but at the same time lateral substituents may increase

the intermolecular attractions. Normally the first effect predominates i.e. a lateral substituent decreases the mesophase thermal stabilities. However, if the substituents do not have fullest breadth increasing effect as in the case of the 5-substituted 6-n-alkoxy-2-naphthoic acids [85], then the second effect predominates i.e. the thermal stability of substituted mesogens increases.

Common lateral substituents are halogens, methyl, ethyl, cyano and other smaller groups [86-88]; however, liquid crystals having large lateral substituents are also known [89-93]. Every lateral substitution leads to an increase in the breadth of the molecule and thus a reduction in length to breadth ratio which in turn usually reduces the clearing temperatures.

The effect of lateral substitution of a type which, in addition to broadening the molecule, increases its thickness by imposing its steric effect on the system i.e. by causing a twisting about one of the bonds, so that parts of the molecule are related out of the plane of the remainder of the molecule are also reported [94, 95]. A combination of both breadth and steric effects greatly reduces the thermal stabilities of the ordered arrangement of molecules in the liquid crystals. There are compounds in which the lateral substituents are shielded so that they are less effective in broadening the molecules and at the same time improve the thermal stability [96]. This gives rise to notably high clearing temperatures. Demus et al. [97] have studied the effect of long lateral substituents having aromatic rings.

The lateral group efficiency order which has been compiled [98] for smectic phase is



The lateral group efficiency order which has been compiled [98] for nematic phase is



1.6 Mesomorphism in homologous series

For a homologous series, when the mesomorphic transition temperatures e.g. nematic-isotropic, smectic-isotropic, smectic-nematic or smectic-smectic are plotted against the number of carbon atoms in the alkoxy groups smooth curves may be drawn for like or related transitions. Usually the crystal-mesomorphic transitions do not exhibit regular

trends. The mesomorphic-isotropic temperatures lie on two falling curves; the upper one for even and lower one for odd number of carbon atoms in the n-alkoxy chain. The odd-even effect usually becomes less marked as the series is ascended and the two curves merge later in the series. The smectic-nematic transition temperatures usually do not alternate and lie on a smooth curves, which rises steeply at first, then levels off and may or may not merge with the falling nematic-isotropic, smectic-isotropic curves.

1.7 Banana Shaped Liquid Crystals

The first compound with a bent molecular geometry exhibiting mesomorphic properties is synthesized by Vorlander and his group [99] and explored the structure property relationship. These materials form new smectic and two-dimensional phases, which are unlike those obtained from normal calamatic molecules [100]. A real breakthrough in bent-core liquid crystals came in 1996, when Niori et al [101] reported ferroelectricity in a smectic phase formed by an achiral banana shaped compound. In 1997, Sekine et al. reported [102] a spontaneous helix formation in the smectic phase of an achiral bent-core compound. The origin of the helix is discussed in view of the twisted molecular conformation and the escape from microscopic polarization. In the last few years hundreds of compounds composed of bent-core molecules have been synthesized [103-111] with a view to understand the relationship between structure and the mesomorphic properties exhibited by such compounds. At least seven of these phases have been described [112] and preliminarily designated by the code letters B1 – B7. The general formula and different possibilities for variation of the chemical structure can be seen in figure 1.8.

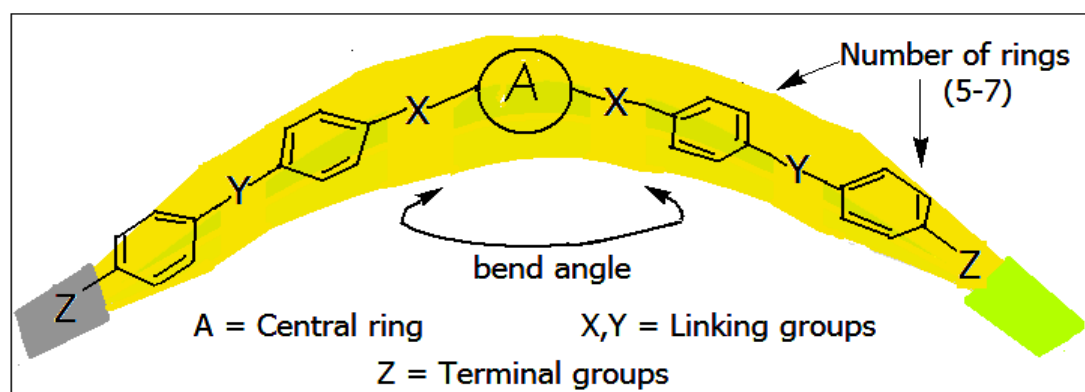


Figure 1.8 General structure of Banana shaped mesogens

Most of the compounds reported so far contain at least five phenyl rings. The angle results from a central 1,3- phenylene unit. The 2,7-disubstituted naphthalene unit is also a suitable central unit for banana shaped molecules [113]. The compounds with six or seven aromatic rings have also been reported [111, 112, 114, 115]. The transition temperatures increase with increasing number of phenyl rings. The exchange of phenyl rings with six-member heterocyclic rings like pyridine or pyrimidine is reported for seven-ring compounds [115]. The substitution of the central ring by a five-member heterocyclic ring such as 2,5-disubstituted-1,3,4-thiadiazole or 1,3,4-oxadiazole results in nematic or smectic mesophases, typical of calamatic liquid crystals [116,117].

1.8 Mesogenic oligomers having flexible spacers:

Dimers, Trimers, Tetramers

Liquid crystalline oligomers, which consist of molecules composed of semi-rigid mesogenic or non-mesogenic units interconnected via flexible spacers, have attracted considerable interest [118-119]. Mesogens containing two, three or four mesogenic or non mesogenic units connected by flexible spacers are called as dimers, trimers or tetramers respectively. Liquid crystal dimers, trimers, and tetramers are also of interest as models for main chain liquid crystal polymers [120]. Schematic representation of dimers, trimers and tetramers is shown in figure 1.9.

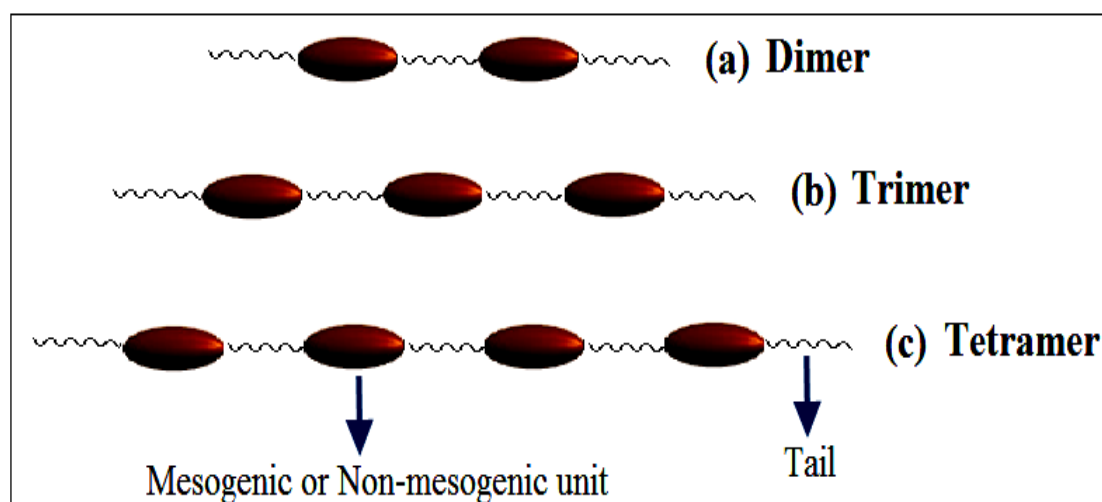


Figure 1.9 Schematic representation of mesogens with flexible spacers

1.8.1 Mesogenic Dimers

The first mesogenic dimer made of rod-like units is reported [121] by Vorlander long ago. Interesting mesophases exhibited by the dimeric system [122-125] depending upon the variation in structure. The first liquid crystalline dimer composed of banana-shaped mesogenic units are reported by Dantlgraber et al. [126]. Recently, Kosata et al. reported [127] symmetric dimers showing columnar phase. Several H-shaped dimers [128-130] with different spacers are reported. Prasad et al [131] synthesized anthraquinone based discotic dimers exhibiting columnar mesophases. Majmudar et al [132] synthesized and characterized cholesterol based liquid crystalline dimers.

1.8.2 Mesogenic Trimers

The significant findings on the dimers have prompted researchers to also synthesize its longer counterpart with three mesogenic groups connected by two spacers which are known as the trimers or trimesogens [133]. The trimers show different mesomorphic properties as compared to those of the dimers. A few chiral trimeric liquid crystals are reported [134-135]. Variety of trimers are synthesized with different mesogenic or non-mesogenic units and different flexible spacers or terminal chain lengths [136- 141]. Trimers containing three biphenyl groups are reported by Itahara et al [142].

1.8.3 Mesogenic Tetramers

Liquid crystalline tetramers are prepared by many groups of researchers [143-145]. These compounds exhibit a remarkable odd–even effect in their transition properties, depending on the length and parity of the flexible spacers [146-147]. The variation in smectic behavior of mesogenic tetramers containing four mesogenic units and three flexible spacers is studied [148-149].

1.9 Polymer Liquid Crystals

After the initial discovery of liquid crystallinity in polymeric solutions by Oster [150] and Robinson [151] number of liquid crystalline polymers have been reported. The high strength, high modulus fibers have given an impetus in the study and synthesis of liquid crystals, yet retain many of the useful and versatile properties of polymers. The

molecular structure and mesomorphic character of liquid crystal polymers is discussed in detail by Finkleman [152] and Ober [153].

The classification of liquid crystal polymers is based on the mesogen used in the construction of the liquid crystal polymer, which can be rod-like, disc-like or amphiphilic [154]. They are broadly classified into main chain liquid crystal polymers and side chain liquid crystal polymers. Figure 1.10 shows the molecular geometry of liquid crystal polymers.

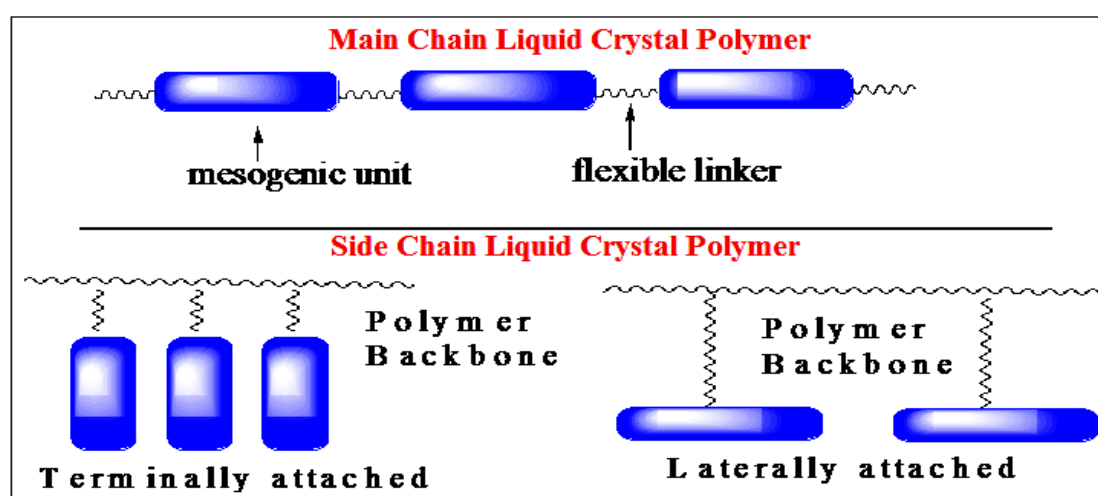


Figure 1.10 Molecular geometry of liquid crystal polymers.

1.9.1 Main Chain Polymer Liquid Crystals (MC-PLCs)

Main chain liquid crystal polymers are formed when rigid elements are incorporated into the backbone of normally flexible polymers. These stiff regions along the chain allow the polymer to orient in a manner similar to ordinary liquid crystals, and thus display liquid crystal, characteristics.

There are two distinct groups of MC- PLCs, differentiated by the manner in which the stiff regions are formed. The first group of main chain polymer liquid crystals is characterized by stiff, rod-like monomers. These monomers are typically made up of several aromatic rings, which provide the necessary size. The second and more prevalent group of main chain polymer liquid crystals is different because it incorporates a mesogen directly into the chain. Main chain liquid crystal polymers are reported by various workers [155-159].

1.9.2 Side Chain Polymer Liquid Crystals (SC-PLCs)

It has been demonstrated that main chain polymer liquid crystals often cannot show mesogenic behavior over a wide temperature range. Side chain polymer liquid crystals, however, are able to expand this scale. These materials are formed when mesogenic units are attached to the polymer as side chains; which are very well summarized by Blumstein and Hsu [160] and Ciferri et al. [161].

Generally acrylates or methacrylates which form a vinyl backbone are prepared as polymerizable groups [162]. Side chain cholesteric mesogenic polymers having isosorbide chiral agent are synthesized by He et al [163]. The first side chain polymer liquid crystals with incorporated bent-core mesogens is reported by Keith et al. [164]. Numbers of side chain liquid crystalline polymer are reported by various researchers [165-169].

1.10 Metallomesogens

In recent years, there is a growing interest in synthesis of liquid crystals containing metal atoms. These have been termed as metallomesogens. Metallomesogens have combination of properties of both of organic liquid crystalline ligand and metal atom [170]. Coordination of liquid crystalline ligands to metal ions can give variety of molecular shapes and phase changes [171]. The first thermotropic metal containing liquid crystals are reported by Vorlander [172] in 1910. He found that the alkali metal carboxylates – $(\text{CH}_2)_n - \text{COONa}$ forms classical lamellar phase on heating. Many thermotropic metallomesogens have been prepared over the years and many of these are discussed in the review articles by Pucci [173] and Espinet et al [174]. Both the rod-like [175-176] and disc-like [177-178] metallomesogens are known and examples of all the main mesophase types have been observed. Varieties of monodentate ligands, such as distilbazole [179], 4-substituted pyridines [180], Ferrocenes [181-182] etc. Synthesis of macrocyclic liquid crystalline ligands and their metal complexes are reported by C. R. Jejurkar et al [183]. A literature survey shows that several metallomesogens containing different metal atoms are synthesized [184-192].

1.11 Mixed mesomorphism

When mesomorphs are mixed, their melting points as well as transition temperatures depress in the usual way following more or less the law of mixtures. Different types of mixtures where none, one or both the components are mesomorphs have been investigated. Tamman [193], Lehmann [194], Smiths [195] and Vorlander and Ost [196] showed the depression of melting points and transition points in the phase diagrams of the mixtures showing liquid crystalline property. Schenck [197] and Schenck and Schneider [198] reported long back that nematic- isotropic temperature of p-azoxyanisole is lowered by the addition of other substances. The extent of mixed mesophase and the effect of terminal substituents in the exhibition of mixed mesomorphism have been studied in greater details by Dave and Dewar [199]. Dave and Lohar [200], Dave and Vasanth [201], Lohar and Shah [202], Lohar and Patel [203], Lohar and Mashru [204], Lohar and Jayrang Dave [205], Jayrang Dave and Menon [206] and Jayrang Dave and Pratik Patel [207]. Many researchers have given a detailed account on the studies of mixed mesomorphism [208-212].

Much earlier Bogojawlensky and Winogrodow [213] deduced from their study of mixed mesomorphism the latent transition temperatures of non-mesomorphic substances by extrapolation method. Walter [214] reported similar cases. Dave and Dewar [199], however, criticized the extrapolation method since they obtained different values for latent transition temperatures of a non-mesomorphic substance depending upon whether the liquid crystalline component was p-azoxyanisole or p-azoxyphenetole. Later on Dave and Lohar [200] found better evidence in favour of the accuracy of the extrapolation method; Lohar and Shah [202], Dewar and Goldberg [215], Lohar and Patel [203], Lohar and Mashru [204] and Lohar and Jayrang Dave [205] have brought out more evidences in support of the extrapolation method, prescribing certain definite conditions for better reliability.

De kock's [216] contention that there should exist a range of temperature over which two liquid phases- one isotropic and another anisotropic co- exist has been questioned by Dave and Dewar [199] who re-examined the system studied by de kock. showing that the mixed liquid crystalline region is a single homogenous phase. Dave and Dewar [199] and Dave and Lohar [200] obtained quite interesting results by mixing

p-azoxyanisole with different Schiff's bases and deduced an order of efficiency of the terminal groups for exhibiting nematic mixed mesophases.

Sackmann and Demus [217] have identified smectic mesophase on the basis of miscibility criteria and texture phenomena. Madhusudana [218] synthesized some liquid crystals made of banana-shaped molecules and studied their binary mixtures with rod-like molecules.

1.12 Physical properties of Liquid Crystals

Large volume of work to study the physical properties of liquid crystals has been carried out by scientists in early days of liquid crystals. Vander Lingen [219], and Huckel [220], Dabrowski et al [221] Yang et al. [222] and Iida et al. [223] carried out X-ray studies. NMR and DSC studies are carried out by Tanaka et al. [224] Domenici et al [225] and Lippmann et al [226, 227] and Saupe and Englert [228]. The studies of Ultra Violet and Infrared Spectroscopy are carried out by a number of researchers like Sun et al. [229] and Khoo et al. [230]. Viscosity studies are done by Schafer [231].

The use of liquid crystals as stationary phase in chromatography is initiated by Dewar et al. [232] and Kelker [233] used few liquid crystalline compounds as stationary phase in gas chromatography. Many other researchers worked in this field [234-237]. Number of reviews and books are published where detailed studied of physical properties are discussed [238-239]. The study of physical properties is important as it decides the applicability of liquid crystals so that they can be exploited for practical advantages.

1.13 Biological Systems

Mesomorphic property in the form of Myelin in biological system is first shown by Virchow [240] in 1854. Biological systems are multicomponent and contain numerous types of macromolecules, organic ions etc. One of the first demonstrations of liquid crystalline phenomenon in a well characterized biological system is given by Bernal and Faukuchen [241] who used X-ray diffraction to investigate solutions of tobacco mosaic virus. A definite claim that liquid crystals entered the structure of living cells and tissues is made in 1959 [242] when it is shown that complex lipids present in

adrenal cortex, ovaries, myelin and also in atheromatous arteries existed at body temperature in a characteristic mesophase. Stewart [243] studied in detail the mesomorphism in biological systems and gave reason why mesomorphism is observed in biological systems. Liquid crystals are abundant in nature and intrinsically linked to a multitude of biological processes, as discussed in several reviews [244-245]. Jewell discussed in detail on living systems and liquid crystals [246]. The lung liquid crystal droplets are capable of phase transitions between liquid crystal, crystal, and isotropic phases which are dependent on the rate of temperature change as in liver, kidney and other major tissues of the embryo [247]. The exploration of liquid crystalline materials at the interface between physics, chemistry and biology is particularly lucrative, providing a greater insight into the mechanisms by which living systems function as well as leading to new biomedical applications in the understanding, diagnosis and treatment of disease [248]. Naturally occurring biological materials that spontaneously form liquid crystal phases *in vivo* include DNA [249-250], chromosomes [251] and collagen [252] as well as the lyotropic phases formed by proteins in the production of spider silk [253] and lipids in the membrane of living cells.

1.14 Applications of Liquid Crystals

From the application point of view, 'liquid crystals' are one of the most developing and fascinating fields of current research. Liquid crystalline compounds have found ways for numerous potential applications because of their characteristic physical and optical properties. Now a days liquid crystals are used in many fields, particularly in the fields of electro-optical applications [254] and in biological systems.

1.14.1 Display applications of Liquid Crystals [255]

Liquid crystal displays (LCDs) had a humble beginning with wrist watches in the seventies. Continued research and development in this multidisciplinary field have resulted on displays with increased size and complexity. After three decades of growth in performance, LCDs now a formidable challenge to cathode ray tubes (CRT). Liquid crystal displays (LCDs) have many advantages over other display types. They are flat

and compact, possess extremely low power consumption (Microwatts per square centimeter in the case of the twisted nematic display).

For simple calculator and watch displays TN (Twisted Nematic) mixtures based on cyanobiphenyls are used. These materials are first invented by G. W. Gray 39 years ago [256, 257]. Broad range TN mixtures with improved viewing angle using phenylcyclohexanes [258, 259] are then used for automotive applications. The introduction of STN displays required materials with large dielectric anisotropy, eg. Cyanoesters with lateral fluoro substitution [260]. Thin film technology (TFT) displays require liquid crystalline materials with high stability like fluorinated liquid crystals [261-265]. Kim et al [266] has fabricated a novel Switchable Transmissive and Reflective (STR) LCD based on dual gap TN (Twisted-Nematic) mode.

1.14.2 Non display applications of Liquid Crystals

1.14.2.1 Thermal mapping and non-destructive testing [267, 268]

A film of cholesteric liquid crystal may be applied to large uneven area. This makes it an ideal tool for thermal mapping and non-destructive testing. The great deal of flexibility in the colour play range allows for a great diversity in potential applications ranging from food processing to electronics and space applications e.g. thermochromic paints have been used on printed circuit boards to examine overheating of components. Liquid crystal thermography is used in non-destructive testing and continuously growing due to the development on new chiral nematic materials to offer improved performance over the cholesteryl esters used in early applications.

1.14.2.2 Liquid crystals lenses

The ability to control the refractive index of a liquid crystal allows the implementation of liquid crystal lenses. The refractive index profile in these devices acts as a curved surface of a glass and hence acts as a lens [269].

1.14.2.3 Medical thermography [270]

Thermochromic liquid crystals are extensively used in medical applications, Forehead thermometers also known as 'fever strips' are based on different thermochromic liquid crystal materials. Thermal mapping of various areas of the body has been used as a diagnostic technique for a wide ranging group of medical conditions in which a temperature differential near the skin surface may be related to the disorder. Subcutaneous and intracutaneous malignant tumors are typically 0.9-3.3°C warmer than the surrounding tissues. Therefore, thermography is an interesting candidate for cancer screening.

1.14.2.4 Radiation detection [271]

Films containing cholesteric liquid crystals are inexpensive and versatile tools for visualizing invisible radiation.

1.14.2.5 Liquid Crystals in gas (GLC) liquid chromatography

The molecular structure of liquid crystals allows for their application in gas and liquid chromatography as highly selective stationary phase. A number of models have been developed to describe more quantitatively the enhancement in selectivity that is obtained the anisotropic orientational ordering of liquid crystals [272-274]. Earlier uses of liquid crystals as stationary phases in gas chromatography are available [275-277]. Stationary phases can be prepared from either monomeric or side chain polymeric liquid crystals.

1.14.2.6 Liquid crystals as solvents in spectroscopy [278]

Liquid crystalline media, particularly nematic, provide the bulk molecular orientation necessary for observation of spectroscopic details analogous to those obtained in solid state experiments. These media have been widely used as solvents in NMR, EPR and Optical spectroscopic studies on oriented molecules. A few general reviews in this area of applications have appeared [279].

1.14.2.7 Liquid crystals as solvents in chemical reactions

Thermotropic liquid crystals have been used as solvents to alter course or rates of uni and bi-molecular thermal and photochemical reactions. The unique anisotropic properties of liquid crystals are utilized to control the efficiency and specificity in micro synthesis elucidation of reaction mechanism etc. Factors that are important in defining the ability of liquid crystals to control solute reactivity have been reviewed to be able to choose the liquid crystals of proper morphology as a solvent [280- 282].

1.14.2.8 High- Strength Fibers

An application of polymer liquid crystals that has been successfully developed for industry is the area of high strength fibers. e. g. Kevlar fibers, which are used to make such things as helmets and bulletproof vests, is just one example of the use of polymer liquid crystals in applications calling for strong light weight materials [283].

1.14.2.9 Optical Applications

The use of polymer liquid crystals in the display industry is an exciting area of research. A twisted nematic polymer liquid crystal cell can be used to make energy efficient displays. Highly polarizable thiophene derivatives are used in nonlinear optical applications [284-286]. Nematic triphenylenes have found application as the principle components in optical compensation films to improve the viewing angle of liquid crystal displays [287]. Liquid crystalline polymers containing azo group have been widely studied overall in the field of optical materials [288-289].

1.14.2.10 Discotic liquid crystals for solar cells

Discotic liquid crystals have very high charge carrier mobility in columnar mesophases which offers potential applications as charge transport materials in a variety of devices like conductors, field-effect transistors, photovoltaic solar cells, etc. [290]. Some other studies on charge and energy migration in discotic liquid crystals [291-292] lead us closer to a long-desired goal of achieving cheaper, clean, eco-friendly energy for the benefit of mankind. The application is of great importance to developing countries.

1.14.2.11 Thermotropic Liquid Crystals as lubricating agent

The mechanism of lubrication is based on the creation of adsorbed layer by a lubricating agent fulfilling irregularities of the surface. Liquid crystals are used as lubricating agents [293-295]. Such compounds have polar groups which let the adsorption on the metal surface and formation of protecting ordered layers. Different liquid crystalline compounds are tested as lubricating agents to check the influence of chemical structure and the mechanism of action of these substances.

1.15 Polarizing Optical Microscopy

The transition temperatures are determined by using a “Leitz Labourlux Microscope”, polarizing microscope provide with Kofler heating stage.

The figure below is a schematic representation of polarizing optical microscope.

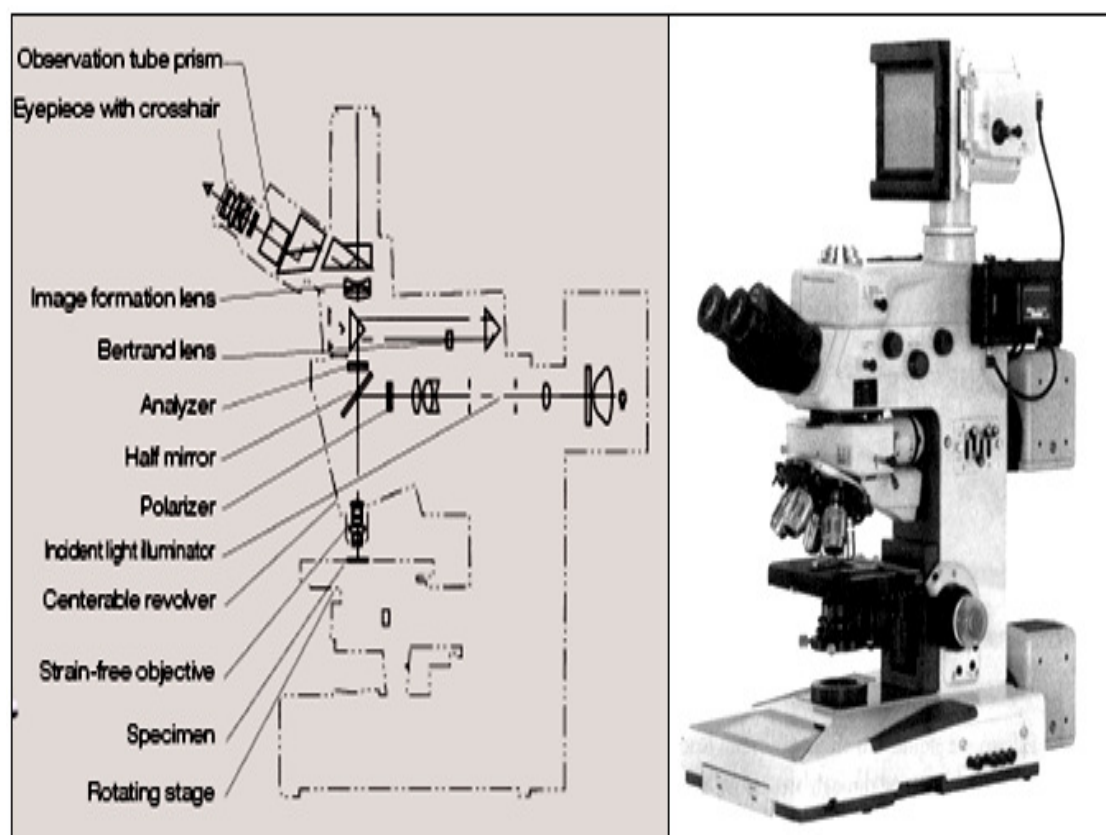


Figure 1.11 Polarizing optical microscope provided with heating stage.

The microscope is standardized by taking melting points and transition temperatures of very pure and known substances like benzoic acid, succinic acid, p-azoxyanisole, vanillin, p-anisaldehyde.

To determine the various transitions, a glass slide carrying a thin section of the material with cover slip on it is heated and observed under the microscope. The slide is inserted into the specimen chamber and the temperature is raised $5^{\circ}\text{C}/\text{min}$ to find the approximate transition temperatures. The measurements are repeated and the rate of heating is regulated to about $1^{\circ}\text{C}/\text{min}$, near the transition to be observed. The changing texture over the temperature ranges are carefully observed and recorded as focal-conic, plane, homeotropic and threaded textures of smectic and nematic phases as they appeared under the polarized light. All observations are repeated several times. In case of any doubt the compounds are purified again and are subjected to study under the microscope a fresh.

1.16 Differential Scanning Calorimetry

This technique maintained the sample and reference materials isothermal to each other by proper application of electrical energy, as they are heated or cooled at a linear rate. The curve obtained is a recording of heat flow dH/dt , in m.cal/sec. as a function of temperature.

In the true thermodynamic sense, an endotherm curve peak is indicated by a peak in the upward direction (increase in enthalpy) while an exotherm curve peak is recorded by a peak in the opposite direction. In all appearances a DSC curve looks very similar to that of a DTA curve, except for the ordinate axis units. As in DTA, the area enclosed by the DSC curve peak is directly proportional to enthalpy change.

$$\text{Area} = K \times \Delta H_m$$

Except that K is independent of temperature.

In the present work, calorimetry study is carried out for number of compounds on Mettler Toledo Star SW 7.01 in nitrogen environment.

Liquid crystalline materials are in good demand these days. Mesogenic materials have become relevant to the needs of the society due to their versatile applications. The fields of liquid crystals have fascinated chemists, physicists as well as technologists, over several decades by now. Their applications in numerous fields of modern technology like, electro optical display, medical thermography, high strength fibre, liquid crystal in gas liquid chromatography etc., devices has developed further interest in search for new mesogens and exploration of fundamental causes of the captivating phenomenon. The synthesis and study of liquid crystalline materials has been continually contributing to the advancement in science and technology. Synthesizing and studying new mesomorphic compounds can yield interesting and useful information and results.

Thus the prime and foremost aim set forth for this investigation is to synthesize new homologous series of high mesomorphic value by varying certain categorical units of the moieties; with specific considerations, certain structural features have been altered, while some have been mentioned as common to newly synthesized homologues series. To synthesize homologous series having ester and azo central linkages with different lateral substitutions and one homologous series with naphthalene central ring containing terminal fluoro group.

To synthesize homologous series having heterocyclic furfural moiety and chalcone as one of the central linkages.

To synthesize homologous series having ester and ethylideneamino central linkages with different terminal groups.

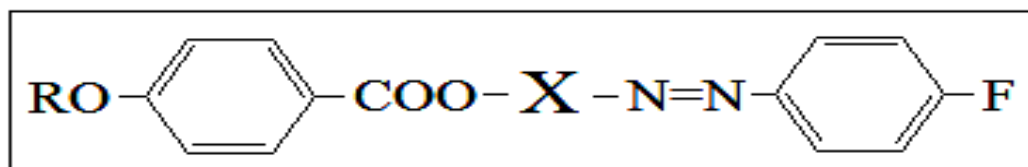
Potential applications of the bent-shaped liquid crystals in non-linear optics, optical storage and electro optical devices has developed considerable interest in the synthesis and structural investigations of these bent-shaped mesogens. The diphenylether moiety makes molecule bent. Thus, in view of this synthesis of mesogens having diphenylether moiety as central core has been planned and their mesomorphic properties are studied.

Study of mixed mesomorphism in binary systems by varying in structural features and mesomorphic characteristics of components has been considered of interest; it has helped revealing some characteristics of liquid crystals. Study of binary systems is important as it depresses the transition temperatures, with changes in mesophase texture. Thus some binary systems comprising structurally dissimilar components have been examined and their mixed mesomorphism has been studied.

Lastly, but not the least the purpose of this investigation is to arrive at certain specific conclusions to the existing knowledge in the subject matter as viewed from the background of the study of large number of newly synthesized liquid crystals under this investigation, their mesomorphic characteristics and also the study of mixed mesomorphism in binary systems.

3.1 Introduction

The properties of liquid crystals depend on the structure of liquid crystal molecules [296]. A number of homologous series with ester and azo central linkages have been synthesized having different terminal groups [297-300]. Introduction of lateral substitution makes molecules broad and plays an effective role in variation in mesogenic properties of mesogenic compounds [301]. A survey of the literature indicates that generally the average thermal stability of the mesogens having lateral substituent is less than laterally unsubstituted mesogens [302-304]. Similarly introduction of central naphthalene ring in mesogenic homologues increases the breadth of the molecules and plays an important role in variation in their mesomorphic properties [305]. In this connection, systematic studies have been carried out by various researchers [306-309]. In order to investigate the effect of lateral substituents and central naphthalene moiety on fluoro liquid crystalline compounds five homologous series having ester and azo central linkages with different lateral substituents and one series having central naphthalene moiety with terminal fluoro group are synthesized. General molecular structure of the series is



Where, R is C_nH_{2n+1} $n= 1$ to 8, 10, 12, 14 and 16

Series	I	II	III	IV	V	VI
X						

3.2 Experimental

3.2.1 Materials

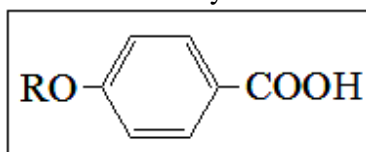
4-hydroxybenzoicacid, n-alkyl halides, phenol, 2-chloro phenol, m-cresol, 3-chloro phenol, o-cresol, α -naphthol and all other chemicals are of Merck, SRL or Loba grade and used as received.

3.2.2 Synthesis

3.2.2.1 Series I: 4-(4'-n-alkoxybenzoyloxy)phenylazo-4''-fluorobenzenes

3.2.2.1.a 4-n-alkoxybenzoicacids

General molecular structure of 4-n-alkoxybenzoicacids



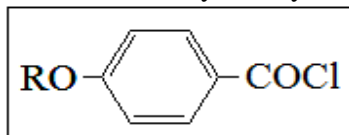
Where, R is C_nH_{2n+1} $n= 1$ to 8, 10, 12, 14 and 16

Commercially available 4-methoxybenzoicacid (anisicacid, Loba) is used. Number of methods are known for the alkylation of 4-hydroxybenzoicacid [310-312]. In the present study, following modified method is used [312].

0.1 mole of 4-hydroxybenzoicacid and 0.25 mole of KOH pellets are dissolved in the 100 ml ethanol. 0.12 mole of respective n-alkylhalide is added and the solution is refluxed for 8 hours. 10% of 25 ml aq. KOH solution is added after the reflux period, and the reflux is continued for two more hours to hydrolyze any ester formed. The solution is cooled to room temperature and acidified with 1:1 HCl to precipitate the acid. They are recrystallised several times from ethanol until constant transition temperatures are obtained. The transition temperatures are in good accordance with the reported values [312].

3.2.2.1.b 4-n-alkoxybenzoylchlorides [312]

General molecular structure of 4-n-alkoxybenzoylchlorides

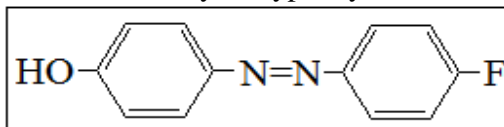


Where, R is C_nH_{2n+1} $n= 1$ to 8, 10, 12, 14 and 16

4-n-alkoxybenzoylchlorides are prepared by refluxing the corresponding 0.005 mole 4-n-alkoxybenzoicacids with an excess of thionylchloride (10-12 ml) under moisture free condition in a water bath, till the evolution of hydrogen chloride gas cased. Excess of thionylchloride is distilled off under reduced pressure and the acidchloride left behind as a residue, which is used in the next reaction without further purification.

3.2.2.1.c 4-hydroxyphenylazo-4'-fluorobenzene

General molecular structure of 4-hydroxyphenylazo-4'-fluorobenzene



The dye is prepared by the reported method [313], in two steps.

(i) Preparation of Diazonium salt of 4-fluororanine

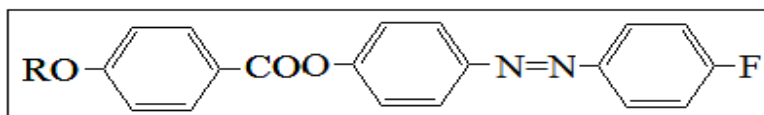
0.05 mol of 4-fluoroaniline is dissolved in a mixture of 20 ml of conc. HCl and 20 ml of water and cooled to 0° - 5° C in a bath of ice and salt. A cold solution of 0.05 mole of $NaNO_2$ in 10 ml of water is added in small portions at 5° C. During addition the mixture is stirred vigorously. The completion of diazotization is checked by using KI-starch paper. The diazonium salt is used immediately in next step.

(ii) Coupling of 4-fluorobenzenediazoniumchloride with phenol

0.05 mol of phenol is dissolved in 25 ml of 20% NaOH solution; while maintaining temperature below 5° C. The mixture is stirred continuously and the cold diazonium salt is added slowly, maintaining the pH 8 to 9. Crystals of the sodium salt of the dye separated out; its mixture is allowed to stand for half an hour; after which it is acidified with 1:1 HCl. The dye obtained is filtered and washed with hot water to remove any decomposed diazonium salt; it is recrystallised twice from methanol.

3.2.2.1.d 4-(4'-n-alkoxybenzoyloxy)phenylazo-4''-fluorobenzenes

General molecular structure of 4-(4'-n-alkoxybenzoyloxy)phenylazo-4''-fluorobenzenes



Where, R is C_nH_{2n+1} $n= 1$ to 8, 10, 12, 14 and 16

0.005 mole 4-hydroxyphenylazo-4'-fluorobenzene is dissolved in 10 ml of dry pyridine and is added slowly to a cold solution of respective 4-n-alkoxybenzoyl chloride in pyridine. The mixture is refluxed in a water bath for an hour and is allowed to stand overnight at room temperature. It is acidified with 1:1 cold HCl and the separated solid is filtered, washed with water, $NaHCO_3$ and NaOH solutions to remove any unreacted acid and phenol. The precipitates are again washed with water and the final product is recrystallised from ethanol until constant transition temperatures are obtained. They are recorded in table 3.1. The elemental analysis of some of the representative compounds are found to be satisfactory and are recorded in table 3.2.

3.2.2.2 Series II: 4-(4'-n-alkoxybenzoyloxy)3-chlorophenylazo-4''-fluorobenzenes**3.2.2.2.a 4-n-alkoxybenzoicacids**

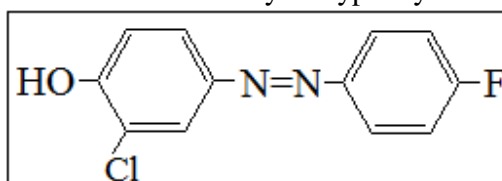
They are synthesized following the procedure reported in 3.2.2.1.a [312].

3.2.2.2.b 4-n-alkoxybenzoylchlorids

They are synthesized following the procedure reported in 3.2.2.1.b [312].

3.2.2.2.c 3-chloro-4-hydroxyphenylazo-4''-fluorobenzene

General molecular structure of 3-chloro-4-hydroxyphenylazo-4''-fluorobenzene



The dye is prepared by the reported method [313], in two steps.

(i) Preparation of Diazonium salt of 4-fluororanimine

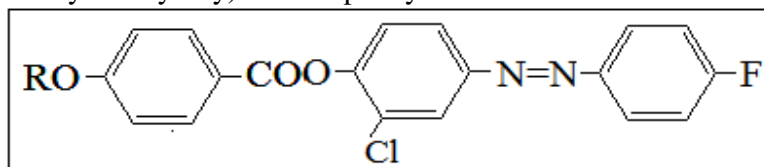
The diazonium salt is prepared by the procedure described in 3.2.2.1.c

(ii) Coupling of 4-fluorobenzediazoniumchloride with 2-chlorophenol

The coupling is carried out by the procedure described in 3.2.2.1.c

3.2.2.2.d 4-(4'-n-alkoxybenzoyloxy)3-chlorophenylazo-4''-fluorobenzenes

General molecular structure of

4-(4'-n-alkoxybenzoyloxy)3-chlorophenylazo-4''-fluorobenzenes

Where, R is C_nH_{2n+1} $n= 1$ to 8, 10, 12, 14 and 16

0.005 mol 3-chloro-4-hydroxyphenylazo-4'-fluorobenzene is dissolved in 10 ml of dry pyridine and is added slowly to a cold solution of respective 4-n-alkoxy benzoylchloride in pyridine. The mixture is refluxed in a water bath for an hour and is allowed to stand overnight at room temperature. It is acidified with 1:1 cold HCl and the separated solid is filtered, washed with water, $NaHCO_3$ and NaOH solutions to remove any unreacted acid and phenol. The precipitates are again washed with water and the final product is recrystallised from ethanol until constant transition temperatures are obtained. They are recorded in table 3.5. The elemental analysis of some of the representative compounds are found to be satisfactory and are recorded in table 3.6.

3.2.2.3 Series III: 4-(4'-n-alkoxybenzoyloxy)3-methylphenylazo-4''-fluoro benzenes**3.2.2.3.a 4-n-alkoxybenzoicacids**

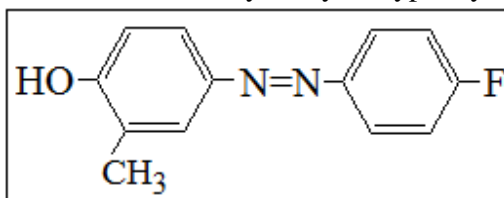
They are synthesized following the procedure reported in 3.2.2.1.a [312].

3.2.2.3.b 4-n-alkoxybenzoylchlorids

They are synthesized following the procedure reported in 3.2.2.1.b [312].

3.2.2.3.c 3-methyl-4-hydroxyphenylazo-4'-fluorobenzene

General molecular structure of 3-methyl-4-hydroxyphenylazo-4'-fluorobenzene



The dye is prepared by the reported method [313], in two steps.

(i) Preparation of Diazonium salt of 4-fluororiline

The diazonium salt is prepared by the procedure described in 3.2.2.1.c

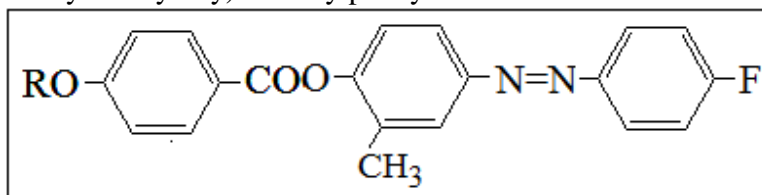
(ii) Coupling of 4-fluorobenzenediazoniumchloride with o-cresol

The coupling is carried out by the procedure described in 3.2.2.1.c

3.2.2.3.d 4-(4'-n-alkoxybenzoyloxy)3-methylphenylazo-4'-fluorobenzenes

General molecular structure of

4-(4'-n-alkoxybenzoyloxy)3-methylphenylazo-4'-fluorobenzenes



Where, R is C_nH_{2n+1} $n=1$ to 8, 10, 12, 14 and 16

0.005 mol 3-methyl-4-hydroxyphenylazo-4'-fluorobenzene is dissolved in 10 ml of dry pyridine and is added slowly to a cold solution of respective 4-n-alkoxy benzoylchloride in pyridine. The mixture is refluxed in a water bath for an hour and is allowed to stand overnight at room temperature. It is acidified with 1:1 cold HCl and the separated solid is filtered, washed with water, $NaHCO_3$ and NaOH solutions to remove any unreacted acid and phenol. The precipitates are again washed with water and the final product is recrystallised from ethanol until constant transition temperatures are obtained. They are recorded in table 3.9. The elemental analysis of some of the representative compounds are found to be satisfactory and are recorded in table 3.10.

3.2.2.4 Series IV: 4-(4'-n-alkoxybenzoyloxy)2-chlorophenylazo-4''-fluoro benzenes

3.2.2.4.a 4-n-alkoxybenzoicacids

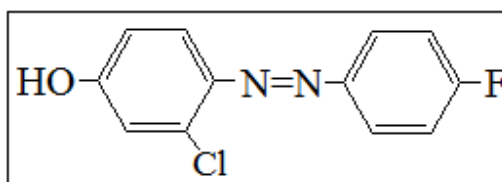
They are synthesized following the procedure reported in 3.2.2.1.a [312].

3.2.2.4.b 4-n-alkoxybenzoylchlorids

They are synthesized following the procedure reported in 3.2.2.1.b [312].

3.2.2.4.c 2-chloro-4-hydroxyphenylazo-4'-fluorobenzene

General molecular structure of 2-chloro-4-hydroxyphenylazo-4'-fluorobenzene



The dye is prepared by the reported method [313], in two steps.

(i) Preparation of Diazonium salt of 4-fluororanine

The diazonium salt is prepared by the procedure described in 3.2.2.1.c

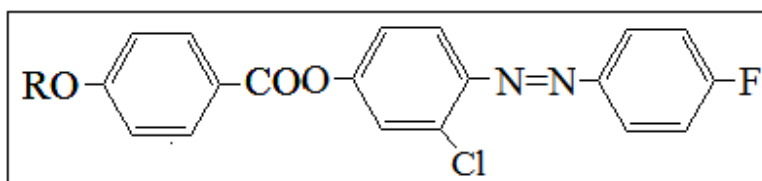
(ii) Coupling of 4-fluorobenzenediazoniumchloride with 3-chlorophenol

The coupling is carried out by the procedure described in 3.2.2.1.c

3.2.2.4.d 4-(4'-n-alkoxybenzoyloxy)2-chlorophenylazo-4''-fluorobenzenes

General molecular structure of

4-(4'-n-alkoxybenzoyloxy)2-chlorophenylazo-4''-fluorobenzenes



Where, R is C_nH_{2n+1} $n= 1$ to 8, 10, 12, 14 and 16

0.005 mol 2-chloro-4-hydroxyphenylazo-4'-fluorobenzene is dissolved in 10 ml of dry pyridine and is added slowly to a cold solution of respective 4-n-alkoxy benzoylchloride in pyridine. The mixture is refluxed in a water bath for an hour and is allowed to stand overnight at room temperature. It is acidified with 1:1 cold HCl and the separated solid is filtered, washed with water, NaHCO₃ and NaOH solutions to remove any unreacted acid and phenol. The precipitates are again washed with water and the final product is recrystallised from ethanol until constant transition temperatures are obtained. They are recorded in table 3.13. The elemental analysis of some of the representative compounds are found to be satisfactory and are recorded in table 3.14.

3.2.2.5 Series V: 4-(4'-n-alkoxybenzoyloxy)2-methylphenylazo-4''-fluoro benzenes

3.2.2.5.a 4-n-alkoxybenzoicacids

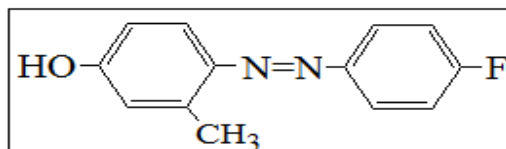
They are synthesized following the procedure reported in 3.2.2.1.a [312].

3.2.2.5.b 4-n-alkoxybenzoylchlorids

They are synthesized following the procedure reported in 3.2.2.1.b [312].

3.2.2.5.c 2-methyl-4-hydroxyphenylazo-4'-fluorobenzene

General molecular structure of 2-methyl-4-hydroxyphenylazo-4'-fluorobenzene



The dye is prepared by the reported method [313], in two steps.

(i) Preparation of Diazonium salt of 4-fluororanine

The diazonium salt is prepared by the procedure described in 3.2.2.1.c

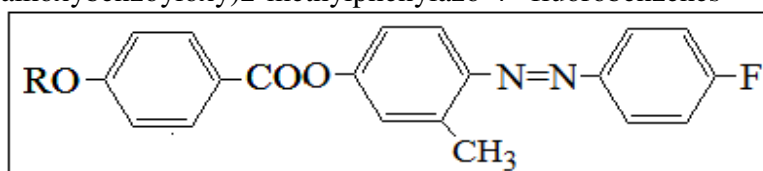
(ii) Coupling of 4-fluorobenzenediazoniumchloride with m-cresol

The coupling is carried out by the procedure described in 3.2.2.1.c

3.2.2.5.d 4-(4'-n-alkoxybenzoyloxy)2-methylphenylazo-4''-fluorobenzenes

General molecular structure of

4-(4'-n-alkoxybenzoyloxy)2-methylphenylazo-4''-fluorobenzenes



Where, R is C_nH_{2n+1} $n= 1$ to 8, 10, 12, 14 and 16

0.005 mol 2-methyl-4-hydroxyphenylazo-4'-fluorobenzene is dissolved in 10 ml of dry pyridine and is added slowly to a cold solution of respective 4-n-alkoxy benzoylchloride in pyridine. The mixture is refluxed in a water bath for an hour and is allowed to stand overnight at room temperature. It is acidified with 1:1 cold HCl and the separated solid is filtered, washed with water, $NaHCO_3$ and NaOH solutions to remove any unreacted acid and phenol. The precipitates are again washed with water and the final product is recrystallised from ethanol until constant transition temperatures are obtained. They are recorded in table 3.17. The elemental analysis of some of the representative compounds are found to be satisfactory and are recorded in table 3.18.

3.2.2.6 Series VI: 4-(4'-n-alkoxybenzoyloxy)naphthylazo-4''-fluorobenzenes**3.2.2.6.a 4-n-alkoxybenzoicacids**

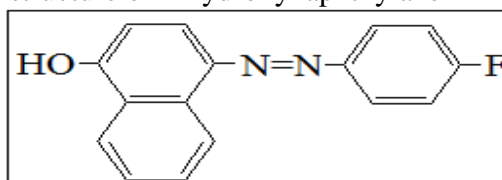
They are synthesized following the procedure reported in 3.2.2.1.a [312].

3.2.2.6.b 4-n-alkoxybenzoylchlorides

They are synthesized following the procedure reported in 3.2.2.1.b [312].

3.2.2.6.c 4-hydroxynaphthylazo-4'-fluorobenzene

General molecular structure of 4-hydroxynaphthylazo-4'-fluorobenzene



Dye is prepared by the reported method [313], in two steps.

(i) Preparation of Diazonium salt of 4-fluororanimine

The diazonium salt is prepared by the procedure described in 3.2.2.1.c

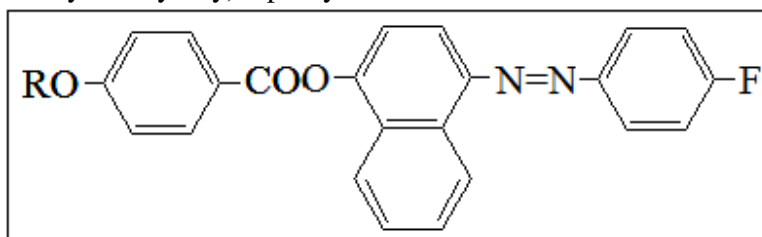
(ii) Coupling of 4-fluorobenzenediazoniumchloride with α -naphthol

The coupling is carried out by the procedure described in 3.2.2.1.d

3.2.2.6.d 4-(4'-n-alkoxybenzoyloxy)naphthylazo-4''-fluorobenzenes

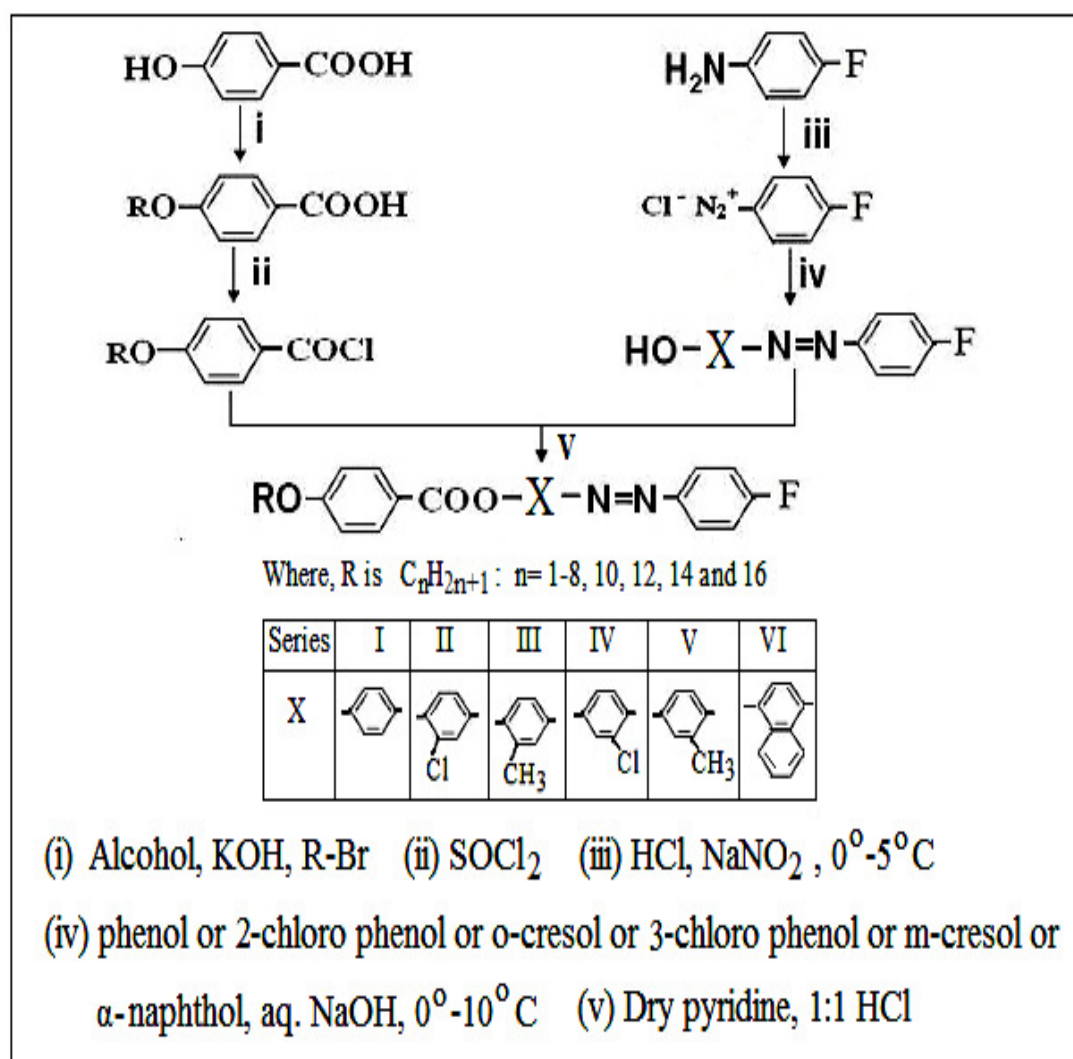
General molecular structure of

4-(4'-n-alkoxybenzoyloxy)naphthylazo-4''-fluorobenzenes



Where, R is C_nH_{2n+1} $n= 1$ to 8, 10, 12, 14 and 16

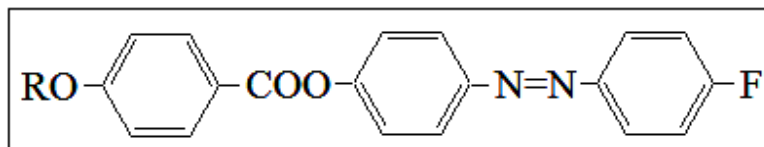
0.005 mol 4-hydroxynaphthylazo-4''-fluorobenzene is dissolved in 10 ml of dry pyridine and is added slowly to a cold solution of respective 4-n-alkoxy benzoylchloride in pyridine. The mixture is refluxed in a water bath for an hour and is allowed to stand overnight at room temperature. It is acidified with 1:1 cold HCl and the separated solid is filtered, washed with water, $NaHCO_3$ and NaOH solutions to remove any unreacted acid and phenol. The precipitates are again washed with water and the final product is recrystallised from ethanol until constant transition temperatures are obtained. They are recorded in table 3.21. The elemental analysis of some of the representative compounds are found to be satisfactory and are recorded in table 3.22. The synthetic route of series I to VI is shown in scheme 3.1.



Scheme 3.1: Synthetic route for series I to VI

3.2.3 Characterization

Elemental analysis of some of the homologues are performed on Perkin Elmer Series II 2400-CHN analyzer, Electronic spectra are recorded on a Shimadzu UV-2450 UV-visible spectrophotometer, IR spectra are recorded on a Perkin Elmer GX-FTIR, 1H NMR spectra are measured on a Bruker Avance II-500 spectrometer. Mass spectra are recorded on Thermoscientific DSQ II mass spectrometer. Transition temperatures and the textures of the mesophases are studied using Leitz Laborlux 12 POL polarizing microscope provided with a Kofler heating stage. DSC are performed on a Mettler Toledo Star SW 7.01.

Table 3.1: Transition temperatures: 4-(4'-n-alkoxybenzoyloxy)phenylazo-4''-fluorobenzenes (Series I)

Homologue	Transition Temperatures °C		
	Smectic C	Nematic	Isotropic
Methyl	—	130	206
Ethyl	—	122	208
Propyl	—	115	205
Butyl	—	110	209
Pentyl	—	100	198
Hexyl	—	91	194
Heptyl	—	83	182
Octyl	85	93	164
Decyl	89	110	142
Dodecyl	93	—	131
Tetradecyl	104	—	126
Hexadecyl	109	—	124

Table 3.2: Elemental analysis

Homologue	Calculated			Found		
	C %	H %	N %	C %	H %	N %
Ethyl	69.23	4.67	7.69	69.20	4.69	7.73
Butyl	70.40	5.35	7.14	70.24	5.29	7.18
Tetradecyl	74.43	7.70	5.26	74.31	7.84	5.34

FTIR (Nujol, KBr pellets, cm⁻¹)

Butyl homologue: 2958, 2937, 1739 (-COO-), 1597, 1496, 1389, 1258, 1199 (-N=N-), 1073 (-CH₂-O-), 969, 761, 692.

Dodecyl homologue: 2955, 2924, 1737 (-COO-), 1606, 1496, 1359, 1259, 1170 (-N=N-), 1064 (-CH₂-O-), 962, 758, 690.

¹H NMR: (CDCl₃, 500 MHz, δ , ppm, standard TMS)

Butyl homologue: δ 1.0 (3H, t, -CH₃), 1.48-1.84 (m, alkyl chain), 4.05 (2H, t, -OCH₂-CH₂), 6.98 (2H, d, H⁵), 7.02 (2H, d, H⁴), 7.36 (2H, d, H²), 7.9 (2H, d, H⁶), 8.0 (2H, d, H¹), 8.1 (2H, d, H³)

Hexyl homologue: δ 0.93 (3H, t, -CH₃), 1.40-1.85 (m, alkyl chain), 4.04 (2H, t, -OCH₂-CH₂), 6.99 (2H, d, H⁵), 7.18 (2H, d, H⁴), 7.36 (2H, d, H²), 7.93 (2H, d, H⁶), 7.99 (2H, d, H¹), 8.1 (2H, d, H³)

Mass Spectra:

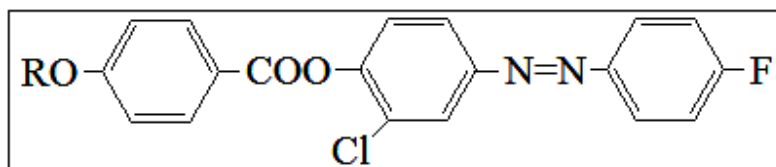
Butyl homologue: MS m/z: 393.75 (M+1)

Table 3.3: DSC data

Series	Homologue	Transition Temperature °C	$\Delta H/Jg^{-1}$	$\Delta S/Jg^{-1}K^{-1}$
I	Butyl	Cr-N 113	61.49	0.160
		N-I 211	2.73	0.0066
	Decyl	Cr-S 88	60.62	0.1673
		S-N 110	3.52	0.0092
		N-I 141	0.91	0.0021

Table 3.4: UV data

Series	Homologue	UV λ max values nm (solvent- ethyl acetate)	
		$\pi \longrightarrow \pi^*$	$n \longrightarrow \pi^*$
I	Pentyl	327	492
	Octyl	327	492

Table 3.5: Transition temperatures: 4-(4'-n-alkoxybenzoyloxy)3-chlorophenylazo-4''-fluorobenzenes (Series II)

Homologue	Transition Temperatures $^{\circ}\text{C}$		
	Smectic C	Nematic	Isotropic
Methyl	—	121	159
Ethyl	—	113	167
Propyl	—	105	163
Butyl	—	95	156
Pentyl	—	89	150
Hexyl	—	85	146
Heptyl	—	80	139
Octyl	—	77	126
Decyl	—	75	119
Dodecyl	83	93	113
Tetradecyl	92	—	110
Hexadecyl	96	—	108

Table 3.6: Elemental analysis

Homologue	Calculated			Found		
	C %	H %	N %	C %	H %	N %
Propyl	64.00	4.36	6.78	64.13	4.27	6.64
Octyl	67.15	5.80	5.80	67.02	5.66	5.72
Hexadecyl	70.64	7.40	4.70	70.58	7.31	4.67

FTIR (Nujol, KBr pellets, cm^{-1})

Pentyl homologue: 2955, 2928, 1739 (-COO-), 1600, 1469, 1357, 1253, 1161 (-N=N-), 1082 (-CH₂-O-), 939, 758, 692.

Octyl homologue: 2944, 2919, 1731 (-COO-), 1606, 1476, 1399, 1264, 1163 (-N=N-), 1066 (-CH₂-O-), 953, 755, 689.

¹H NMR: (CDCl₃, 500 MHz, δ , ppm, standard TMS)

Ethyl homologue: δ 0.98 (3H, t, -CH₃), 1.48-1.83 (m, alkyl chain), 4.09 (2H, t, -OCH₂-CH₂), 6.91 (2H, d, H³), 7.21 (2H, d, H⁵), 7.48 (2H, d, H⁴), 7.78 (2H, d, H²), 7.98 (2H, d, H⁶), 8.0 (2H, d, H¹)

Octyl homologue: δ 0.9 (3H, t, -CH₃), 1.3-1.85 (m, alkyl chain), 4.04 (2H, t, -OCH₂-CH₂), 6.98 (1H, s, H³), 7.0 (2H, d, H⁵), 7.24 (2H, d, H⁴), 7.9 (2H, d, H²), 8.0 (2H, d, H⁶), 8.1 (2H, d, H¹)

Mass Spectra:

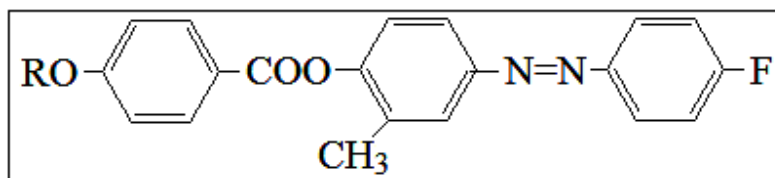
Propyl homologue: MS m/z: 412 (M⁺)

Table 3.7: DSC data

Series	Homologue	Transition Temperature °C	$\Delta H/\text{Jg}^{-1}$	$\Delta S/\text{Jg}^{-1}\text{K}^{-1}$
II	Octyl	Cr-N 78	83.00	0.237
		N-I 125	1.65	0.0041
	Dodecyl	Cr-S 81	63.54	0.1784
		S-N 90	4.20	0.0115
		N-I 112	1.13	0.0029

Table 3.8: UV data

Series	Homologue	UV λ max values nm (solvent- ethyl acetate)	
		$\pi \longrightarrow \pi^*$	$n \longrightarrow \pi^*$
II	Heptyl	327	487
	Decyl	327	487

Table 3.9: Transition temperatures: 4-(4'-n-alkoxybenzoyloxy)3-methylphenylazo-4''-fluorobenzenes (Series III)

Homologue	Transition Temperatures °C		
	Smectic C	Nematic	Isotropic
Methyl	—	113	148
Ethyl	—	109	139
Propyl	—	100	133
Butyl	—	90	128
Pentyl	—	84	125
Hexyl	—	78	116
Heptyl	—	73	109
Octyl	—	69	103
Decyl	—	72	98
Dodecyl	—	78	96
Tetradecyl	81	85	93
Hexadecyl	86	—	91

Table 3.10: Elemental analysis

Homologue	Calculated			Found		
	C %	H %	N %	C %	H %	N %
Pentyl	71.42	5.95	6.66	71.49	5.90	6.51
Hexyl	71.88	6.22	6.45	71.60	5.46	6.31
Octyl	72.72	6.70	6.06	72.63	6.82	6.17

FTIR (Nujol, KBr pellets, cm^{-1})

Hexyl homologue: 2946, 1729 (-COO-), 1603, 1498, 1317, 1260, 1165 (-N=N-), 1065 (-CH₂-O-), 842, 724, 689.

Tetradecyl homologue: 2955, 2916, 1737(-COO-), 1606, 1500, 1307, 1259, 1170 (-N=N-), 1064 (-CH₂-O-), 956, 846, 719, 650.

¹H NMR: (CDCl₃, 500 MHz, δ , ppm, standard TMS)

Butyl homologue: δ 1.0 (3H, t, -CH₃), 1.5-1.8 (m, alkyl chain), 2.46 (3H, s, Ar-CH₃), 4.0 (2H, t, -OCH₂-CH₂), 6.98-8.24 (m, Ar-H)

Hexyl homologue: δ 0.93 (3H, t, -CH₃), 1.3-1.8 (m, alkyl chain), 2.33 (3H, s, Ar-CH₃), 4.0 (2H, t, -OCH₂-CH₂), 6.99 (1H, s, H³), 7.1 (2H, d, H⁵), 7.30 (2H, d, H⁴), 7.93 (2H, d, H²), 7.99 (2H, d, H⁶), 8.1 (2H, d, H¹)

Mass Spectra:

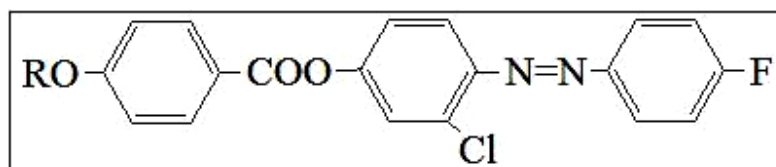
Hexyl homologue: MS m/z: 469 (M⁺)

Table 3.11: DSC data

Series	Homologue	Transition Temperature °C	$\Delta H/\text{Jg}^{-1}$	$\Delta S/\text{Jg}^{-1}\text{K}^{-1}$
III	Hexyl	Cr-N 78	72.77	0.207
		N-I 116	0.92	0.0023
	Decyl	Cr-N 70	66.44	0.1924
		N-I 97	0.9744	0.0026

Table 3.12: UV data

Series	Homologue	UV λ max values nm (solvent- ethyl acetate)	
		$\pi \longrightarrow \pi^*$	$n \longrightarrow \pi^*$
III	Dodecyl	327	462
	Tetradecyl	327	462

Table 3.13: Transition temperatures: 4-(4'-n-alkoxybenzoyloxy)2-chlorophenylazo-4''-fluorobenzenes (Series IV)

Homologue	Transition Temperatures °C		
	Smectic C	Nematic	Isotropic
Methyl	—	114	182
Ethyl	—	104	170
Propyl	—	102	163
Butyl	—	90	158
Pentyl	—	78	160
Hexyl	—	71	157
Heptyl	—	65	149
Octyl	—	62	144
Decyl	—	85	138
Dodecyl	—	79	129
Tetradecyl	70	86	114
Hexadecyl	68	92	111

Table 3.14: Elemental analysis

Homologue	Calculated			Found		
	C %	H %	N %	C %	H %	N %
Pentyl	65.38	4.99	6.35	65.42	4.95	6.43
Heptyl	66.59	5.54	5.97	66.51	5.48	5.81
Decyl	68.16	6.26	5.48	68.20	6.90	5.26

FTIR (Nujol, KBr pellets, cm^{-1})

Pentyl homologue: 2949, 2928, 1739 (-COO-), 1606, 1259, 1170 (-N=N-), 1082 (-CH₂-O-), 879, 754, 692.

Decyl homologue: 2921, 1735 (-COO-), 1596, 1271, 1176 (-N=N-), 1066 (-CH₂-O-), 936, 888, 756, 693.

¹H NMR: (CDCl₃, 500 MHz, δ , ppm, standard TMS)

Pentyl homologue: δ 0.98 (3H, t, -CH₃), 1.45-1.82 (m, alkyl chain), 4.05 (2H, t, -OCH₂-CH₂), 6.95 (1H, s, H⁴), 7.0 (2H, d, H⁵), 7.38 (2H, d, H²), 7.94 (2H, d, H¹), 7.95 (2H, d, H⁶), 8.15 (2H, d, H³)

Decyl homologue: δ 0.9 (3H, t, -CH₃), 1.4-1.85 (m, alkyl chain), 4.03 (2H, t, -OCH₂-CH₂), 6.98 (1H, s, H⁴), 7.2 (2H, d, H⁵), 7.48 (2H, d, H²), 7.9 (2H, d, H¹), 8.0 (2H, d, H⁶), 8.1 (2H, d, H³)

Mass Spectra:

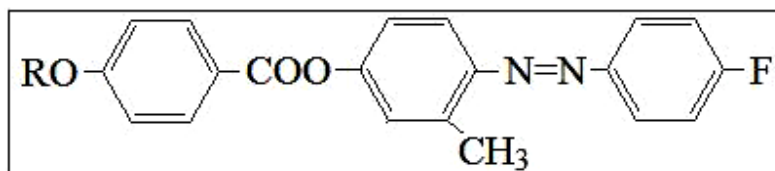
Decyl homologue: MS m/z: 510 (M⁺)

Table 3.15: DSC data

Series	Homologue	Transition Temperature °C	$\Delta H/\text{Jg}^{-1}$	$\Delta S/\text{Jg}^{-1}\text{K}^{-1}$
IV	Decyl	Cr-N 87	48.00	0.1330
		N-I 136	1.038	0.0025
	Tetradecyl	Cr-S 71	80.85	0.2343
		S-N 85	2.26	0.0063
		N-I 114	0.483	0.0012

Table 3.16: UV data

Series	Homologue	UV λ max values nm (solvent- ethyl acetate)	
		$\pi \longrightarrow \pi^*$	$n \longrightarrow \pi^*$
IV	Ethyl	326	430
	Propyl	326	430

Table 3.17: Transition temperatures: 4-(4'-n-alkoxybenzoyloxy)2-methylphenylazo-4'-fluorobenzenes (Series V)

Homologue	Transition Temperatures $^{\circ}\text{C}$		
	Smectic C	Nematic	Isotropic
Methyl	—	120	165
Ethyl	—	122	158
Propyl	—	110	138
Butyl	—	92	140
Pentyl	—	84	135
Hexyl	—	78	131
Heptyl	—	63	129
Octyl	—	67	128
Decyl	—	61	122
Dodecyl	—	72	117
Tetradecyl	—	76	112
Hexadecyl	—	68	98

Table 3.18: Elemental analysis

Homologue	Calculated			Found		
	C %	H %	N %	C %	H %	N %
Butyl	70.93	5.66	6.89	70.81	5.57	6.92
Heptyl	72.32	6.47	6.25	72.19	6.50	6.20
Hexadecyl	75.26	8.18	4.87	75.21	8.10	4.96

FTIR (Nujol, KBr pellets, cm⁻¹)

Butyl homologue: 2961, 2934, 1730 (-COO-), 1601, 1392, 1165 (-N=N-), 1098 (-CH₂-O-), 842, 759, 691.

Heptyl homologue: 2955, 2928, 1739 (-COO-), 1600, 1394, 1161 (-N=N-), 1082 (-CH₂-O-), 848, 758, 692.

¹H NMR: (CDCl₃, 500 MHz, δ , ppm, standard TMS)

Butyl homologue: δ 0.9 (3H, t, -CH₃), 1.5-1.8 (m, alkyl chain), 2.33 (3H, s, Ar-CH₃), 4.0 (2H, t, OCH₂-CH₂), 6.98 (1H, s, H⁴), 7.0 (2H, d, H⁵), 7.30 (2H, d, H²), 7.9 (2H, d, H⁶), 8.1 (2H, d, H¹), 8.2 (2H, d, H³)

Heptyl homologue: δ 0.9 (3H, t, -CH₃), 1.4-1.85 (m, alkyl chain), 2.30 (3H, s, Ar-CH₃), 4.0 (2H, t, -OCH₂-CH₂), 6.98 (1H, s, H⁴), 7.1 (2H, d, H⁵), 7.26 (2H, d, H²), 7.93 (2H, d, H¹), 7.95 (2H, d, H⁶), 8.1 (2H, d, H³)

Mass Spectra:

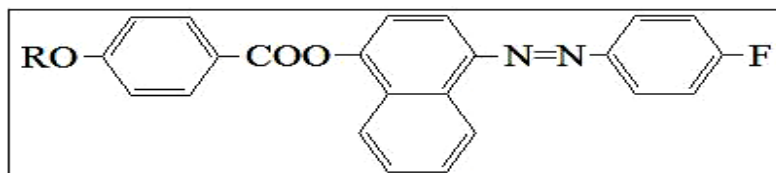
Butyl homologue: MS m/z: 406 (M⁺)

Table 3.19: DSC data

Series	Homologue	Transition Temperature °C	$\Delta H/Jg^{-1}$	$\Delta S/Jg^{-1}K^{-1}$
V	Butyl	Cr-N 91	41.29	0.1133
		N-I 137	0.62	0.0015
	Dodecyl	Cr-N 71	80.08	0.2323
		N-I 118	0.79	0.0020

Table 3.20: UV data

Series	Homologue	UV λ max values nm (solvent- ethyl acetate)	
		$\pi \longrightarrow \pi^*$	$n \longrightarrow \pi^*$
V	Ethyl	326	431
	Pentyl	326	431

Table 3.21: Transition temperatures: 4-(4'-n-alkoxybenzoyloxy)naphthylazo-4''-fluorobenzenes (Series VI)

Homologue	Transition Temperatures °C	
	Nematic	Isotropic
Methyl	148	181
Ethyl	139	175
Propyl	125	170
Butyl	120	161
Pentyl	103	145
Hexyl	90	130
Heptyl	82	126
Octyl	71	120
Decyl	90	108
Dodecyl	(50)	90
Tetradecyl	(58)	87
Hexadecyl	(68)	86

Values in parentheses indicates monotropic transitions

Table 3.22 : Elemental analysis

Homologue	Calculated			Found		
	C %	H %	N %	C %	H %	N %
Butyl	76.59	5.43	6.61	76.51	5.57	6.64
Heptyl	77.41	6.23	6.02	77.46	6.21	6.08
Hexadecyl	79.18	7.95	4.73	79.00	7.90	4.71

FTIR (Nujol, KBr pellets, cm⁻¹)

Propyl homologue: 2914, 1739 (-COO-), 1608, 1473, 1390, 1253, 1158 (-N=N-), 1073 (-CH₂-O-), 758, 688.

Hexadecyl homologue: 2919, 1734 (-COO-), 1646, 1468, 1390, 1253, 1158 (-N=N-), 1086 (-CH₂-O-), 758, 691.

¹H NMR: (CDCl₃, 500 MHz, δ , ppm, standard TMS)

Octyl homologue: δ 0.88 (3H, t, -CH₃), 1.4-1.8 (m, alkyl chain), 4.0 (2H, t, -OCH₂-CH₂), 6.91 – 8.04 (m, Ar-H)

Hexadecyl homologue: δ 0.86 (3H, t, -CH₃), 1.4-1.85 (m, alkyl chain), 4.0 (2H, t, -OCH₂-CH₂), 7.03 – 8.04 (m, Ar-H)

Mass Spectra:

Dodecyl homologue: MS m/z: 554 (M⁺)

Table 3.23: DSC data

Series	Homologue	Transition Temperature °C	$\Delta H/Jg^{-1}$	$\Delta S/Jg^{-1}K^{-1}$
VI	Pentyl	Cr-N 104	70.83	0.1866
		N-I 144	0.8922	0.0021
	Dodecyl	Cr-I 49	0.89	0.0024
		I-N 90	61.40	0.1892

Table 3.24 UV data

Series	Homologue	UV λ max values nm (solvent- ethyl acetate)	
		$\pi \longrightarrow \pi^*$	$n \longrightarrow \pi^*$
VI	Ethyl	326	433
	Hexyl	326	433

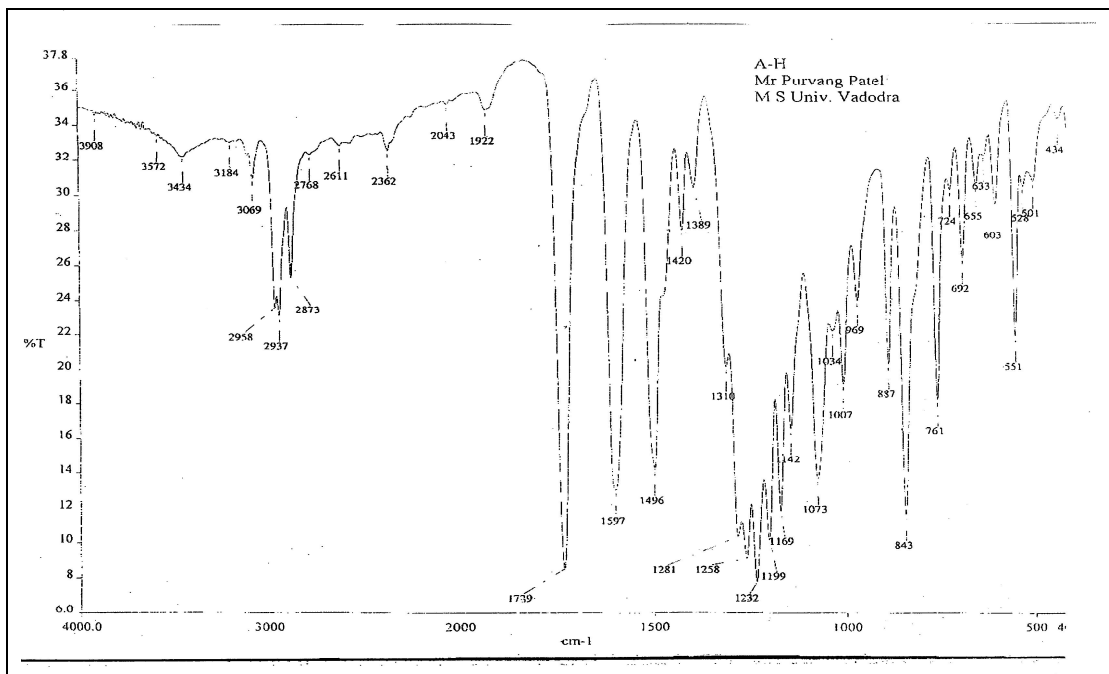


Figure 3.1 (a): IR spectra of C4 homologue of series I

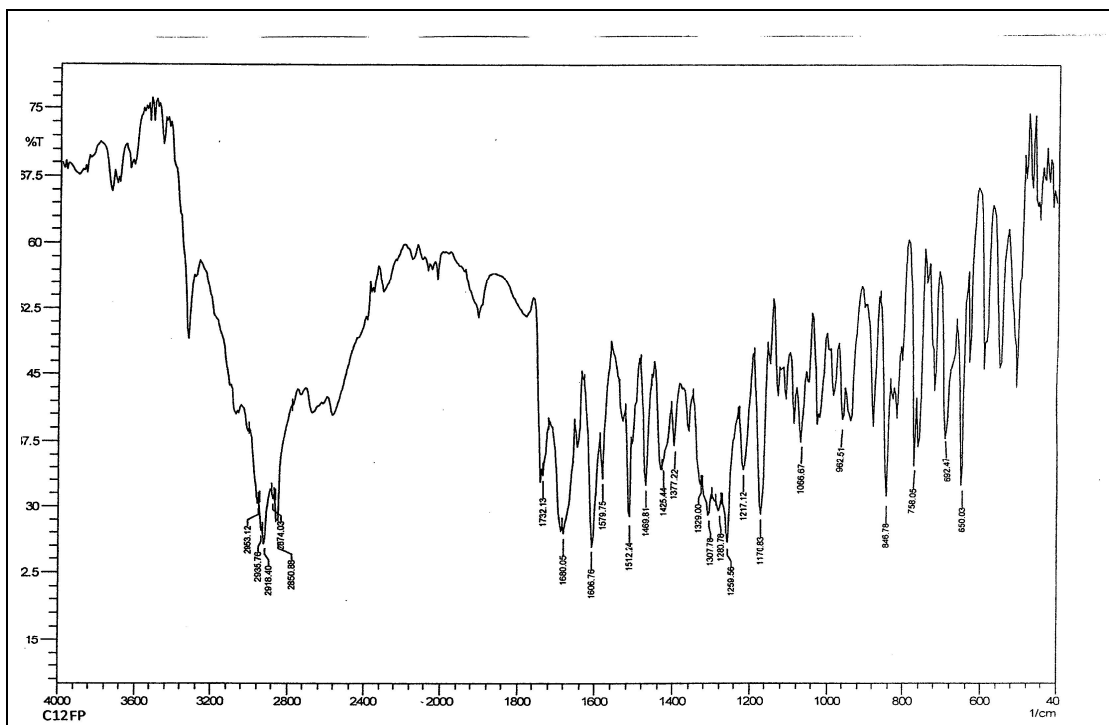


Figure 3.1 (b): IR spectra of C12 homologue of series I

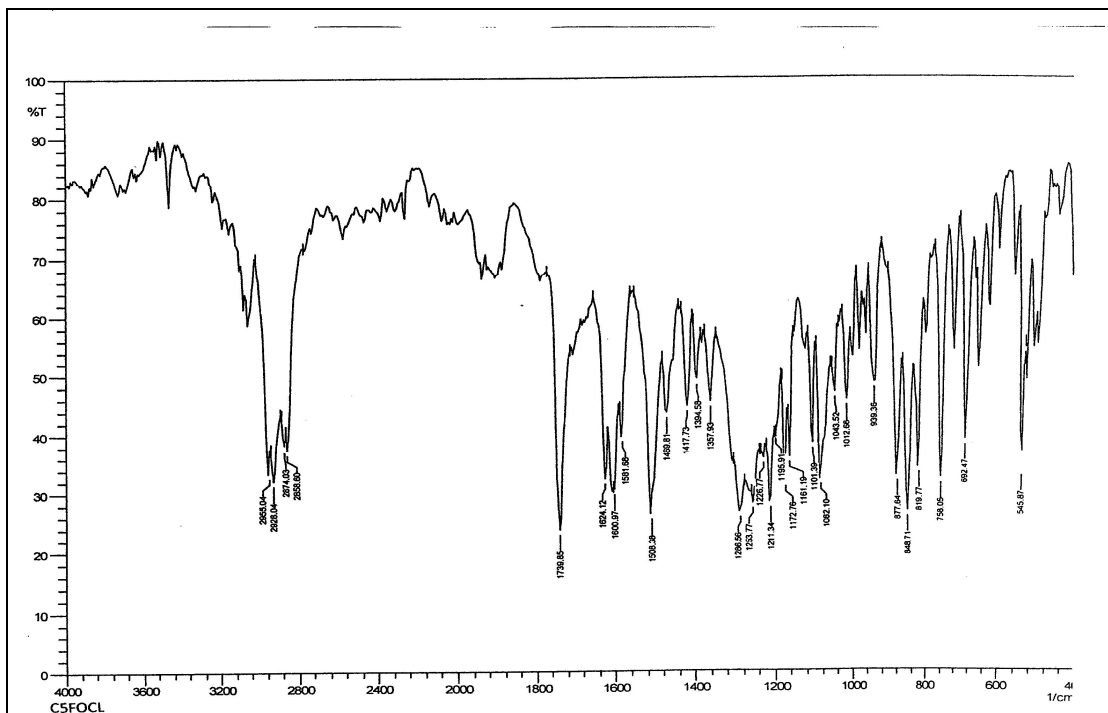


Figure 3.1 (c): IR spectra of C5 homologue of series II

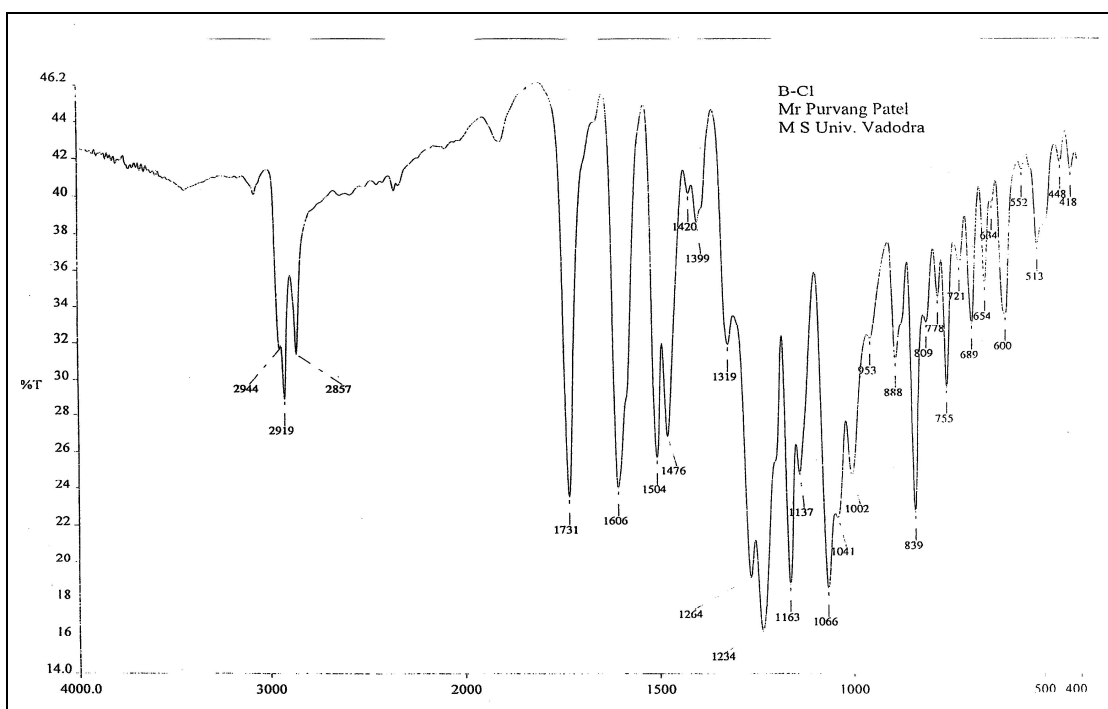


Figure 3.1 (d): IR spectra of C8 homologue of series II

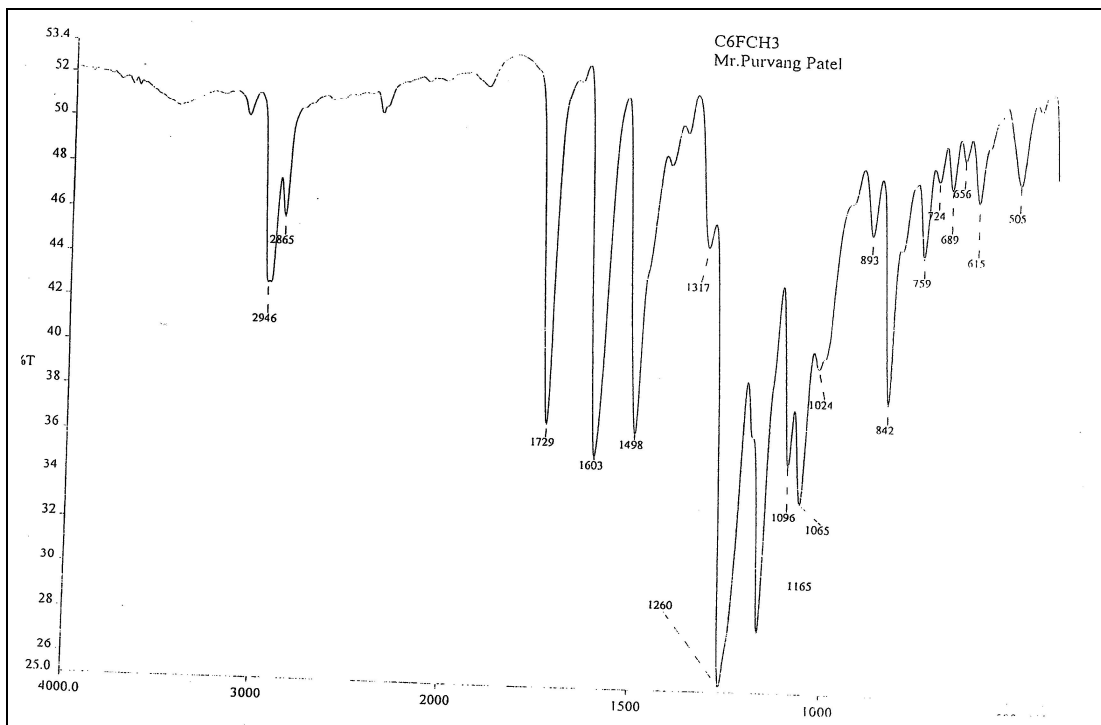


Figure 3.1 (e): IR spectra of C6 homologue of series III

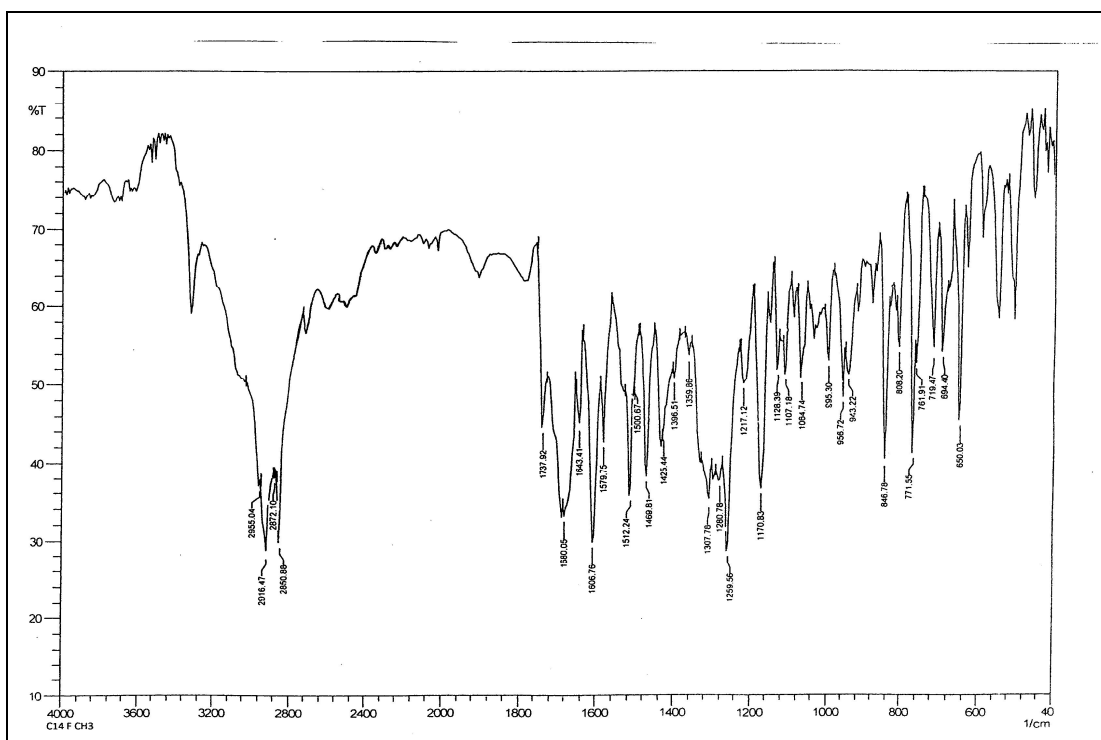


Figure 3.1 (f): IR spectra of C14 homologue of series III

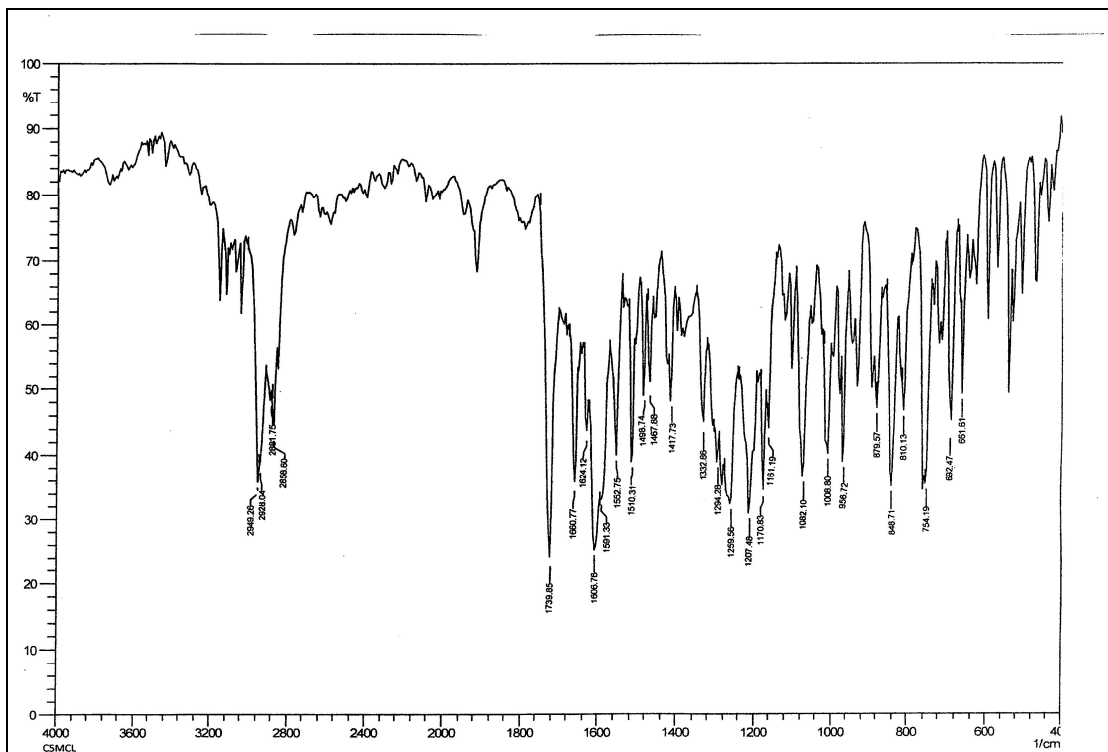


Figure 3.1 (g): IR spectra of C5 homologue of series IV

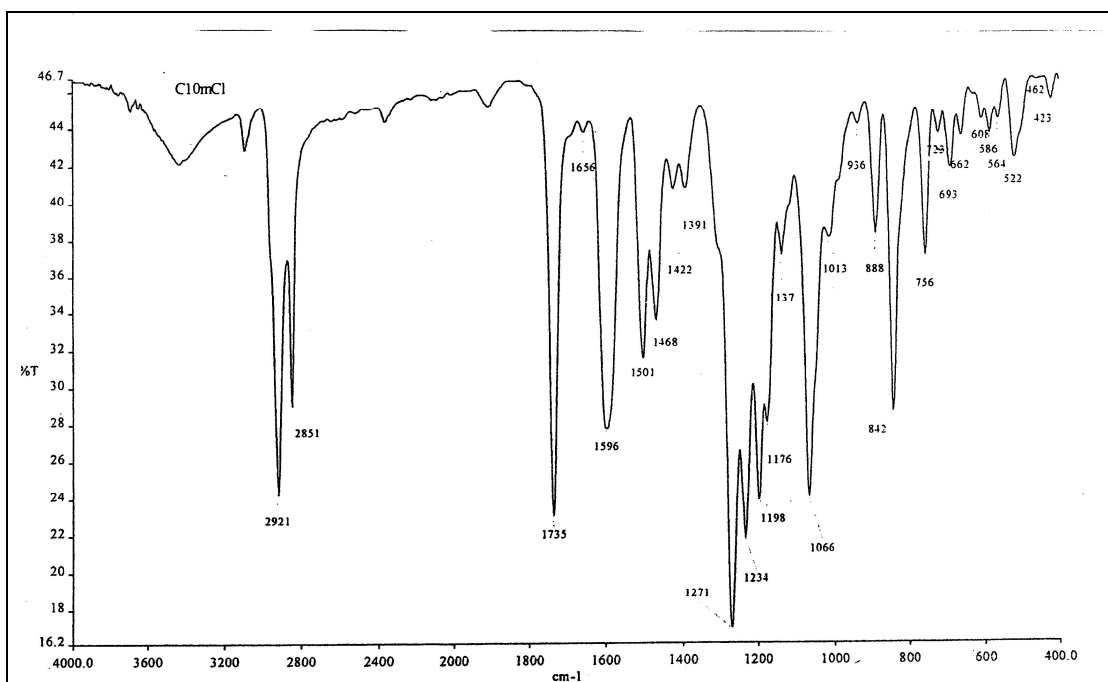


Figure 3.1 (h): IR spectra of C10 homologue of series IV

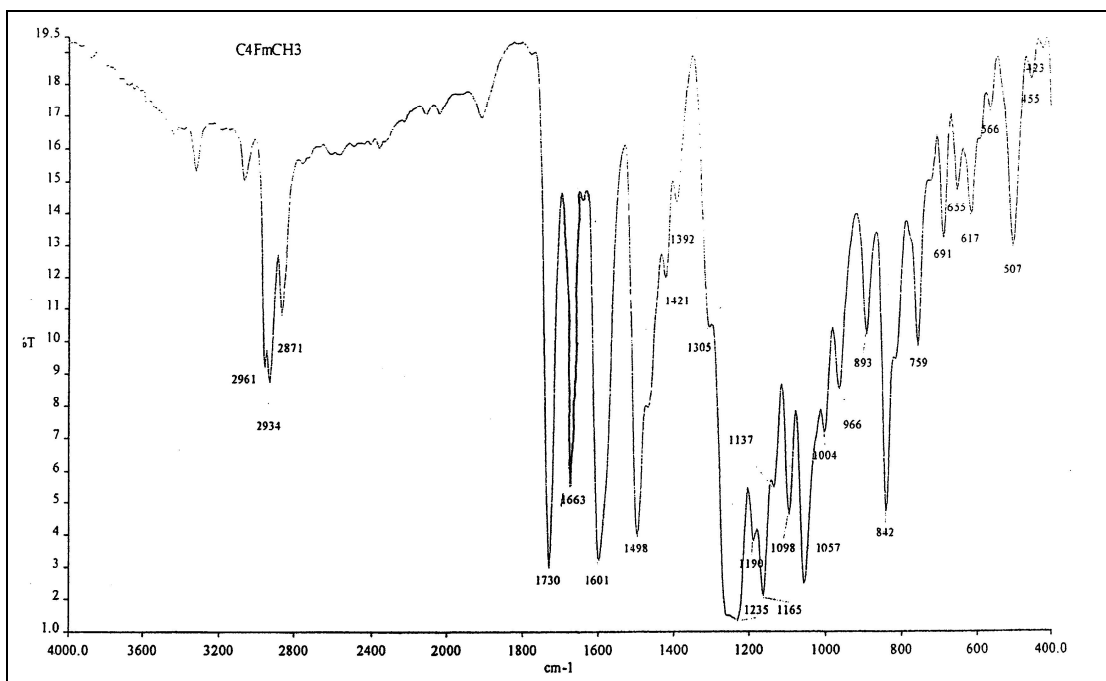


Figure 3.1 (i): IR spectra of C4 homologue of series V

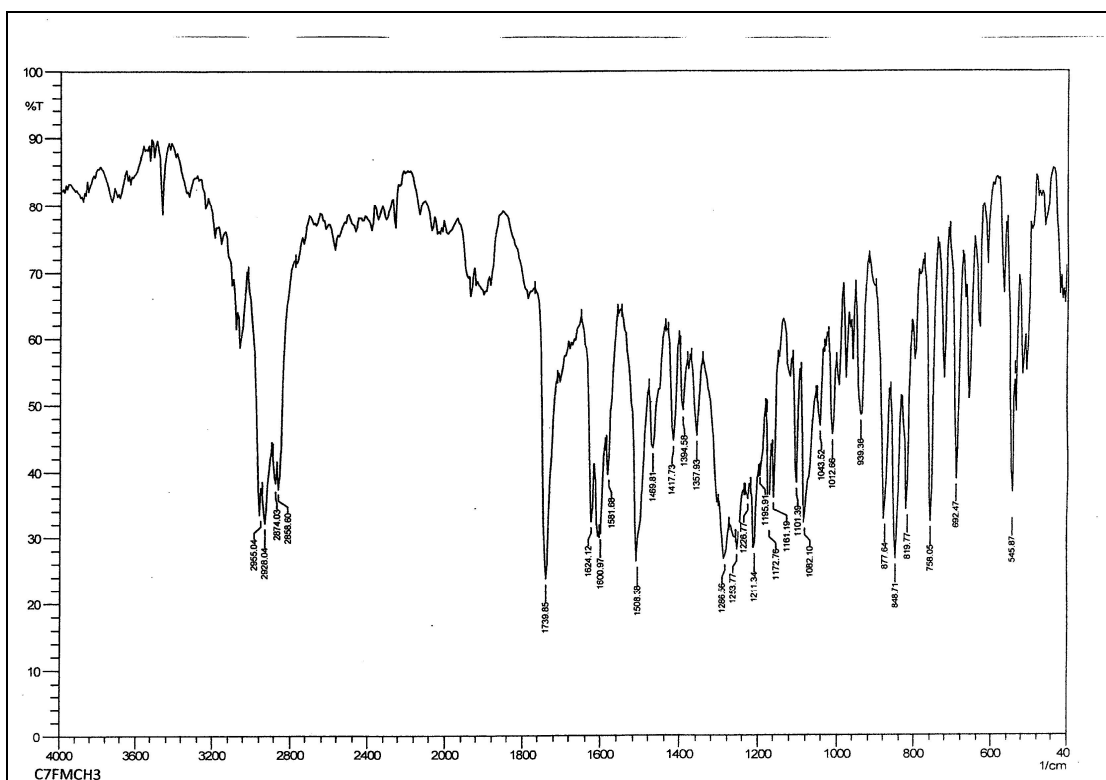


Figure 3.1 (j): IR spectra of C7 homologue of series V

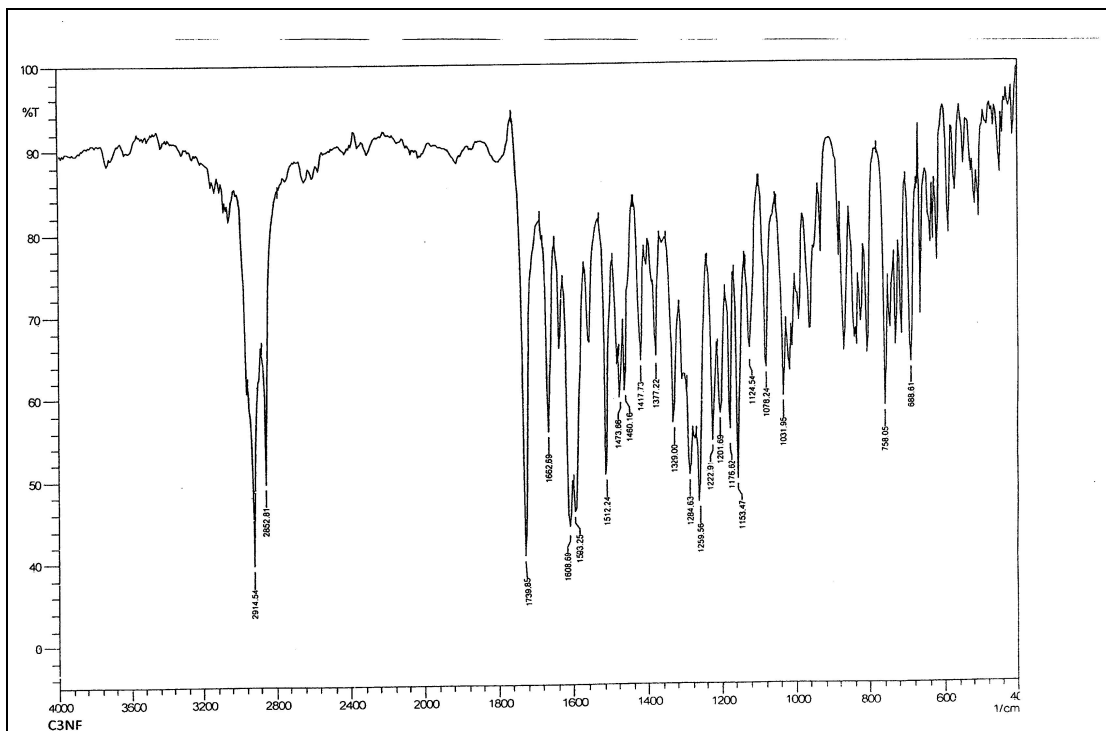


Figure 3.1 (k): IR spectra of C3 homologue of series VI

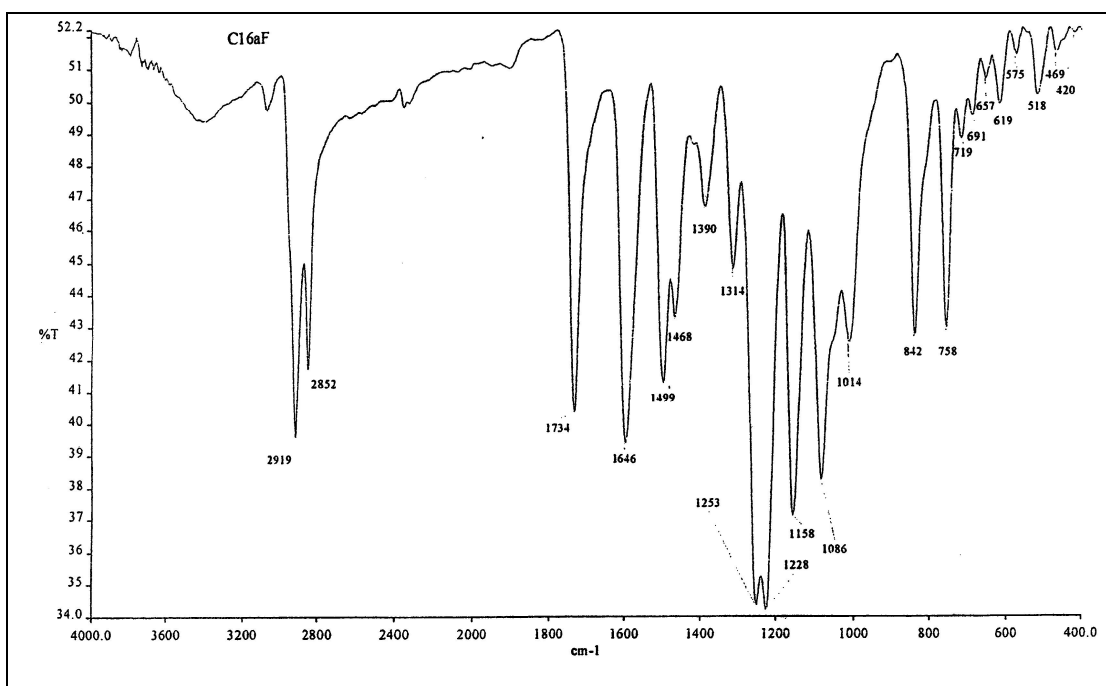
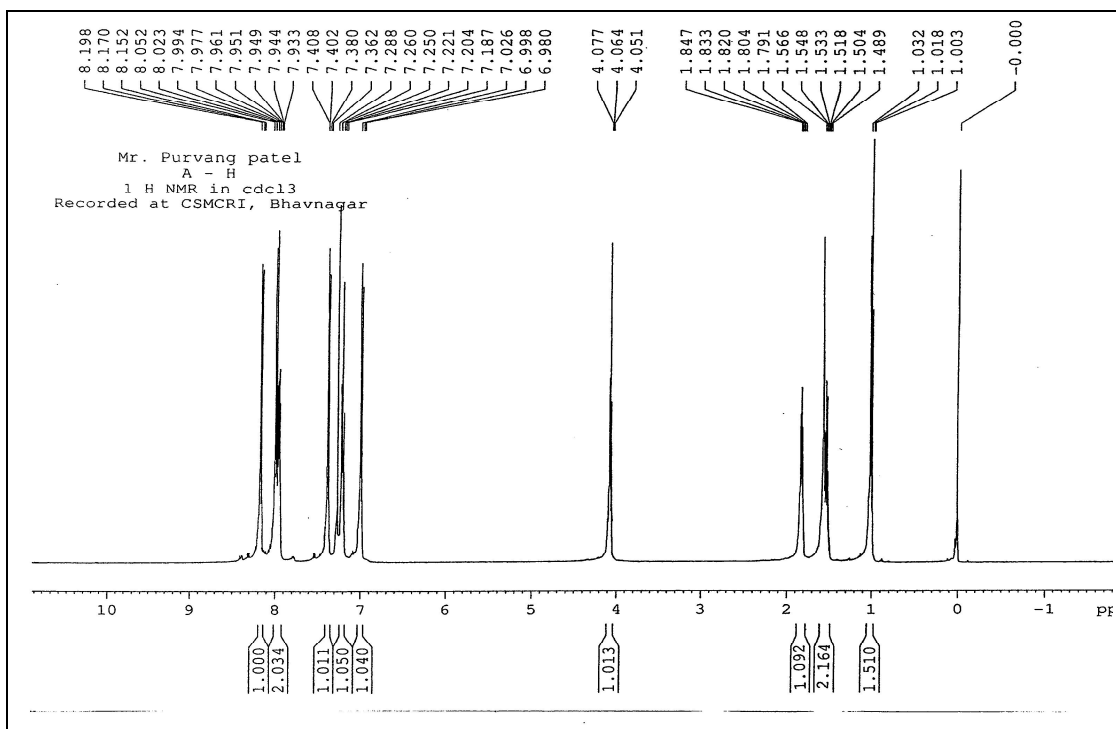
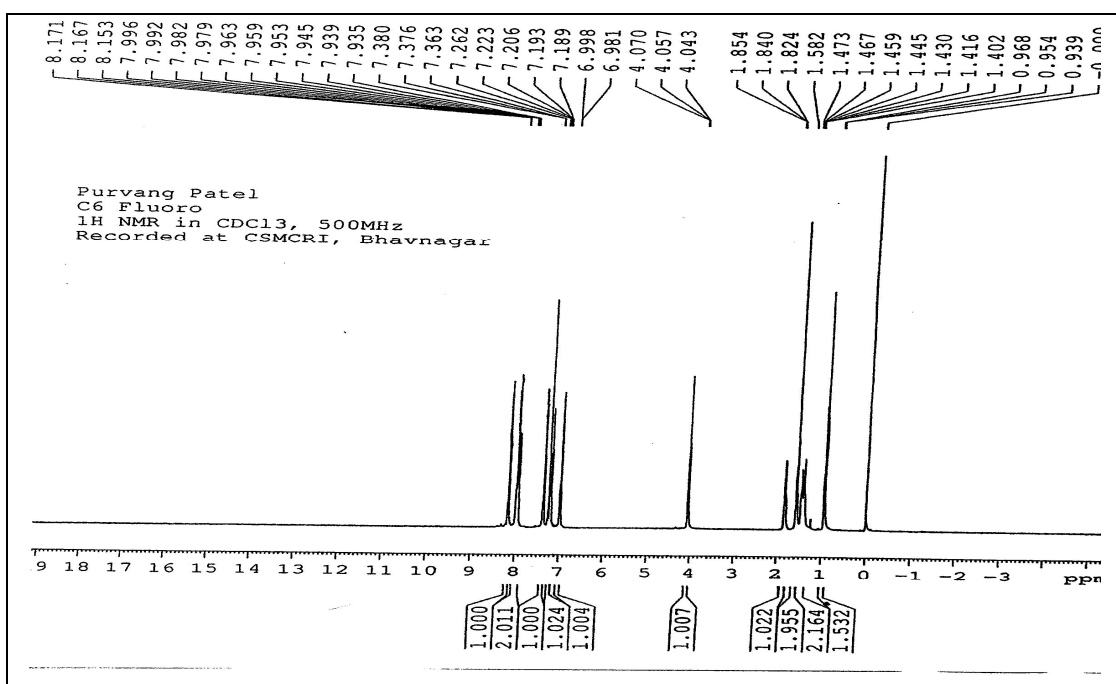
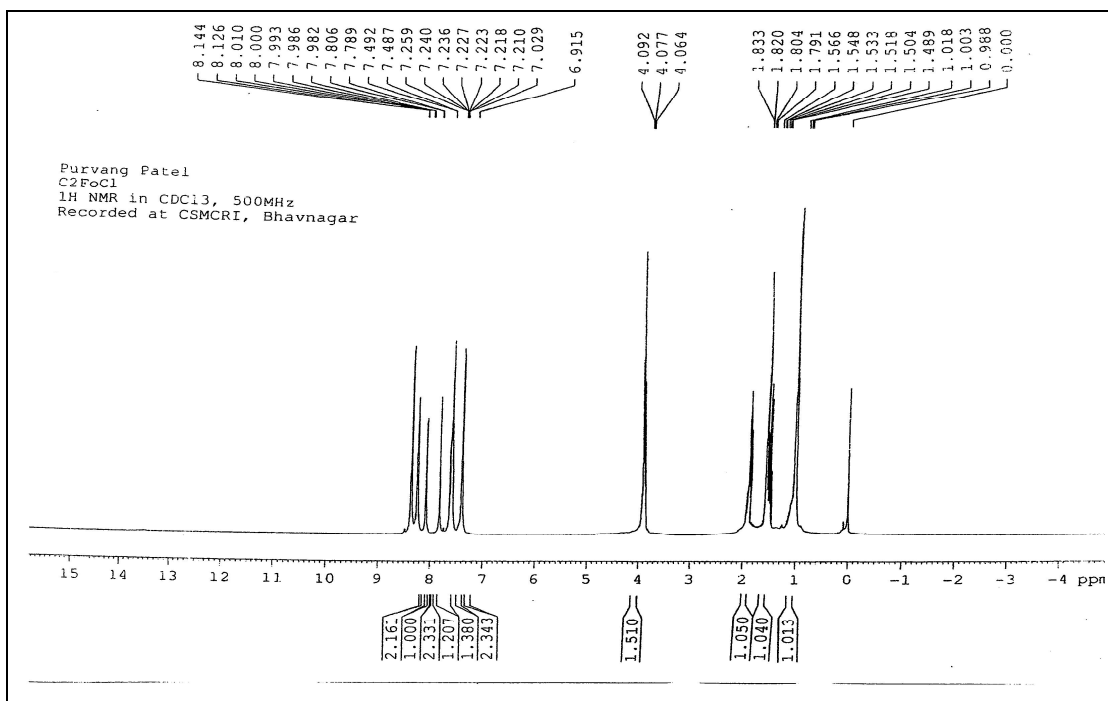
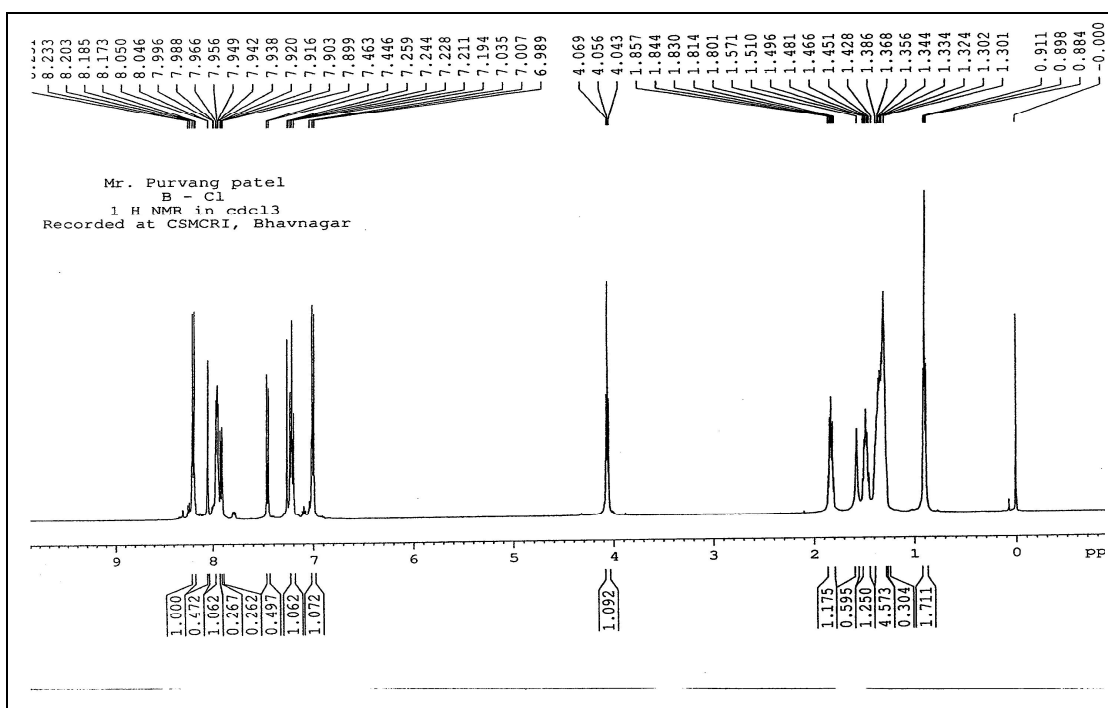
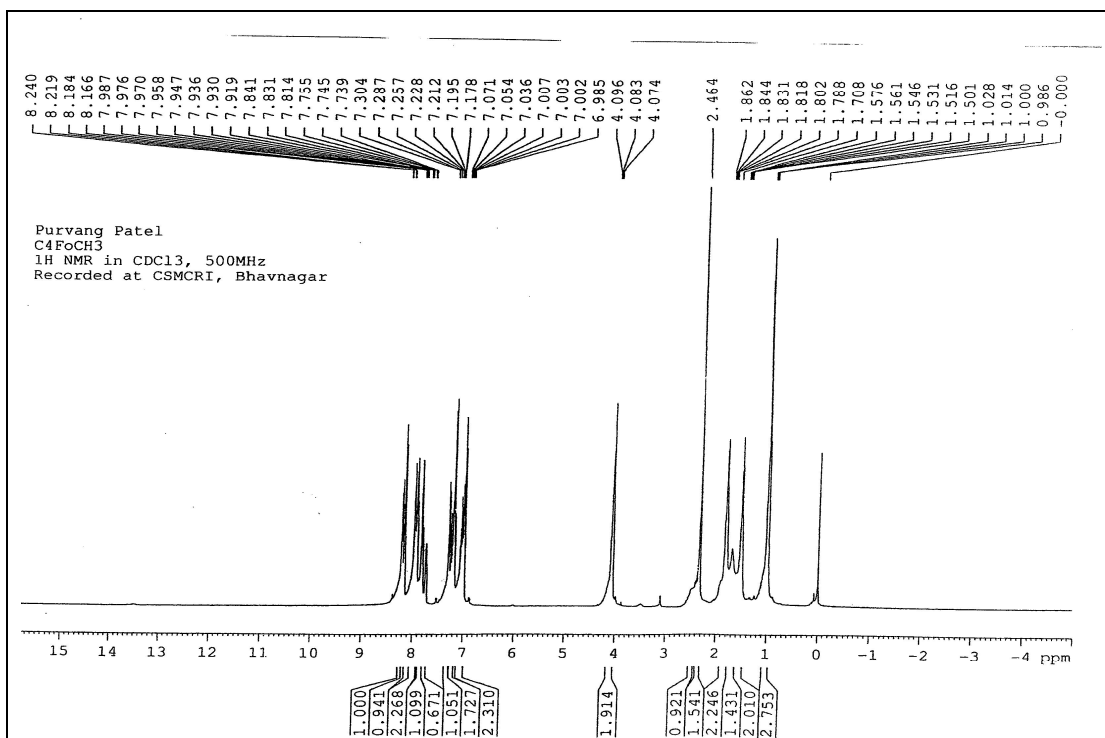
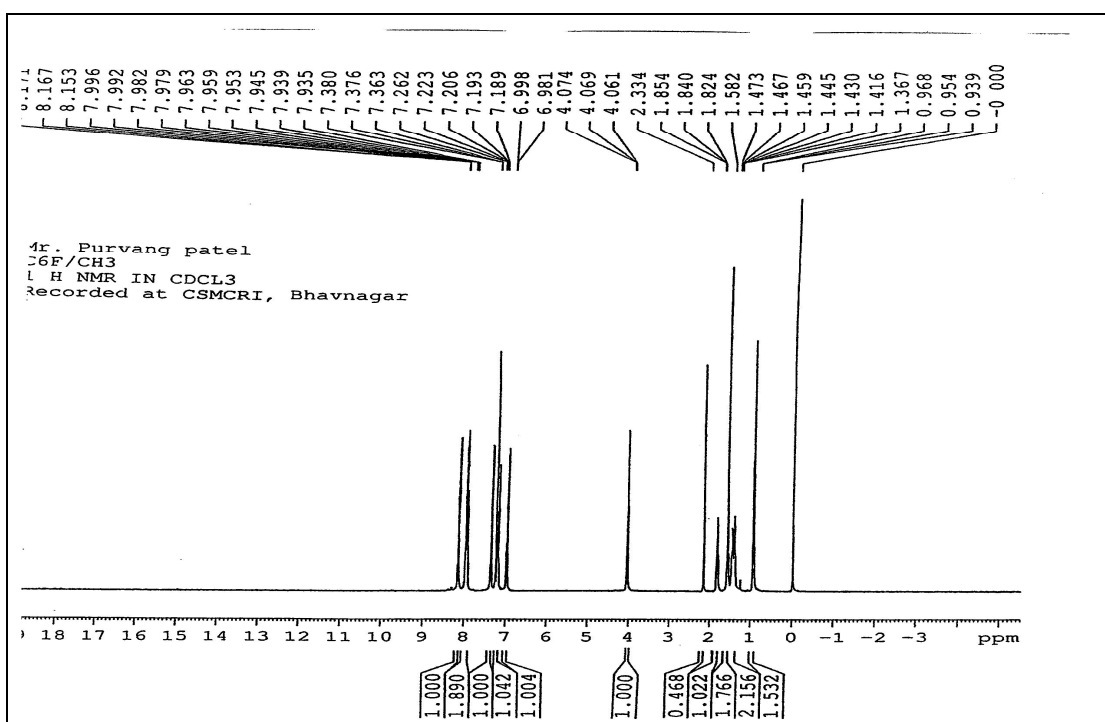
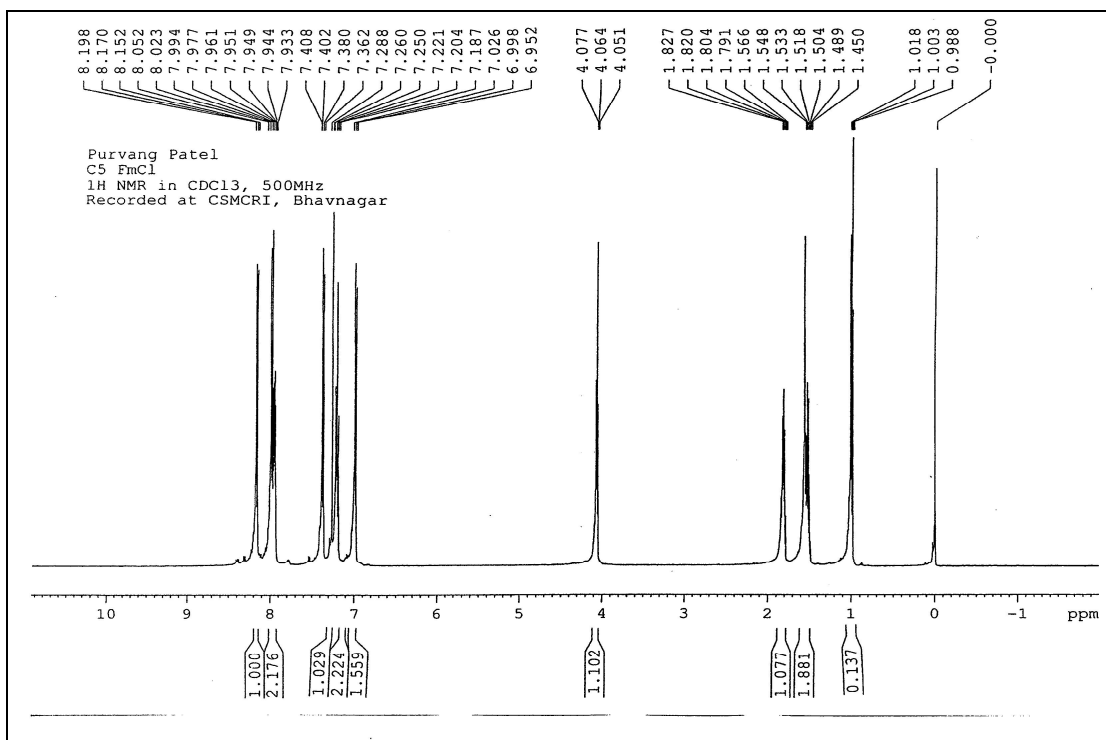
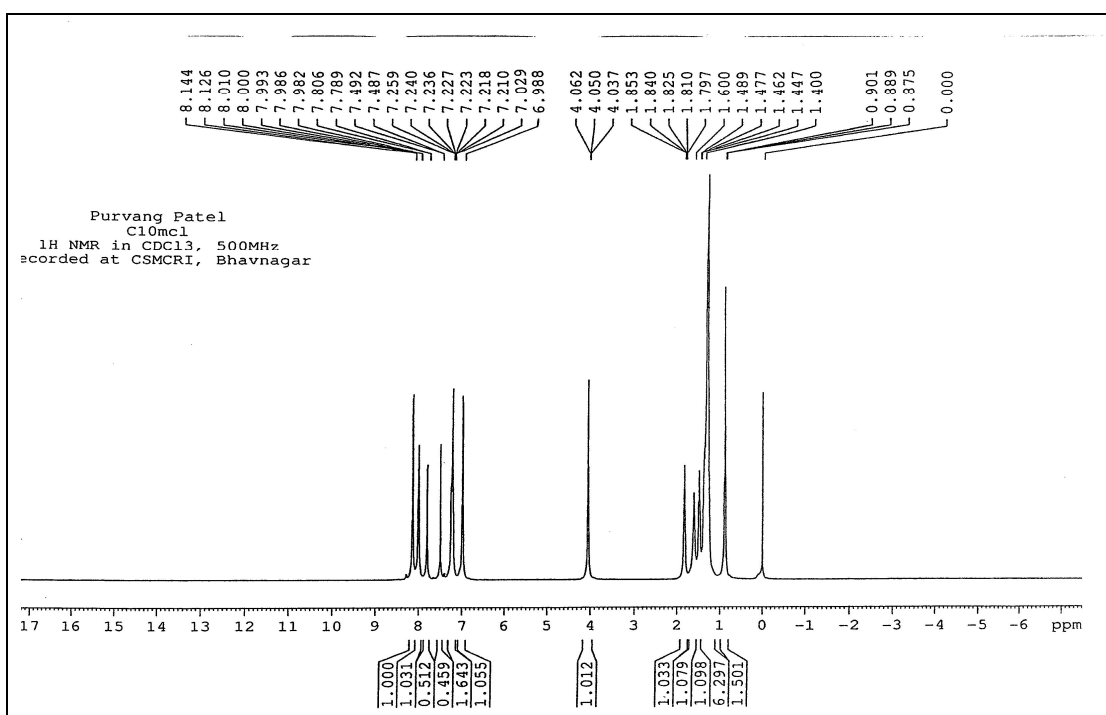


Figure 3.1 (l): IR spectra of C16 homologue of series VI

Figure 3.2 (a): ^1H NMR spectra of C4 homologue of series IFigure 3.2 (b): ^1H NMR spectra of C6 homologue of series I

Figure 3.2 (c): ^1H NMR spectra of C2 homologue of series IIFigure 3.2 (d): ^1H NMR spectra of C8 homologue of series II

Figure 3.2 (e): ^1H NMR spectra of C4 homologue of series IIIFigure 3.2 (f): ^1H NMR spectra of C6 homologue of series III

Figure 3.2 (g): ¹H NMR spectra of C5 homologue of series IVFigure 3.2 (h): ¹H NMR spectra of C10 homologue of series IV

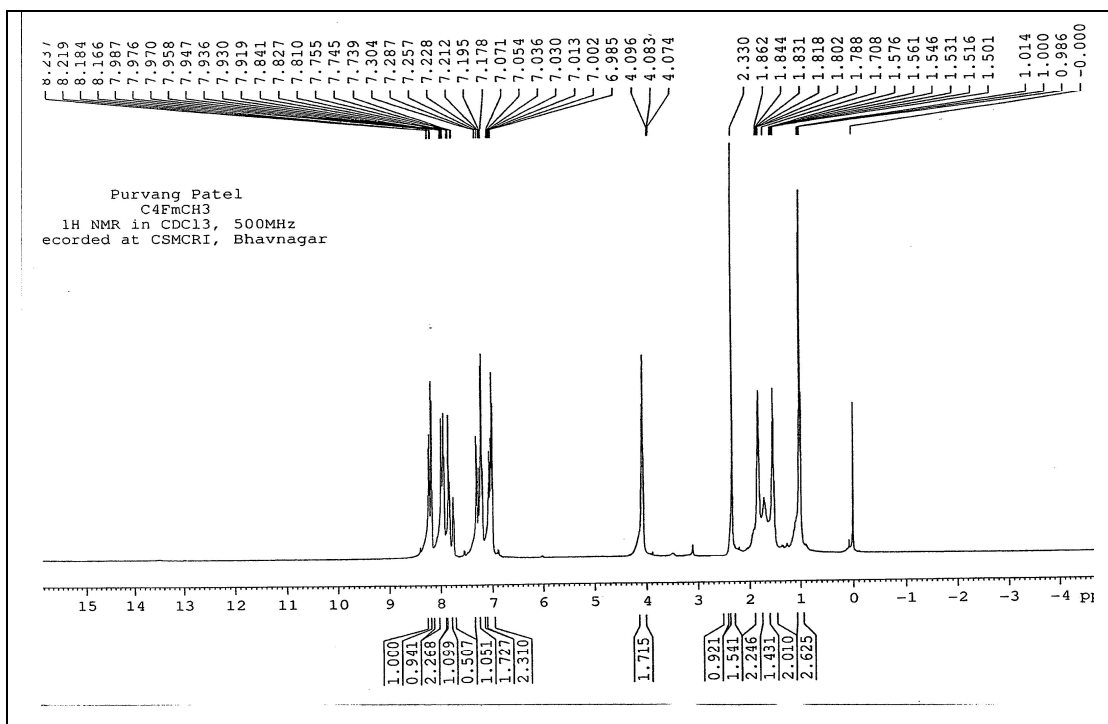


Figure 3.2 (i): ¹H NMR spectra of C4 homologue of series V

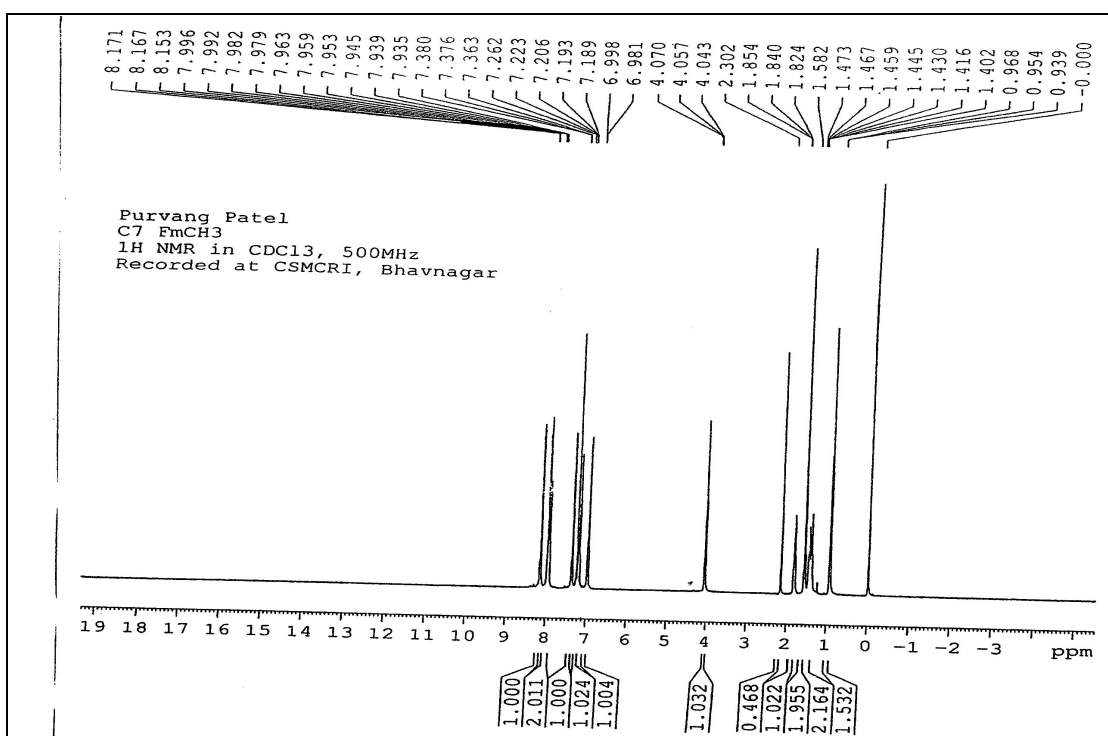
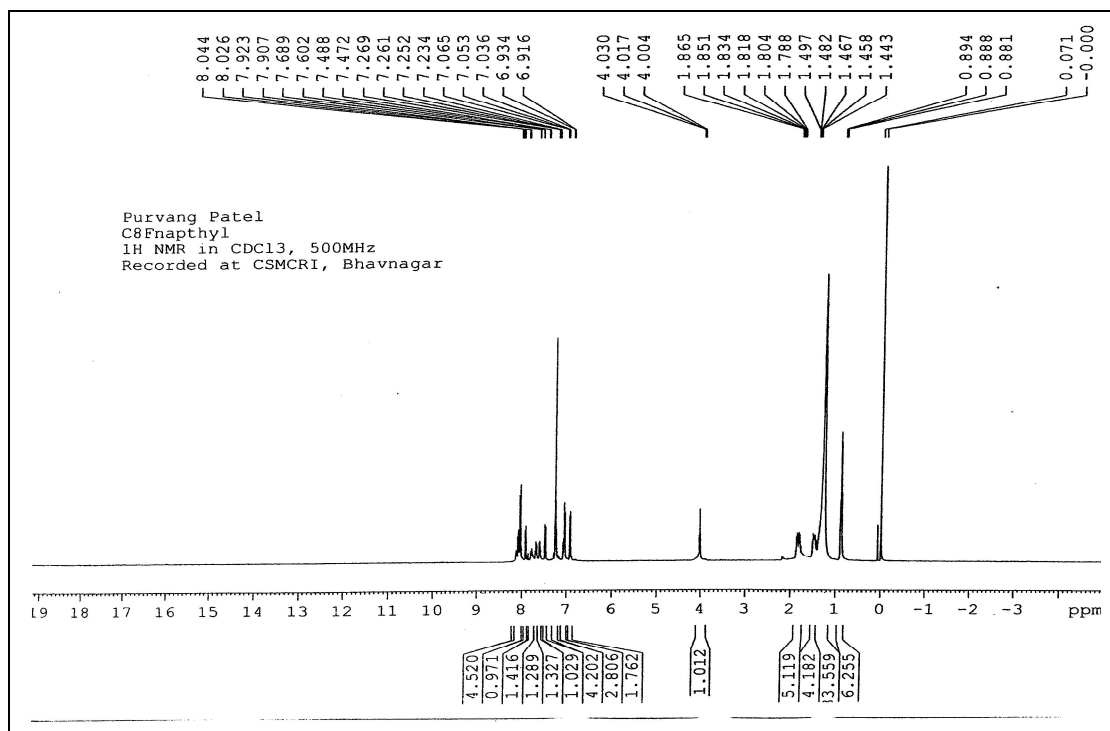
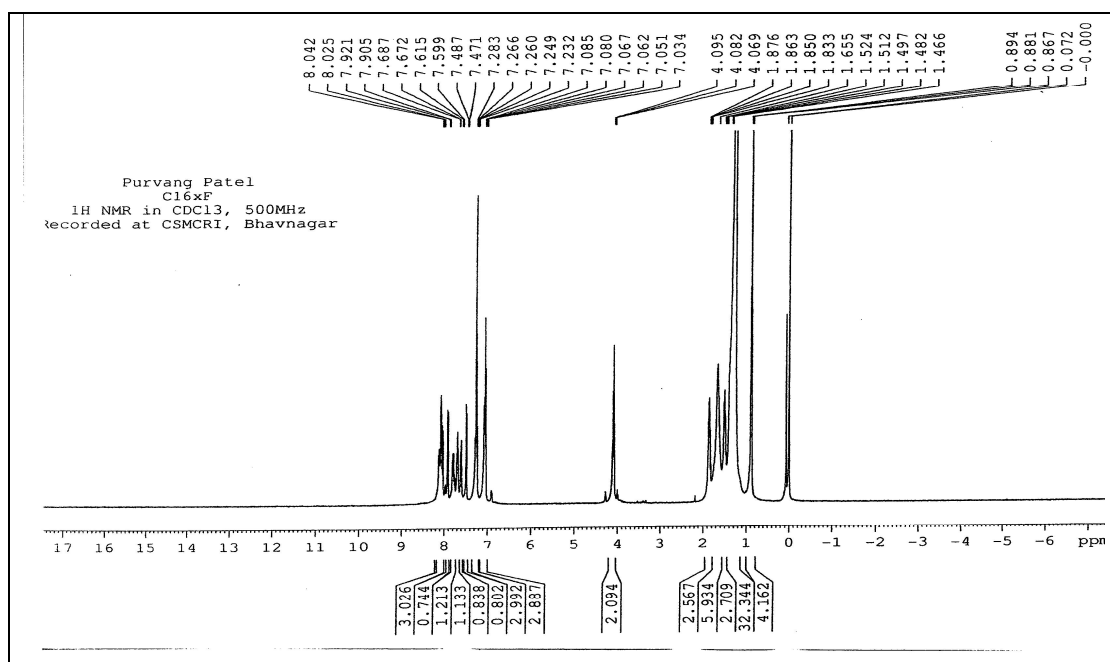


Figure 3.2 (j): ¹H NMR spectra of C7 homologue of series V

Figure 3.2 (k): ¹H NMR spectra of C8 homologue of series VIFigure 3.2 (l): ¹H NMR spectra of C16 homologue of series VI

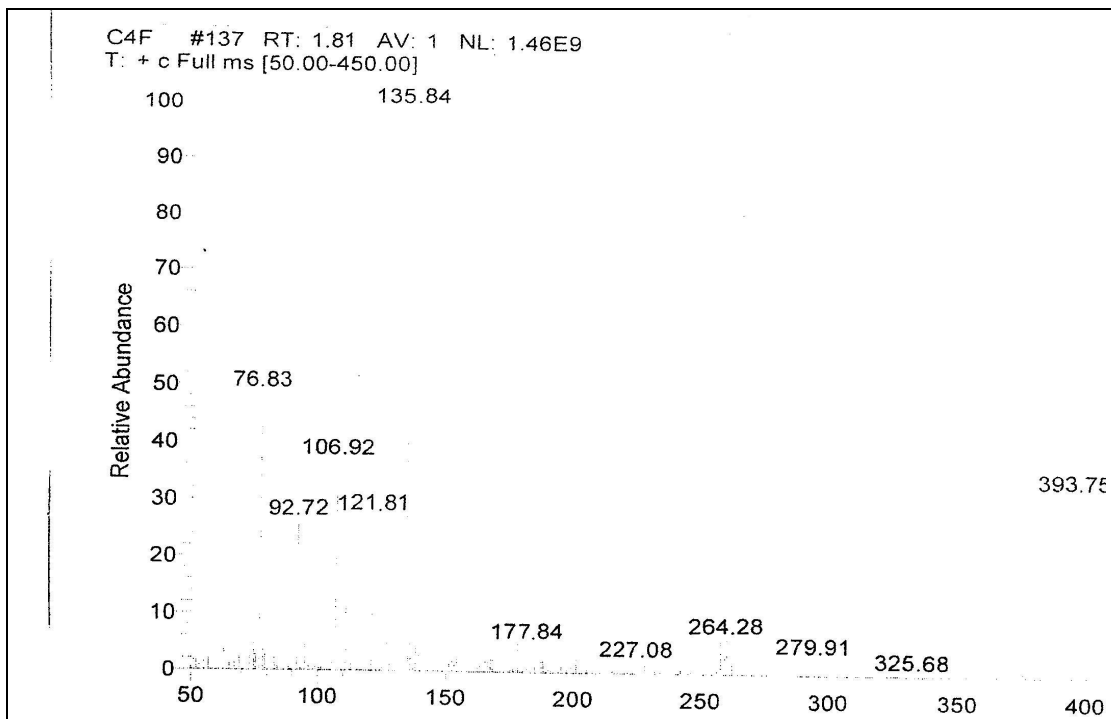


Figure 3.3 (a): Mass spectra of C4 homologue of series I

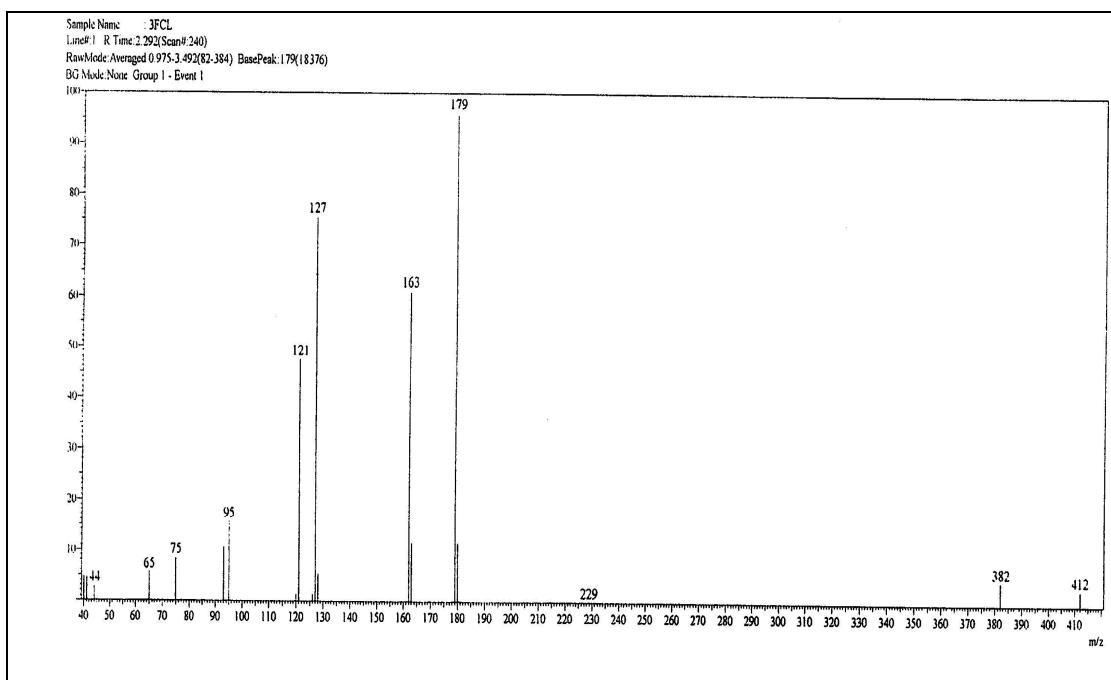


Figure 3.3 (b): Mass spectra of C3 homologue of series II

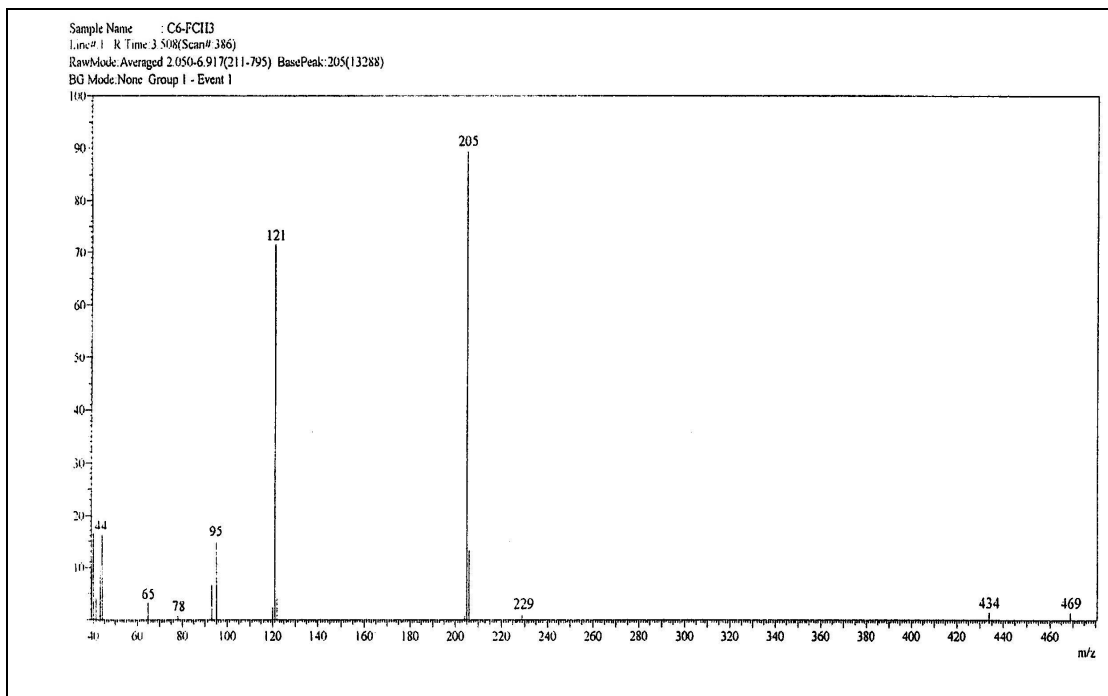


Figure 3.3 (c): Mass spectra of C6 homologue of series III

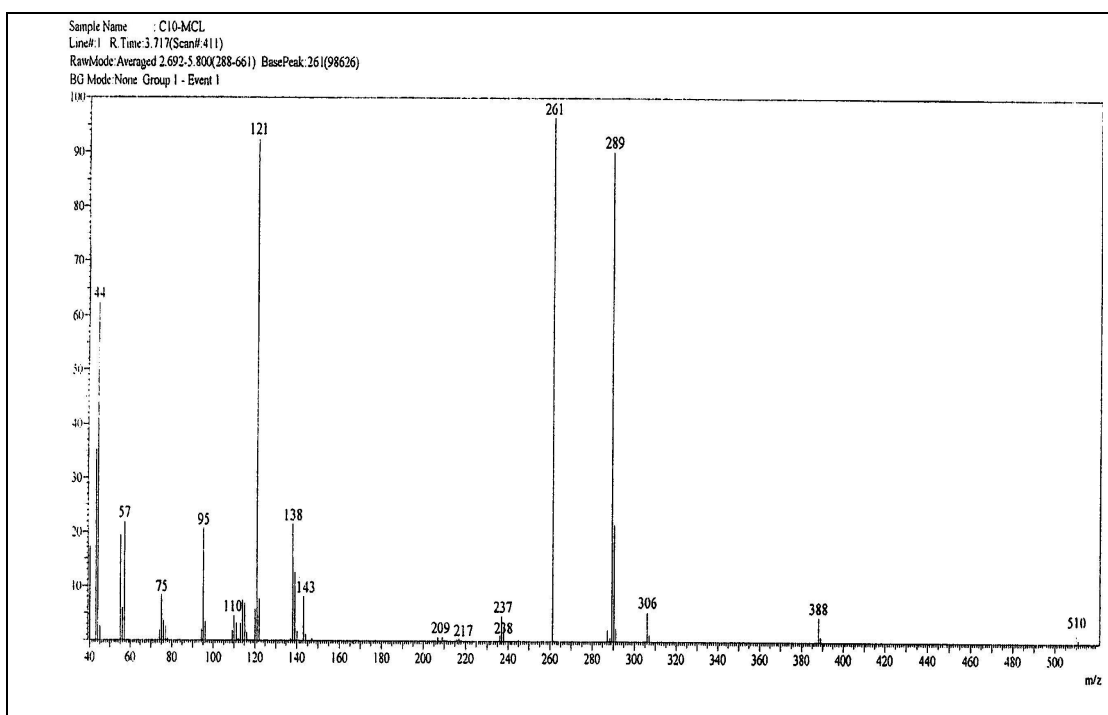


Figure 3.3 (d): Mass spectra of C10 homologue of series IV

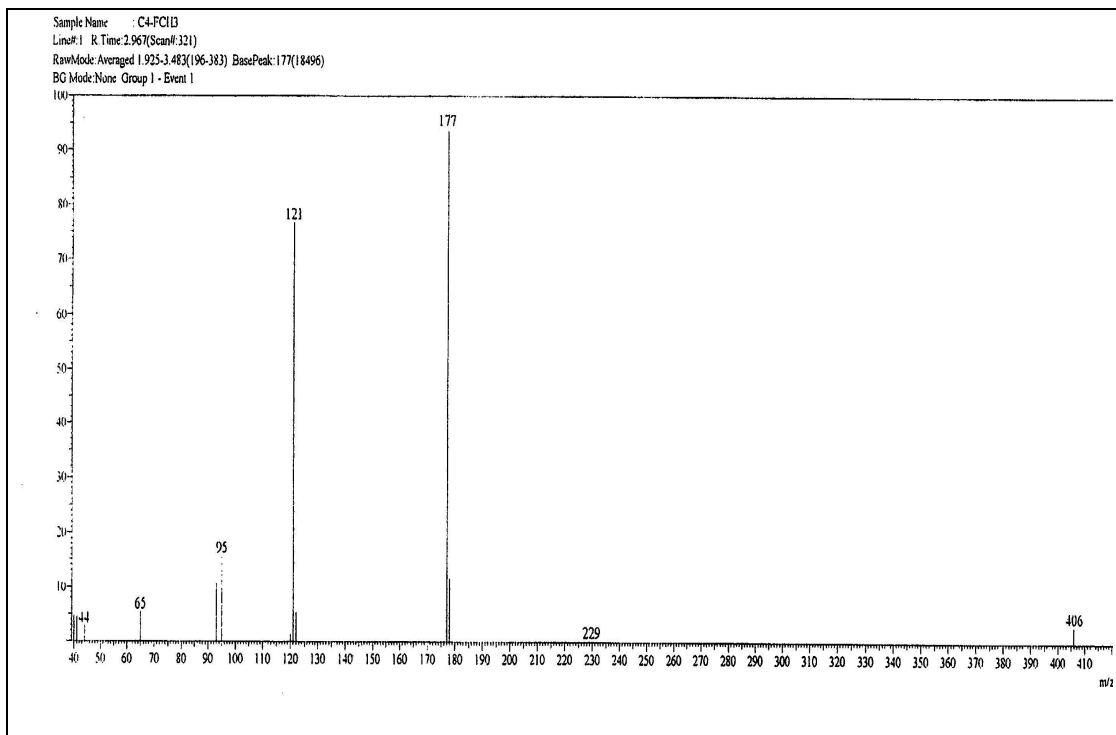


Figure 3.3 (e): Mass spectra of C6 homologue of series V

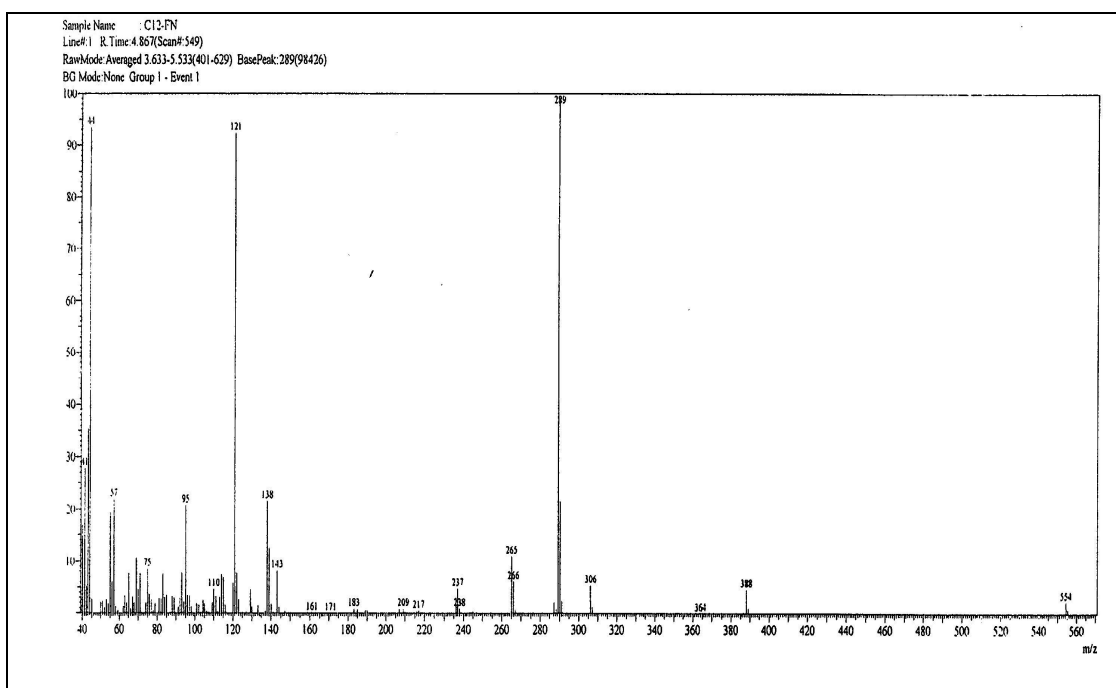


Figure 3.3 (f): Mass spectra of C10 homologue of series VI

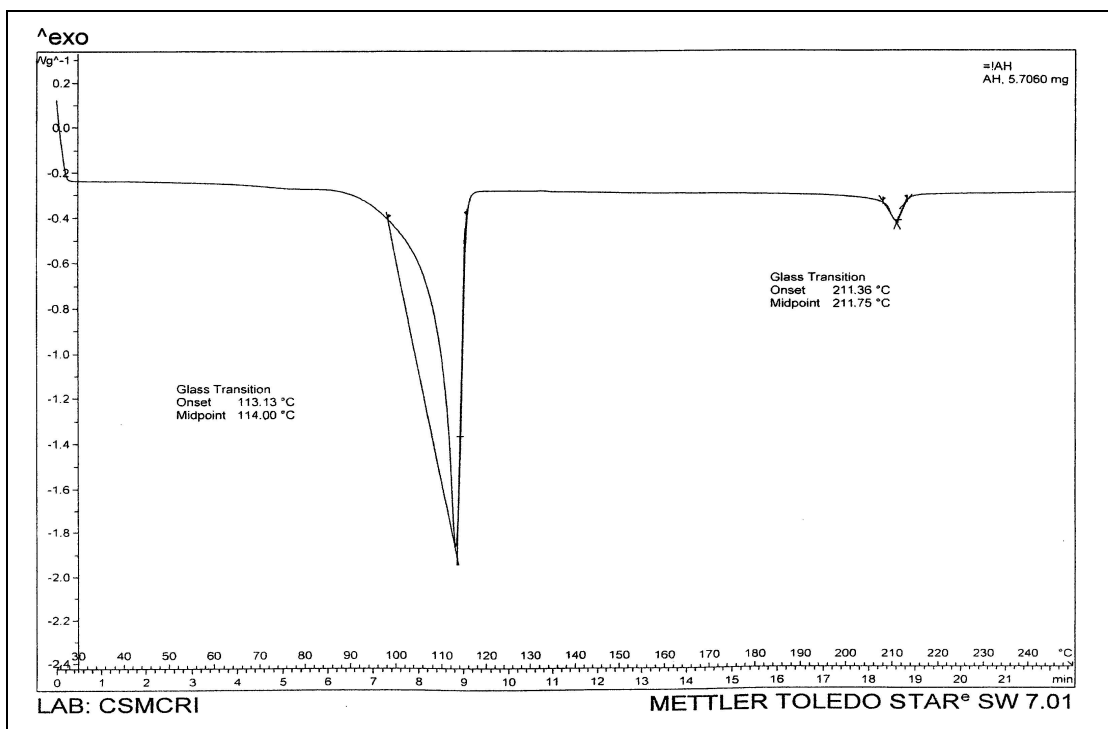


Figure 3.4 (a): DSC Thermogram of C4 homologue of series I

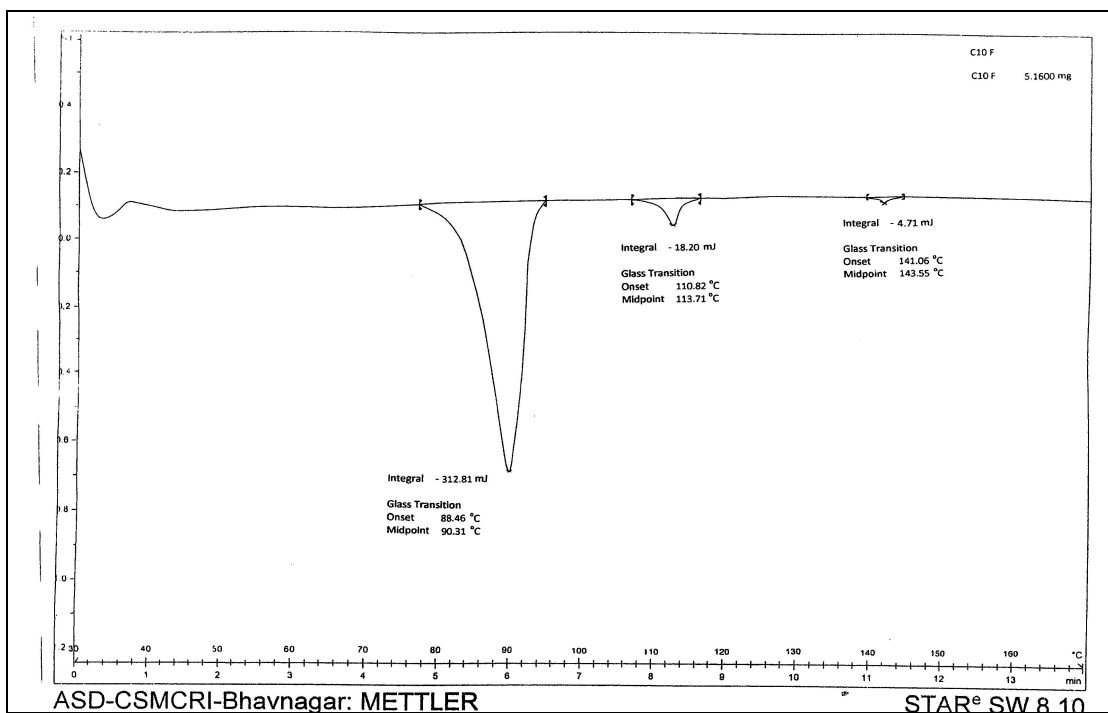


Figure 3.4 (b): DSC Thermogram of C10 homologue of series I

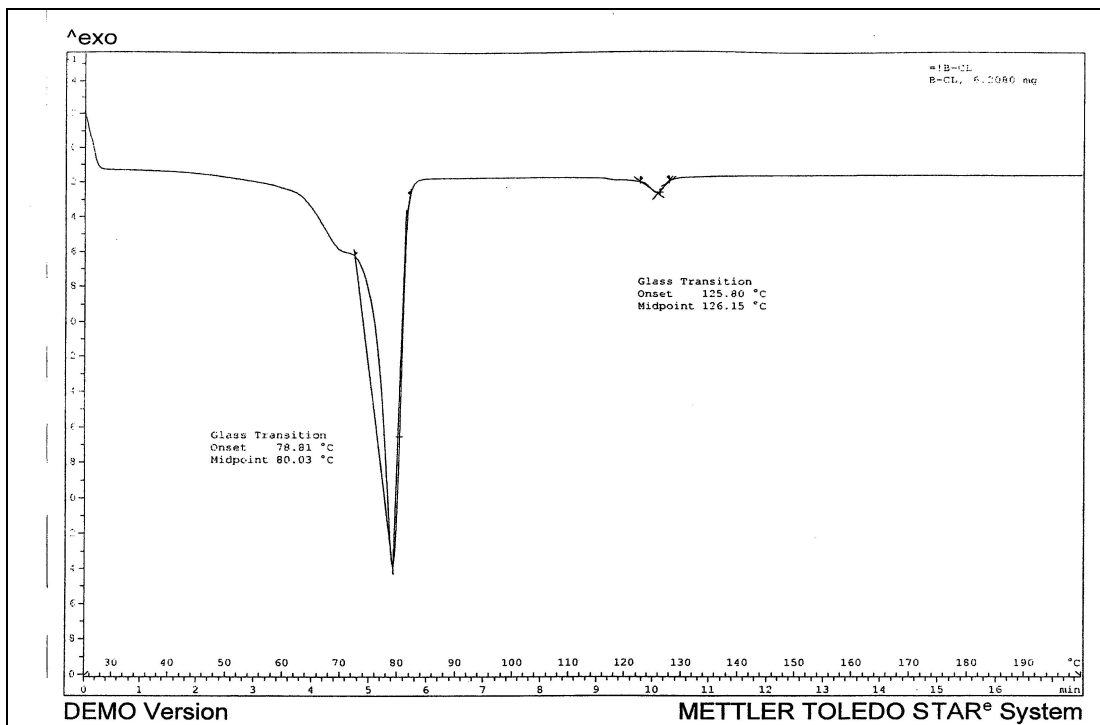


Figure 3.4 (c): DSC Thermogram of C8 homologue of series II

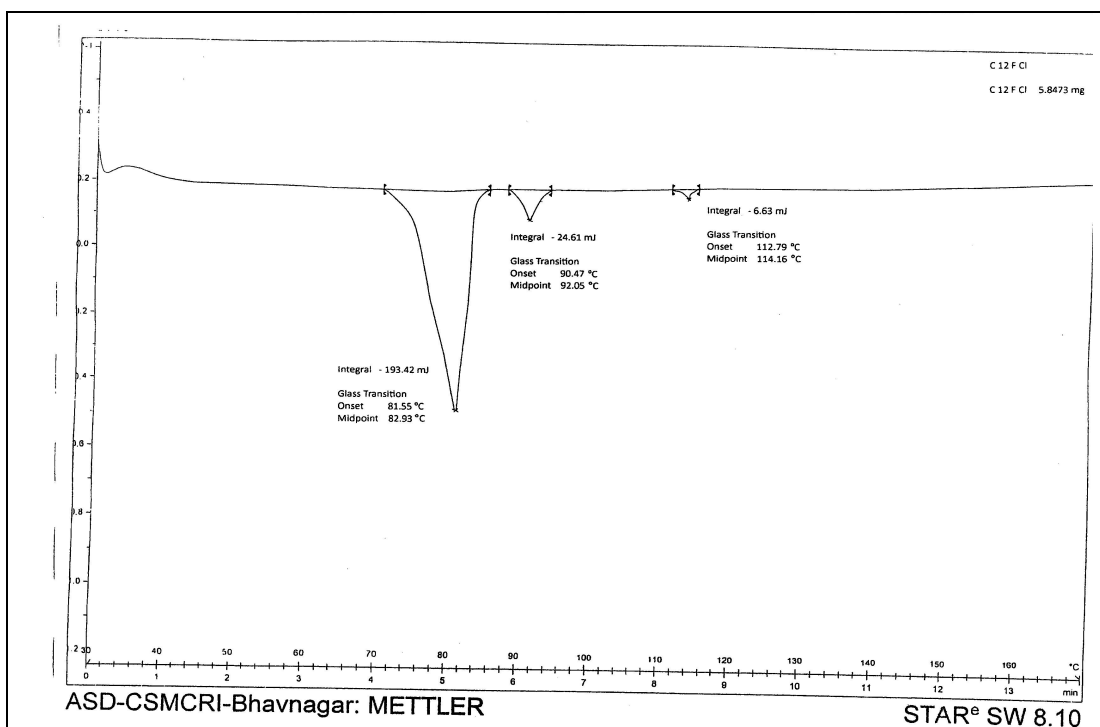


Figure 3.4 (d): DSC Thermogram of C12 homologue of series II

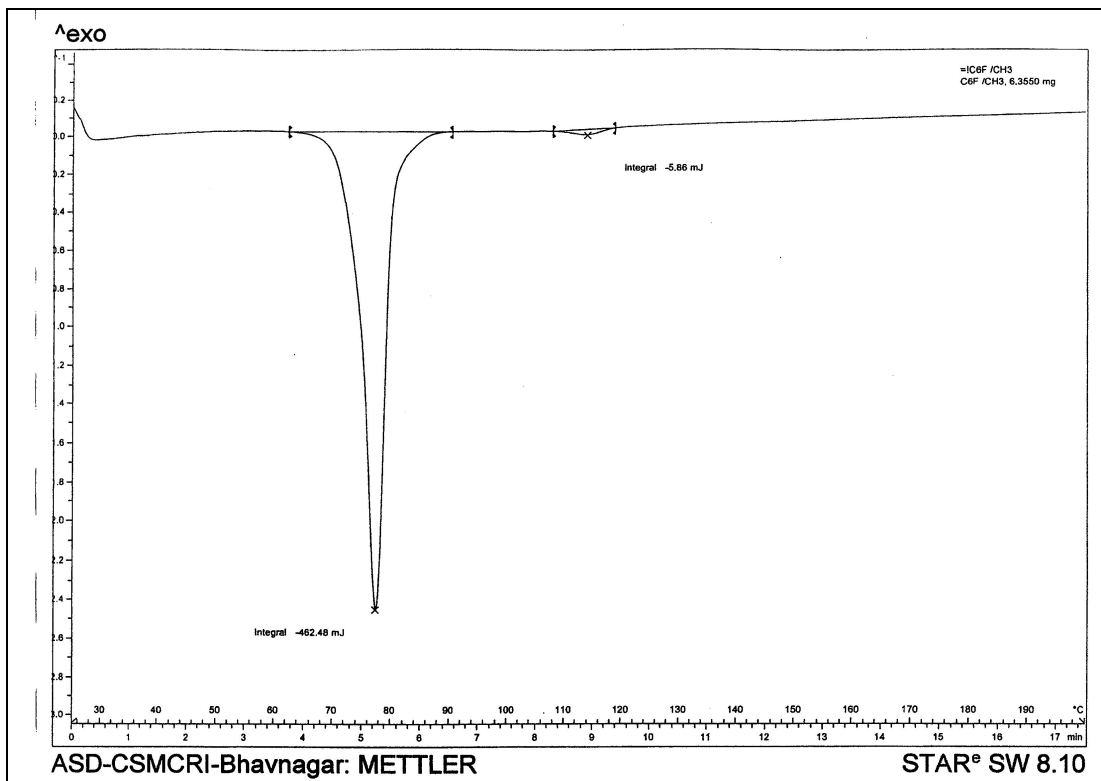


Figure 3.4 (e): DSC Thermogram of C6 homologue of series III

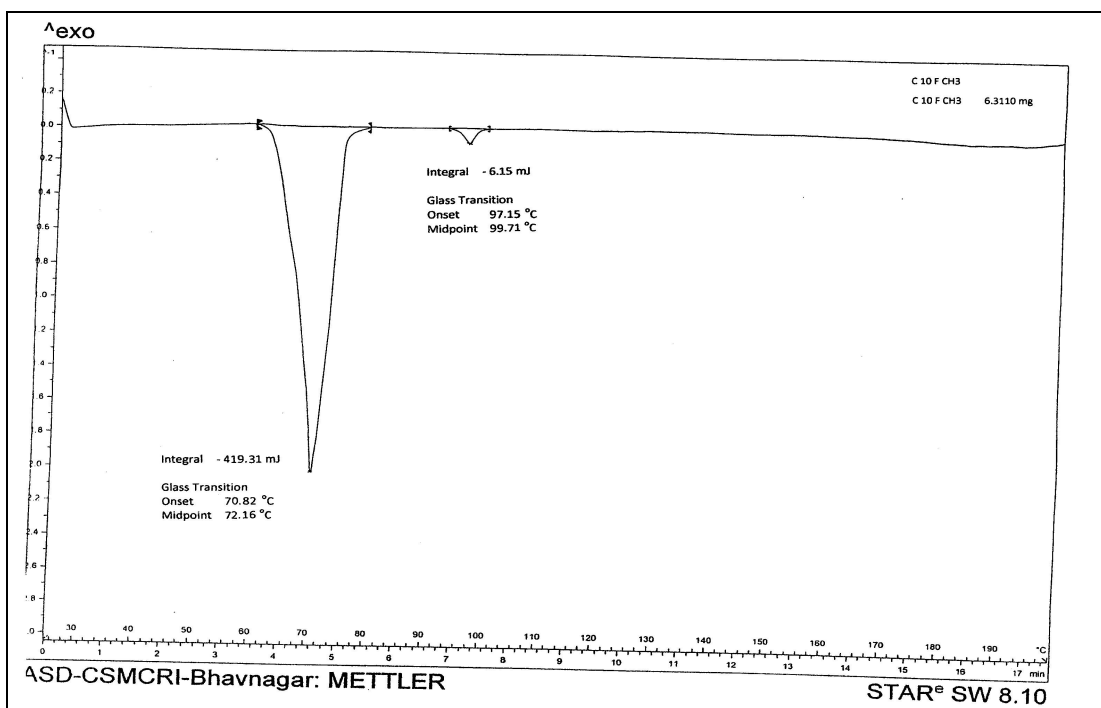


Figure 3.4 (f): DSC Thermogram of C10 homologue of series III

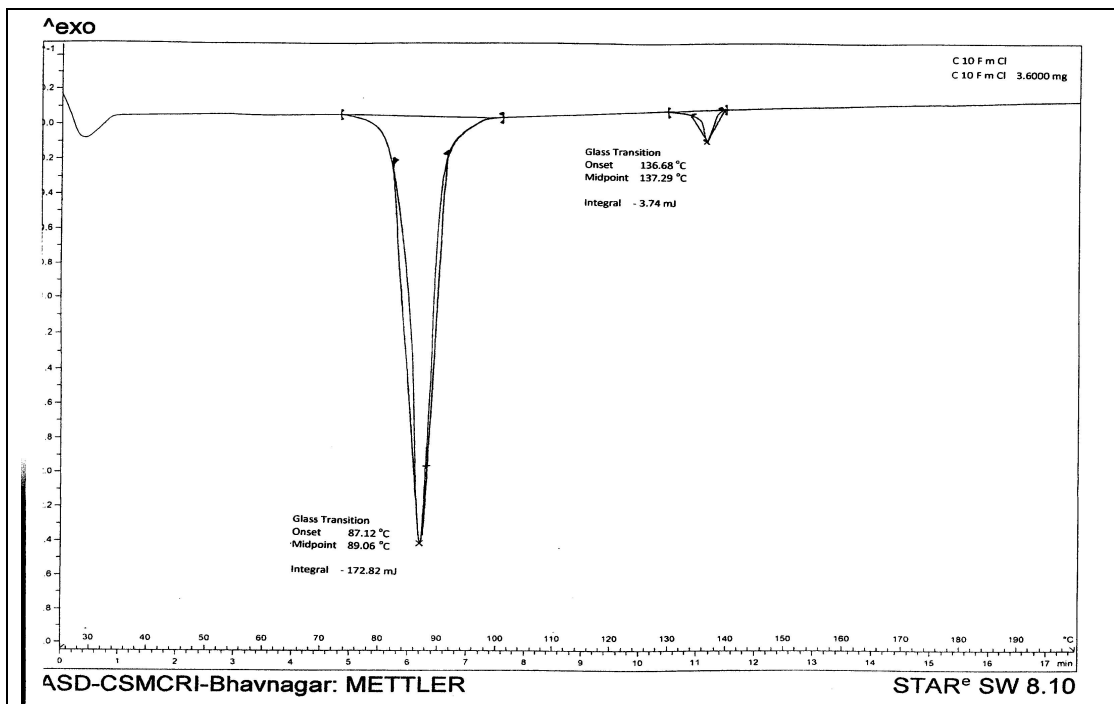


Figure 3.4 (g): DSC Thermogram of C10 homologue of series IV

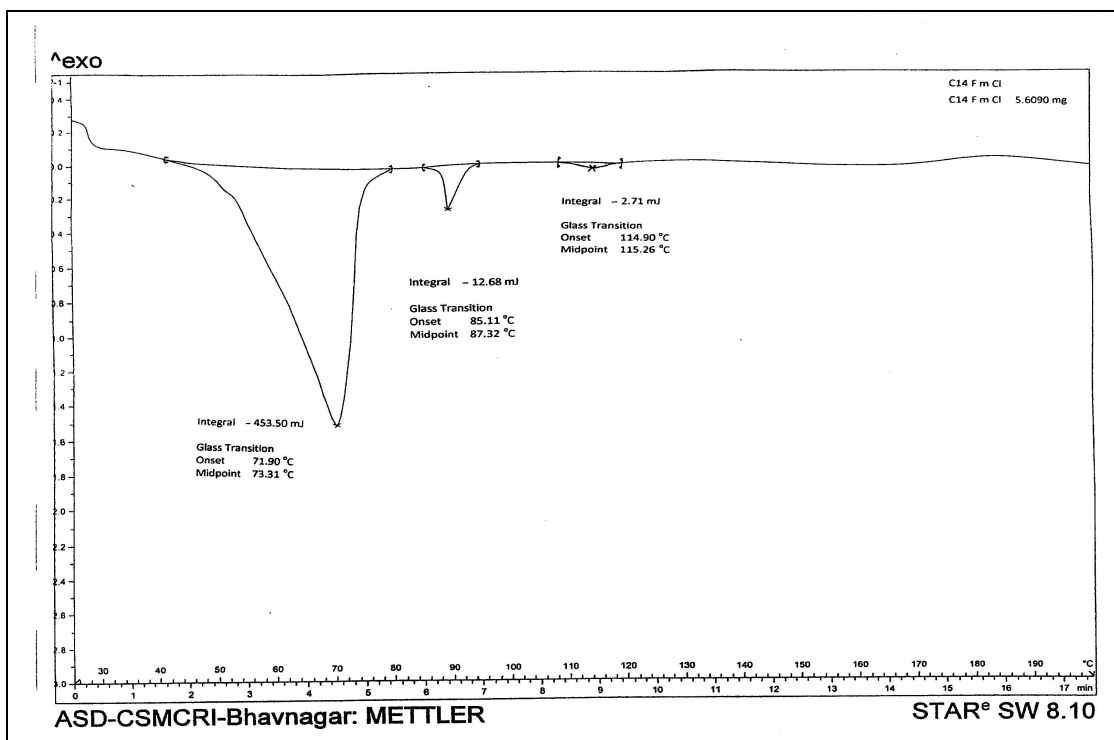


Figure 3.4 (h): DSC Thermogram of C14 homologue of series IV

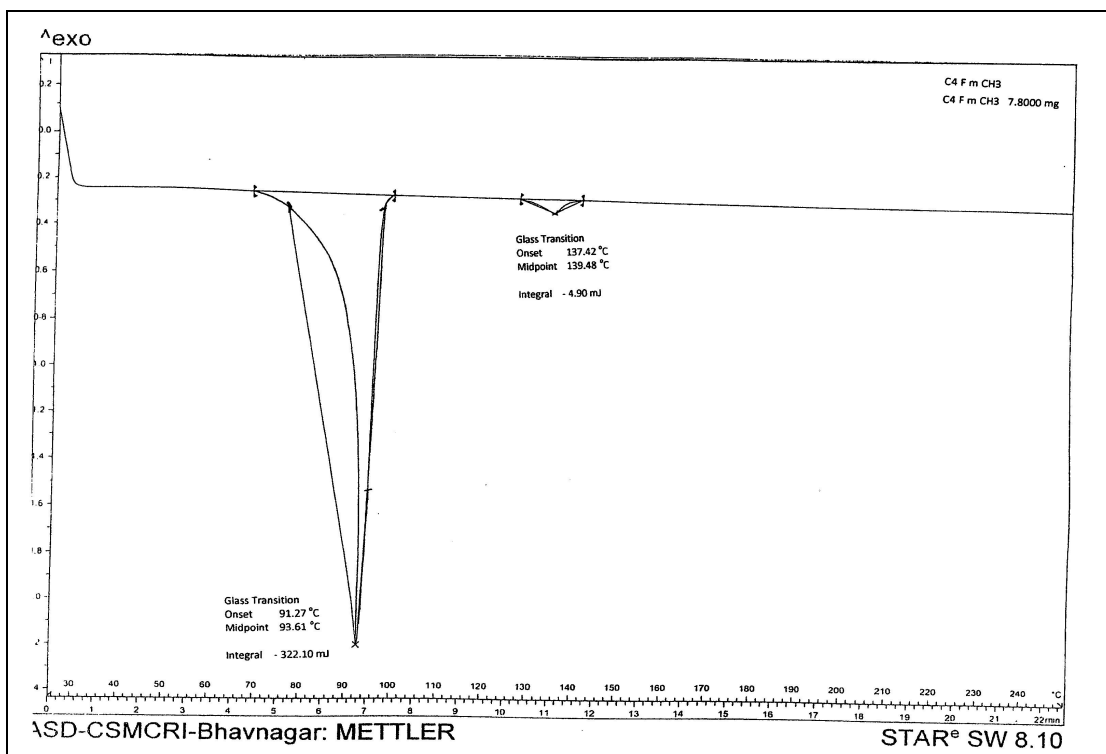


Figure 3.4 (i): DSC Thermogram of C4 homologue of series V

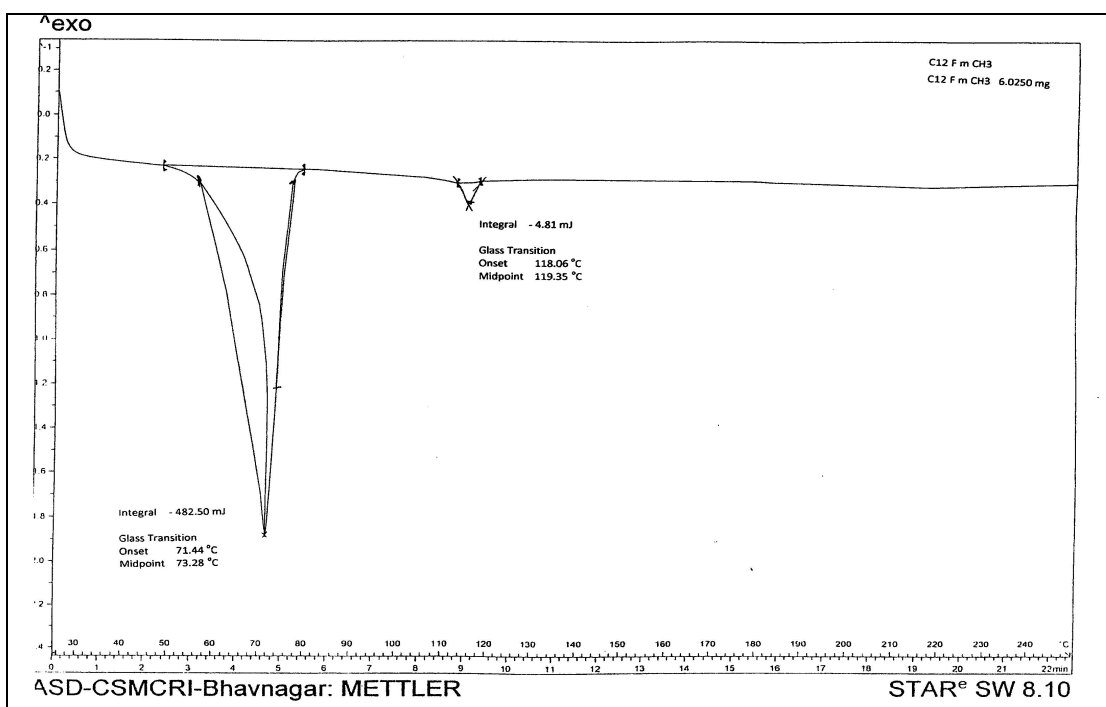


Figure 3.4 (j): DSC Thermogram of C12 homologue of series V

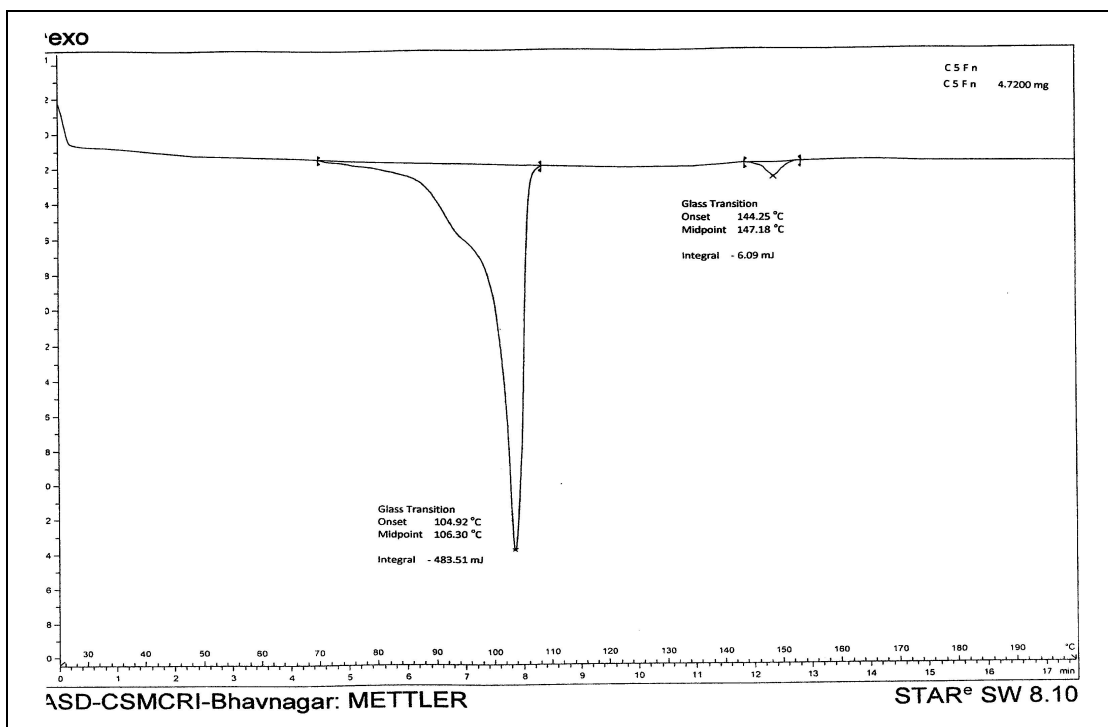


Figure 3.4 (k): DSC Thermogram of C5 homologue of series VI

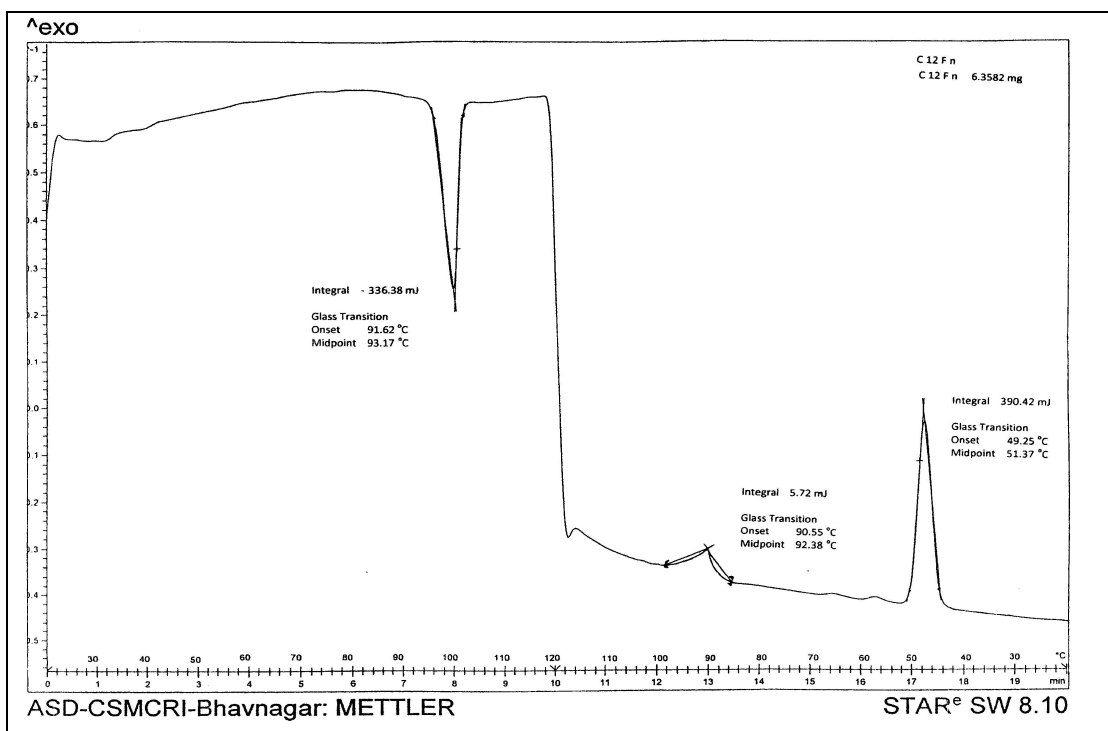


Figure 3.4 (l): DSC Thermogram of C12 homologue of series VI

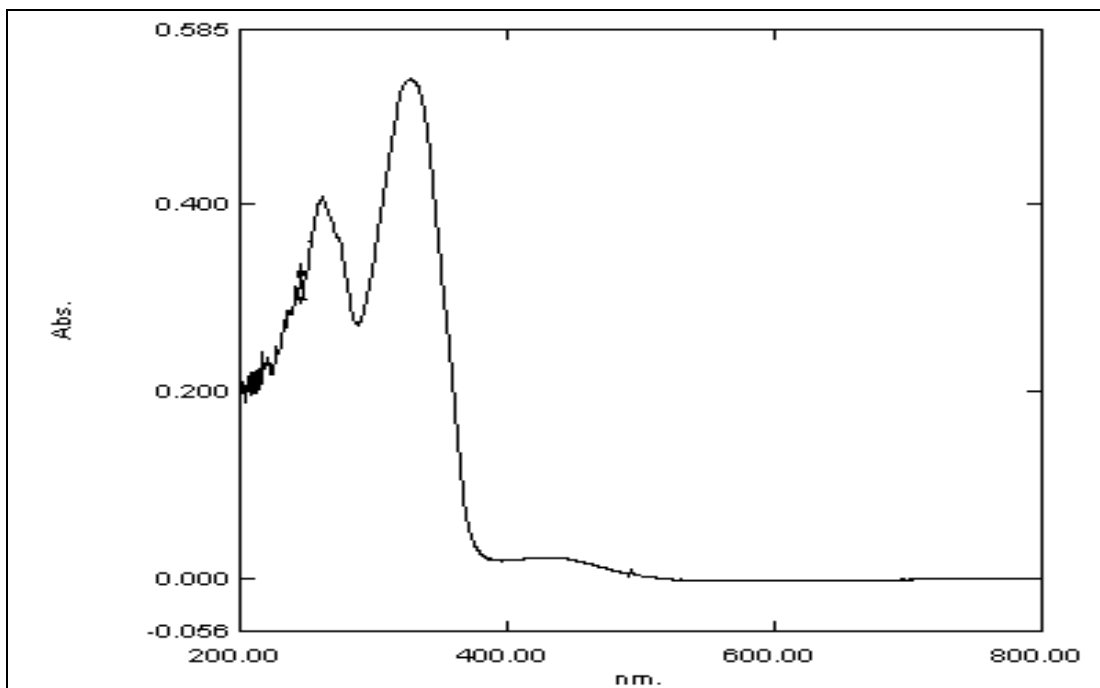


Figure 3.5 (a): UV spectra of C5 homologue of series I

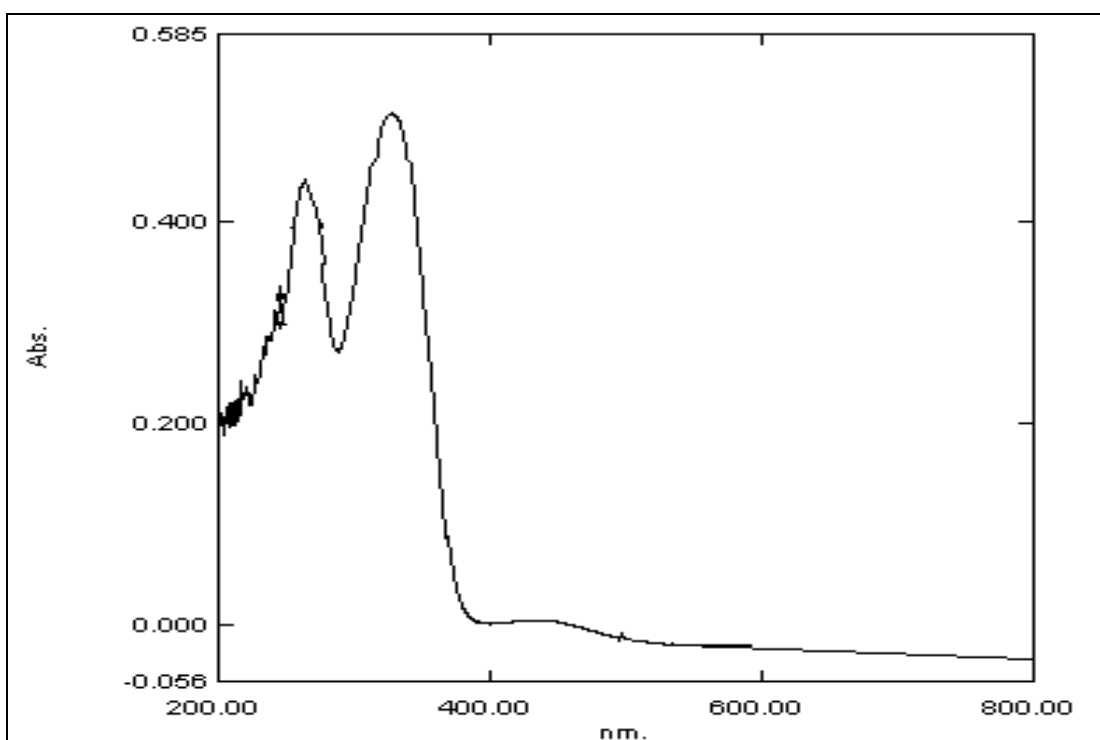


Figure 3.5 (b): UV spectra of C8 homologue of series I

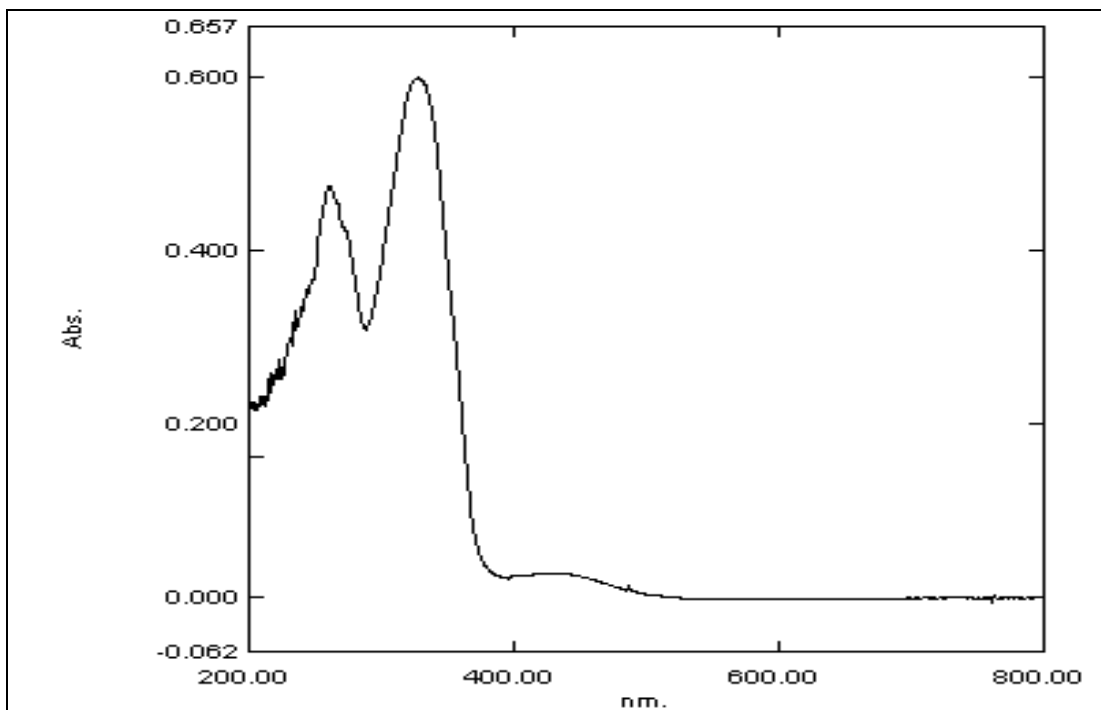


Figure 3.5 (c): UV spectra of C7 homologue of series II

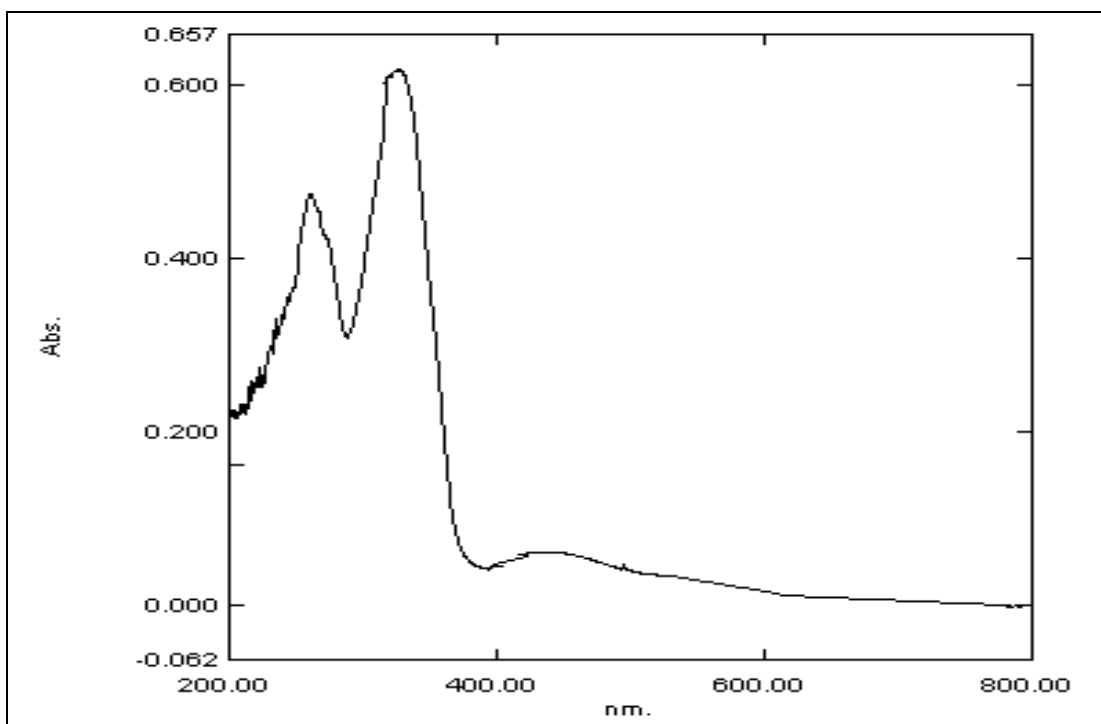


Figure 3.5 (d): UV spectra of C10 homologue of series II

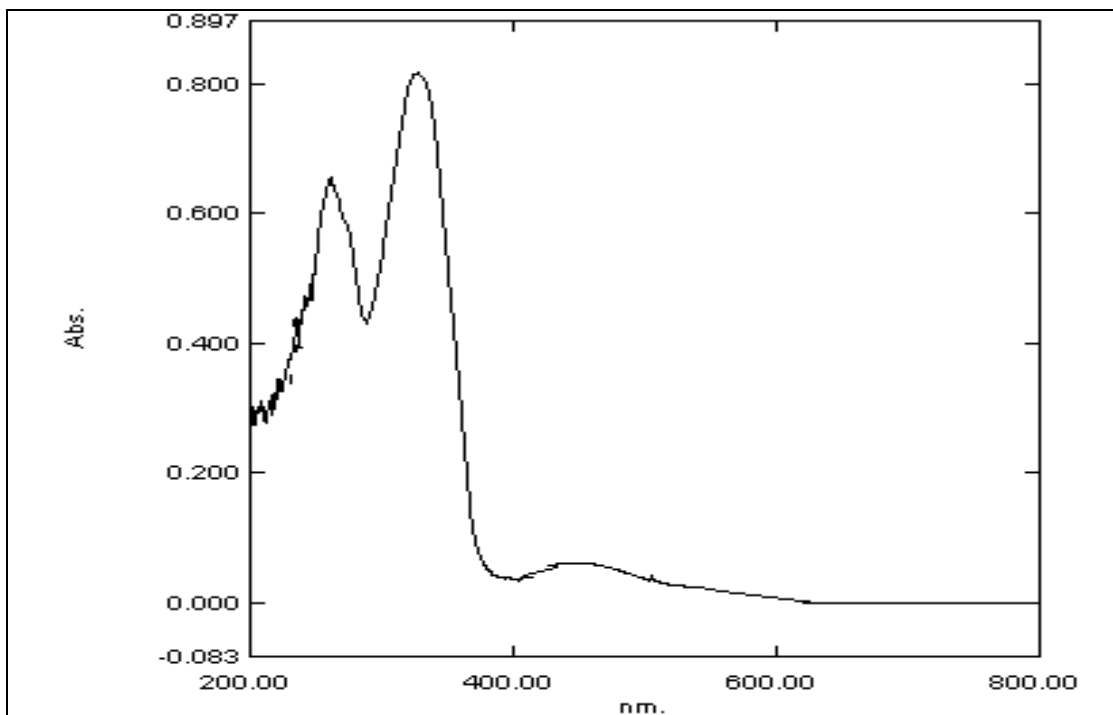


Figure 3.5 (e): UV spectra of C12 homologue of series III

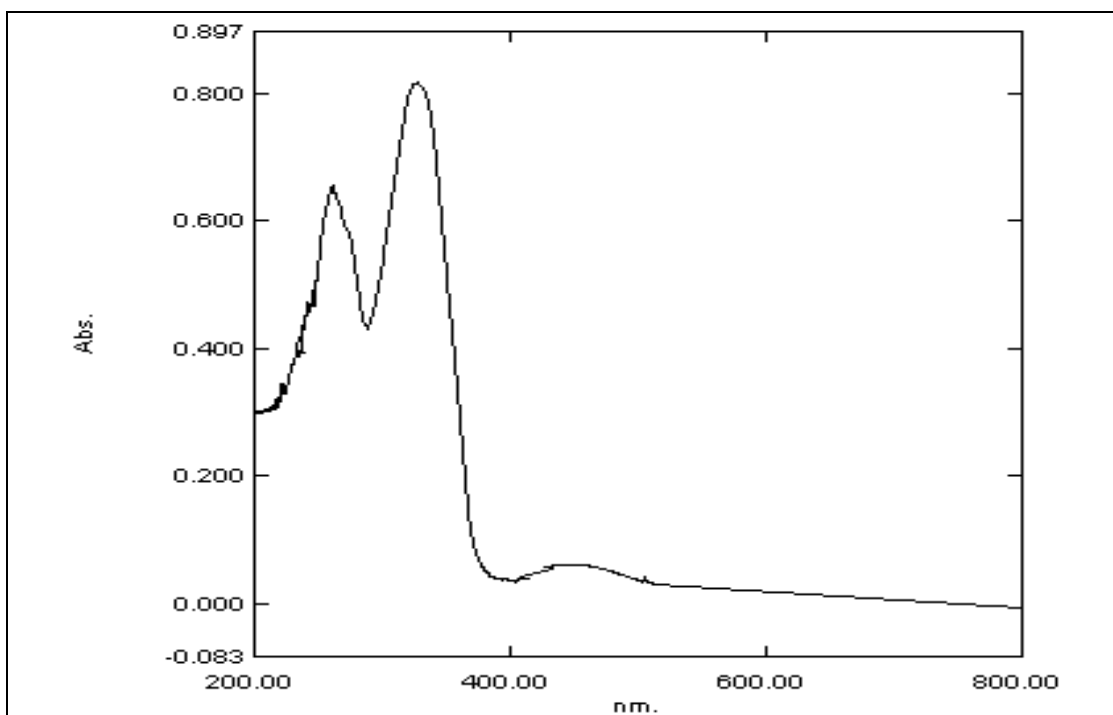


Figure 3.5 (f): UV spectra of C14 homologue of series III

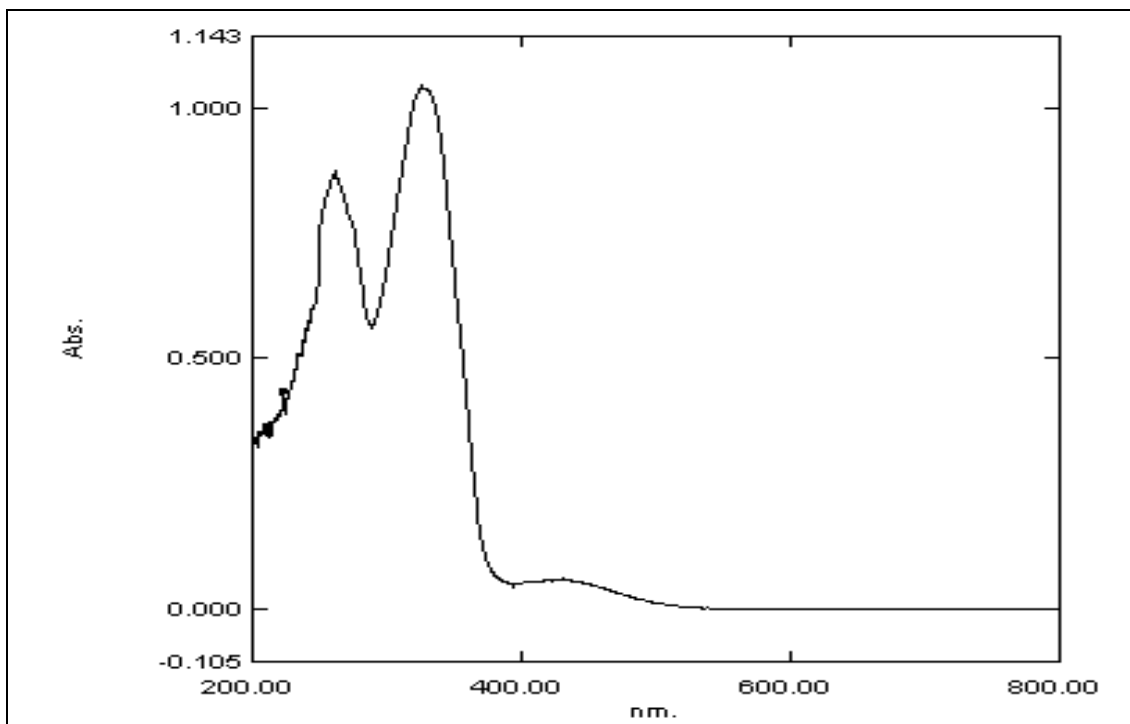


Figure 3.5 (g): UV spectra of C2 homologue of series IV

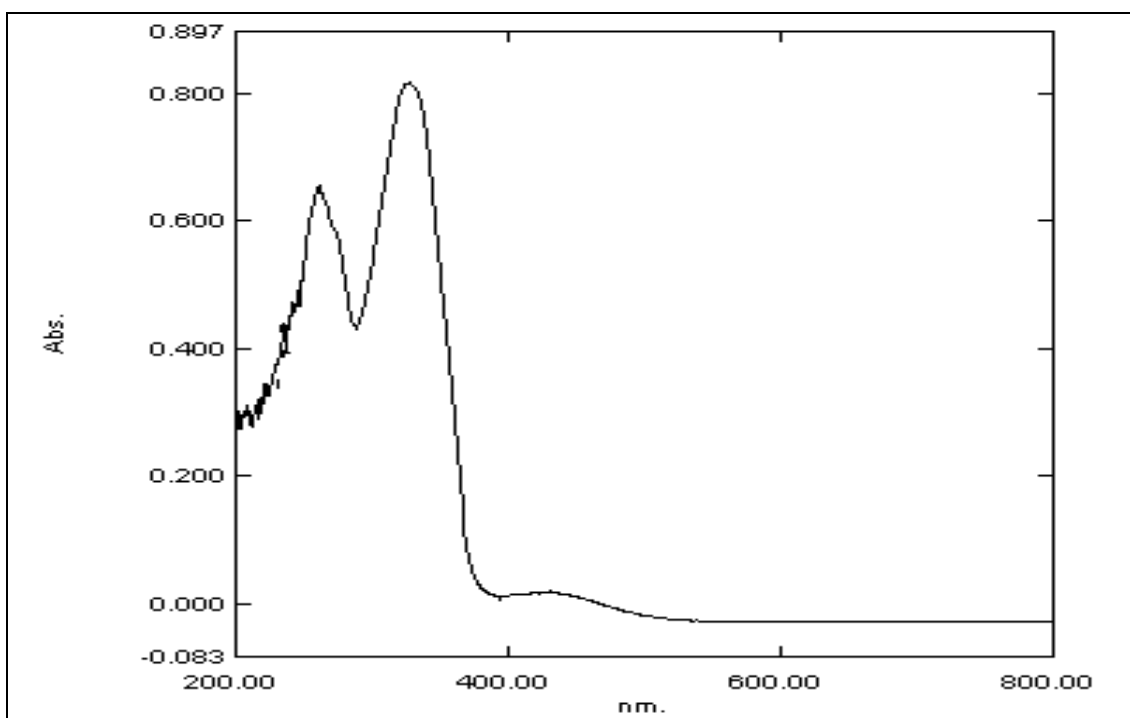


Figure 3.5 (h): UV spectra of C3 homologue of series IV

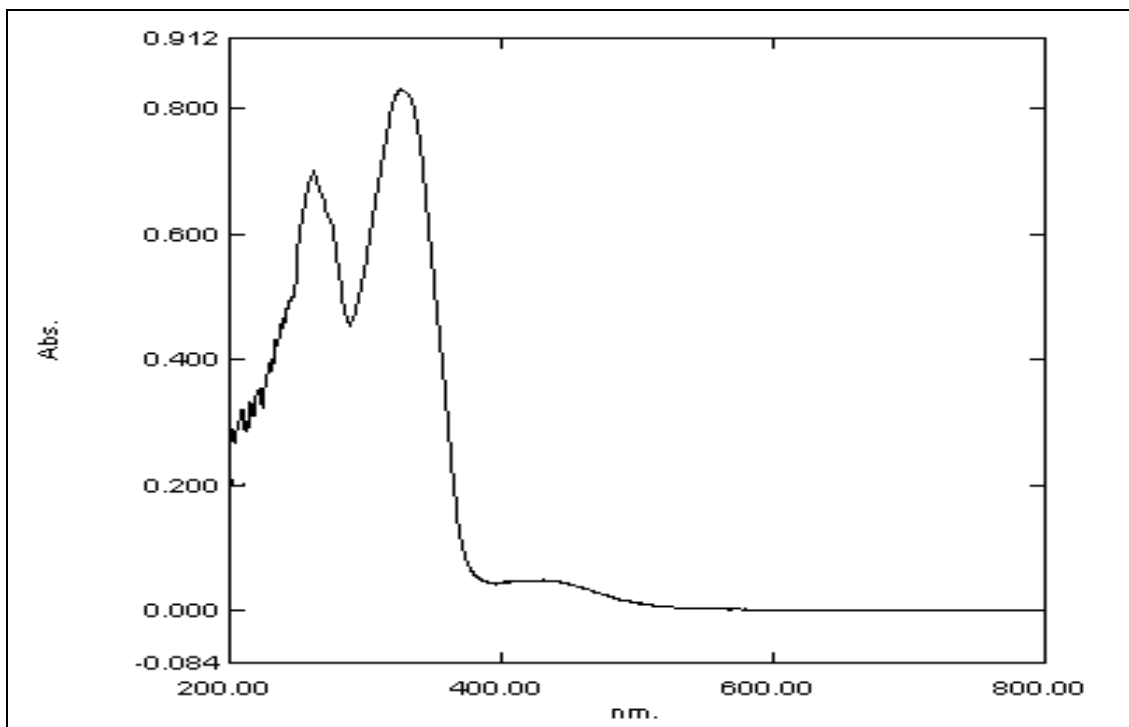


Figure 3.5 (i): UV spectra of C2 homologue of series V

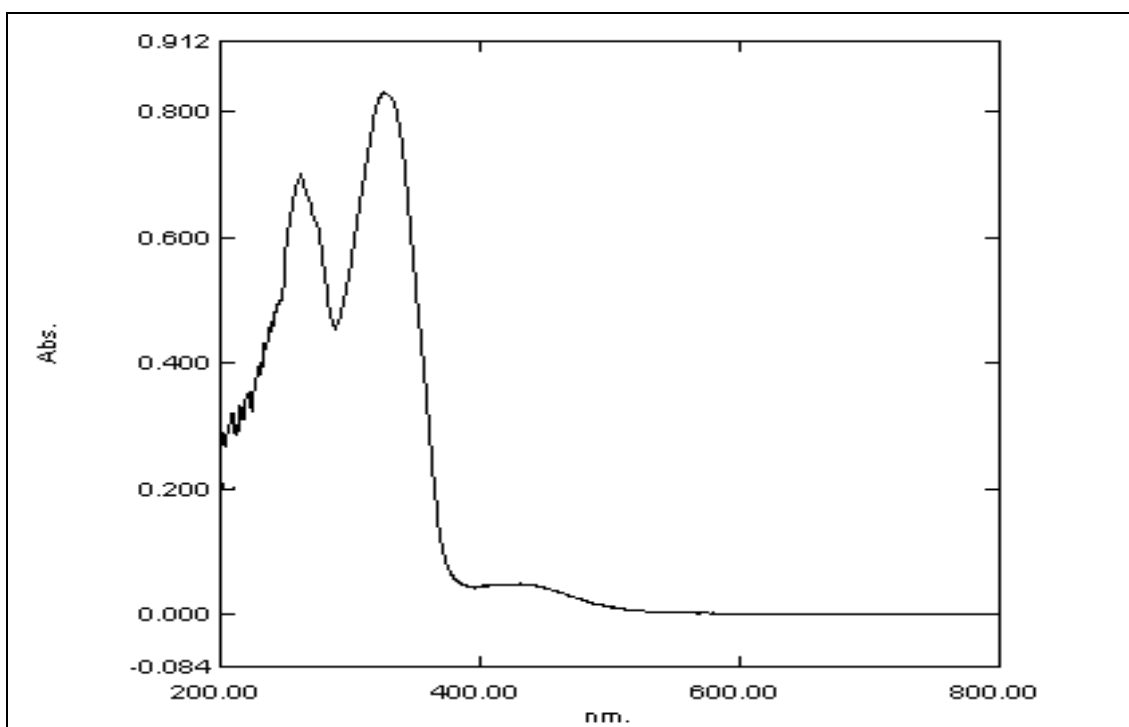


Figure 3.5 (j): UV spectra of C5 homologue of series V

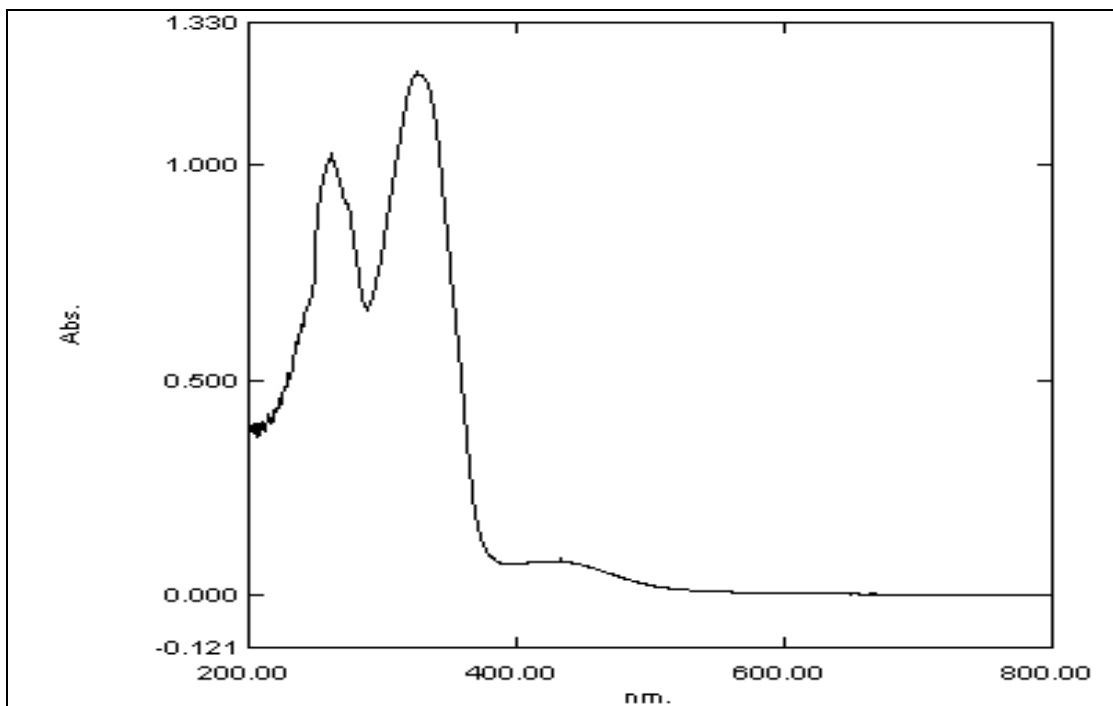


Figure 3.5 (k): UV spectra of C2 homologue of series VI

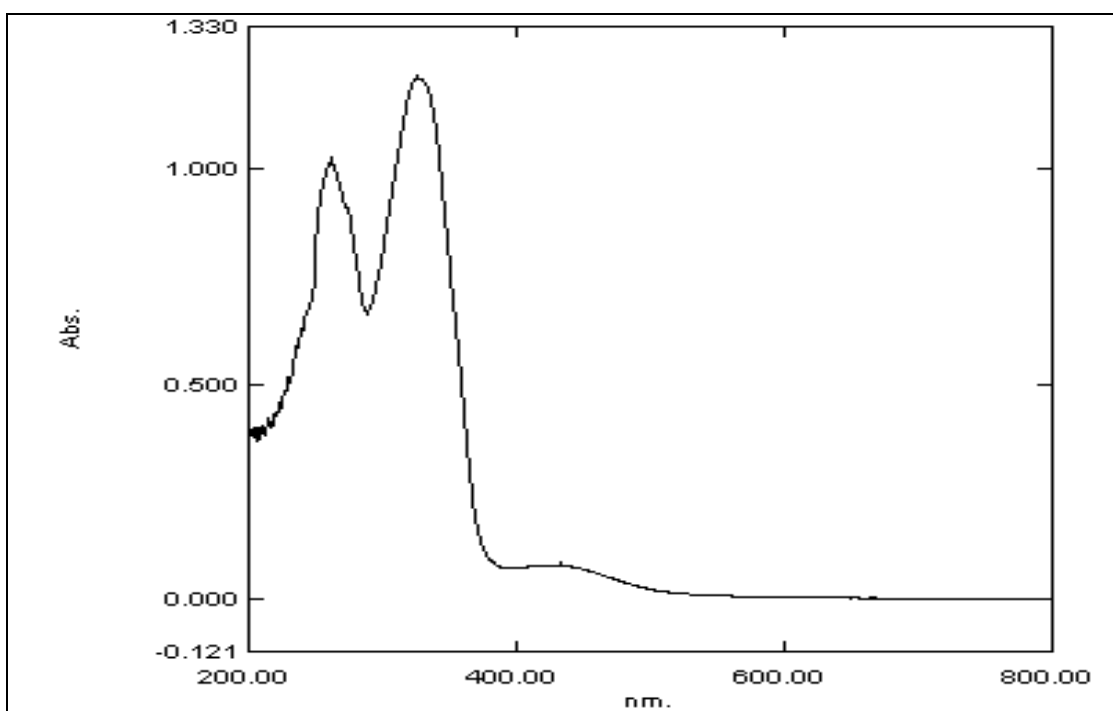
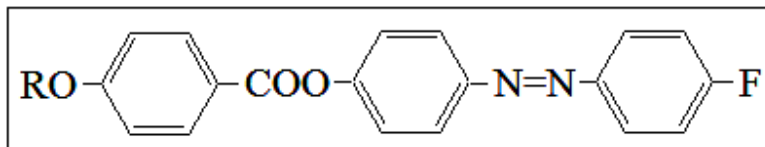


Figure 3.5 (l): UV spectra of C6 homologue of series VI

3.3 Results and Discussion

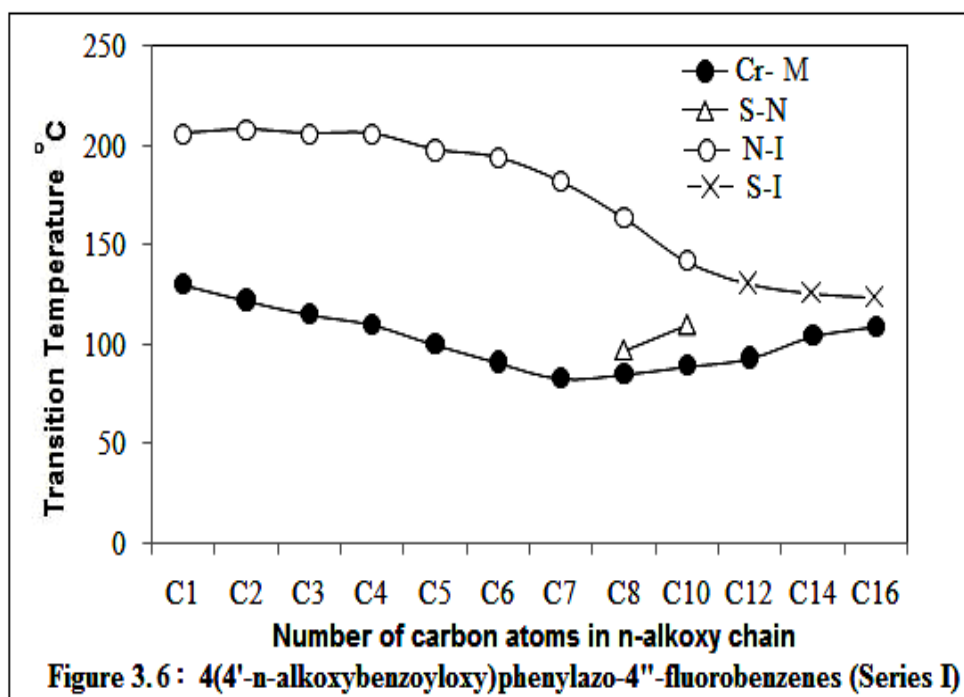
3.3.1 Series I: 4-(4'-n-alkoxybenzoyloxy)phenylazo-4''-fluorobenzenes

General molecular structure of the series is



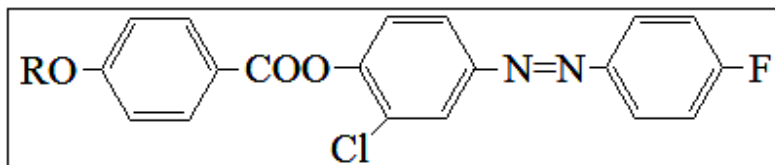
Where, R is C_nH_{2n+1} $n= 1$ to 8, 10, 12, 14 and 16

All the twelve homologues of the series I are mesogens (Table 3.1); the nematic phase commences from first derivative and remains up to the decyl derivative while Smectic C phase commences from the octyl derivative and remains to be exhibited up to the last hexadecyl derivative synthesised. Figure 3.6 i.e., the plot of transition temperatures against number of carbon atoms in alkoxy chain; it indicates that N-I curve shows overall falling tendency with slight increase at fourth derivative and merges with falling S-I curve as the series is ascended. No odd-even effect is observed in N-I curve as well as S-I curves. The Cr-M transitions show falling tendency from methyl to heptyl derivative and then rising tendency from octyl derivative to hexadecyl derivative. Nematic phase of the series shows marble texture and the smectic phase shows schlieren texture of smectic C variety.



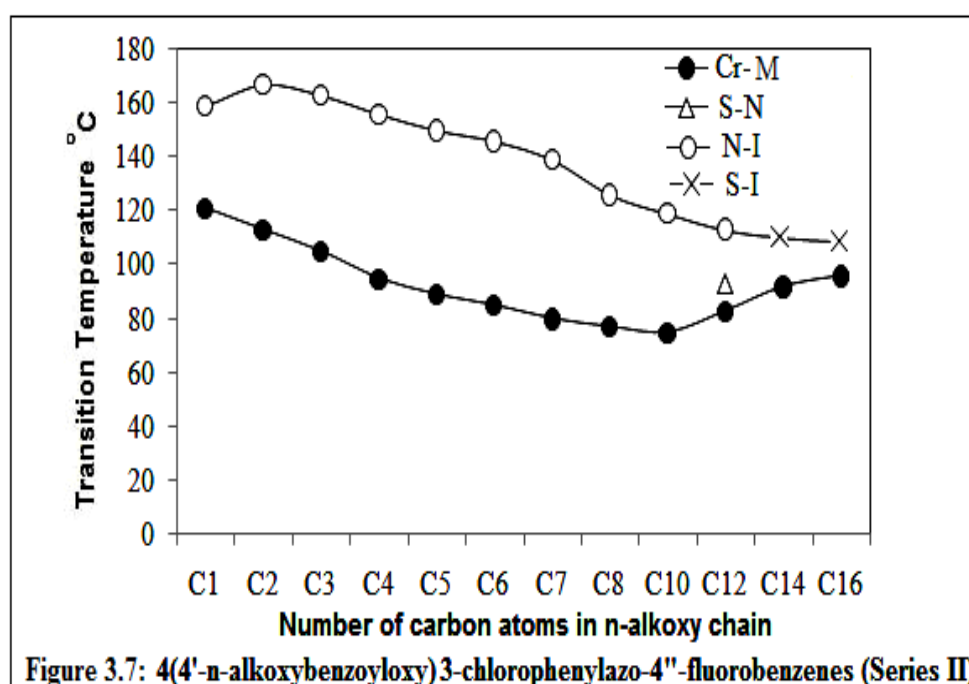
3.3.2 Series II: 4-(4'-n-alkoxybenzoyloxy)3-chlorophenylazo-4''-fluoro benzenes

General molecular structure of the series is



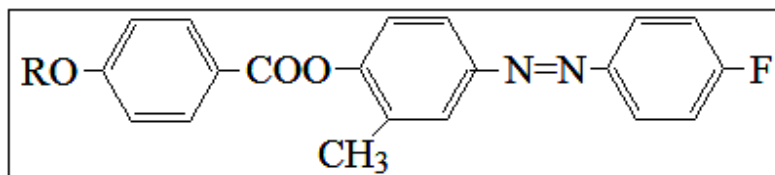
Where, R is C_nH_{2n+1} $n= 1$ to 8, 10, 12, 14 and 16

All the twelve homologues of the series II are mesogens (Table 3.5); the nematic phase commences from first derivative and remains up to the dodecyl derivative while Smectic C phase commences from the dodecyl derivative and remains to be exhibited up to the last hexadecyl derivative synthesised. Figure 3.7 i.e., the plot of transition temperatures against number of carbon atoms in alkoxy chain; it indicates that N-I curve shows overall falling tendency with slight increase at second derivative and merges with falling S-I curve as the series is ascended. Here no odd-even effect is observed in N-I curve as well as S-I curves. The Cr-M transitions show falling tendency from methyl to decyl derivative and rising tendency from dodecyl derivative to hexadecyl derivative. Here too, nematic phase of the series shows marble texture and the smectic phase shows schlieren texture of smectic C variety.



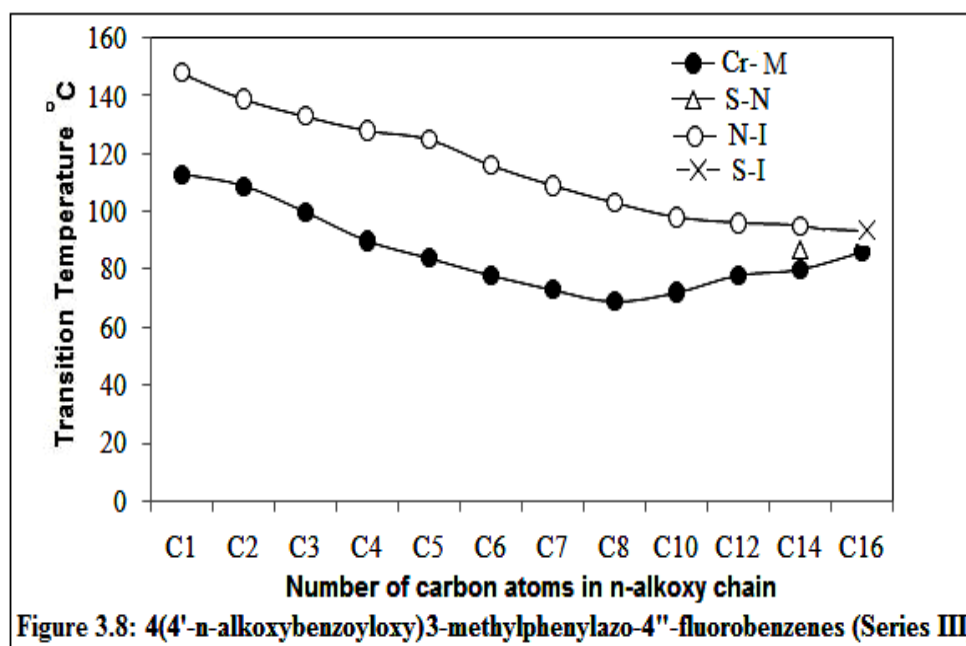
3.3.3 Series III: 4-(4'-n-alkoxybenzoyloxy)3-methylphenylazo-4''-fluorobenzenes

General molecular structure of the series is



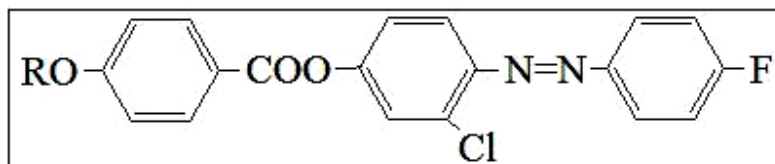
Where, R is C_nH_{2n+1} $n=1$ to 8, 10, 12, 14 and 16

All the twelve homologues of the series III are mesogens (Table 3.9); the nematic phase commences from first derivative and remains up to the tetradecyl derivative while Smectic C phase commences from the tetradecyl derivative and remains to be exhibited up to the last hexadecyl derivative synthesised. Figure 3.8 i.e., the plot of transition temperatures against number of carbon atoms in alkoxy chain; it indicates that N-I curve shows overall falling tendency with slight increase at fifth derivative and merges with falling S-I curve as the series is ascended. No odd-even effect is observed in N-I curve as well as S-I curves. The Cr-M transitions show falling tendency from methyl to dodecyl derivative and rising tendency from dodecyl derivative to hexadecyl derivative. Like other two series, here also nematic phase of the series shows marble texture and the smectic phase shows schlieren texture of smectic C variety.



3.3.4 Series IV: 4-(4'-n-alkoxybenzoyloxy)2-chlorophenylazo-4''-fluorobenzenes

General molecular structure of the series is



Where, R is C_nH_{2n+1} $n=1$ to 8, 10, 12, 14 and 16

All the twelve homologues of the series IV are mesogens (Table 3.13); the nematic phase commences from the very first derivative and remains up to the last hexadecyl derivative synthesised while Smectic C phase commences from the tetradecyl derivative and remains to be exhibited upto the last hexadecyl derivative synthesised. Figure 3.9 i.e., the plot of transition temperatures against number of carbon atoms in alkoxy chain; it indicates that N-I curve shows overall falling tendency and merges as the series is ascended; no odd-even effect is observed in N-I curves. The Cr-M transitions show overall falling tendency with a rising jump at decyl derivative. The nematic phase of the series shows marble texture and the smectic phase shows schlieren texture of smectic C variety.

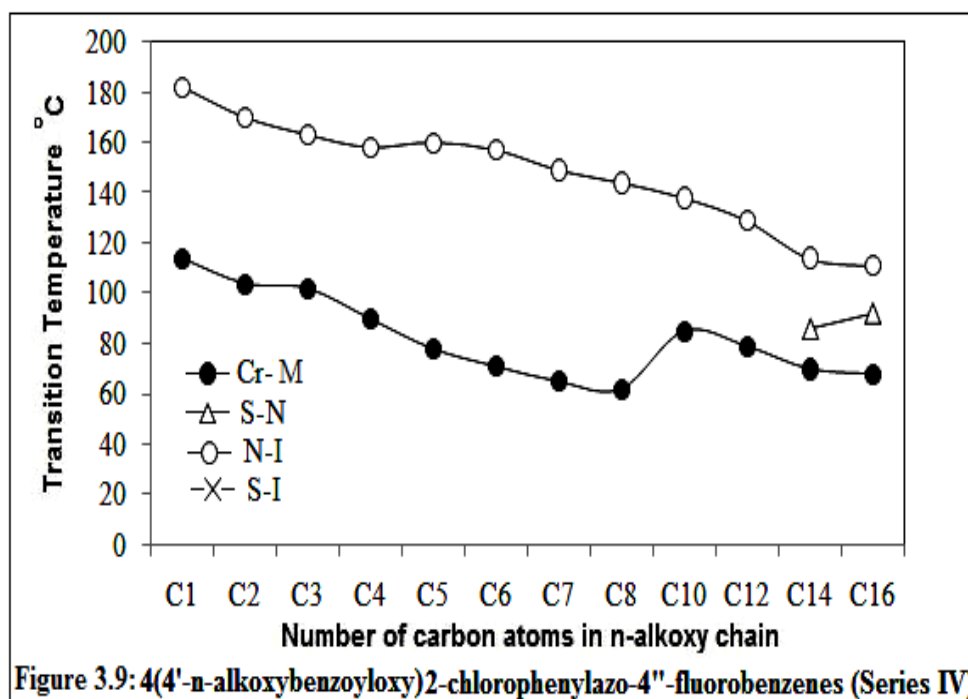
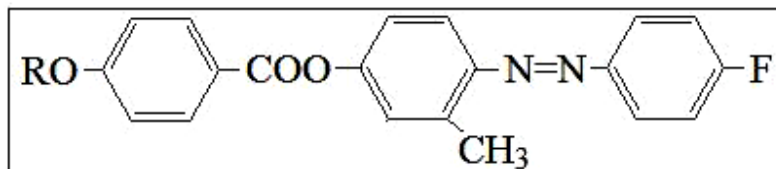


Figure 3.9: 4-(4'-n-alkoxybenzoyloxy)2-chlorophenylazo-4''-fluorobenzenes (Series IV)

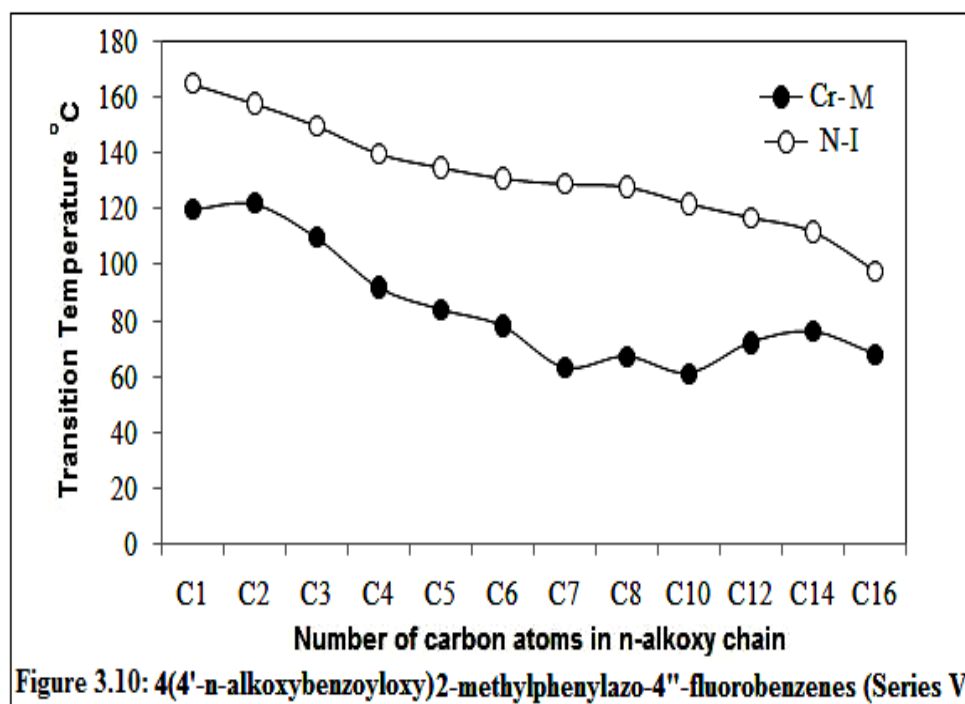
3.3.5 Series V: 4-(4'-n-alkoxybenzoyloxy)2-methylphenylazo-4''-fluoro benzenes

General molecular structure of the series is



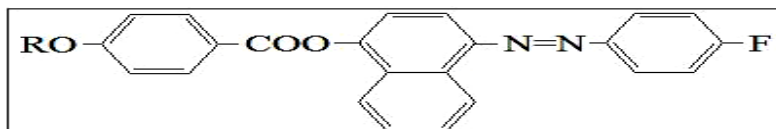
Where, R is C_nH_{2n+1} $n=1$ to 8, 10, 12, 14 and 16

All the twelve homologues of the series V are mesogens (Table 3.17); the nematic phase commences from the very first derivative and remains upto the last hexadecyl derivative synthesized. Figure 3.10 i.e., the plot of transition temperatures against number of carbon atoms in alkoxy chain; it indicates that N-I curve shows overall falling tendency as the series is ascended. Here also no odd-even effect is observed in N-I curve. The Cr-M transitions show overall falling tendency from methyl to hexadecyl derivative with slight rise at ethyl, octyl and tetradecyl derivative. Here also nematic phase of the series shows marble texture.



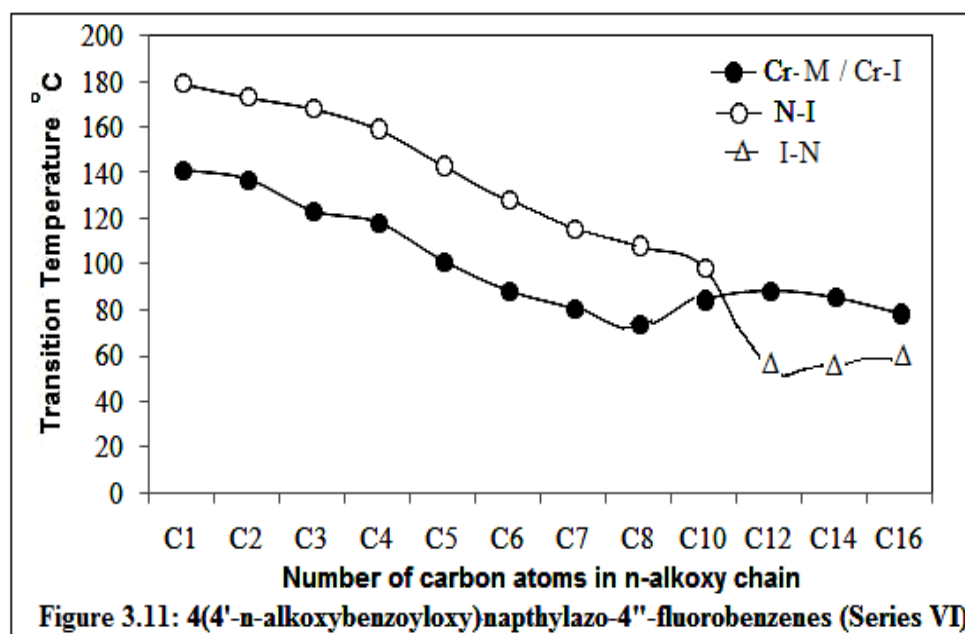
3.3.6 Series VI: 4-(4'-n-alkoxybenzoyloxy)naphthylazo-4''-fluorobenzenes

General molecular structure of the series is



Where, R is C_nH_{2n+1} $n=1$ to 8, 10, 12, 14 and 16

All the twelve homologues of the series VI are mesogens (Table 3.21); the nematic phase commences from the very first methyl derivative and remains upto the last hexadecyl derivative synthesized. Methyl to decyl derivatives show enantiotropic nematic phase where as the last three dodecyl, tetradecyl and hexadecyl derivatives show monotropic nematic phase. Figure 3.11 i.e., the plot of transition temperatures against number of carbon atoms in alkoxy chain; it indicates that N-I curve shows overall falling tendency upto decyl derivative; the curve then merges with I-N curve at dodecyl derivative and then rises upto the last hexadecyl derivative. Here also no odd-even effect is observed in N-I curve. The Cr-M transitions show overall falling tendency from methyl to octyl derivative and then rises upto decyl derivative; the curve then merges with Cr-I curve at dodecyl derivative and then shows overall falling tendency upto the last hexadecyl derivative. Here nematic phase of the series shows schlieren texture.



The average thermal stabilities of all the six series are compared internally with each other. Table 3.25 and figure 3.12 show the average thermal stability for the homologous series.

Table 3.25: Average thermal stability °C

Series	N-I	S-N or S-I	Commencement of smectic mesophase
I	189.70 (C ₁ to C ₁₀)	116.80 (C ₈ to C ₁₆)	C ₈
II	143.80 (C ₁ to C ₁₂)	103.66 (C ₁₂ to C ₁₆)	C ₁₂
III	117.09 (C ₁ to C ₁₄)	88.00 (C ₁₄ to C ₁₀)	C ₁₄
IV	147.19 (C ₁ to C ₁₆)	89.00 (C ₁₂ to C ₁₆)	C ₁₄
V	131.08 (C ₁ to C ₁₆)	–	–
VI	131.58 (C ₁ to C ₁₆)	–	–

Comparison of average thermal stabilities of all six series (Table 3.25) shows that both the N-I and S-N/S-I average thermal stabilities of series I are higher than series II, III and IV. Series V and VI show only nematic mesophase and the average N-I thermal stabilities of both the series are lower than that of series I. Compared to the laterally unsubstituted analogous series I, the breadth of the molecules of series II to V is increased due to the presence of a lateral group on central benzene ring and both the S-N/S-I and N-I average thermal stabilities are decreased [301]. The difference in commencement of mesophase type is because of the different nature and position of lateral substitution [301]. The average N-I thermal stability of series I is 189.7 °C, series II is 143.8 °C and series III is 117.09 °C similarly the average S-N/S-I thermal stability of the series I is 116.8 °C and that of series II is 103.6 °C and series III is 88 °C. Series II and series III has lateral chloro and lateral methyl group on ortho position to the -COO- central linkage respectively, whereas series I is laterally unsubstituted. Thus, average N-I and S-N/S-I thermal stabilities of series II and series III are lower than those of series I, whereas both the N-I and S-N/S-I thermal stabilities of series III are lower than those of series II. The average N-I thermal stability of series I is

189.7 °C, series IV is 147.19 °C and series V is 131.08 °C similarly the average S-N/S-I thermal stability of the series I is 116.8 °C and that of series IV is 89 °C; whereas series V shows only nematic mesophase. Series IV and series V has lateral chloro and lateral methyl group on ortho position to the azo central linkage respectively, whereas series I is laterally unsubstituted. Thus, average N-I thermal stabilities of series IV and series V are lower than those of series I, while the average S-N thermal stability of series IV is lower than that of series I; whereas series V shows only nematic mesophase. The N-I thermal stability of series V is lower than that of series IV. The lateral group order can be derived from the comparison of average thermal stabilities of the current series II to V is,

Nematic order : decreasing sequence: CH₃ > Cl

Smectic order : decreasing sequence: CH₃ > Cl

The average N-I thermal stability of series I is 189.7 °C, and series VI is 131.58 °C. Series I and series VI differ only in their central ring system; series I has central phenyl ring and series VI has central naphthalene ring while other features are same. In series VI with central naphthalene ring, the axes of the substituents are collinear, but the second ring protrudes from the molecule like a large substituent [314] to increases the breadth of the molecule and last three members of the series VI show monotropic mesophase [315-317]; moreover, the effect of the central naphthalene ring causes disruption in the molecular packing, because of all these factors the smectic mesophase is disappeared and N-I thermal stability is decreased compared to series I.

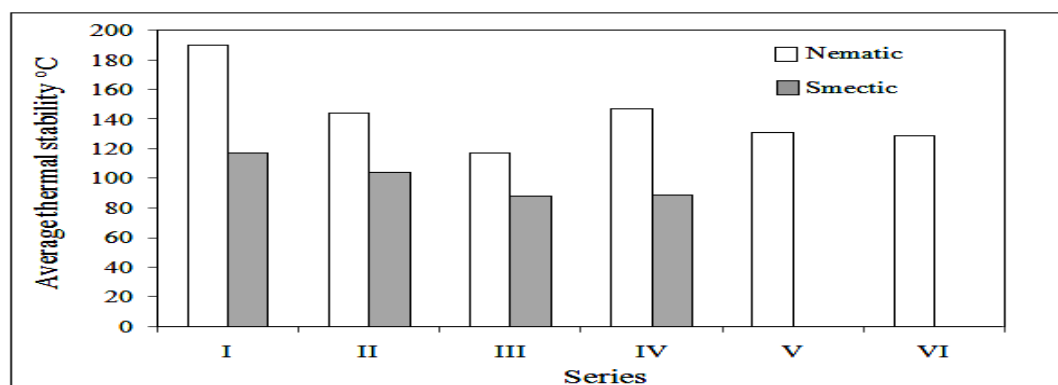
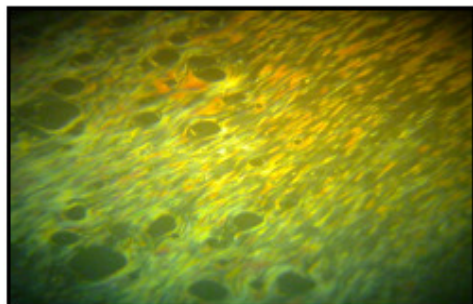
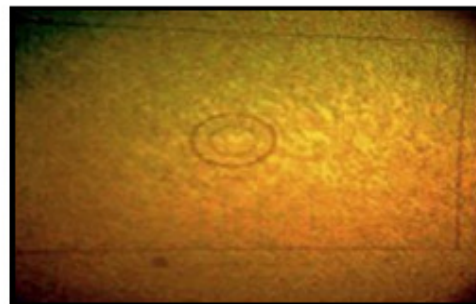


Figure 3.12: Average thermal stability for the series I to VI.

Figure 3.13 shows the photomicrographs of textures of the representative derivatives.

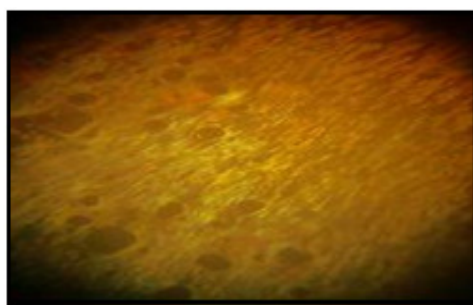


(a) Schlieren texture of Smectic phase



(b) Marble texture of nematic phase

Photomicrographs of the textures of Decyl homologue of series I



(c) Schlieren texture of Smectic phase

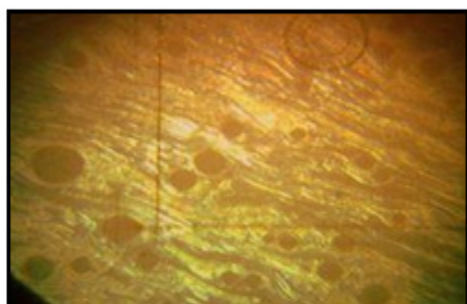
Tetradecyl homologue



(d) Marble texture of nematic phase

Butyl homologue

Photomicrographs of series II



(e) Schlieren texture of Smectic phase

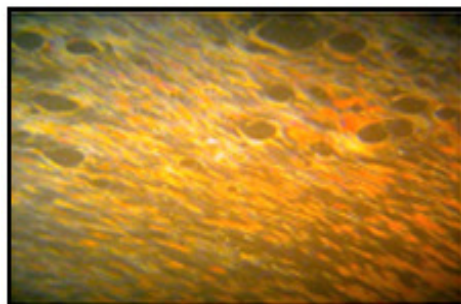
Hexadecyl homologue



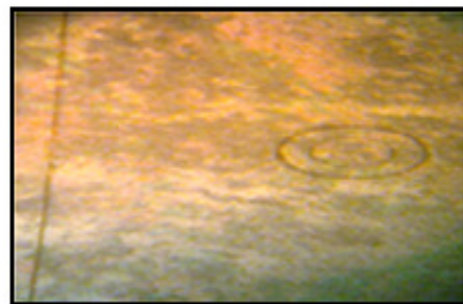
(f) Marble texture of nematic phase

Propyl homologue

Photomicrographs of series III

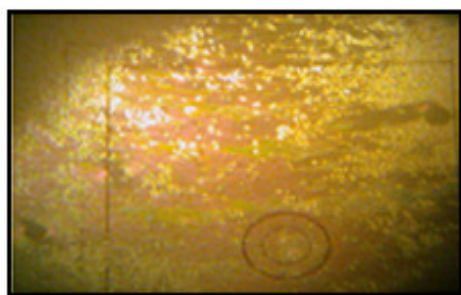


(g) Schlieren texture of Smectic phase



(h) Marble texture of nematic phase

Photomicrographs of the textures of Hexadecyl homologue of series IV

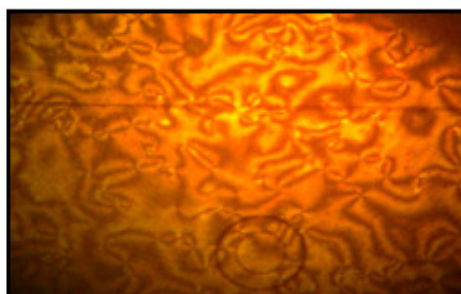


(i) Marble texture of nematic phase
Ethyl homologue



(j) Marble texture of nematic phase
Hexadecyl homologue

Photomicrographs of series V



(k) Schlieren texture of nematic phase
Butyl homologue



(l) Schlieren texture of nematic phase
Heptyl homologue

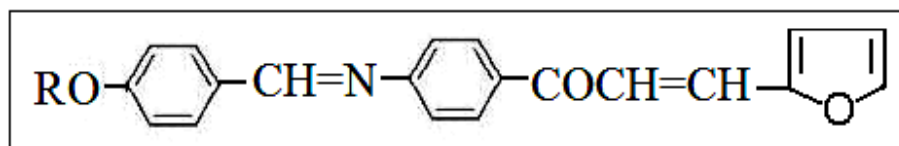
Photomicrographs of series VI

Figure 3.13: Photomicrographs of the textures of the representative homologues

4.1 Introduction

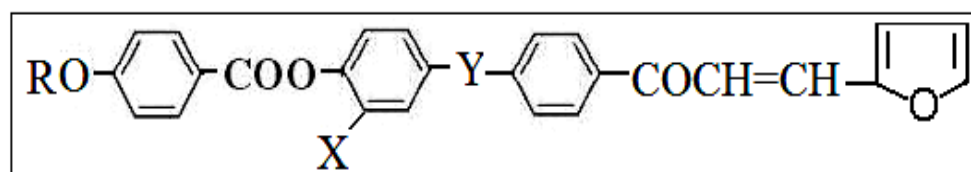
Central linkage is an important part of chemical structure of liquid crystals molecule and effects mesomorphic properties of liquid crystals [318]. It has been observed that chalcone central linkage is comparatively less conducive to mesomorphism as compared to azomethine, azo and ester central linkages due to the non linearity and angle strain arising from the keto group; however, when chalcone linkage is present with other central linkages it becomes conducive to mesomorphism [319-323]. Liquid crystalline derivatives having heterocyclic moieties with chalcone as one of the central linkages are comparatively less explored [324-327]. In view of this four homologous series (VII to X) are synthesized consisting of furfural moiety and chalcone as one of the central linkages along with other central linkages.

General molecular structure of series VII



Where, R is C_nH_{2n+1} $n=1$ to 8, 10, 12, 14 and 16

General molecular structure of series VIII, IX, X



Where, R is C_nH_{2n+1} $n=1$ to 8, 10, 12, 14 and 16

Series	X	Y
VIII	-H	-CH=N-
IX	-OCH ₃	-CH=N-
X	-H	-C=N- CH ₃

4.2 Experimental

4.2.1 Materials

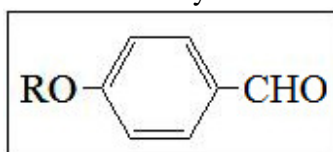
4-hydroxybenzoic acid, 4-hydroxybenzaldehyde, 3-methoxy-4-hydroxybenzaldehyde, 4-hydroxyacetophenone, n-alkyl halides, thionylchloride, 4-aminoacetophenone, furfural and all other chemicals are of Merck, SRL or Loba grade and used as received.

4.2.2 Synthesis

4.2.2.1 Series VII : 1-(4-(4'-n-alkoxybenzylideneamino)-phenyl)-3-(furan-2-yl)-prop-2-en-1-ones

4.2.2.1.a 4-n-alkoxybenzaldehydes

General molecular structure of 4-n-alkoxybenzaldehydes



Where, R is C_nH_{2n+1} $n= 1$ to 8, 10, 12, 14 and 16

Commercially available 4-methoxybenzaldehyde (anisaldehyde, SRL make) is used. Number of methods are known for the alkylation of 4-hydroxybenzaldehyde [328-329]. In the present study, the method developed by Gray and Jones [328] is followed.

0.1 mol of 4-hydroxybenzaldehyde is dissolved in 80 ml dry acetone. 0.15 mol anhydride potassium carbonate and 0.15 mol of n-alkylbromide are added and the solution is refluxed in water bath for five hours. In the case of higher members the reflux period is extended upto 8 hours. The mass is added to water and aldehyde thus separated is extracted with ether. Ether extract is washed with dil. NaOH to remove unreacted 4-hydroxyaldehyde followed by water and dried.

4.2.2.1.b 1-(4-aminophenyl)-3-(furan-2-yl)-prop-2-en-1-one

Molecular structure of 1-(4-aminophenyl)-3-(furan-2-yl)-prop-2-en-1-one



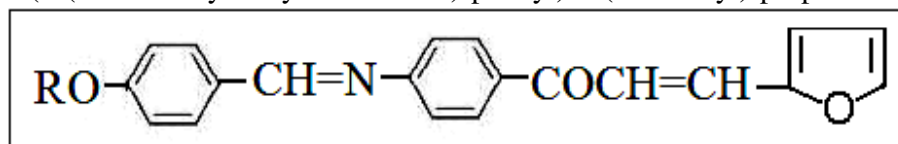
1-(4-aminophenyl)-3-(furan-2-yl)-prop-2-en-1-one is synthesised by known method [330].

0.1 mol 4-aminoacetophenone and 0.1 mol furfural are dissolved in 50 ml ethanol. 10 ml of 20 % aq. NaOH solution is added with stirring. The reaction mixture is stirred for 3 hours and then left over night at room temperature. The product is added to cold solution of 1:1 HCl with stirring. Separated product is filtered, washed with water and dried. The product is recrystallised from acetone.

4.2.2.1.c 1-(4-(4'-n-alkoxybenzylideneamino)-phenyl)-3-(furan-2-yl)-prop-2-en-1-ones

General molecular structure of

1-(4-(4'-n-alkoxybenzylideneamino)-phenyl)-3-(furan-2-yl)-prop-2-en-1-ones



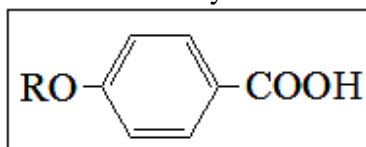
Where, R is C_nH_{2n+1} $n= 1$ to 8, 10, 12, 14 and 16

1-(4-(4'-n-alkoxybenzylideneamino)-phenyl)-3-(furan-2-yl)-prop-2-en-1-ones are synthesised by taking equimolar quantities of appropriate 4-n-alkoxybenzaldehyde and 1-(4-aminophenyl)-3-(furan-2-yl)-prop-2-en-1-one in minimum quantity of ethanol with a few drops of glacial acetic acid and refluxing it for a period of 6 hours. The products are filtered, dried and recrystallized from acetone until constant transition temperatures are obtained. They are recorded in table 4.1. The elemental analysis of all the compounds are found to be satisfactory and are recorded in table 4.2.

4.2.2.2 Series VIII : 1-(4-(4'-(4''-n-alkoxybenzoyloxy)-benzylidene amino)-phenyl)-3-(furan-2-yl)-prop-2-en-1-ones

4.2.2.2.a 4-n-alkoxybenzoicacids

General molecular structure of 4-n-alkoxybenzoicacids

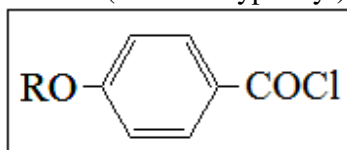


Where, R is C_nH_{2n+1} $n= 1$ to 8, 10, 12, 14 and 16

They are synthesized following the procedure reported in 3.2.2.1.a. [312].

4.2.2.2.b 1-(4-n-alkoxyphenyl)-2-chloroethanones

General molecular structure of 1-(4-n-alkoxyphenyl)-2-chloroethanones

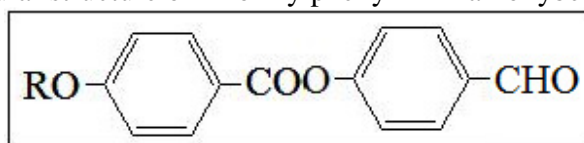


Where, R is C_nH_{2n+1} $n= 1$ to 8, 10, 12, 14 and 16

They are synthesized following the procedure reported in 3.2.2.1.b. [312].

4.2.2.2.c 4-formylphenyl-4'-n-alkoxybenzoates

General molecular structure of 4-formylphenyl-4'-n-alkoxybenzoates



Where, R is C_nH_{2n+1} $n= 1$ to 8, 10, 12, 14 and 16

They are prepared by condensing the appropriate 1-(4-n-alkoxyphenyl)-2-chloroethanones with 4-hydroxybenzaldehyde following the similar method reported in step 3.2.2.1.d. The aldehydes are recrystallized from methanol until constant transition temperatures are obtained [331].

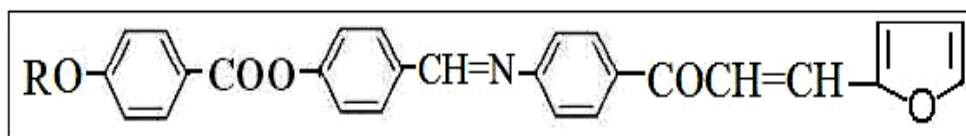
4.2.2.2.d 1-(4-aminophenyl)-3-(furan-2-yl)-prop-2-en-1-one

This is synthesized following the procedure reported in 4.2.2.1.b [330].

4.2.2.2.e 1-(4-(4'-(4''-n-alkoxybenzoyloxy)-benzylideneamino)-phenyl)-3-(furan-2-yl)-prop-2-en-1-ones

General molecular structure of

1-(4-(4'-(4''-n-alkoxybenzoyloxy)-benzylideneamino)-phenyl)-3-(furan-2-yl)-prop-2-en-1-ones



Where, R is C_nH_{2n+1} $n= 1$ to 8, 10, 12, 14 and 16

They are synthesised by taking equimolar quantities of appropriate 4-formylphenyl-4'-n-alkoxybenzoates and 1-(4-aminophenyl)-3-(furan-2-yl)-prop-2-en-1-one following the similar method reported in step 4.2.2.1.c. The products are filtered, dried and recrystallized from acetone until constant transition temperatures are obtained. They are recorded in table 4.5. The elemental analysis of all the compounds are found to be satisfactory and are recorded in table 4.6.

4.2.2.3 Series IX : 1-(4-(4'-(4''-n-alkoxybenzoyloxy)-2'-methoxybenzylideneamino)-phenyl)-3-(furan-2-yl)-prop-2-en-1-ones**4.2.2.3.a 4-n-alkoxybenzoicacids**

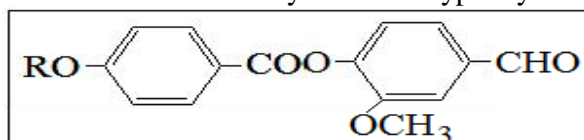
They are synthesized following the procedure reported in 3.2.2.1.a [312].

4.2.2.3.b 1-(4-n-alkoxyphenyl)-2-chloroethanones

They are synthesized following the procedure reported in 3.2.2.1.b [312].

4.2.2.3.c 4-formyl-2-methoxyphenyl-4'-n-alkoxybenzoates

General molecular structure of 4-formyl-2-methoxyphenyl-4'-n-alkoxybenzoates



Where, R is C_nH_{2n+1} $n= 1$ to 8, 10, 12, 14 and 16

They are prepared by condensing the appropriate 1-(4-n-alkoxyphenyl)-2-chloroethanones with 3-methoxy-4-hydroxybenzaldehyde following the similar method reported in step 3.2.2.1.d. The aldehydes are recrystallized from methanol.

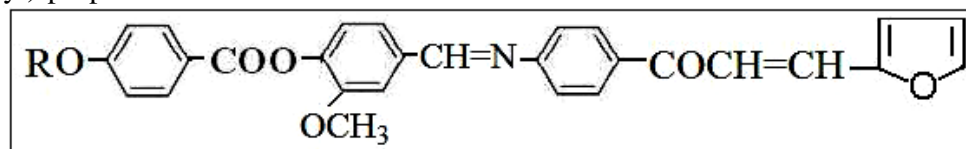
4.2.2.3.d 1-(4-aminophenyl)-3-(furan-2-yl)-prop-2-en-1-one

This is synthesized following the procedure reported in 4.2.2.1.b [330].

4.2.2.3.e 1-(4-(4'-(4''-n-alkoxybenzoyloxy)-2'-methoxybenzylideneamino)-phenyl)-3-(furan-2-yl)-prop-2-en-1-ones

General molecular structure of

1-(4-(4'-(4''-n-alkoxybenzoyloxy)-2'-methoxybenzylideneamino)-phenyl)-3-(furan-2-yl)-prop-2-en-1-ones



Where, R is C_nH_{2n+1} $n = 1$ to 8, 10, 12, 14 and 16

They are synthesised by taking equimolar quantities of appropriate 4-formyl-2-methoxyphenyl-4'-n-alkoxybenzoates and 1-(4-aminophenyl)-3-(furan-2-yl)-prop-2-en-1-one following the similar method reported in step 4.2.2.1.c. The products are filtered, dried and recrystallized from acetone until constant transition temperatures are obtained. They are recorded in table 4.9. The elemental analysis of all the compounds are found to be satisfactory and are recorded in table 4.10.

4.2.2.4 Series X : 1-(4-(4'-(4''-n-alkoxybenzoyloxy)-phenylethylidene amino)-phenyl)-3-(furan-2-yl)-prop-2-en-1-ones

4.2.2.4.a 4-n-alkoxybenzoicacids

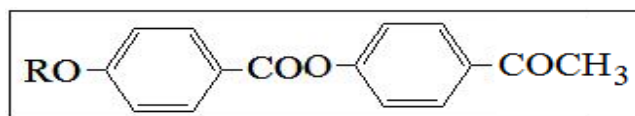
They are synthesized following the procedure reported in 3.2.2.1.a [312].

4.2.2.4.b 1-(4-n-alkoxyphenyl)-2-chloroethanones

They are synthesized following the procedure reported in 3.2.2.1.b [312].

4.2.2.4.c 4-acetylphenyl-4'-n-alkoxybenzoates

General molecular structure of 4-acetylphenyl-4'-n-alkoxybenzoates



Where, R is C_nH_{2n+1} $n= 1$ to 8, 10, 12, 14 and 16

They are prepared by condensing the appropriate 1-(4-n-alkoxyphenyl)-2-chloroethanones with 4-hydroxyacetophenone following the similar method reported in step 3.2.2.1.d. The compounds are recrystallized from methanol until constant transition temperatures are obtained [331].

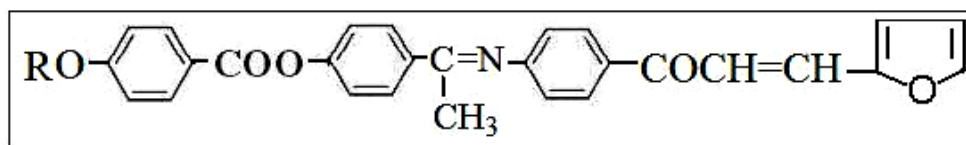
4.2.2.4.d 1-(4-aminophenyl)-3-(furan-2-yl)-prop-2-en-1-one

This is synthesized following the procedure reported in 4.2.2.1.b [330].

4.2.2.4.e 1-(4-(4'-(4''-n-alkoxybenzoyloxy)-phenylethylideneamino)-phenyl)-3-(furan-2-yl)-prop-2-en-1-ones

General molecular structure of

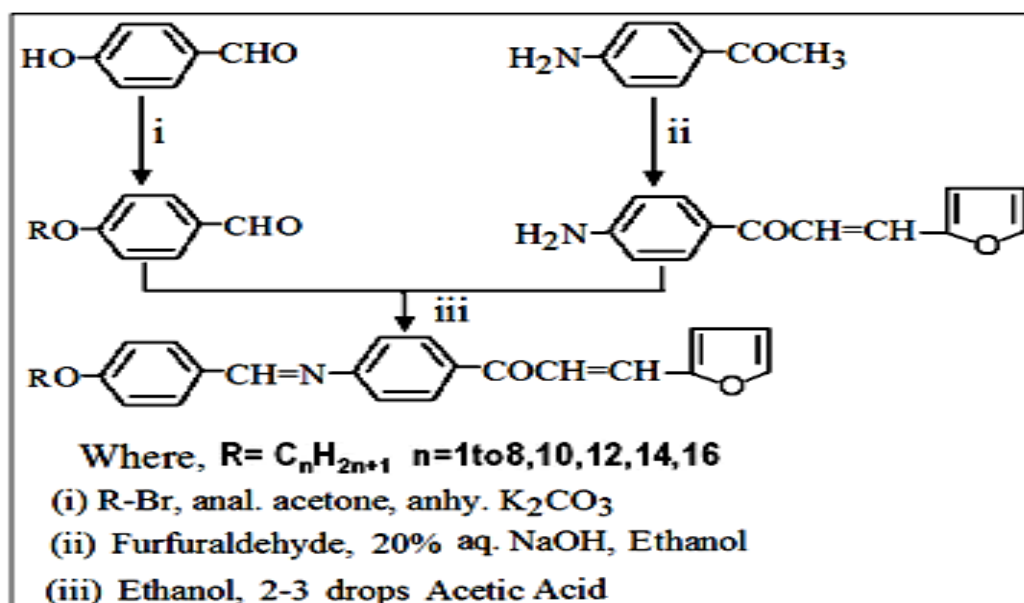
1-(4-(4'-(4''-n-alkoxybenzoyloxy)-ethylideneamino)-phenyl)-3-(furan-2-yl)-prop-2-en-1-ones



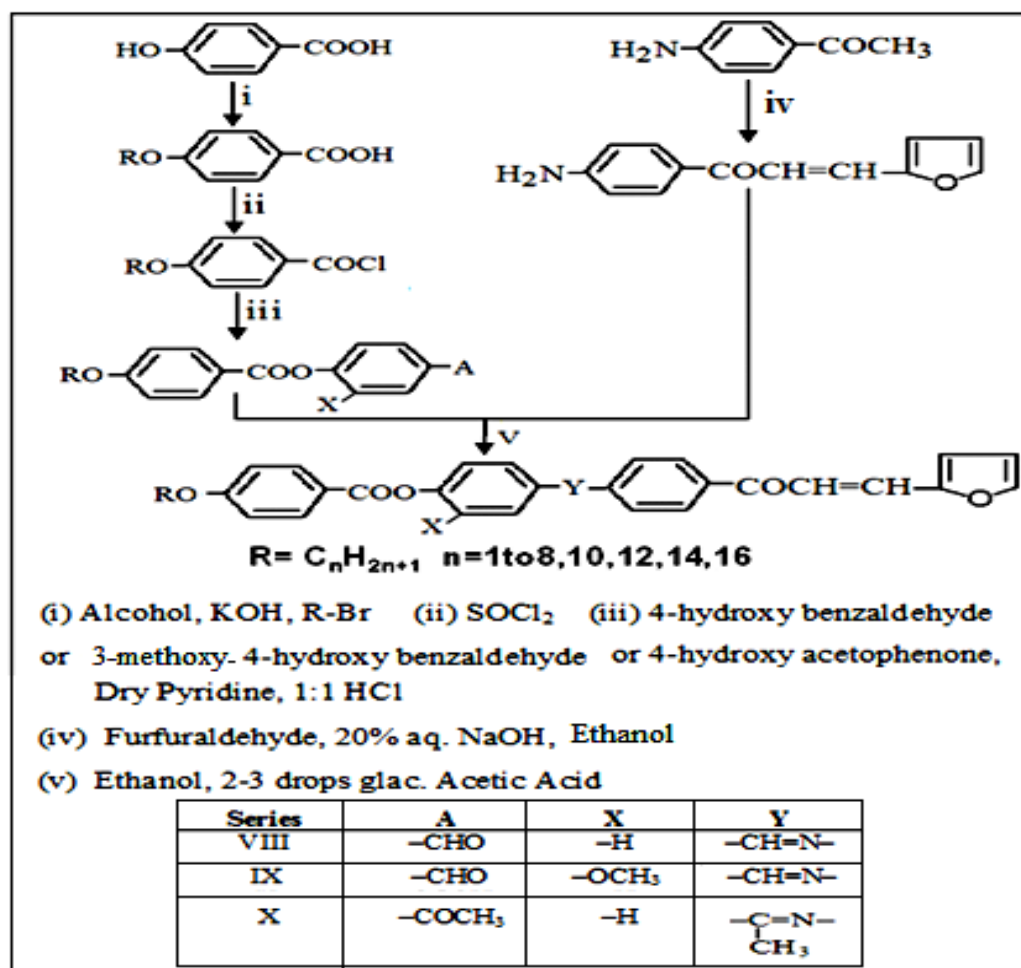
Where, R is C_nH_{2n+1} $n= 1$ to 8, 10, 12, 14 and 16

They are synthesised by taking equimolar quantities of appropriate 4-acetylphenyl-4'-n-alkoxybenzoates and 1-(4-aminophenyl)-3-(furan-2-yl)-prop-2-en-1-one following the similar method reported in step 4.2.2.1.c. The products are filtered, dried and recrystallized from acetone until constant transition temperatures are obtained. They are recorded in table 4.13. The elemental analysis of all the compounds are found to be satisfactory and are recorded in table 4.14.

The synthetic route of series VII and series VIII to X is shown in scheme 4.1 and scheme 4.2 respectively.



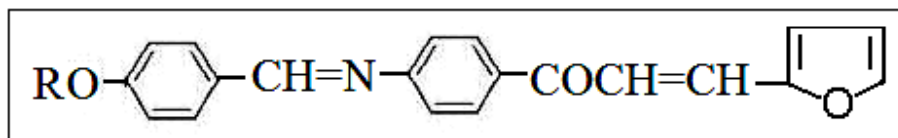
Scheme 4.1: Synthetic route for series VII



Scheme 4.2: Synthetic route for series VIII to X

4.2.3 Characterization

Microanalyses of some of the representative compounds are performed on Perkin Elmer Series II 2400-CHN analyzer, Electronic spectra are recorded on a Shimadzu UV-2450 UV-visible spectrophotometer, IR spectra are recorded on a Perkin Elmer GX-FTIR, ¹H NMR spectra are measured on a Bruker Avance II-500 spectrometer. Mass spectra are recorded on Thermoscientific DSQ II mass spectrometer. Transition temperatures and the textures of the mesophases are studied using Leitz Laborlux 12 POL polarizing microscope provided with a Kofler heating stage. DSC are performed on a Mettler Toledo Star SW 7.01.

Table 4.1: Transition temperatures: 1-(4-(4'-n-alkoxybenzylideneamino)-phenyl)-3-(furan-2-yl)-prop-2-en-1-ones (Series VII)

R=n-alkyl group	Transition Temperatures °C	
	Nematic	Isotropic
Methyl	—	107
Ethyl	—	115
Propyl	—	96
Butyl	(84)	92
Pentyl	(99)	105
Hexyl	(69)	94
Heptyl	(88)	106
Octyl	(100)	114
Decyl	(82)	97
Dodecyl	(90)	103
Tetradecyl	(81)	93
Hexadecyl	(99)	108

Values in parentheses indicates monotropic transitions

Table 4.2: Elemental analysis

Homologue	Calculated			Found		
	C %	H %	N %	C %	H %	N %
Hexyl	77.80	6.73	3.49	77.89	6.84	3.58
Dodecyl	79.17	8.04	2.88	79.45	8.00	2.75
Tetradecyl	79.53	8.38	2.72	79.59	8.25	2.80

FTIR (Nujol, KBr pellets, cm^{-1})

Propyl homologue: 2955, 2928, 1652 (-CH=CH-), 1600, 1394, 1257, 1195 (-CH=N-), 1082 (-CH₂-O-), 939, 848, 692.

Propyl homologue: 2920, 1652 (-CH=CH-), 1590, 1390, 1257, 1168 (-CH=N-), 1082 (-CH₂-O-), 929, 847, 691.

¹H NMR: (CDCl₃, 500 MHz, δ , ppm, standard TMS)

Heptyl homologue: δ 0.91 (3H, t, -CH₃), 1.3-1.84 (m, alkyl chain), 4.04 (2H, t, -OCH₂-CH₂), 6.52 - 7.86 (m, Ar-H), 6.73 and 8.09 (2H, 2xd, -CH=CH-), 8.38 (1H, s, -CH=N-)

Dodecyl homologue: δ 0.89 (3H, t, -CH₃), 1.44-1.84 (m, alkyl chain), 4.02 (2H, t, -OCH₂-CH₂), 6.51-7.86 (m, Ar-H), 6.72 and 8.08 (2H, 2xd, -CH=CH-), 8.3 (1H, s, -CH=N-)

Mass Spectra:

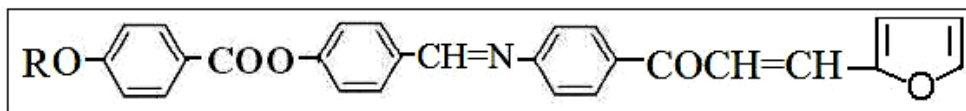
Octyl homologue: MS m/z: 429 (M⁺)

Table 4.3: DSC data

Series	Homologue	Transition Temperature °C	$\Delta H/\text{Jg}^{-1}$	$\Delta S/\text{Jg}^{-1}\text{K}^{-1}$
VII	Butyl	Cr-I 94	74.61	0.2043
		I-N 81	1.0210	0.0028
	Dodecyl	Cr-I 92	57.36	0.1522
		I-N 103	0.9683	0.0026

Table 4.4: UV data

Series	Homologue	UV λ max values nm (solvent- ethyl acetate)	
		$\pi \longrightarrow \pi^*$	$n \longrightarrow \pi^*$
VII	Pentyl	250	352
	Decyl	250	352

Table 4.5: Transition temperatures: 1-(4-(4'-(4''-n-alkoxybenzoyloxy)-benzylideneamino)-phenyl)-3-(furan-2-yl)-prop-2-en-1-ones (Series VIII)

Homologue	Transition Temperatures °C		
	Smectic C	Nematic	Isotropic
Methyl	—	185	273
Ethyl	—	171	286
Propyl	—	148	240
Butyl	—	140	236
Pentyl	—	137	235
Hexyl	129	149	222
Heptyl	113	147	207
Octyl	115	136	194
Decyl	110	129	190
Dodecyl	90	120	156
Tetradecyl	86	116	135
Hexadecyl	90	115	127

Table 4.6: Elemental analysis

Homologue	Calculated			Found		
	C %	H %	N %	C %	H %	N %
Ethyl	74.83	4.94	3.01	74.89	4.91	3.16
Heptyl	76.26	6.16	2.61	76.21	6.10	2.50
Dodecyl	77.35	7.10	2.31	77.39	7.02	2.30

FTIR (Nujol, KBr pellets, cm⁻¹)

Pentyl homologue: 2953, 2939, 1732 (-COO-), 1660 (-CH=CH-), 1606, 1259, 1170 (-CH=N-), 1072 (-CH₂-O-), 962, 754, 690.

Tetradecyl homologue: 2914, 1739 (-COO-), 1662 (-CH=CH-), 1606, 1259, 1176 (-CH=N-), 1078 (-CH₂-O-), 939, 758, 688.

¹H NMR: (CDCl₃, 500 MHz, δ, ppm, standard TMS)

Hexyl homologue: δ 0.9 (3H, t, -CH₃), 1.25-1.85 (m, alkyl chain), 4.04 (2H, t, -OCH₂-CH₂), 6.52 – 8.12 (m, Ar-H), 6.73 and 8.16 (2H, 2xd, -CH=CH-), 8.47 (1H, s, -CH=N-)

Dodecyl homologue: δ 0.89 (3H, t, -CH₃), 1.23-1.84 (m, alkyl chain), 4.0 (2H, t, -OCH₂-CH₂), 6.92-8.12 (m, Ar-H), 6.97 and 8.16 (2H, 2xd, -CH=CH-), 8.47 (1H, s, -CH=N-)

Mass Spectra:

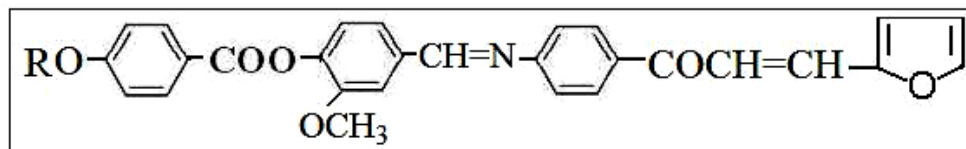
Propyl homologue: MS m/z: 479 (M⁺)

Table 4.7: DSC data

Series	Homologue	Transition Temperature °C	Δ H/Jg ⁻¹	Δ S/Jg ⁻¹ K ⁻¹
VIII	Propyl	Cr-N 146	79.10	1.2600
		N-I 239	0.5403	0.0024
	Hexyl	Cr-S 123	62.85	0.1570
		S-N 151	5.09	0.0119
		N-I 223	1.98	0.0039

Table 4.8: UV data

Series	Homologue	UV λ max values nm (solvent- ethyl acetate)	
		π → π*	n → π*
VIII	Butyl	275	350
	Hexadecyl	275	350

Table 4.9: Transition temperatures: 1-(4-(4'-(4''-n-alkoxybenzoyloxy)-2'-methoxybenzylidene amino)-phenyl)-3-(furan-2-yl)-prop-2-en-1-ones (Series IX)

Homologue	Transition Temperatures $^{\circ}\text{C}$	
	Nematic	Isotropic
Methyl	107	200
Ethyl	140	209
Propyl	116	192
Butyl	145	195
Pentyl	106	169
Hexyl	90	189
Heptyl	105	132
Octyl	95	155
Decyl	103	138
Dodecyl	84	135
Tetradecyl	75	126
Hexadecyl	73	124

Table 4.10: Elemental analysis

Homologue	Calculated			Found		
	C %	H %	N %	C %	H %	N %
Propyl	73.08	5.30	2.75	73.19	5.28	2.83
Octyl	74.61	6.39	2.41	74.75	6.47	2.33
Tetradecyl	76.01	7.39	2.11	76.17	7.31	2.27

FTIR (Nujol, KBr pellets, cm^{-1})

Hexyl homologue: 2916, 1726 (-COO-), 1662 (-CH=CH-), 1608, 1377, 1259, 1176 (-CH=N-), 1078 (-CH₂-O-), 754, 690.

Decyl homologue: 2955, 2916, 1737 (-COO-), 1680 (-CH=CH-), 1606, 1359, 1259, 1170 (-CH=N-), 1064 (-CH₂-O-), 962, 771, 690.

¹H NMR: (CDCl₃, 500 MHz, δ , ppm, standard TMS)

Heptyl homologue: δ 0.9 (3H, t, -CH₃), 1.28-1.84 (m, alkyl chain), 3.88-4.06 (2H, m, -OCH₂-CH₂ and 3H, -OCH₃), 6.52-8.17 (m, Ar-H), 6.73 and 8.10 (2H, 2xd, -CH=CH-), 8.43 (1H, s, -CH=N-)

Hexadecyl homologue: δ 0.89 (3H, t, -CH₃), 1.35-1.83 (m, alkyl chain), 3.88-4.06 (2H, m, -OCH₂-CH₂ and 3H, -OCH₃), 6.52-8.17 (m, Ar-H), 6.73 and 8.12 (2H, 2xd, -CH=CH-), 8.43 (1H, s, -CH=N-)

Mass Spectra:

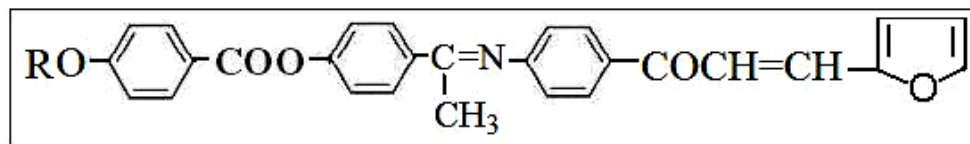
Methyl homologue: MS m/z: 481 (M⁺)

Table 4.11: DSC data

Series	Homologue	Transition Temperature °C	$\Delta H/\text{Jg}^{-1}$	$\Delta S/\text{Jg}^{-1}\text{K}^{-1}$
IX	Hexyl	Cr-N 91	58.93	0.1594
		N-I 192	0.8738	0.0018
	Hexadecyl	Cr-N 70	74.97	0.2120
		N-I 123	1.2128	0.0028

Table 4.12: UV data

Series	Homologue	UV λ max values nm (solvent- ethyl acetate)	
		$\pi \longrightarrow \pi^*$	$n \longrightarrow \pi^*$
IX	Ethyl	275	358
	Pentyl	275	358

Table 4.13: Transition temperatures: 1-(4-(4'-(4''-n-alkoxybenzoyloxy)-phenylethylideneamino)-phenyl)-3-(furan-2-yl)-prop-2-en-1-ones (Series X)

Homologue	Transition Temperatures °C	
	Nematic	Isotropic
Methyl	—	158
Ethyl	—	133
Propyl	—	108
Butyl	(45)	68
Pentyl	(64)	87
Hexyl	86	100
Heptyl	72	108
Octyl	79	110
Decyl	80	114
Dodecyl	78	111
Tetradecyl	80	97
Hexadecyl	75	91

Values in parentheses indicates monotropic transitions

Table 4.8: Elemental analysis

Homologue	Calculated			Found		
	C %	H %	N %	C %	H %	N %
Pentyl	76.00	5.95	2.68	76.06	5.87	2.71
Decyl	77.15	6.93	2.36	77.10	6.90	2.40
Dodecyl	77.54	7.26	2.26	77.53	7.11	2.21

FTIR (Nujol, KBr pellets, cm⁻¹)

Propyl homologue: 2955, 2918, 1732 (-COO-), 1680 (-CH=CH-), 1600, 1359, 1253, 1163 (-C=N-), 1066 (-CH₂-O-), 962, 846, 758, 690.

Heptyl homologue: 2955, 2939, 1739 (-COO-), 1660 (-CH=CH-), 1606, 1359, 1259, 1176 (-C=N-), 1072 (-CH₂-O-), 968, 842, 758, 690.

¹H NMR: (CDCl₃, 500 MHz, δ , ppm, standard TMS)

Butyl homologue: δ 1.0 (3H, t, -CH₃), 1.22 (3H, s, -CH₃ of ethylideneamino), 1.48-1.84 (m, alkyl chain), 4.05 (2H, t, -OCH₂-CH₂), 6.56-7.99 (m, Ar-H), 6.79 and 8.05 (2H, 2xd, -CH=CH-)

Octyl homologue: δ 0.89 (3H, t, -CH₃), 1.25 (3H, s, -CH₃ of ethylideneamino), 1.29-1.84 (m, alkyl chain), 4.03 (2H, t, -OCH₂-CH₂), 6.92 – 8.14 (m, Ar-H), 6.98 and 8.13 (2H, 2xd, -CH=CH-)

Mass Spectra:

Hexyl homologue: MS m/z: 535 (M+1)

Table 4.15: DSC data

Series	Homologue	Transition Temperature °C	$\Delta H/Jg^{-1}$	$\Delta S/Jg^{-1}K^{-1}$
X	Octyl	Cr-N 77	83.37	0.2459
		N-I 111	1.5958	0.0044
	Tetradecyl	Cr-N 80	62.05	0.1850
		N-I 98	1.28	0.0035

Table 4.16: UV data

Series	Homologue	UV λ max values nm (solvent- ethyl acetate)	
		$\pi \longrightarrow \pi^*$	$n \longrightarrow \pi^*$
X	Hexyl	263	351
	Decyl	263	351

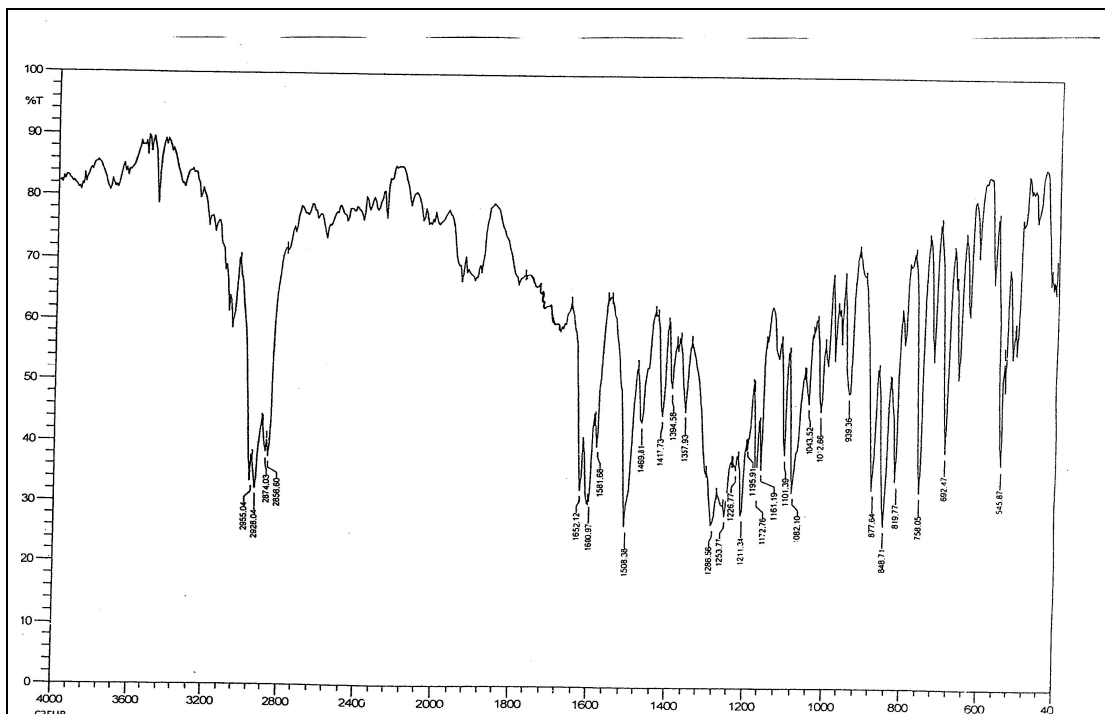


Figure 4.1 (a): IR spectra of C3 homologue of series VII

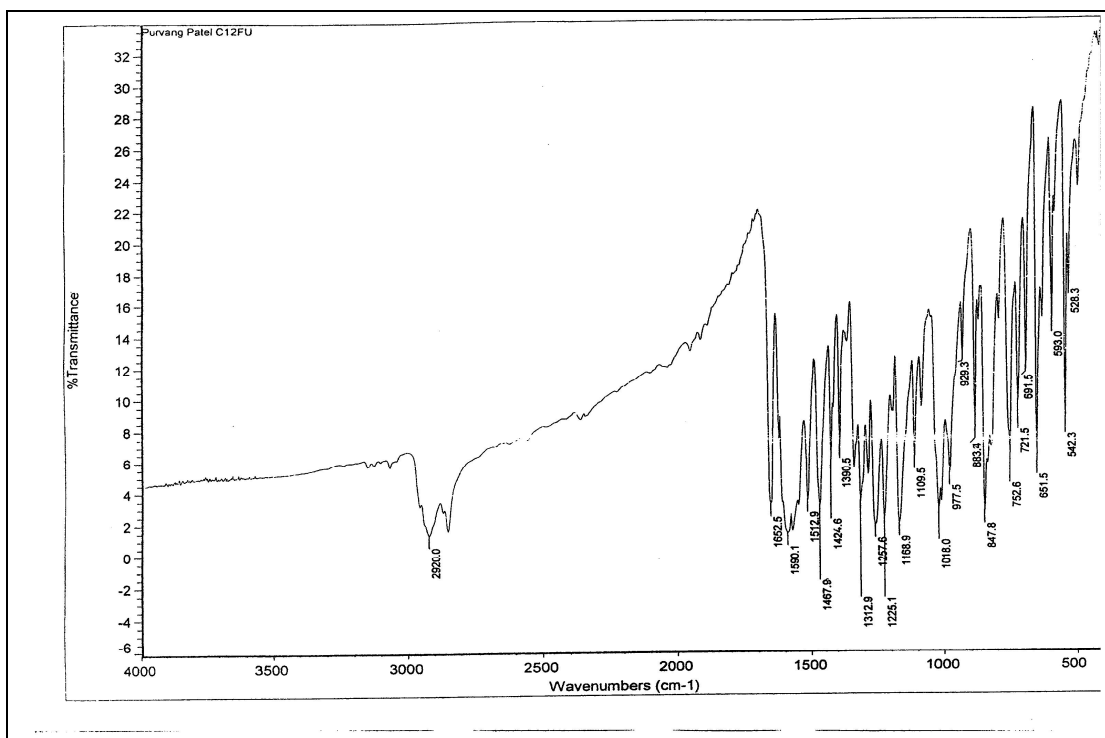


Figure 4.1 (b): IR spectra of C12 homologue of series VII

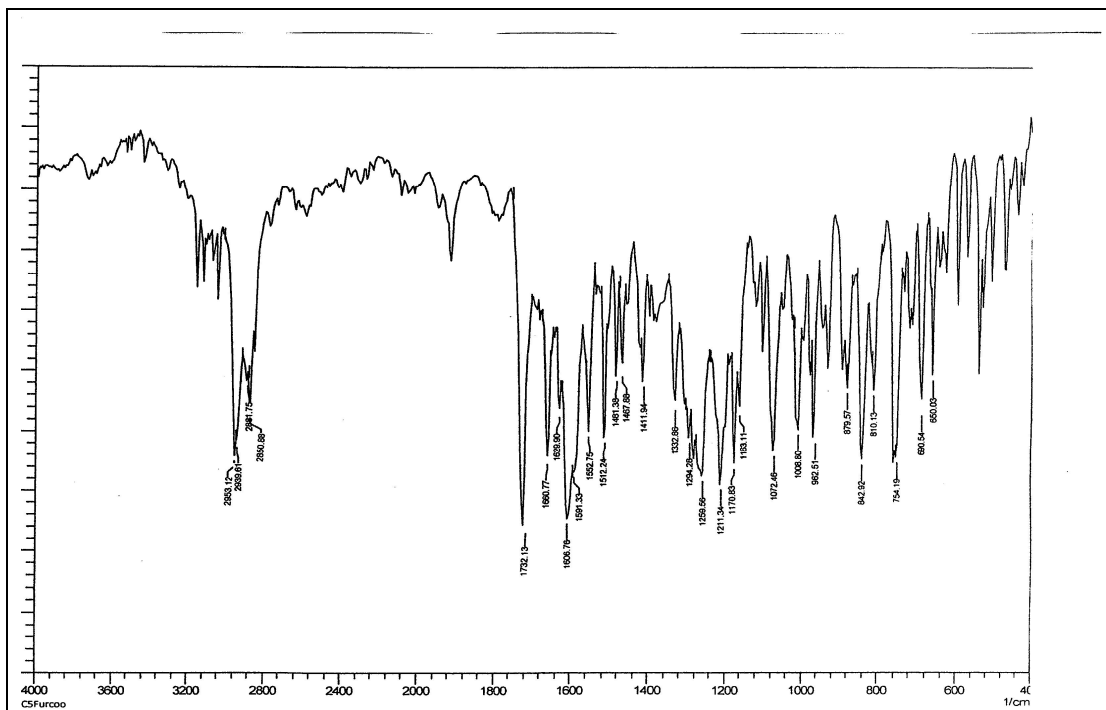


Figure 4.1 (c): IR spectra of C5 homologue of series VIII

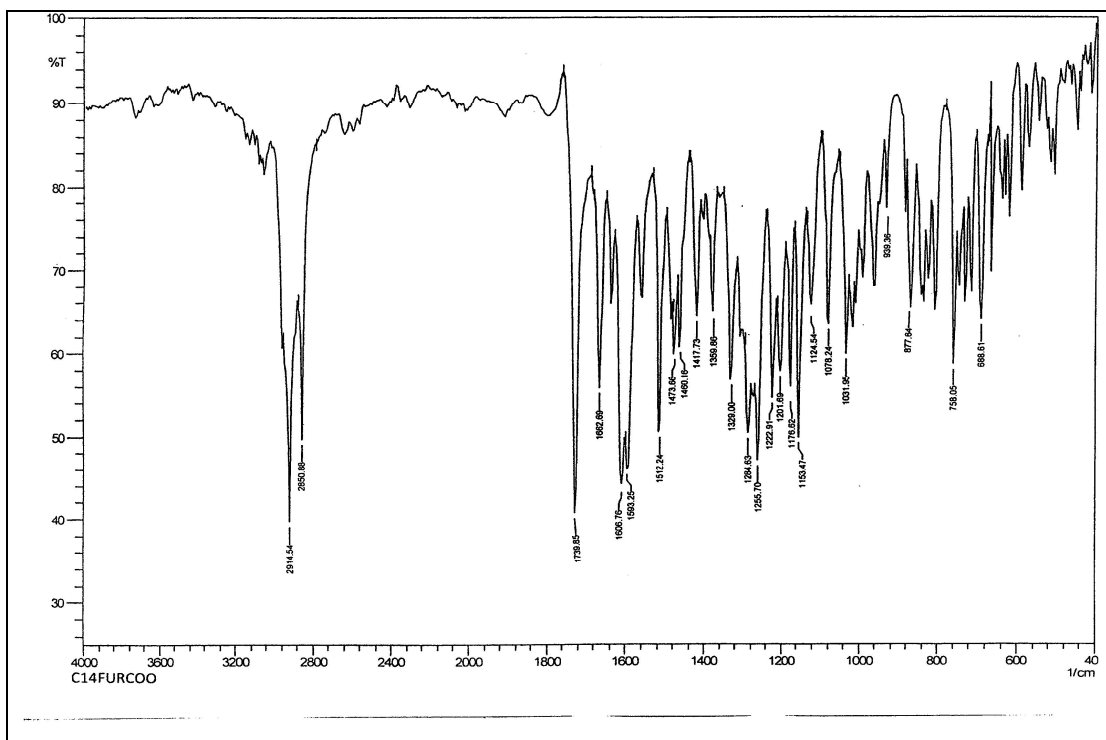


Figure 4.1 (d): IR spectra of C14 homologue of series VIII

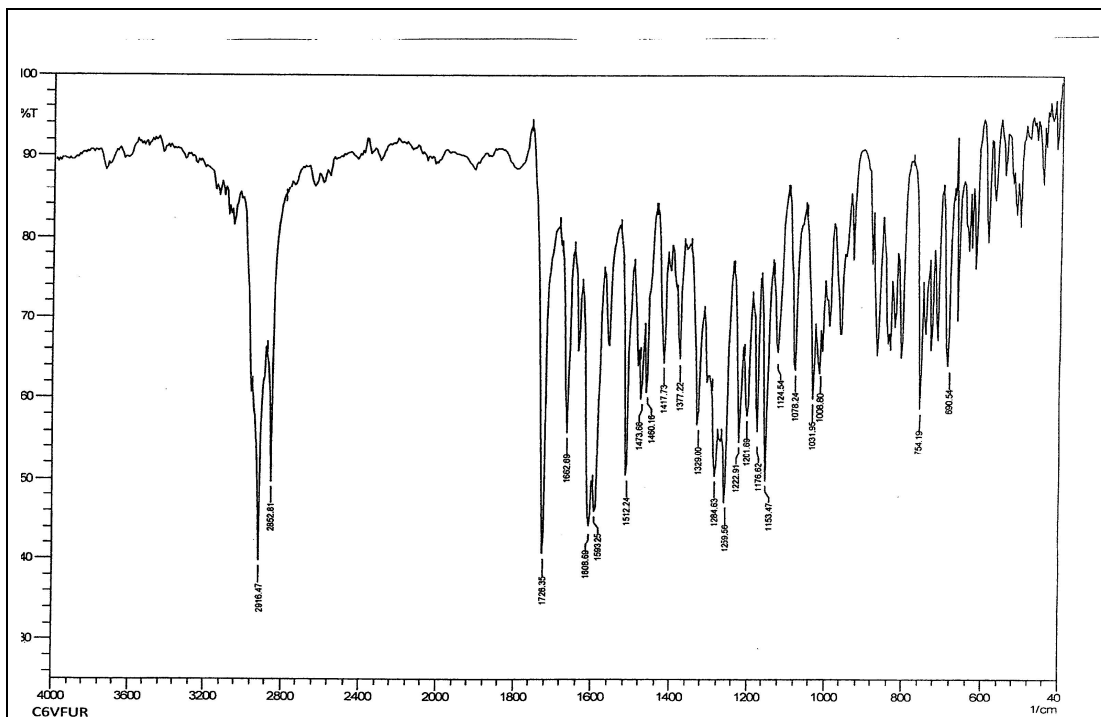


Figure 4.1 (e): IR spectra of C6 homologue of series IX

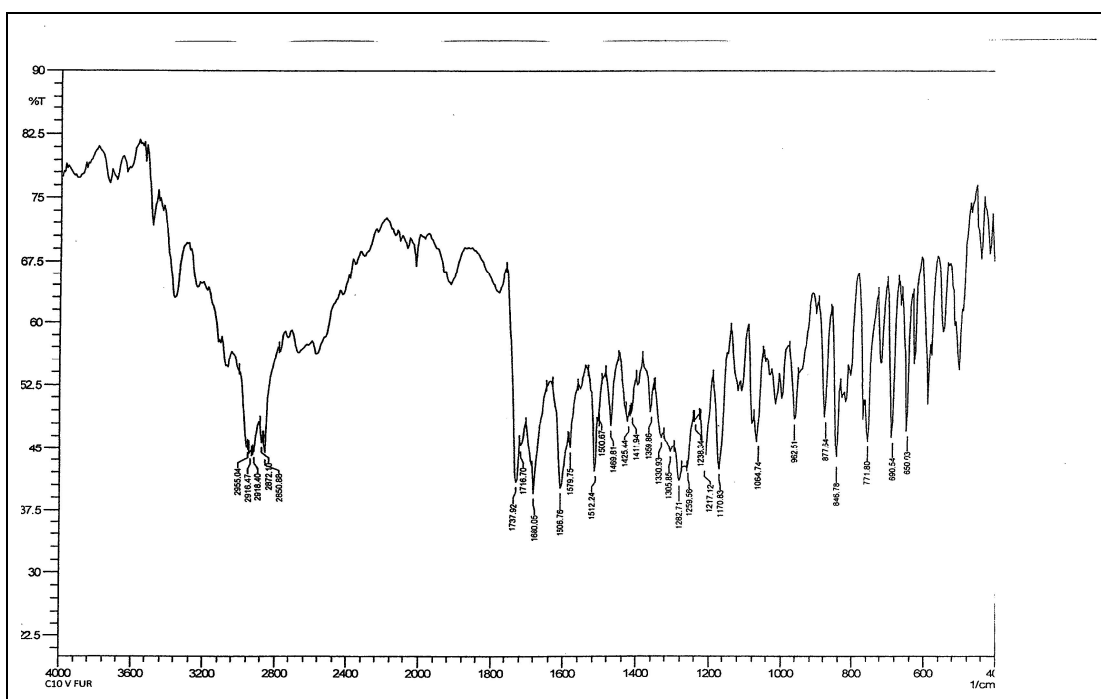


Figure 4.1 (f): IR spectra of C10 homologue of series IX

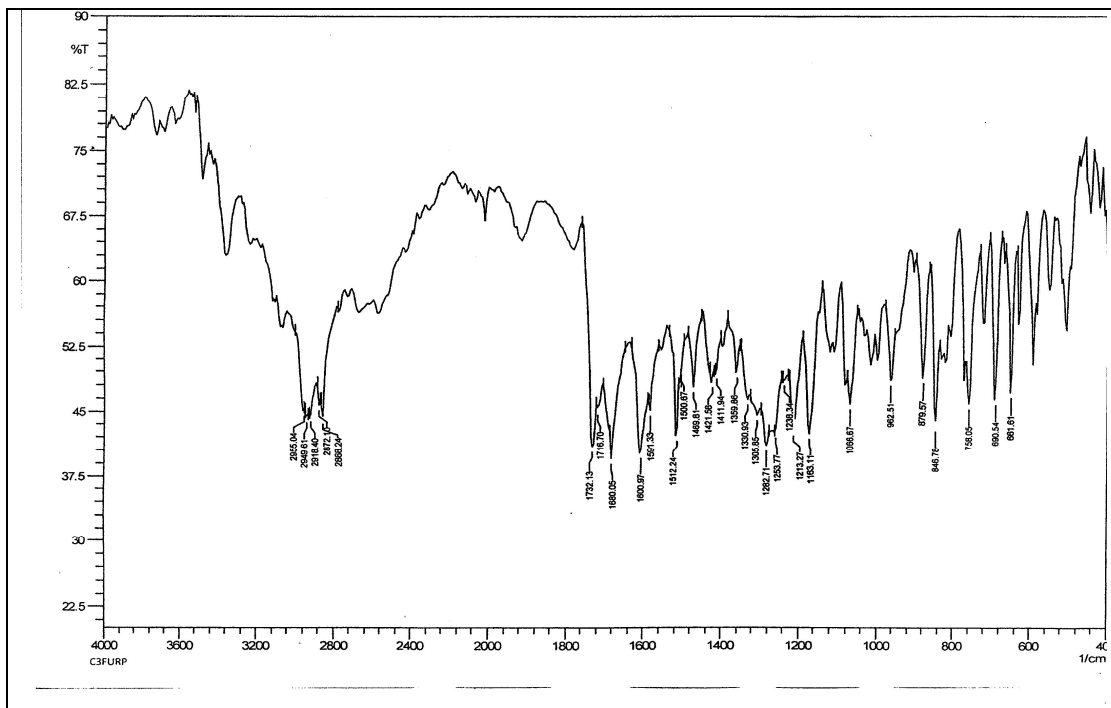


Figure 4.1 (g): IR spectra of C3 homologue of series X

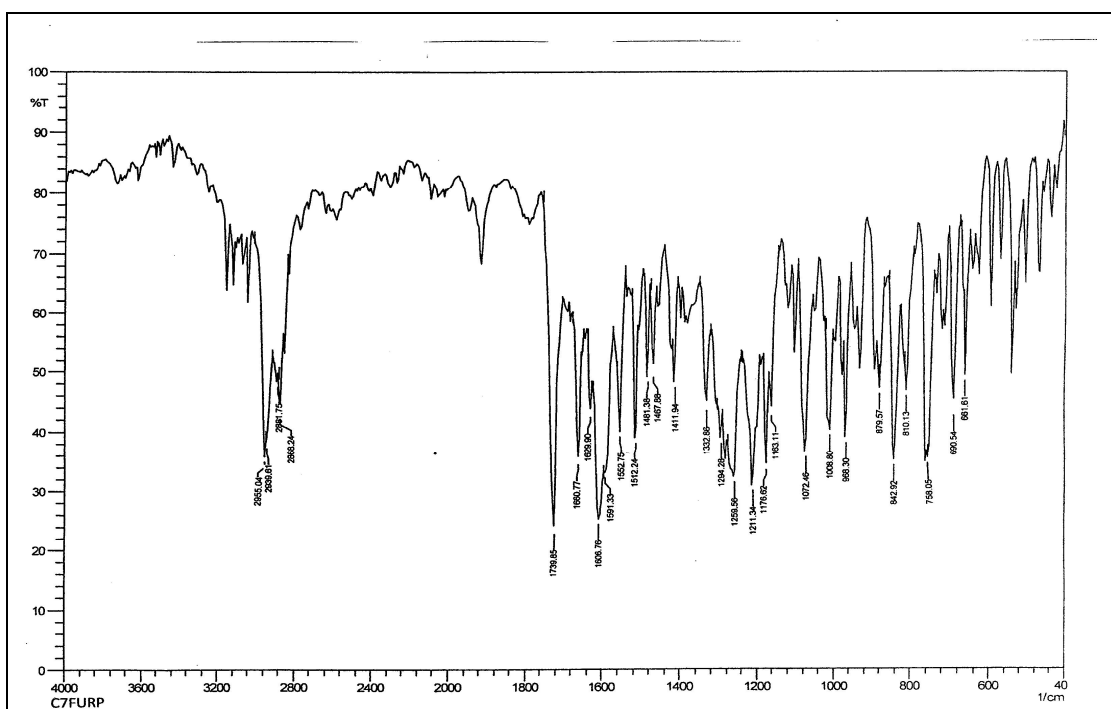


Figure 4.1 (h): IR spectra of C7 homologue of series X

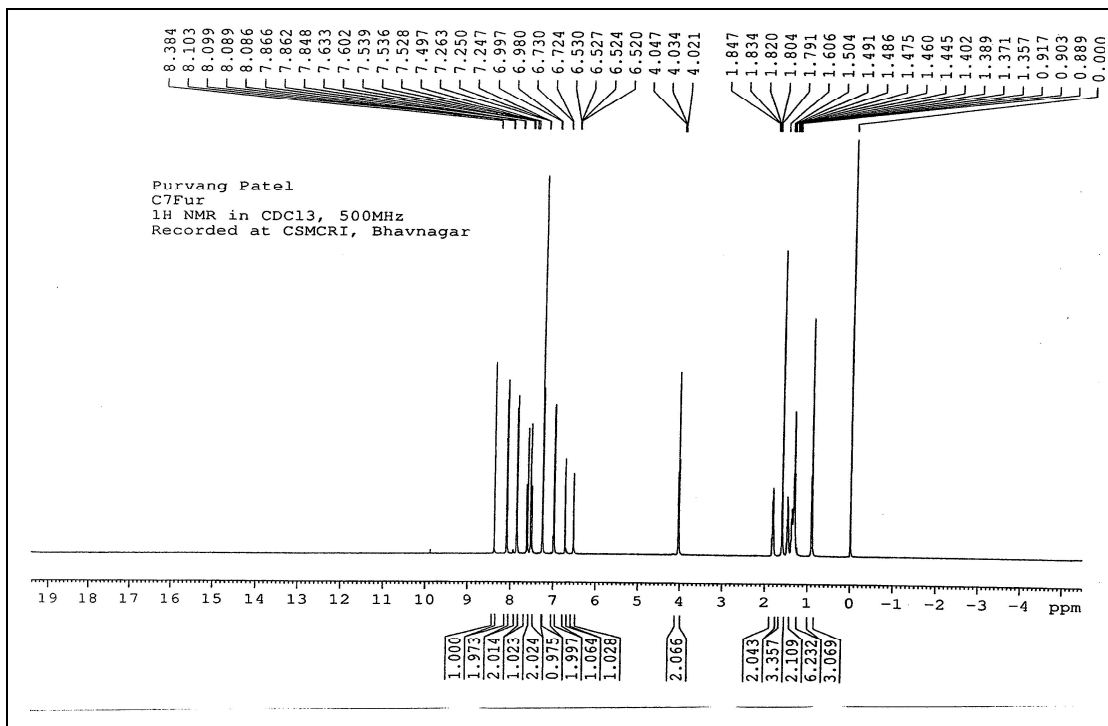


Figure 4.2 (a): ^1H NMR spectra of C7 homologue of series VII

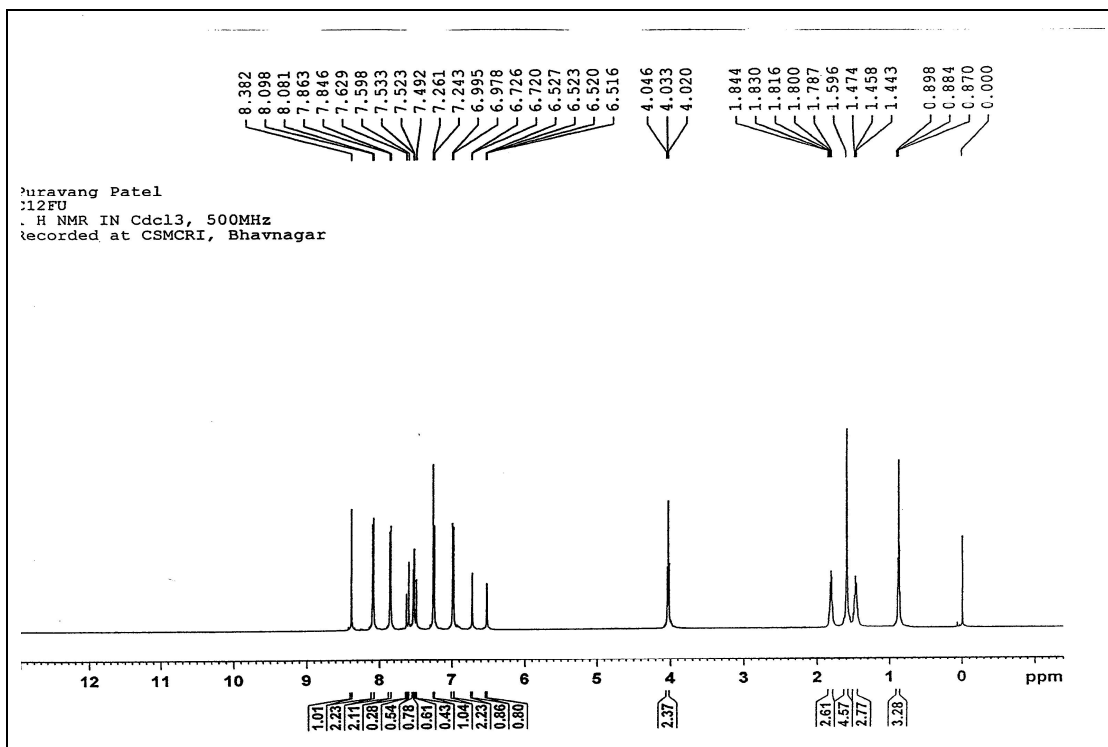


Figure 4.2 (b): ^1H NMR spectra of C12 homologue of series VII

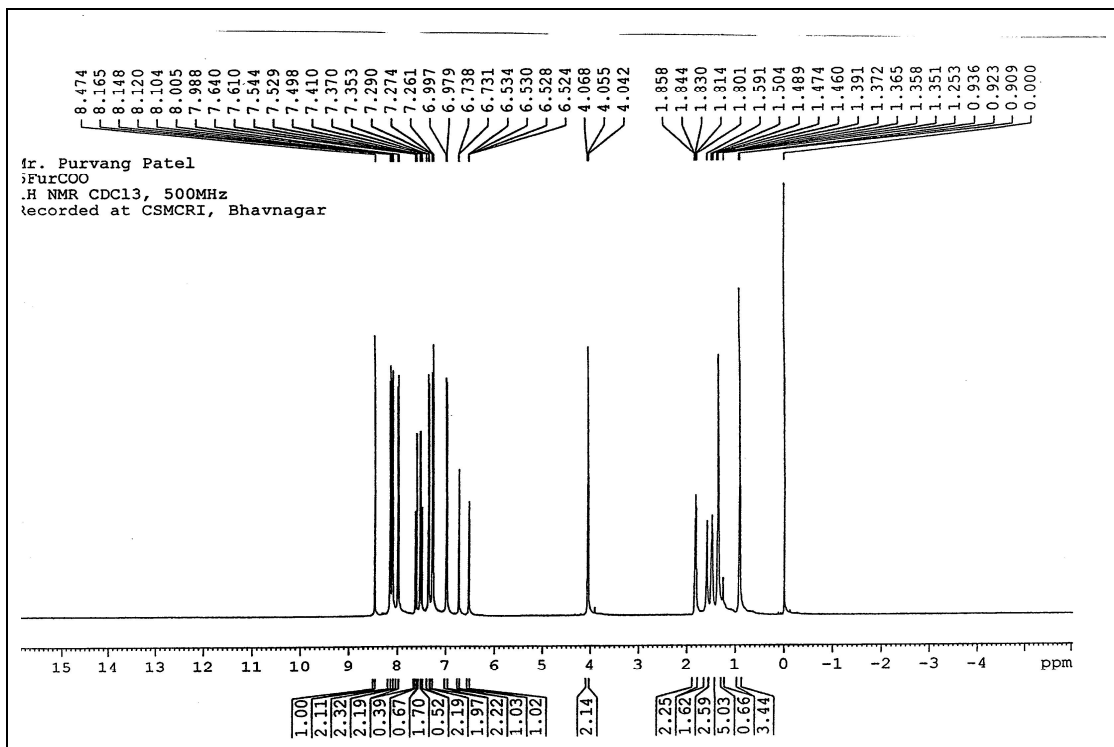


Figure 4.2 (c): ^1H NMR spectra of C6 homologue of series VIII

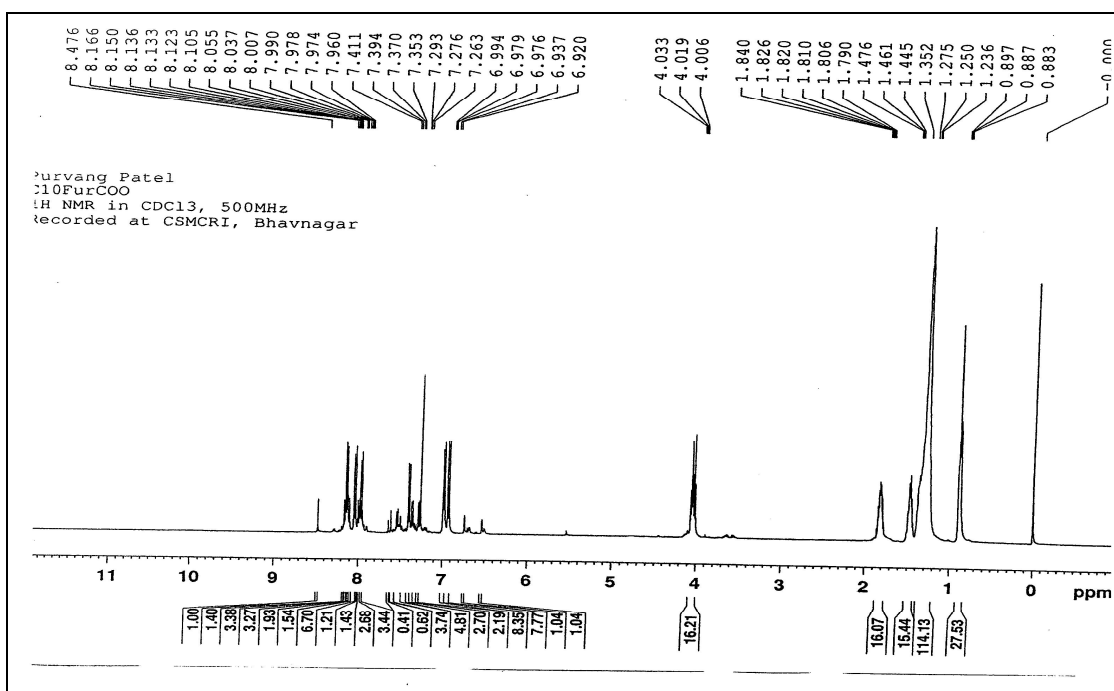


Figure 4.2 (d): ^1H NMR spectra of C10 homologue of series VIII

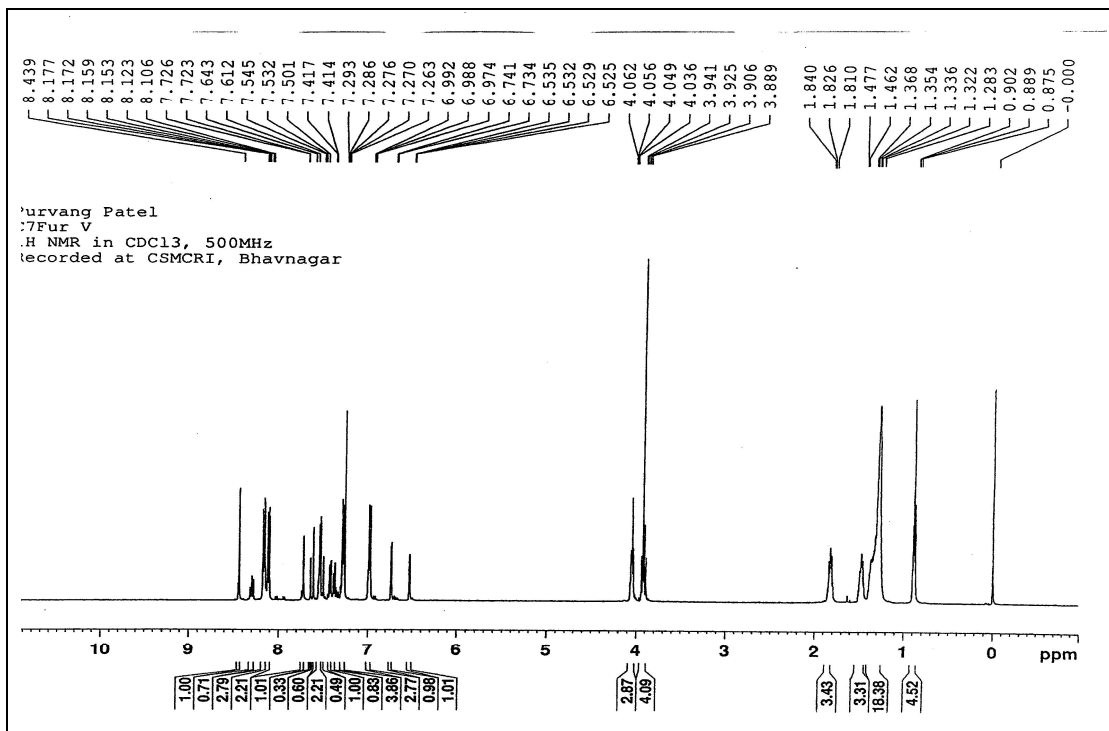


Figure 4.2 (e): ¹H NMR spectra of C7 homologue of series IX

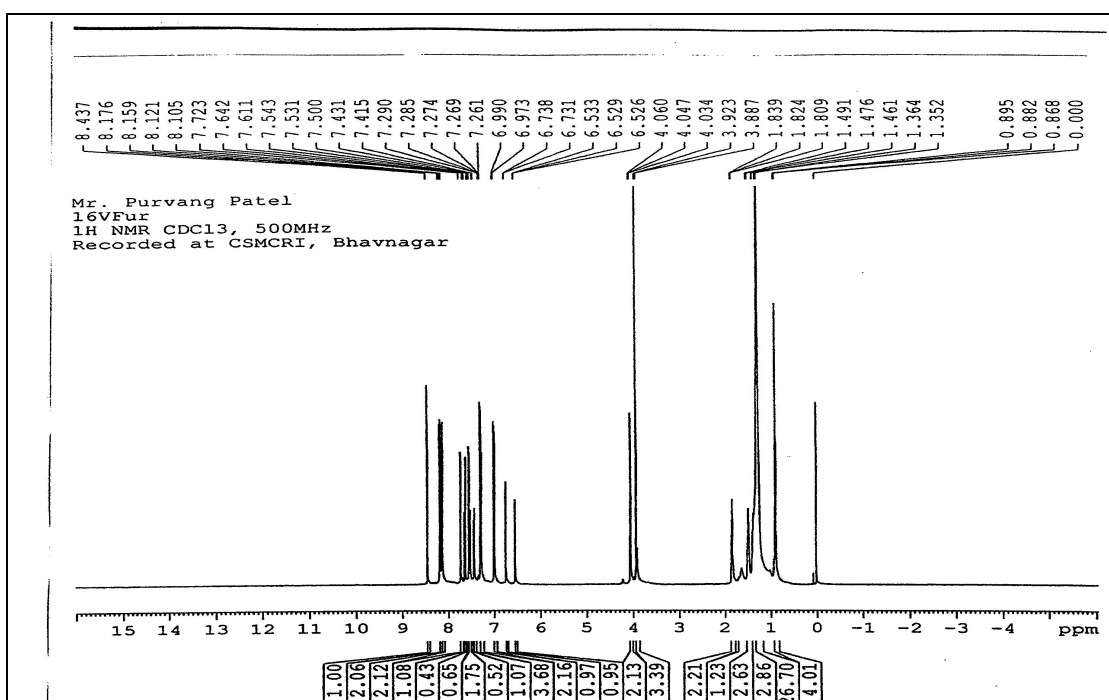


Figure 4.2 (f): ¹H NMR spectra of C16 homologue of series IX

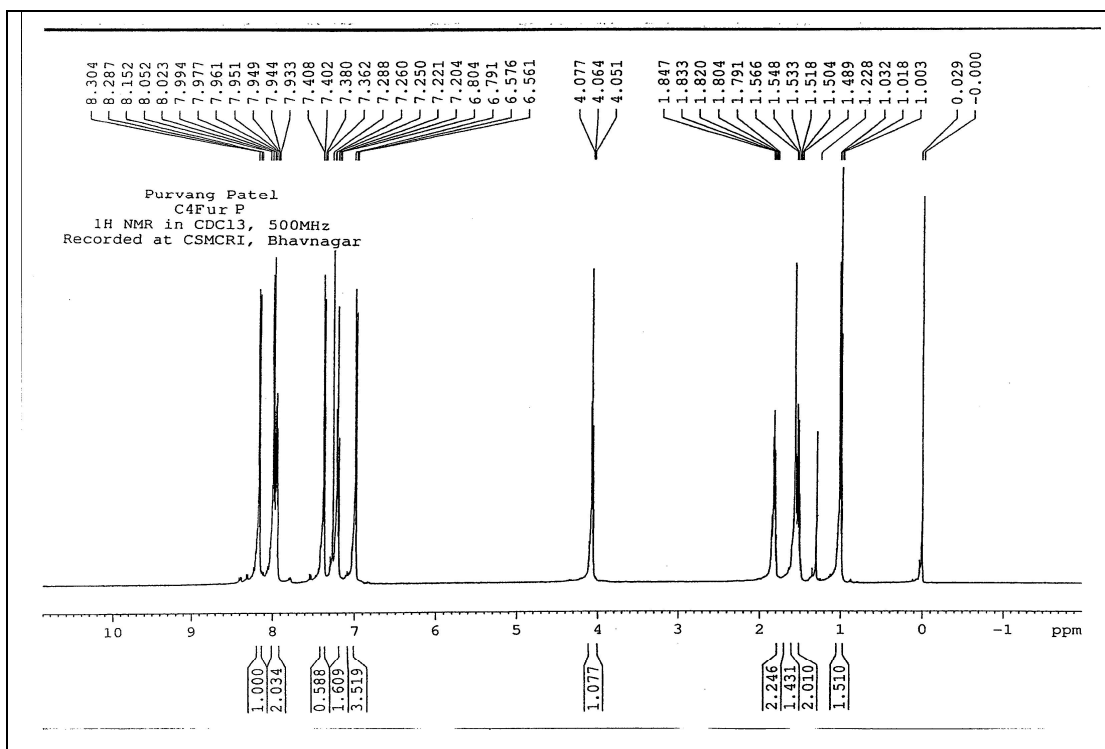


Figure 4.2 (g): ¹H NMR spectra of C4 homologue of series X

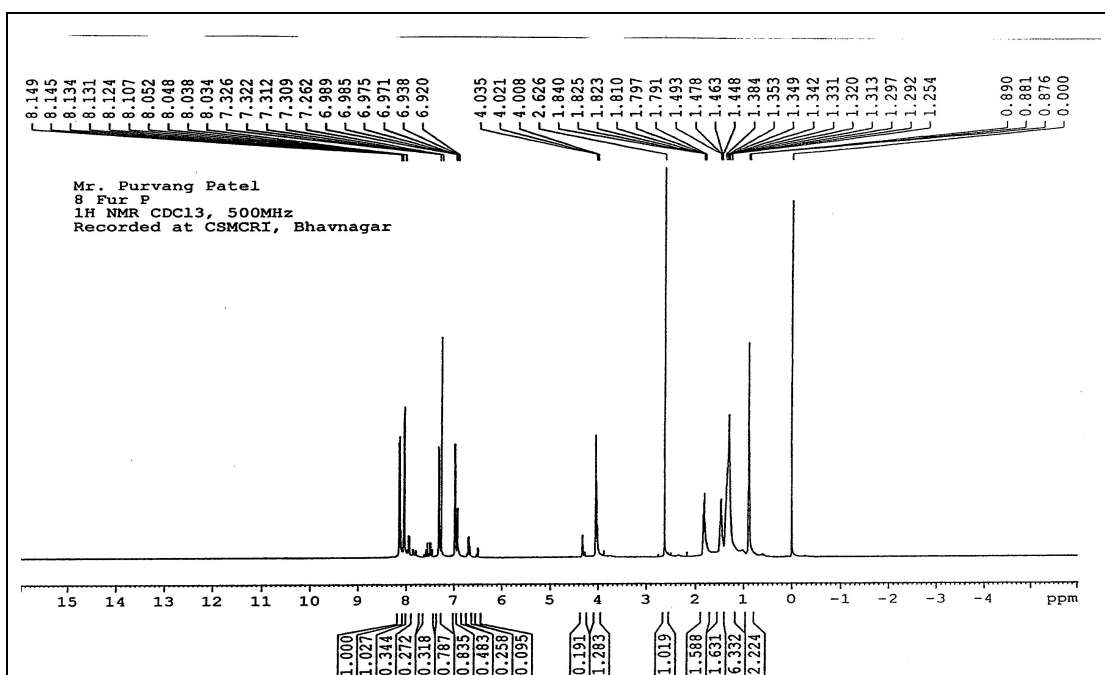


Figure 4.2 (h): ¹H NMR spectra of C8 homologue of series X

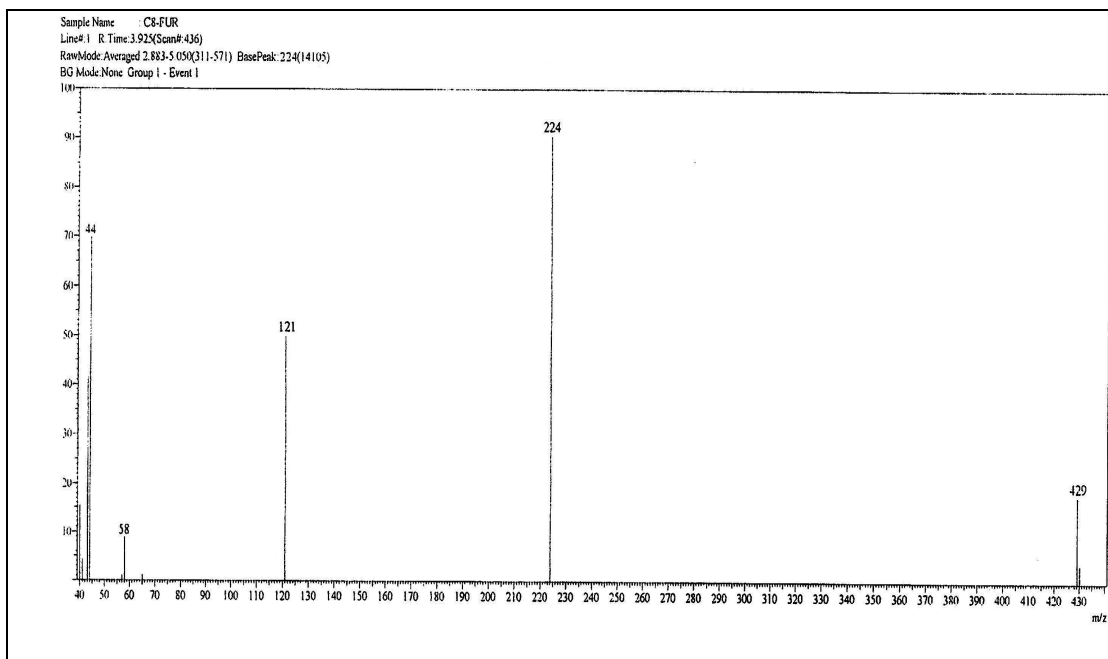


Figure 4.3 (a): Mass spectra of C8 homologue of series VII

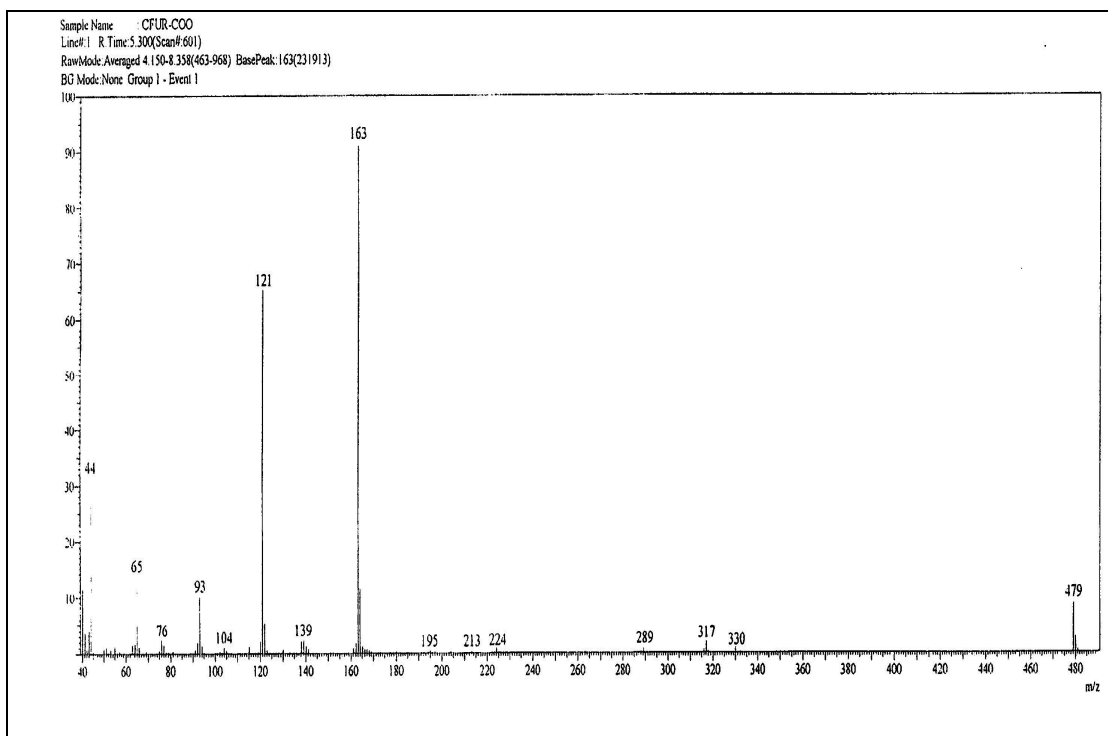


Figure 4.3 (b): Mass spectra of C3 homologue of series VIII

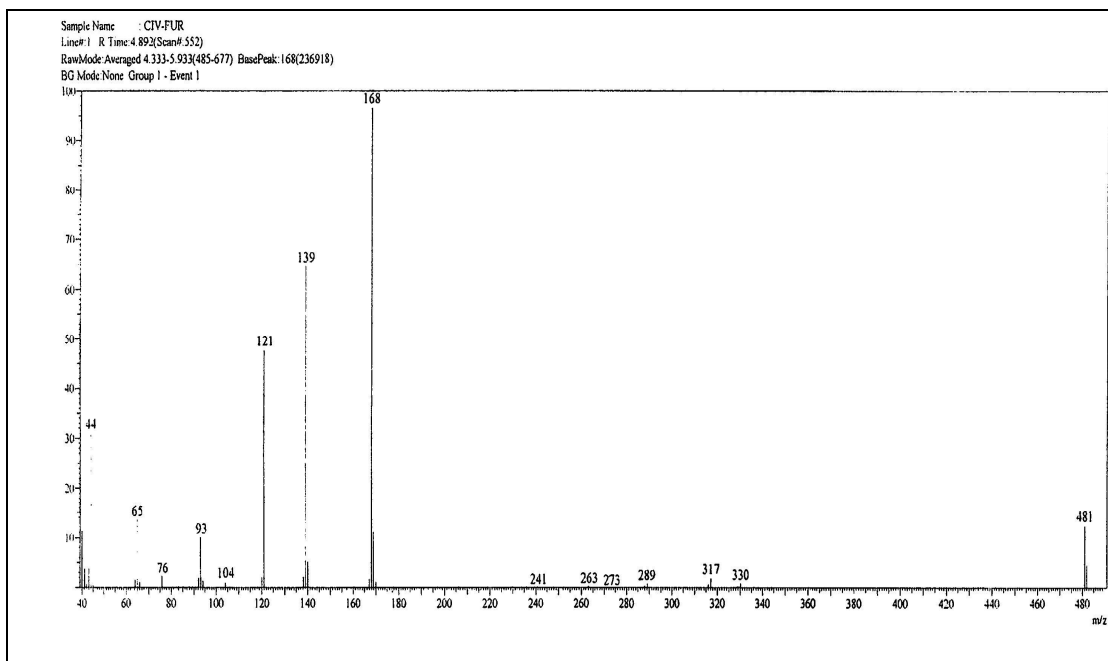


Figure 4.3 (c): Mass spectra of C1 homologue of series IX

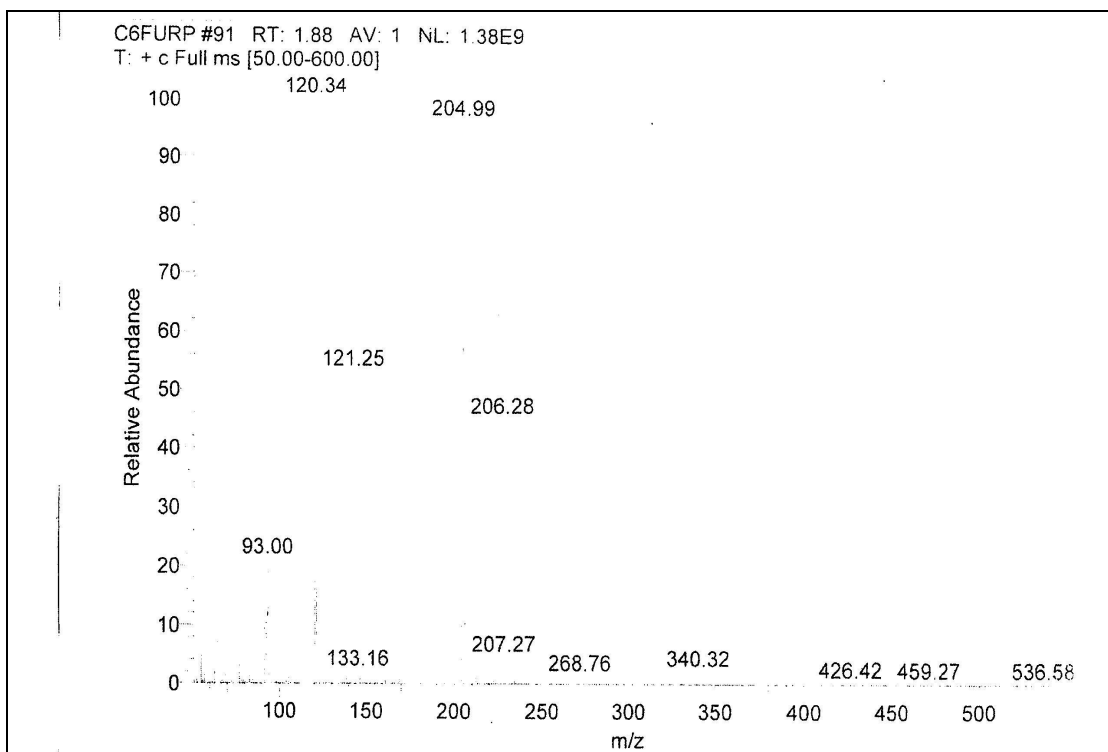


Figure 4.3 (d): Mass spectra of C6 homologue of series X

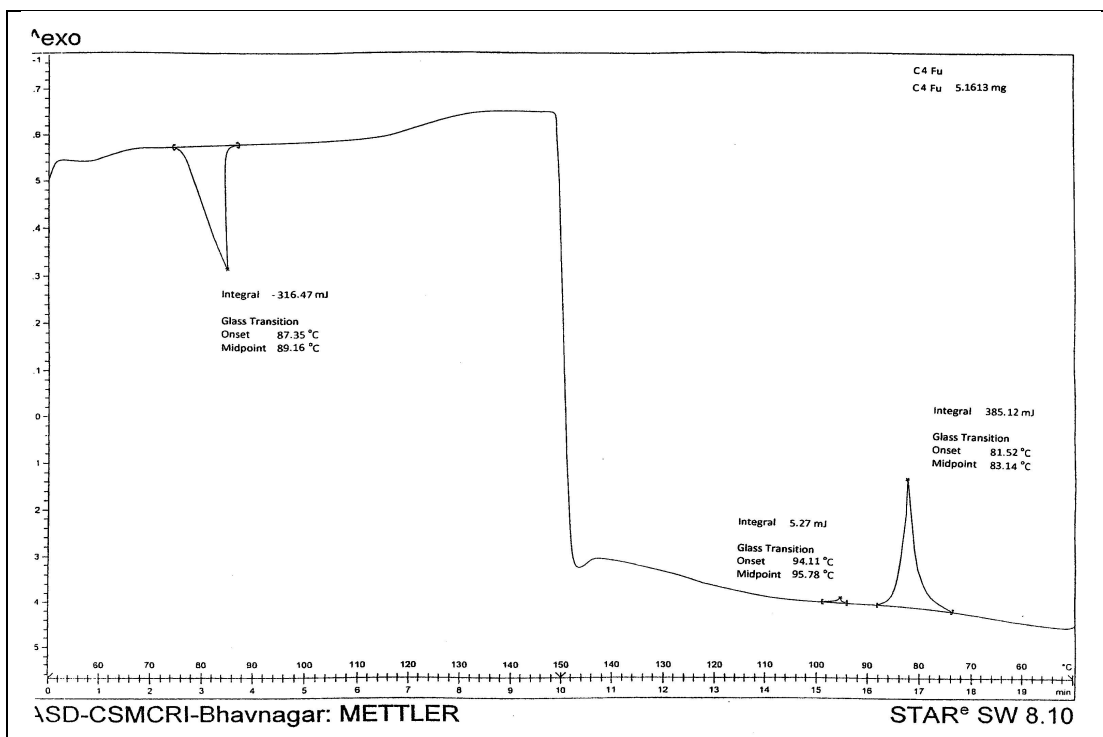


Figure 4.4 (a): DSC Thermogram of C4 homologue of series VII

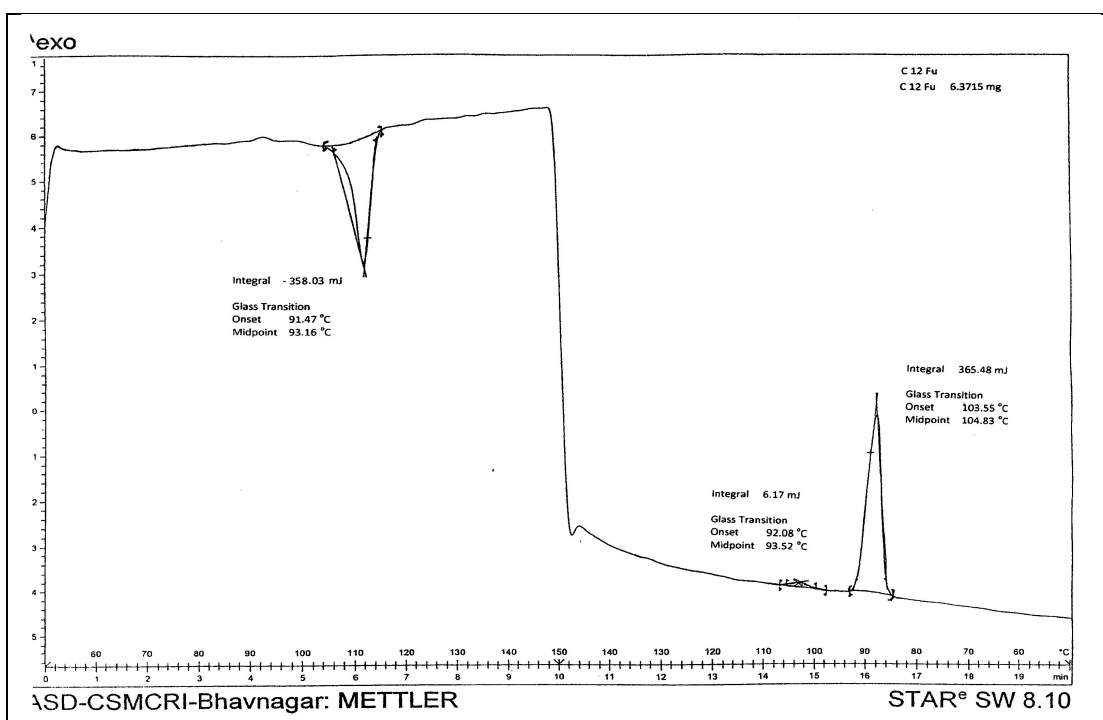


Figure 4.4 (b): DSC Thermogram of C12 homologue of series VII

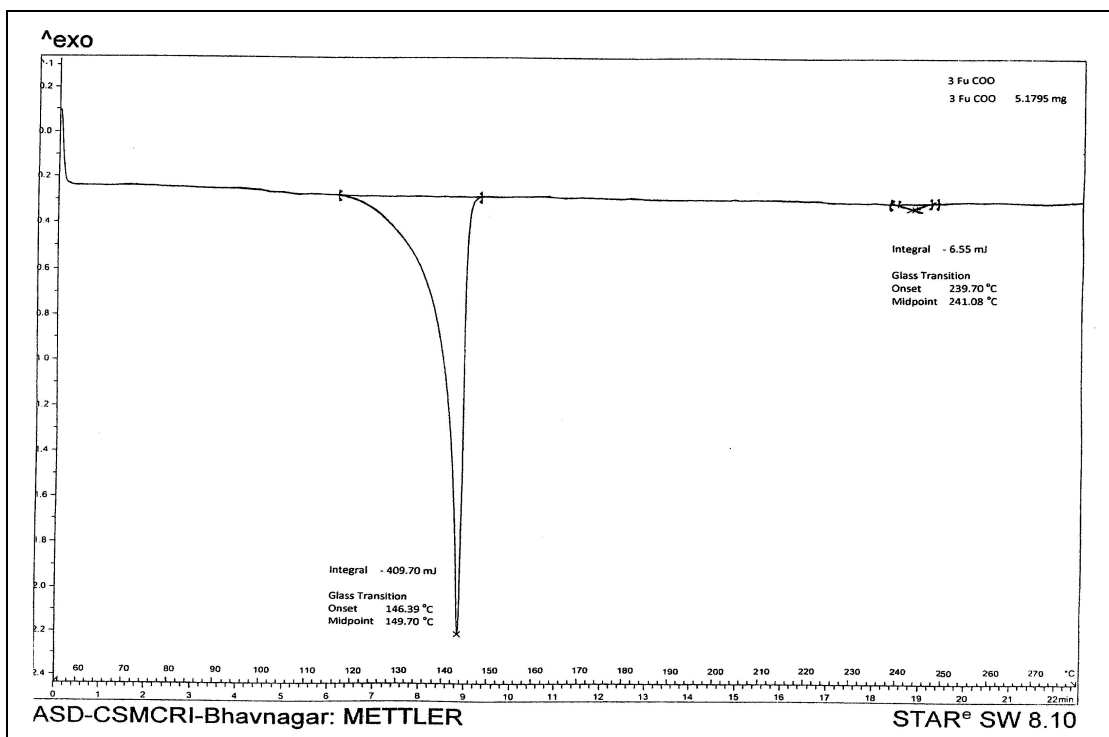


Figure 4.4 (c): DSC Thermogram of C3 homologue of series VIII

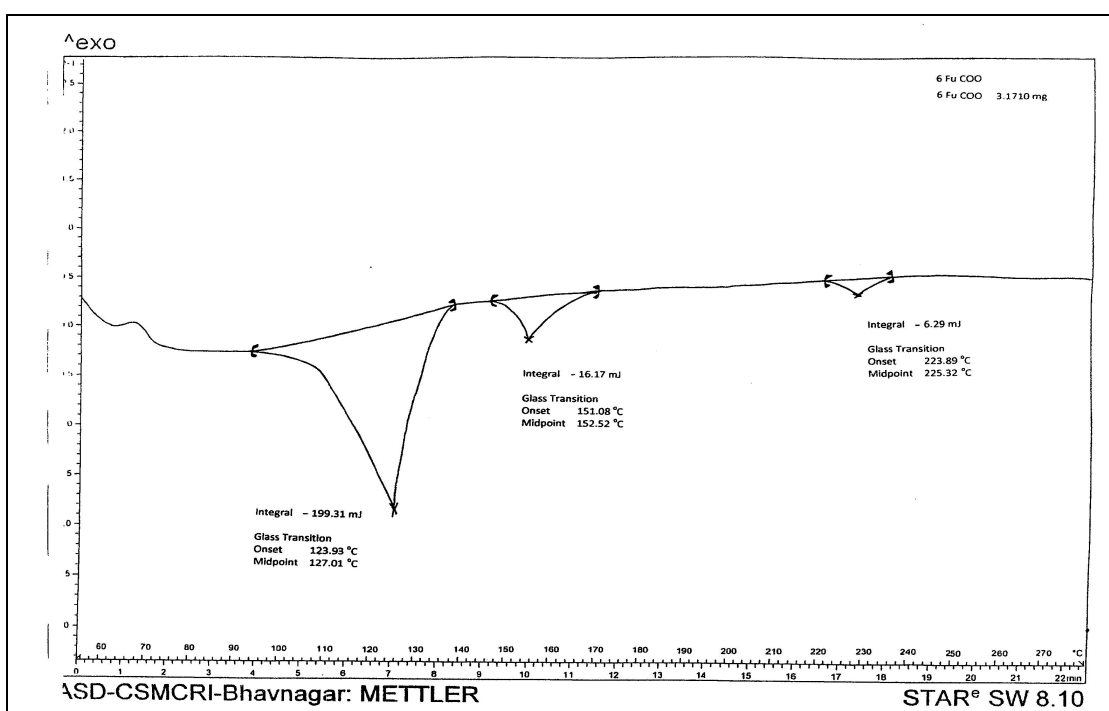


Figure 4.4 (d): DSC Thermogram of C6 homologue of series VIII

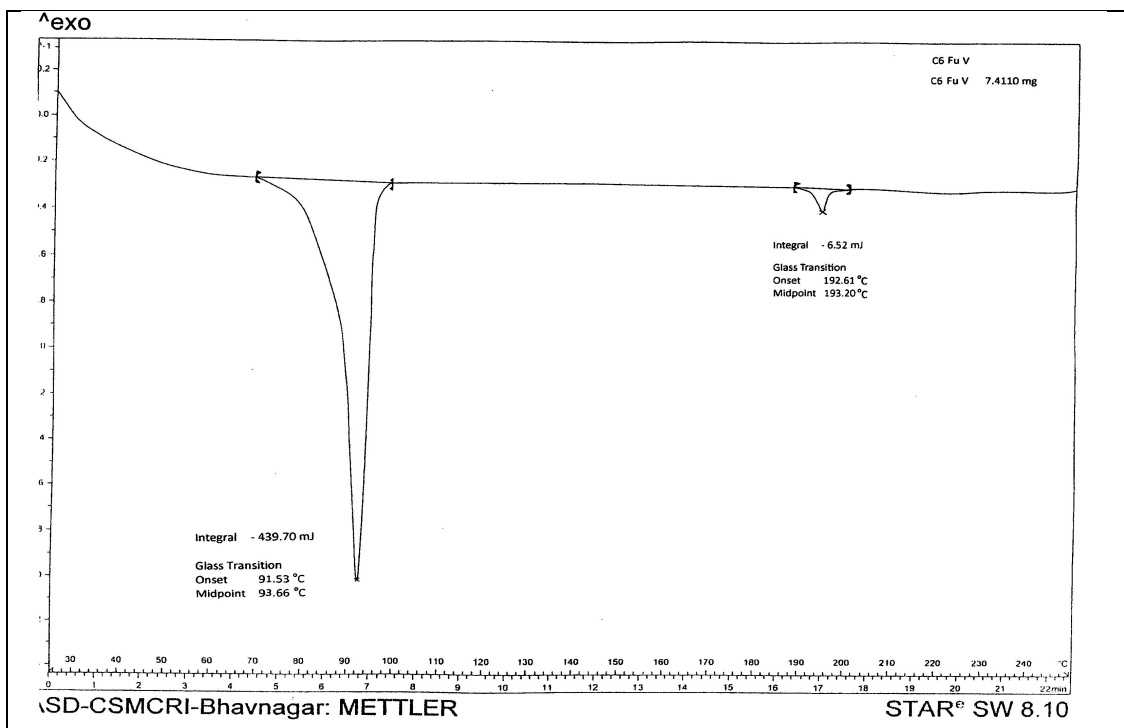


Figure 4.4 (e): DSC Thermogram of C6 homologue of series IX

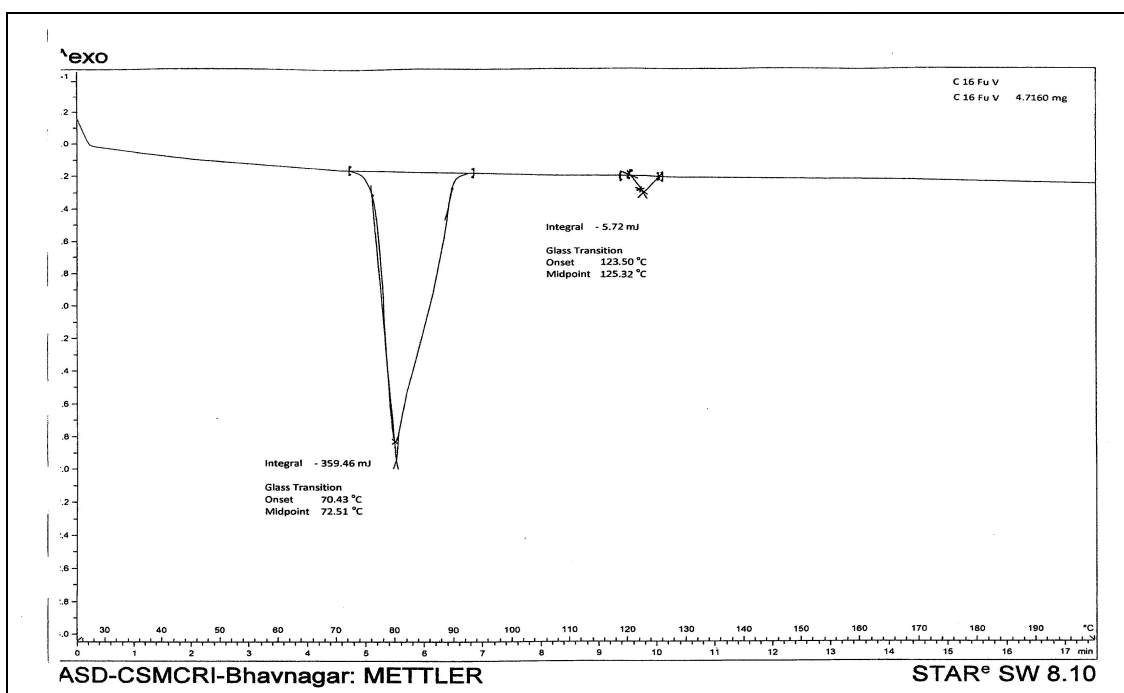


Figure 4.4 (f): DSC Thermogram of C16 homologue of series IX

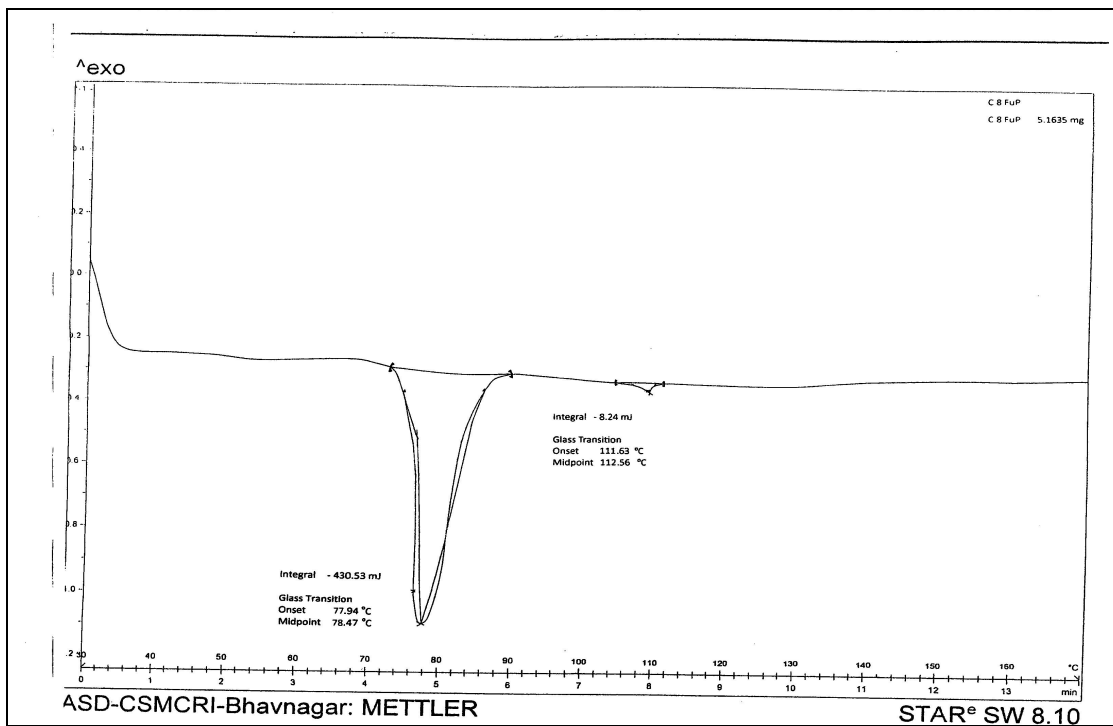


Figure 4.4 (g): DSC Thermogram of C8 homologue of series X

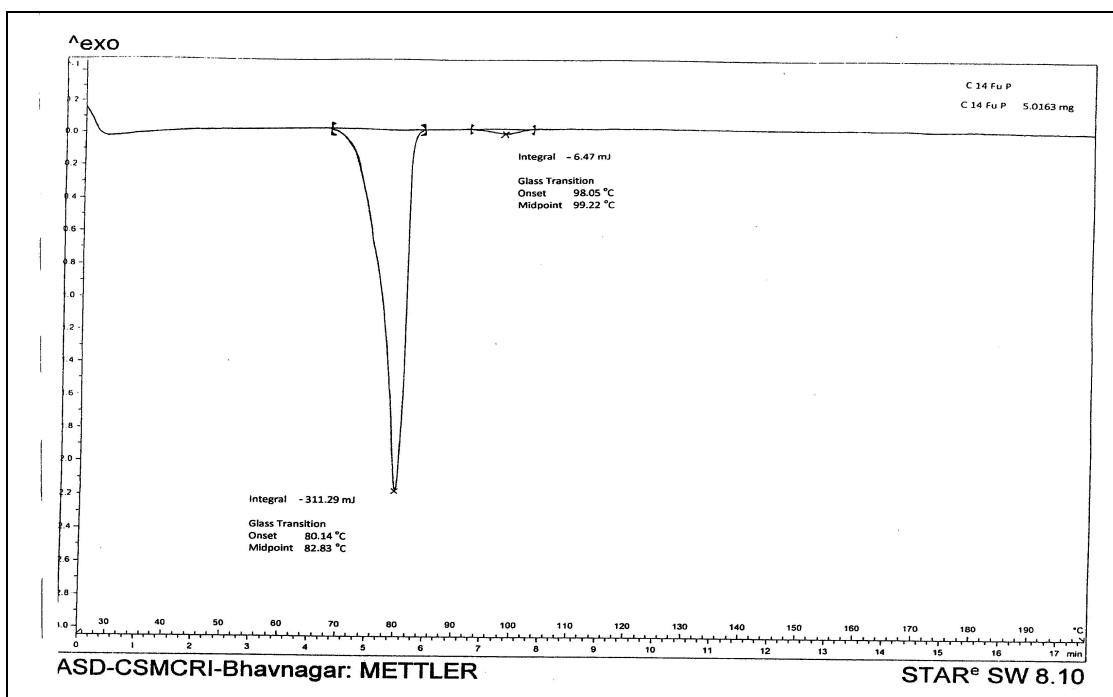


Figure 4.4 (h): DSC Thermogram of C14 homologue of series X

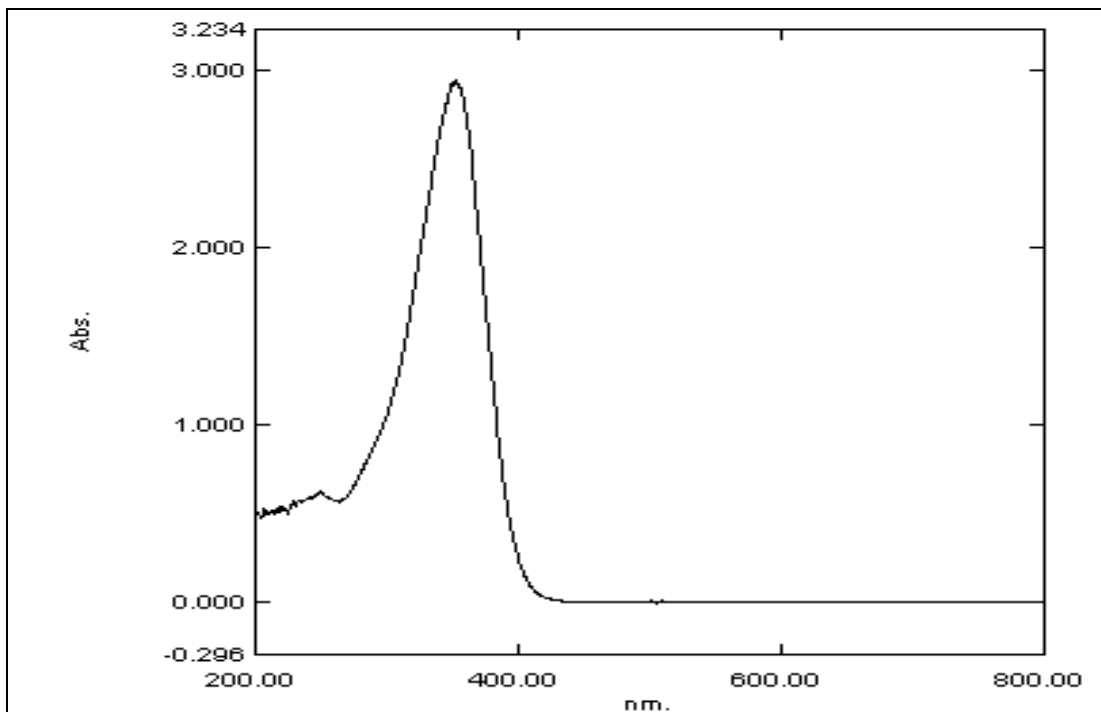


Figure 4.5 (a): UV spectra of C5 homologue of series VII

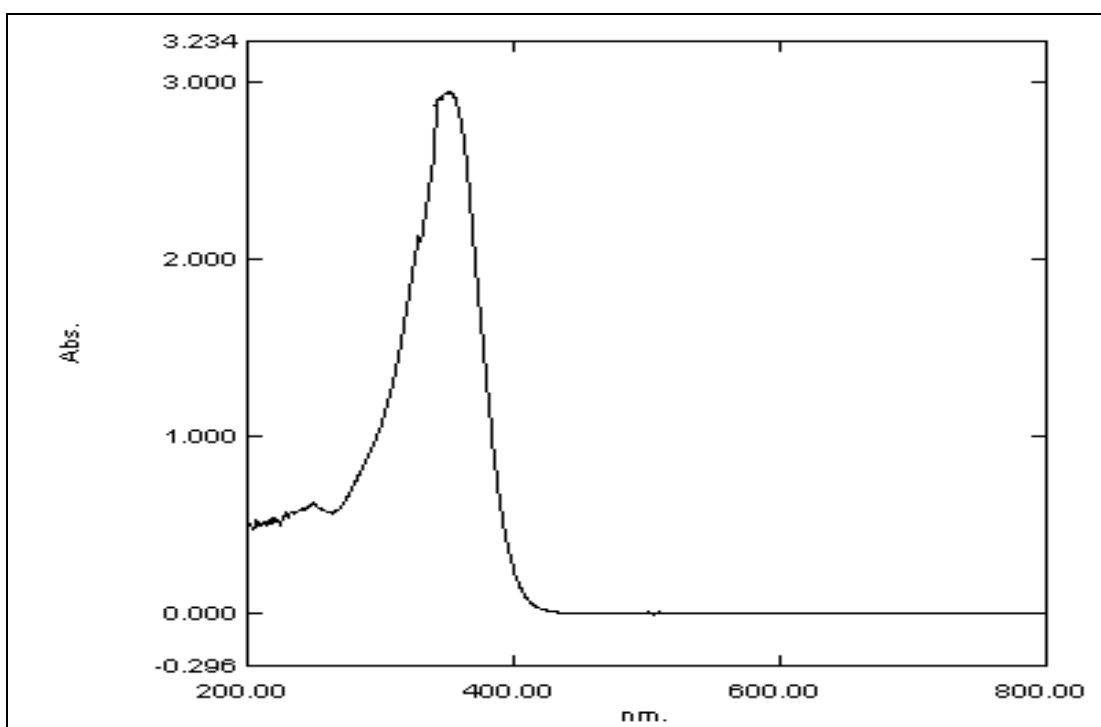


Figure 4.5 (b): UV spectra of C10 homologue of series VII

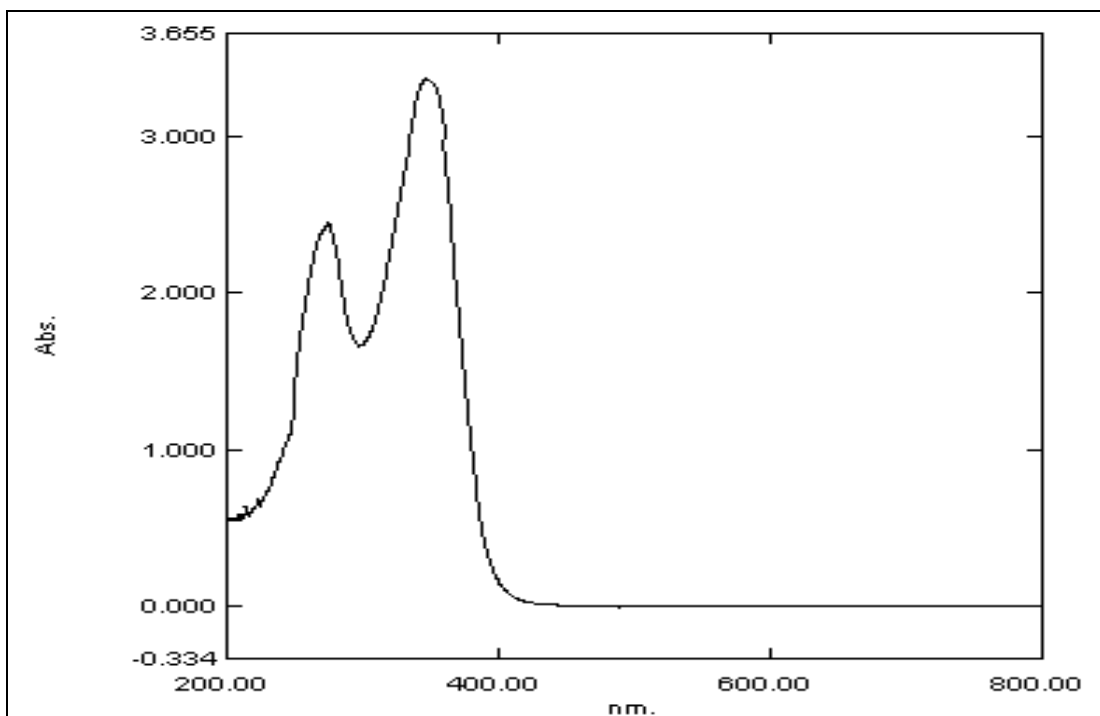


Figure 4.5 (c): UV spectra of C4 homologue of series VIII

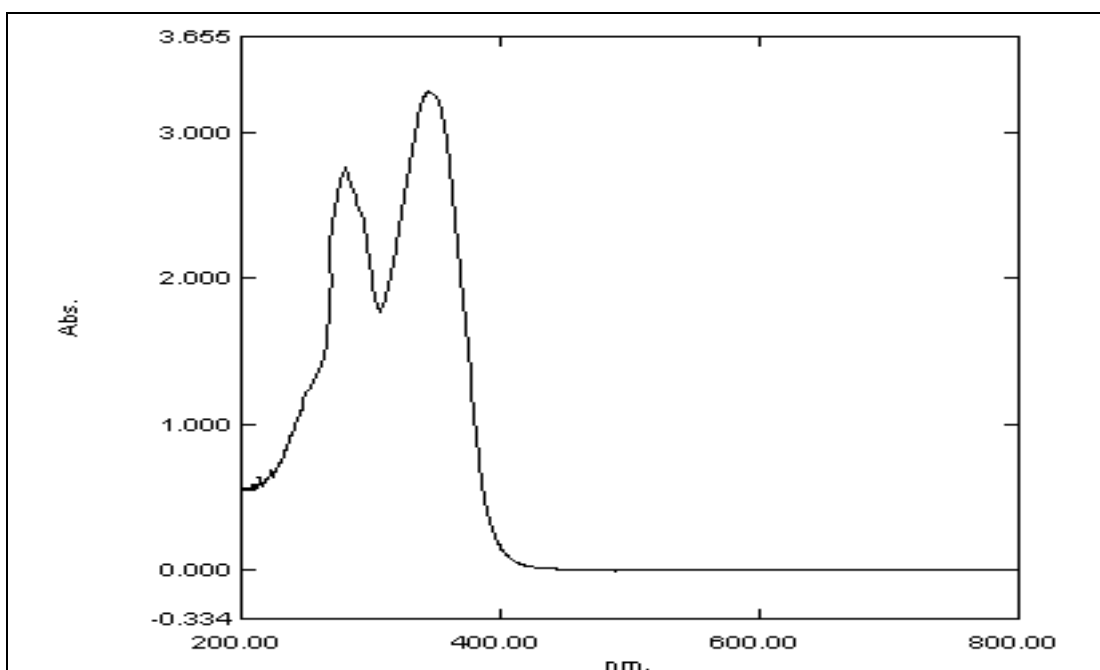


Figure 4.5 (d): UV spectra of C16 homologue of series VIII

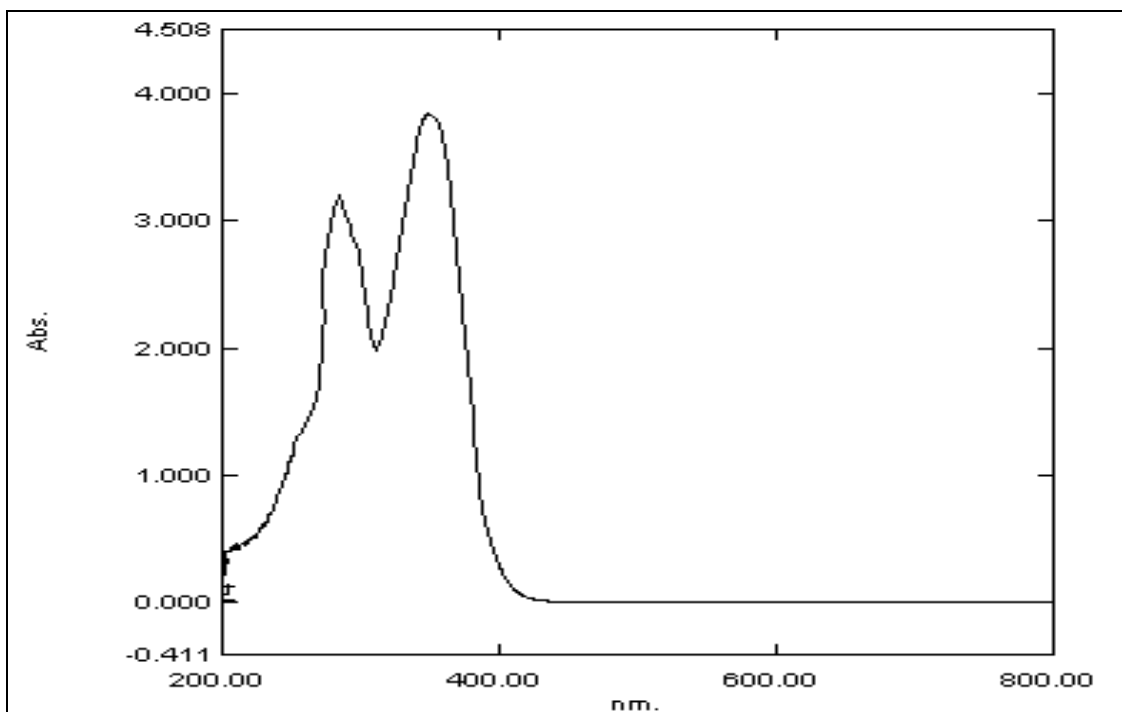


Figure 4.5 (e): UV spectra of C2 homologue of series IX

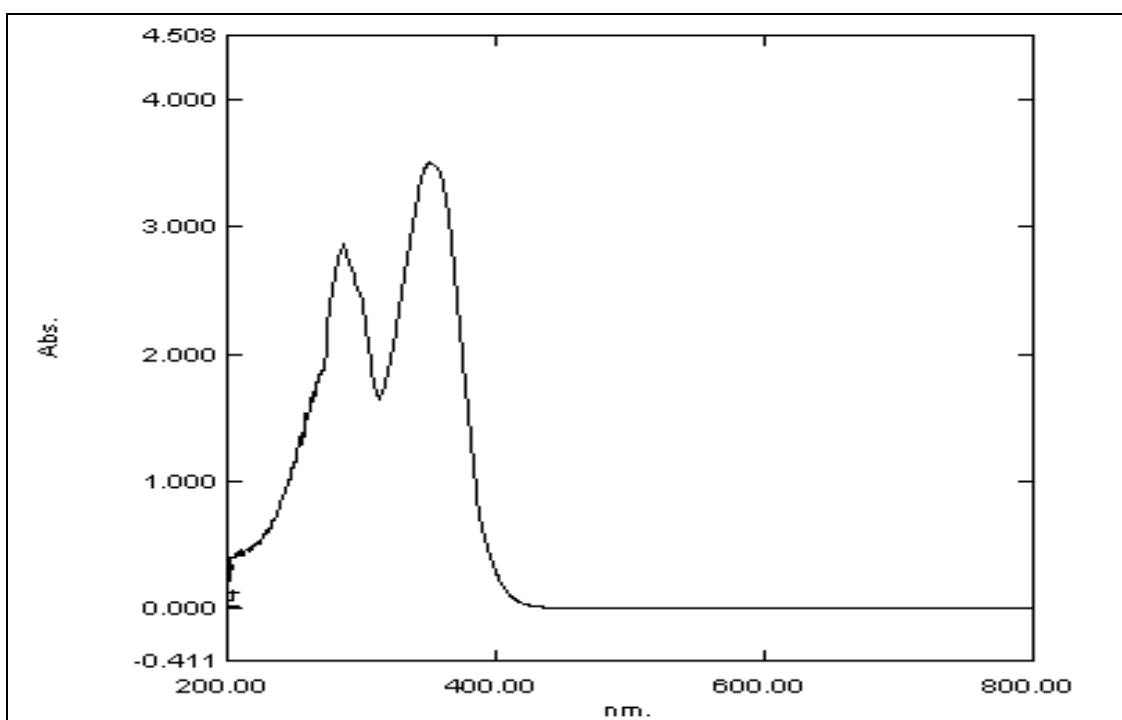


Figure 4.5 (f): UV spectra of C5 homologue of series IX

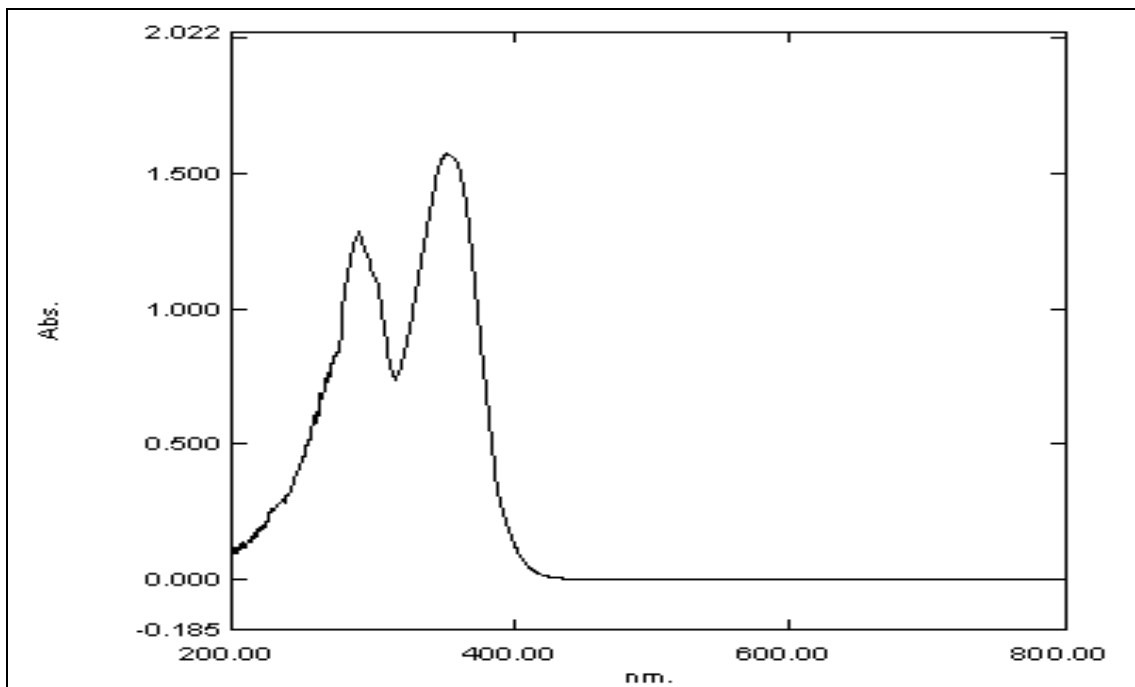


Figure 4.5 (g): UV spectra of C6 homologue of series IX

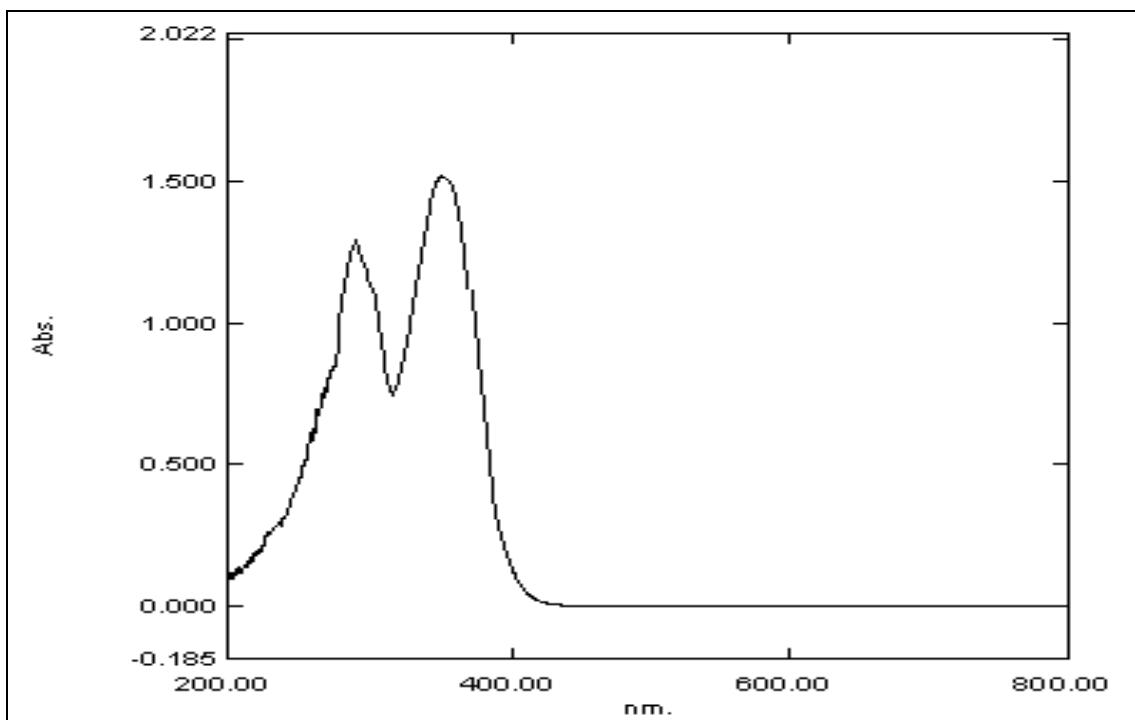
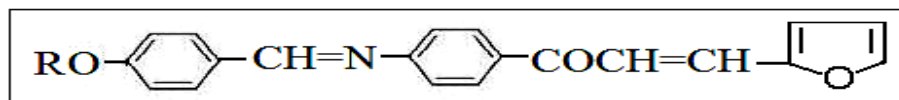


Figure 4.5 (h): UV spectra of C10 homologue of series IX

4.3 Results and Discussion

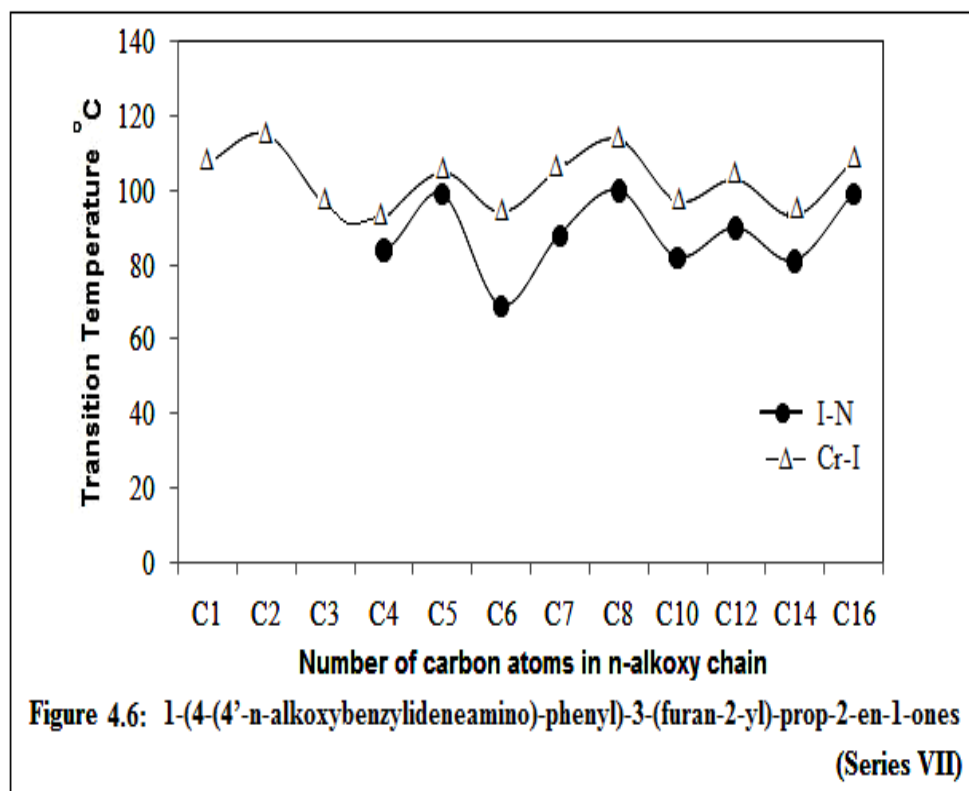
4.3.1 Series VII : 1-(4-(4'-n-alkoxybenzylideneamino)-phenyl)-3-(furan-2-yl)-prop-2-en-1-ones

General molecular structure of series VII



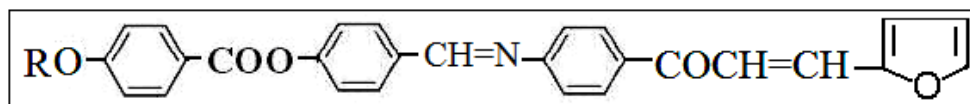
Where, R is C_nH_{2n+1} $n = 1$ to 8, 10, 12, 14 and 16

The first three members of the series VII are non-mesomorphic in nature (Table 4.1); all the other derivatives from butyl onwards exhibit monotropic nematic mesophase. Figure 4.6 shows the plot of transition temperatures against number of carbon atoms in n-alkoxy chain; it indicates that both Cr-I curve and I-N curve show more or less zig-zag tendency as the series is ascended. Nematic phase of the series shows threaded texture.



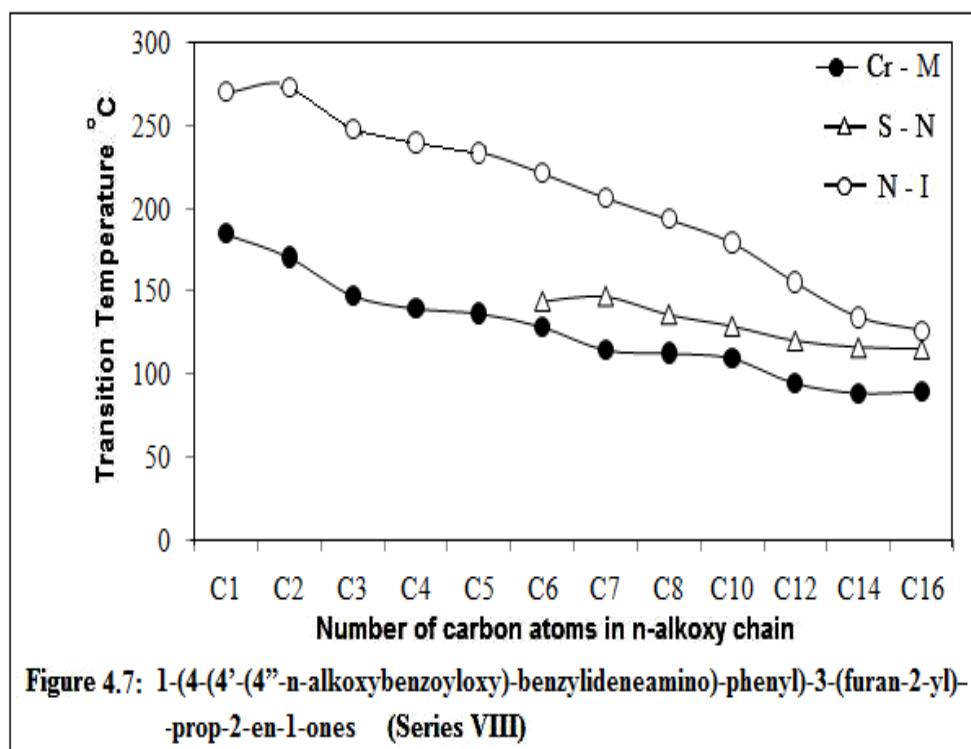
4.3.2 Series VIII : 1-(4-(4'-(4''-n-alkoxybenzoyloxy)-benzylideneamino)-phenyl)-3-(furan-2-yl)-prop-2-en-1-ones

General molecular structure of series VIII



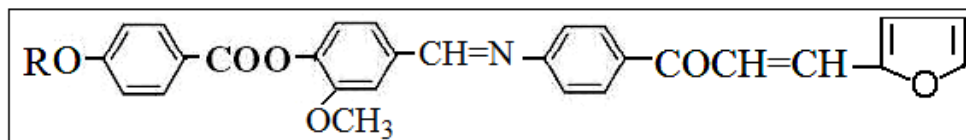
Where, R is C_nH_{2n+1} $n = 1$ to 8, 10, 12, 14 and 16

All the twelve homologues of the series VIII are mesogens (Table 4.5); the nematic mesophase commences from first derivative and remains up to the last hexadecyl derivative synthesised whereas Smectic C phase commences from the hexyl derivative and remains to be exhibited up to the last hexadecyl derivative synthesised. Figure 4.7 shows the plot of transition temperatures against number of carbon atoms in n-alkoxy chain. It indicates that N-I curve shows falling tendency; with a slight rise at ethyl derivative as the series is ascended. No odd-even effect is observed in N-I curve. The S-N curve also shows overall falling tendency as the series is ascended. The Cr-M transitions also show overall falling tendency as the series is ascended. Nematic mesophase of the series shows marble texture and the smectic phase shows schlieren texture of smectic C variety.



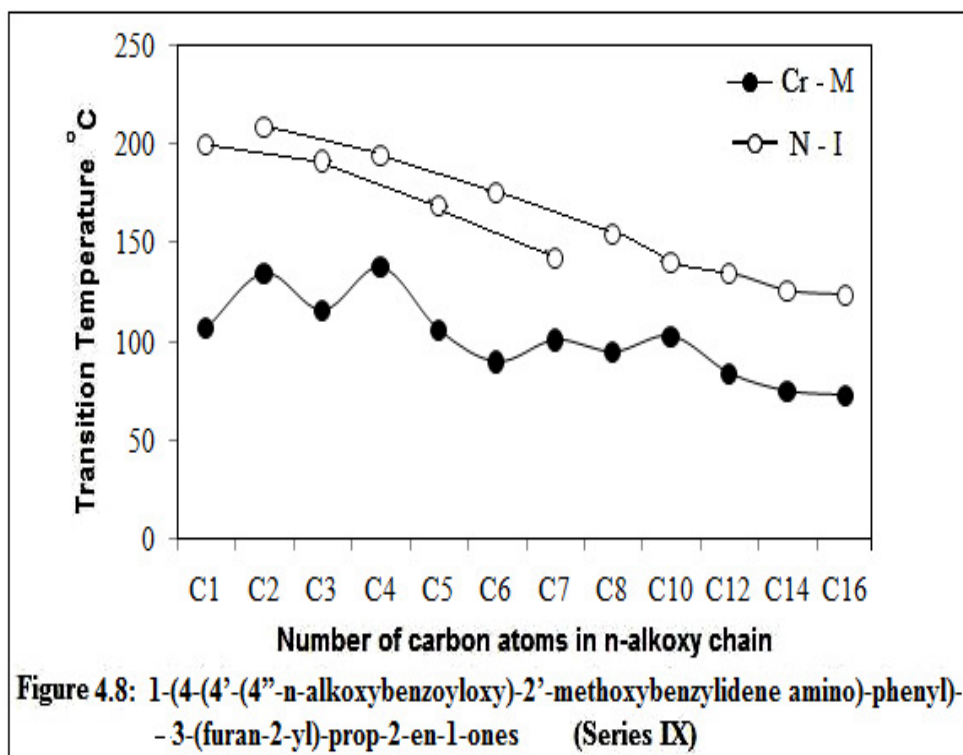
4.3.3 Series IX: 1-(4-(4'-(4''-n-alkoxybenzoyloxy)-2'-methoxybenzylidene amino)-phenyl)-3-(furan-2-yl)-prop-2-en-1-ones

General molecular structure of series IX



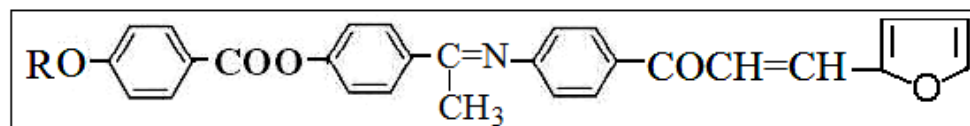
Where, R is C_nH_{2n+1} $n = 1$ to 8, 10, 12, 14 and 16

All the twelve homologues of the series IX are mesogens (Table 4.9); the nematic phase commences from first derivative and remains up to the last hexadecyl derivative synthesised. Figure 4.8 shows the plot of transition temperatures against number of carbon atoms in n-alkoxy chain. It indicates that N-I curves show the odd-even effect with falling tendency as the series is ascended; however both the N-I curves do not show any tendency of merger with each other. The Cr-M transitions show an irregular pattern with overall falling tendency as the series is ascended. Nematic phase of the series shows threaded texture.



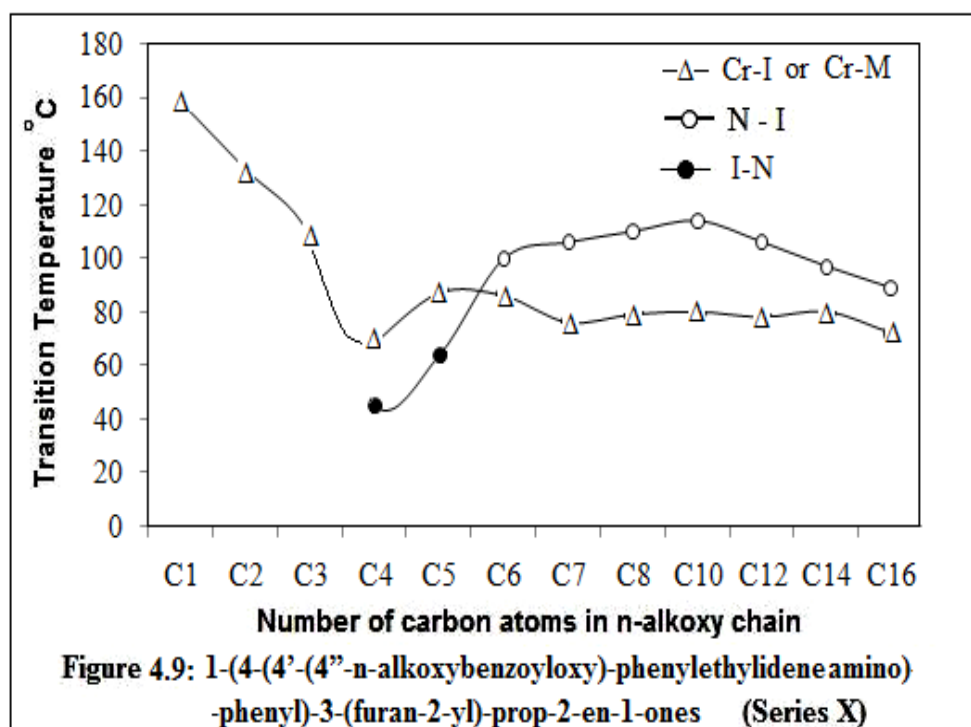
4.3.4 Series X : 1-(4-(4'-(4''-n-alkoxybenzoyloxy)-phenylethylidene amino)-phenyl)-3-(furan-2-yl)-prop-2-en-1-ones

General molecular structure of series X



Where, R is C_nH_{2n+1} $n= 1$ to 8, 10, 12, 14 and 16

The first three members of the series X are non-mesomorphic in nature (Table 4.13); butyl and pentyl derivatives exhibit monotropic nematic mesophase while hexyl to hexadecyl derivatives exhibit enantiotropic nematic mesophase. Figure 4.9 shows the plot of transition temperatures against number of carbon atoms in n-alkoxy chain; it indicates that I-N curve shows step rising tendency from butyl to pentyl derivative and it merges with the rising N-I curve at hexyl derivative. The N-I curve rises upto decyl derivative and then shows falling tendency upto hexadecyl derivative. Cr-I curve shows step fall upto butyl derivative and then rises upto pentyl derivative; the curve then merges with Cr-M curve at hexyl derivative and then shows overall falling tendency upto the last hexadecyl derivative. Nematic phase of the series shows threaded texture.



The average thermal stabilities of the series are compared internally with each other. Table 4.17 and figure 4.10 show the average thermal stability for the homologous series.

Table 4.17 : Average thermal stability °C

Series	N-I	S-N	Commencement of smectic mesophase
VII	88.00 (monotropic) (C ₄ to C ₁₆)	–	–
VIII	208.41 (C ₁ to C ₁₆)	129.57 (C ₆ to C ₁₆)	C ₆
IX	163.66 (C ₁ to C ₁₆)	–	–
X	93.33 (C ₄ to C ₁₆)	–	–

Comparison of average thermal stabilities of all four series (Table 4.17) shows that only series VIII shows both the smectic and nematic mesophase. Series VII shows monotropic nematic phase whereas series VIII, IX and X show enantiotropic nematic phase. Chalcone central linkage generally reduces the tendency to form mesomorphism [321] when present between two benzene rings; however with the introduction of additional –CH=N– central linkage and furfural ring in the present series VII, induces mesomorphism in monotropic form from butyl derivative up to the last hexadecyl derivative. The parent monotropic series VII is transformed into the enantiotropic series VIII, IX and X by addition of one phenyl ring and different central linkages. The average N-I thermal stability of series VIII is 208.41 °C is highest among the present series under comparison. The N-I thermal stability of series VIII is higher than series VII due to the additional of polarizable, planar and rigid phenyl ring with –COO– linkage. The N-I thermal stability of series IX is lower by about 45 °C than series VIII. This may be due to the introduction of lateral –OCH₃ group in the central benzene ring in series IX. The effect of lateral –OCH₃ group in the central benzene ring causes disruption in the molecular packing, which reduces the transition temperatures and melting points as well as decreases the N-I thermal stability with absence of the smectic mesophase as compared to the laterally unsubstituted analogues series VIII [301].

The N-I thermal stability of series X is lower by about 115 °C than series VIII. The first three homologues of series X are non-mesogen whereas butyl to pentyl homologues show monotropic nematic phase and hexyl to hexadecyl homologues show enantiotropic nematic phase; while all the twelve homologues of series VIII are enantiotropic. This may be due to the replacement of the -H of -CH=N- linkage by -CH₃ group in series X. -CH₃ group in ethylideneamino linkage of series X plays an important role to effect their mesomorphic properties. The -CH₃ group in ethylideneamino linkage increases breadth of the molecule and causes disruption in the molecular packing. The broadening effect of the -CH₃ group of ethylideneamino linkage in series X reduces the N-I thermal stability with absence of the smectic mesophase as compared to series VIII [332].

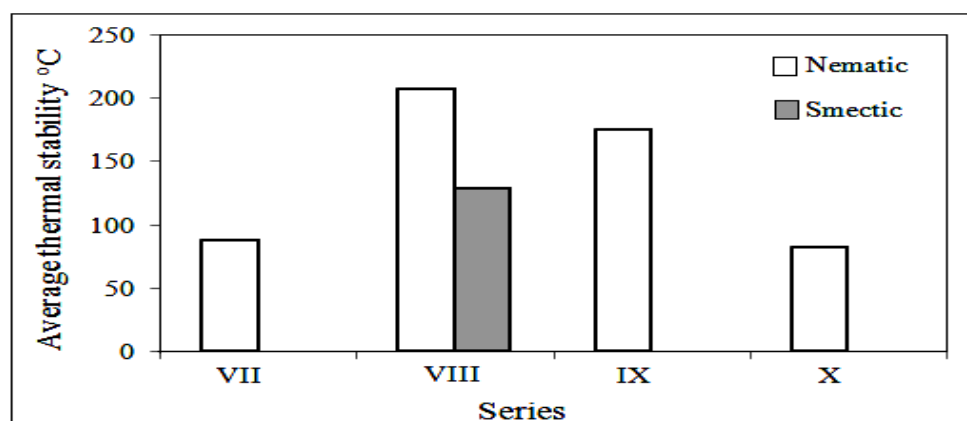
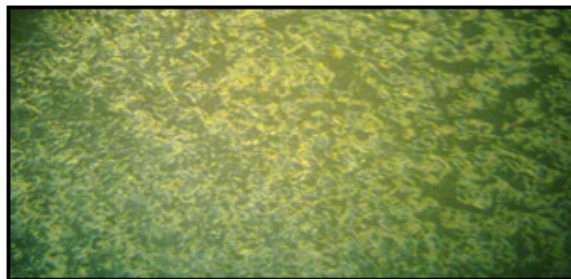


Figure 4.10: Average thermal stability for the series

Figure 4.11 shows the photomicrographs of the textures of representative derivatives.

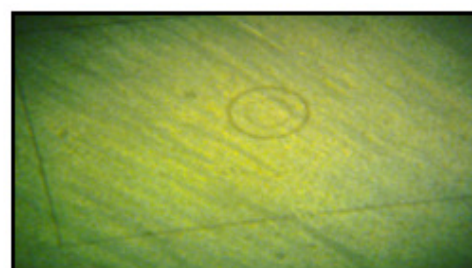


(a) Threaded texture of nematic phase

Photomicrographs of the textures of Octyl homologue of series VII

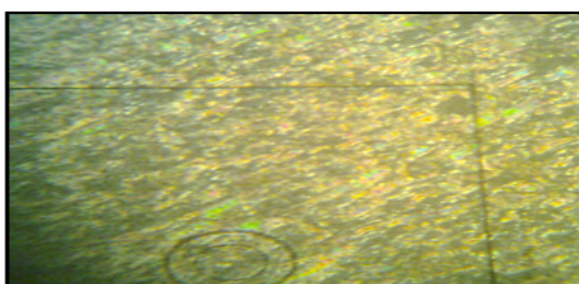


(b) Marble texture of nematic phase



(c) Schlieren texture of smectic phase

Photomicrographs of the textures of Octyl homologue of series VIII



(d) Threaded texture of nematic phase

Photomicrographs of the textures of Propyl homologue of series IX



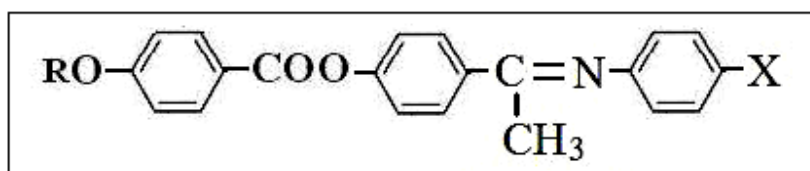
(e) Threaded texture of nematic phase

Photomicrographs of the textures of Hexyl homologue of series X

Figure 4.11: Photomicrographs of the textures of the representative homologues

5.1 Introduction

Molecular structure of an organic compound is one of the responsible factors for its mesomorphic behaviour [296]. Liquid crystalline compounds with different central linkages and terminal groups are known [333-340]; most of these central linkages are ester, azo or azomethine and terminal groups are halogens, cyano, nitro or alkyl chains [341-345]. Central linkages in the molecular constitution of mesogenic compound play an effective role in mesogenic properties. A survey of the literature indicates that mesogens having ethylideneamino central linkage are comparatively less explored [346, 348]. Thus, in order to understand the co-relation between mesomorphic properties and structural variation of the mesogen, three new homologous series with ester and ethylideneamino central linkages having fluoro(series XI), chloro(series XII) and methyl(series XIII) terminal groups respectively are synthesised and their mesomorphic properties are studied. All the three series are compared with each other and with structurally related series. The general molecular structure is



Where, R is C_nH_{2n+1} $n= 1$ to 8, 10, 12, 14 and 16

X = - F (Series XI), - Cl (Series XII), - CH_3 (Series XIII)

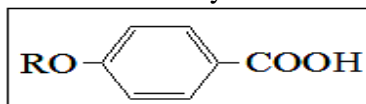
5.2 Experimental

5.2.1 Materials

4-hydroxybenzoic acid, n-alkylhalides, 4-hydroxyacetophenone, 4-fluoroaniline, 4-chloroaniline, 4-toluidine and all other chemicals are of Merck, SRL or Loba grade and used as received.

5.2.2 Synthesis**5.2.2.1 Series XI: 4-(4'-n-alkoxybenzoyloxy)phenylethylidene-4''-fluoroanilines****5.2.2.1.a 4-n-alkoxybenzoicacids**

General molecular structure of 4-n-alkoxybenzoicacids

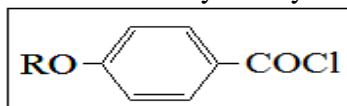


Where, R is C_nH_{2n+1} $n= 1$ to 8, 10, 12, 14 and 16

They are synthesized following the procedure reported in 3.2.2.1.a. [312].

5.2.2.1.b 4-n-alkoxybenzoylchlorides

General molecular structure of 4-n-alkoxybenzoylchlorides

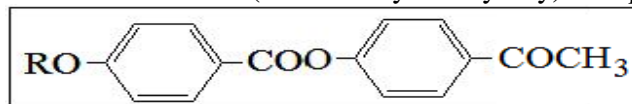


Where, R is C_nH_{2n+1} $n= 1$ to 8, 10, 12, 14 and 16

They are synthesized following the procedure reported in 3.2.2.1.b. [312].

5.2.2.1.c 4-(4'-n-alkoxybenzoyloxy)acetophenones

General molecular structure of 4-(4'-n-alkoxybenzoyloxy)acetophenones

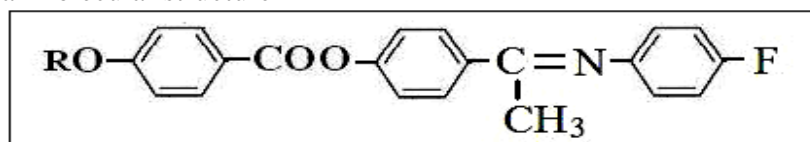


Where, R is C_nH_{2n+1} $n= 1$ to 8, 10, 12, 14 and 16

They are prepared by condensing the appropriate 4-n-alkoxybenzoylchlorides with 4-hydroxyacetophenone following the similar method reported in step 3.2.2.1.d. The compounds are recrystallized from methanol until constant transition temperatures are obtained [331].

5.2.2.1.d 4-(4'-n-alkoxybenzoyloxy)phenylethylidene-4''-fluoroanilines

General molecular structure



Where, R is C_nH_{2n+1} $n= 1$ to 8, 10, 12, 14 and 16

They are synthesised by taking equimolar quantities of appropriate 4-(4'-n-alkoxybenzoyloxy)acetophenones and 4-fluoroaniline following the similar method reported in step 4.2.2.1.c. The products are filtered, dried and recrystallized from acetone until constant transition temperatures are obtained. They are recorded in table 5.1. The elemental analysis of all the compounds are found to be satisfactory and are recorded in table 5.2.

5.2.2.2 Series XII: 4-(4'-n-alkoxybenzoyloxy)phenylethylidene-4''-chloroanilines

5.2.2.2.a 4-n-alkoxybenzoicacids

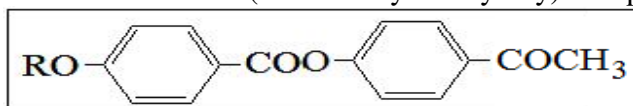
They are synthesized following the procedure reported in 3.2.2.1.a. [312].

5.2.2.2.b 4-n-alkoxybenzoylchlorides

They are synthesized following the procedure reported in 3.2.2.1.b. [312].

5.2.3.2.c 4-(4'-n-alkoxybenzoyloxy)acetophenones

General molecular structure of 4-(4'-n-alkoxybenzoyloxy)acetophenones

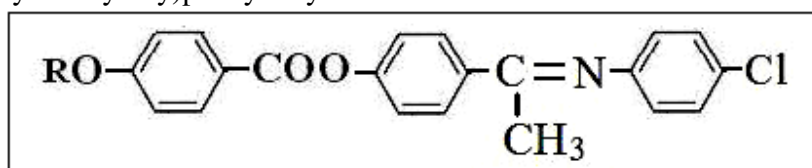


Where, R is C_nH_{2n+1} $n= 1$ to 8, 10, 12, 14 and 16

They are prepared by condensing the appropriate 4-n-alkoxybenzoylchlorides with 4-hydroxyacetophenone following the similar method reported in step 3.2.2.1.d. The compounds are recrystallized from methanol until constant transition temperatures are obtained [331].

5.2.2.2.d 4-(4'-n-alkoxybenzoyloxy)phenylethylidene-4''-chloroanilines

General molecular structure of
4-(4'-n-alkoxybenzoyloxy)phenylethylidene-4''-chloroanilines



Where, R is C_nH_{2n+1} $n= 1$ to 8, 10, 12, 14 and 16

They are synthesised by taking equimolar quantities of appropriate 4-(4'-n-alkoxybenzoyloxy)acetophenones and 4-chloroaniline following the similar method reported in step 4.2.2.1.c. The products are filtered, dried and recrystallized from acetone until constant transition temperatures are obtained. They are recorded in table 5.5. The elemental analysis of all the compounds are found to be satisfactory and are recorded in table 5.6.

5.2.2.3 Series XIII: 4-(4'-n-alkoxybenzoyloxy)phenylethylidene-4''-toluidines

5.2.2.3.a 4-n-alkoxybenzoicacids

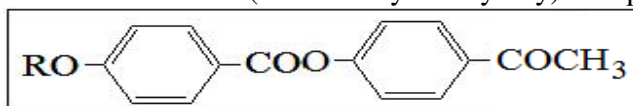
They are synthesized following the procedure reported in 3.2.2.1.a. [312].

5.2.2.3.b 4-n-alkoxybenzoylchlorides

They are synthesized following the procedure reported in 3.2.2.1.b. [312].

5.2.2.3.c 4-(4'-n-alkoxybenzoyloxy)acetophenones

General molecular structure of 4-(4'-n-alkoxybenzoyloxy)acetophenones

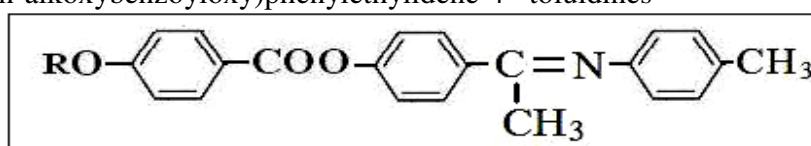


Where, R is C_nH_{2n+1} $n= 1$ to 8, 10, 12, 14 and 16

They are prepared by condensing the appropriate 4-n-alkoxybenzoylchlorides with 4-hydroxyacetophenone following the similar method reported in step 3.2.2.1.d. The compounds are recrystallized from methanol until constant transition temperatures are obtained [331].

5.2.2.3.d 4-(4'-n-alkoxybenzoyloxy)phenylethylidene-4''-toluidines

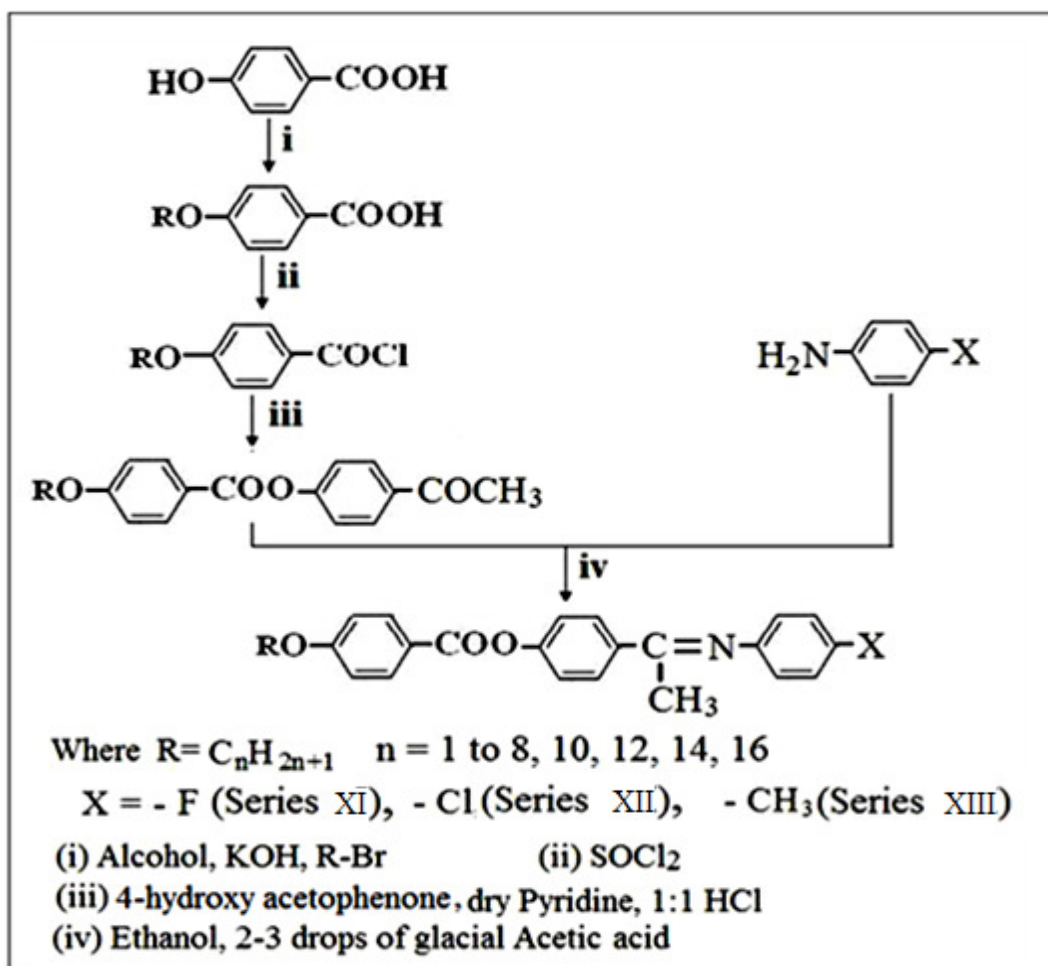
General molecular structure of 4-(4'-n-alkoxybenzoyloxy)phenylethylidene-4''-toluidines



Where, R is C_nH_{2n+1} $n= 1$ to 8, 10, 12, 14 and 16

They are synthesised by taking equimolar quantities of appropriate 4-(4'-n-alkoxybenzoyloxy)acetophenones and 4-toluidine following the similar method reported in step 4.2.2.1.c. The products are filtered, dried and recrystallized from acetone until constant transition temperatures are obtained. They are recorded in table 5.9. The elemental analysis of all the compounds are found to be satisfactory and are recorded in table 5.10.

The synthetic route of series XI to XIII is shown in scheme 5.1.



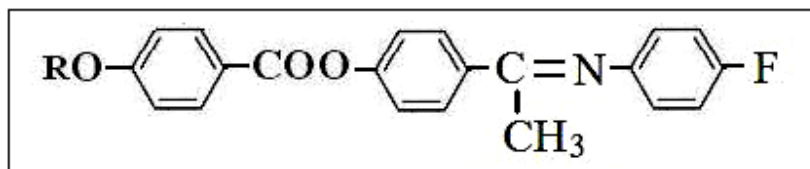
Scheme 5.1: Synthetic route for series XI to XIII

5.2.3 Characterization

Microanalyses of some of the representative compounds are performed on Perkin Elmer Series II 2400-CHN analyzer, Electronic spectra are recorded on a Shimadzu UV-2450 UV-visible spectrophotometer, IR spectra are recorded on a Perkin Elmer GX-FTIR, ¹H NMR spectra are measured on a Bruker Avance II-500 spectrometer. Mass spectra are recorded on Thermoscientific DSQ II mass spectrometer. Transition temperatures and the textures of the mesophases are studied using Leitz Laborlux 12 POL polarizing microscope provided with a Kofler heating stage. DSC are performed on a Mettler Toledo Star SW 7.01.

Table 5.1: Transition temperatures:

4-(4'-n-alkoxybenzoyloxy)phenylethylidene-4''-fluoroanilines (Series XI)



Homologue	Transition Temperatures ^o C		
	Smectic A	Nematic	Isotropic
R=n-alkyl group			
Methyl	—	125	160
Ethyl	—	121	143
Propyl	—	120	140
Butyl	—	117	135
Pentyl	—	93	131
Hexyl	—	84	132
Heptyl	—	81	123
Octyl	—	79	110
Decyl	—	74	104
Dodecyl	75	83	108
Tetradecyl	70	92	105
Hexadecyl	72	98	109

Table 5.2: Elemental analysis

Homologue	Calculated			Found		
	C %	H %	N %	C %	H %	N %
Propyl	73.65	5.62	3.58	73.60	5.56	3.53
Decyl	76.07	7.36	2.88	76.15	7.44	2.87
Dodecyl	76.59	7.73	2.70	76.60	7.85	2.78

FTIR (Nujol, KBr pellets, cm^{-1})

Pentyl homologue: 2955, 2918, 1737 (-COO-), 1606, 1359, 1259, 1176 ($-\overset{\text{I}}{\text{C}}=\text{N}-$), 1041 (-CH₂-O-), 933, 846, 759, 646.

Dodecyl homologue: 2953, 2918, 1732 (-COO-), 1606, 1377, 1259, 1170 ($-\overset{\text{I}}{\text{C}}=\text{N}-$), 1066 (-CH₂-O-), 962, 846, 758, 650.

¹H NMR: (CDCl₃, 500 MHz, δ , ppm, standard TMS)

Decyl homologue: δ 0.8 (3H, t, -CH₃), 1.26 (3H, s, -CH₃ of ethylideneamino), 1.33-1.81 (m, alkyl chain), 4.02 (2H, t, -OCH₂-CH₂), 6.89-8.14 (m, Ar-H)

Hexadecyl homologue: δ 0.8 (3H, t, -CH₃), 1.25 (3H, s, -CH₃ of ethylideneamino), 1.35-1.83 (m, alkyl chain), 4.02 (2H, t, -OCH₂-CH₂), 6.88-8.14 (m, Ar-H)

Mass Spectra:

Heptyl homologue: MS m/z: 447 (M+1)

Table 5.3: DSC data

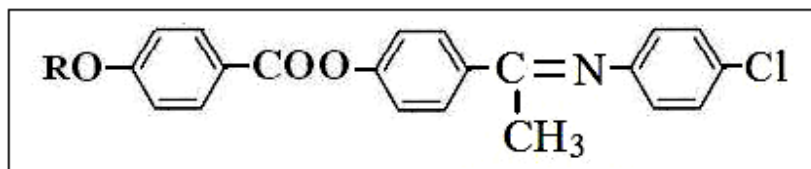
Series	Homologue	Transition Temperature °C	$\Delta H/\text{Jg}^{-1}$	$\Delta S/\text{Jg}^{-1}\text{K}^{-1}$
XI	Octyl	Cr-N 77	55.23	0.1568
		N-I 109	1.0536	0.0027
	Hexadecyl	Cr-S 73	61.82	0.1791
		S-N 99	3.11	0.0083
		N-I 109	0.9240	0.0024

Table 5.4: UV data

Series	Homologue	UV λ max values nm (solvent- ethyl acetate)	
		$\pi \longrightarrow \pi^*$	$n \longrightarrow \pi^*$
XI	Ethyl	266	314
	Hexadecyl	266	314

Table 5.5: Transition temperatures:

4-(4'-n-alkoxybenzoyloxy)phenylethylidene-4''-chloroanilines (Series XII)



Homologue	Transition Temperatures °C		
	Smectic A	Nematic	Isotropic
Methyl	—	133	165
Ethyl	—	127	168
Propyl	—	119	151
Butyl	—	115	140
Pentyl	—	97	134
Hexyl	—	89	126
Heptyl	—	85	124
Octyl	—	71	120
Decyl	—	67	115
Dodecyl	69	95	113
Tetradecyl	70	102	115
Hexadecyl	73	105	116

Table 5.6: Elemental analysis

Homologue	Calculated			Found		
	C %	H %	N %	C %	H %	N %
Ethyl	70.13	5.08	3.55	70.18	5.17	3.52
Heptyl	72.49	6.47	3.02	72.55	6.40	3.08
Tetradecyl	74.79	7.83	2.49	74.88	7.91	2.53

FTIR (Nujol, KBr pellets, cm⁻¹)

Butyl homologue: 2953, 2916, 1726 (-COO-), 1606, 1255, 1172 ($-\overset{|}{\text{C}}=\text{N}-$), 1078 (-CH₂-O-), 933, 846, 688.

Octyl homologue: 2953, 2916, 1732 (-COO-), 1606, 1255, 1172 ($-\overset{|}{\text{C}}=\text{N}-$), 1066 (-CH₂-O-), 933, 846, 647.

¹H NMR: (CDCl₃, 500 MHz, δ , ppm, standard TMS)

Hexyl homologue: δ 0.91 (3H, t, -CH₃), 1.26 (3H, s, -CH₃ of ethylideneamino), 1.36-1.86 (m, alkyl chain), 4.0 (2H, t, -OCH₂-CH₂), 6.91-8.15 (m, Ar-H)

Decyl homologue: δ 0.8 (3H, t, -CH₃), 1.27 (3H, s, -CH₃ of ethylideneamino), 1.31-1.83 (m, alkyl chain), 4.0 (2H, t, -OCH₂-CH₂), 6.91-8.14 (m, Ar-H)

Mass Spectra:

Ethyl homologue: MS m/z: 393 (M+1)

Table 5.7: DSC data

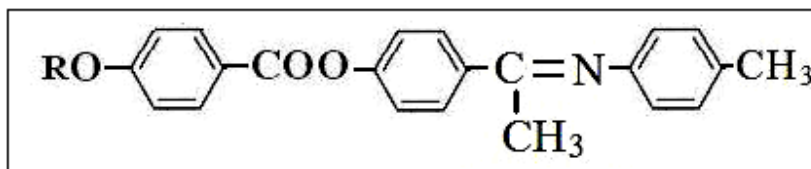
Series	Homologue	Transition Temperature °C	$\Delta H/\text{Jg}^{-1}$	$\Delta S/\text{Jg}^{-1}\text{K}^{-1}$
XII	Hexyl	Cr-N 88	76.11	0.2101
		N-I 127	0.9790	0.0024
	Dodecyl	Cr-S 68	72.69	0.2124
		S-N 96	2.2112	0.0060
		N-I 114	0.9719	0.0025

Table 5.8: UV data

Series	Homologue	UV λ max values nm (solvent- ethyl acetate)	
		$\pi \longrightarrow \pi^*$	$n \longrightarrow \pi^*$
XII	Pentyl	266	313
	Octyl	266	313

Table 5.9: Transition temperatures:

4-(4'-n-alkoxybenzoyloxy)phenylethylidene-4''-toluidines (Series XIII)



Homologue	Transition Temperatures °C	
	Nematic	Isotropic
R=n-alkyl group		
Methyl	110	170
Ethyl	119	165
Propyl	118	161
Butyl	111	150
Pentyl	105	142
Hexyl	98	130
Heptyl	81	124
Octyl	78	111
Decyl	76	110
Dodecyl	72	108
Tetradecyl	69	101
Hexadecyl	67	94

Table 5.10: Elemental analysis

Homologue	Calculated			Found		
	C %	H %	N %	C %	H %	N %
Butyl	77.80	6.73	3.49	77.88	6.79	3.53
Octyl	78.77	7.65	3.06	78.62	7.69	3.03
Hexadecyl	80.14	8.96	2.46	80.16	8.91	2.59

FTIR (Nujol, KBr pellets, cm⁻¹)

Heptyl homologue: 2955, 2916, 1737 (-COO-), 1606, 1359, 1259, 1170 ($-\overset{|}{\text{C}}=\text{N}-$), 1064 (-CH₂-O-), 956, 846, 771, 694.

Decyl homologue: 2953, 2918, 1732 (-COO-), 1606, 1377, 1259, 1170 ($-\overset{|}{\text{C}}=\text{N}-$), 1066 (-CH₂-O-), 962, 846, 758, 692.

¹H NMR: (CDCl₃, 500 MHz, δ , ppm, standard TMS)

Dodecyl homologue: δ 0.8 (3H, t, -CH₃), 1.00 (3H, s, -CH₃ of ethylideneamino), 1.26-1.83 (m, alkyl chain), 4.02 (2H, t, -OCH₂-CH₂), 6.88-8.14 (m, Ar-H)

Tetradecyl homologue: δ 0.8 (3H, t, -CH₃), 1.26 (3H, s, -CH₃ of ethylideneamino), 1.30-1.84 (m, alkyl chain), 4.04 (2H, t, -OCH₂-CH₂), 6.92-8.15 (m, Ar-H)

Mass Spectra:

Heptyl homologue: MS m/z: 443 (M+1)

Table 5.11: DSC data

Series	Homologue	Transition Temperature °C	$\Delta H/\text{Jg}^{-1}$	$\Delta S/\text{Jg}^{-1}\text{K}^{-1}$
XIII	Pentyl	Cr-N 104	73.87	0.1953
		N-I 143	0.9403	0.0022
	Dodecyl	Cr-N 73	58.99	0.1709
		N-I 108	0.9249	0.0024

Table 5.12: UV data

Series	Homologue	UV λ max values nm (solvent- ethyl acetate)	
		$\pi \longrightarrow \pi^*$	$n \longrightarrow \pi^*$
XIII	Propyl	266	313
	Dodecyl	266	313

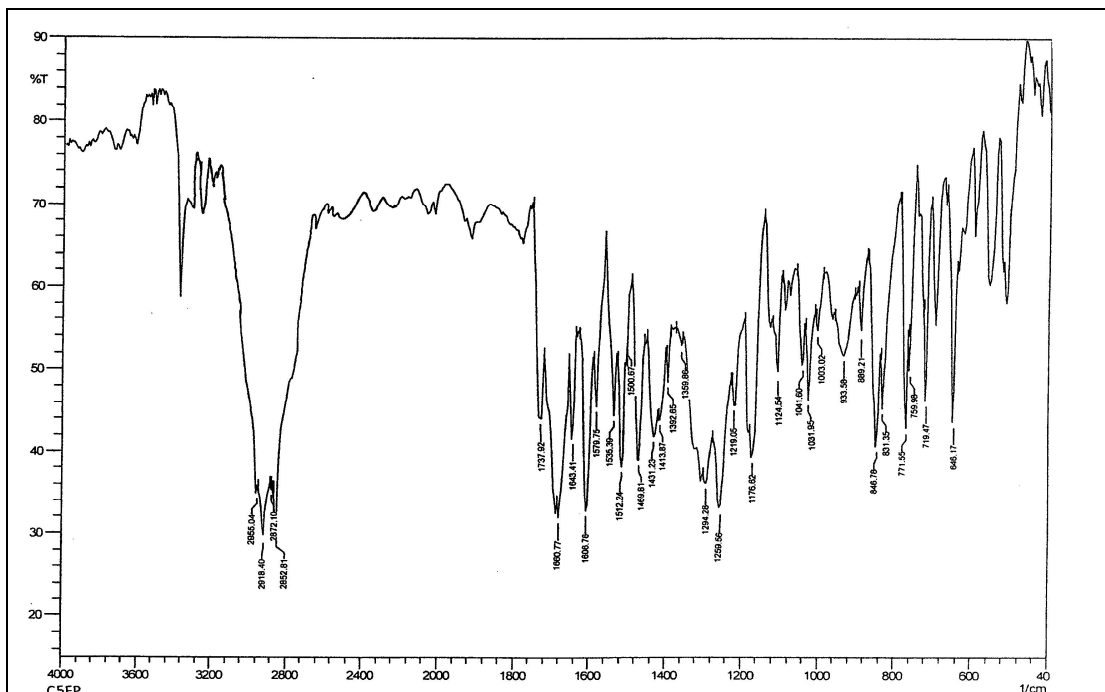


Figure 5.1 (a): IR spectra of C5 homologue of series XI

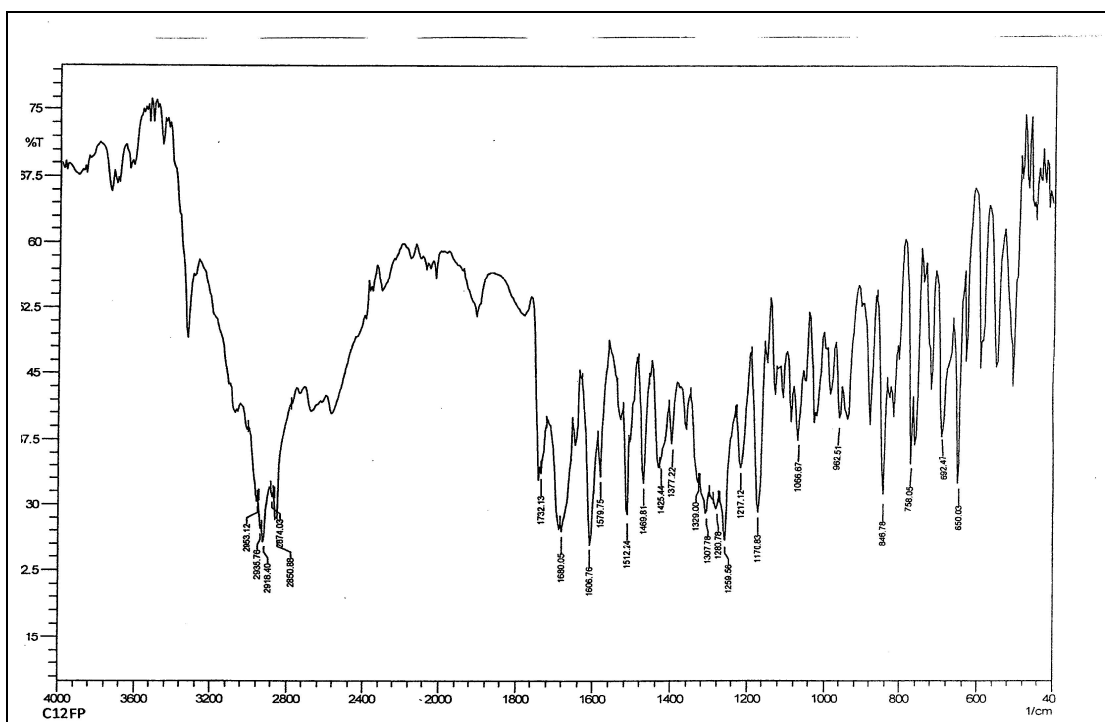


Figure 5.1 (b): IR spectra of C12 homologue of series XI

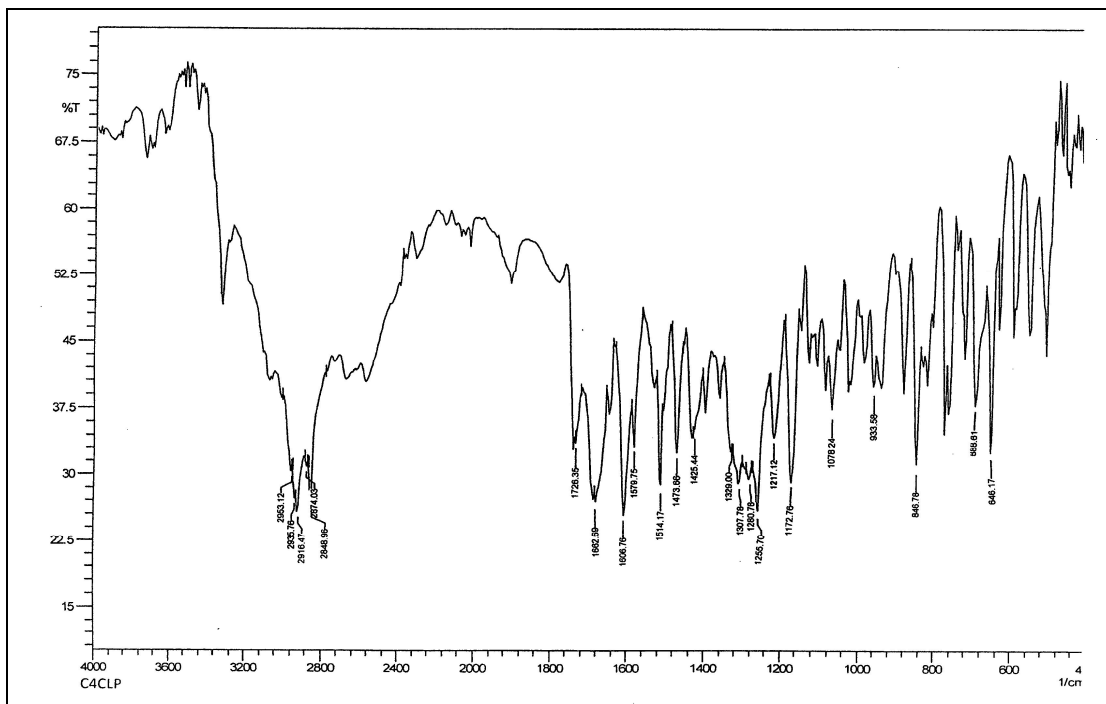


Figure 5.1 (c): IR spectra of C4 homologue of series XII

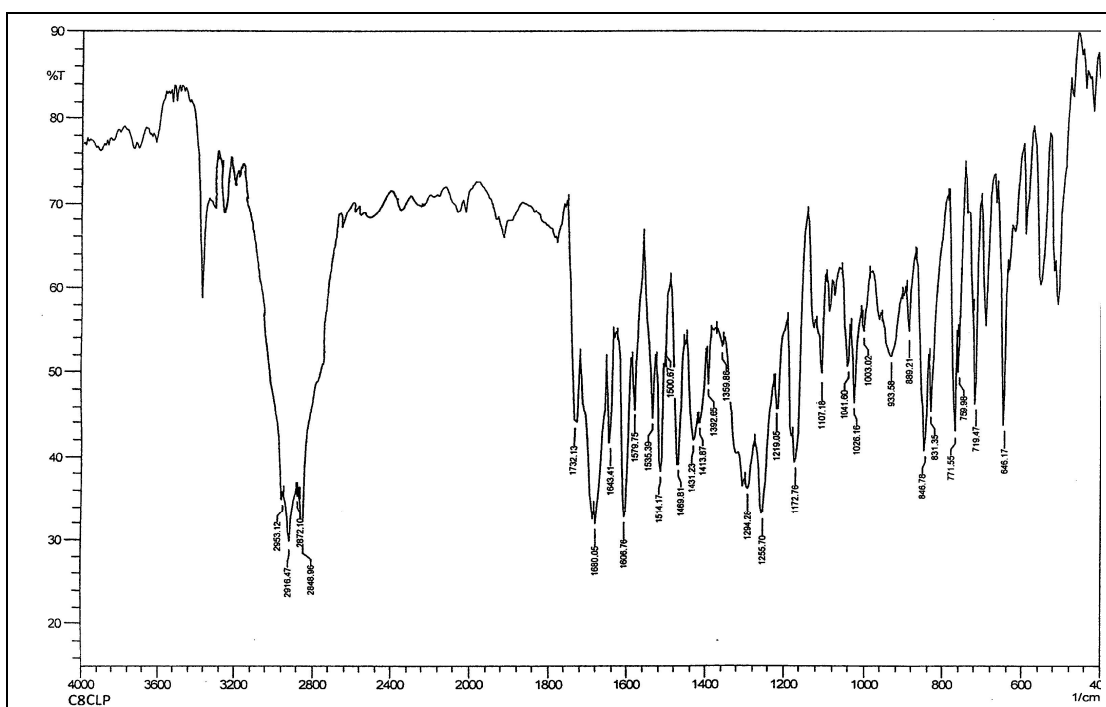


Figure 5.1 (d): IR spectra of C8 homologue of series XII

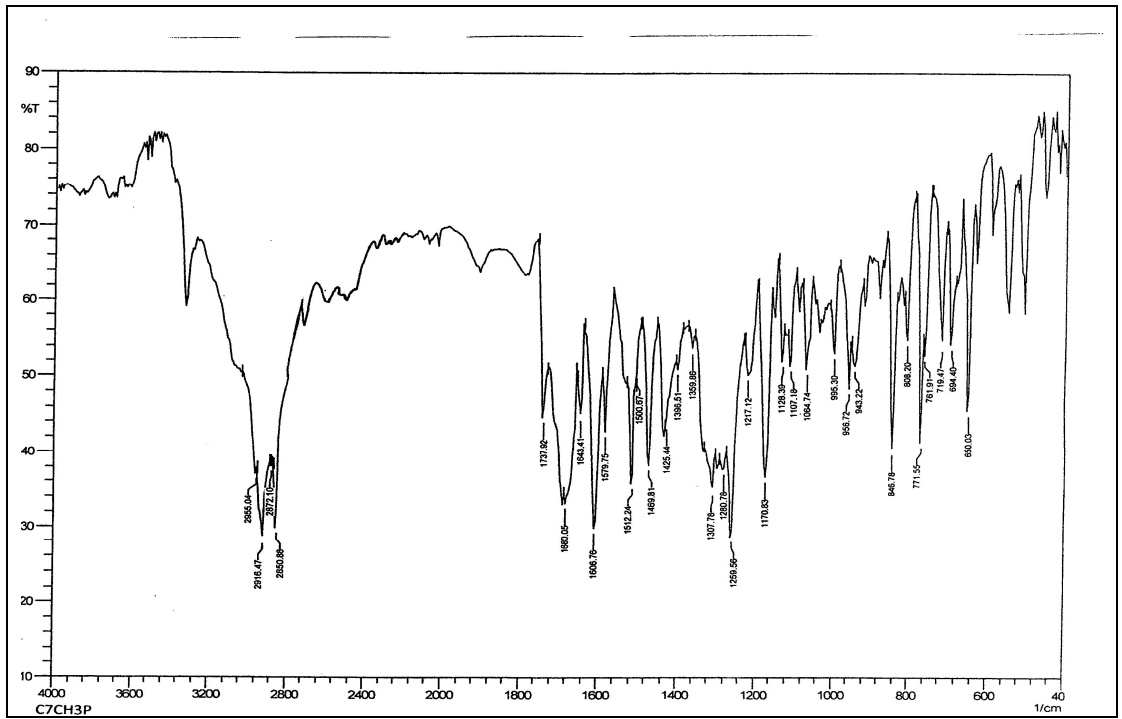


Figure 5.1 (e): IR spectra of C7 homologue of series XIII

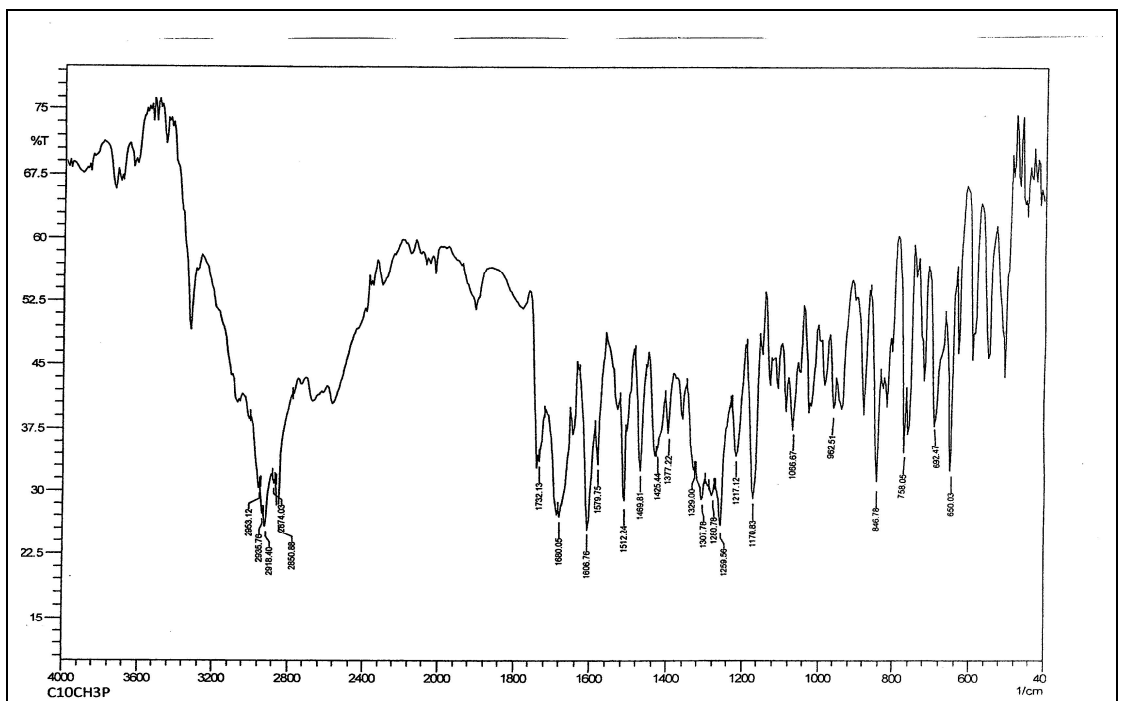


Figure 5.1 (f): IR spectra of C10 homologue of series XIII

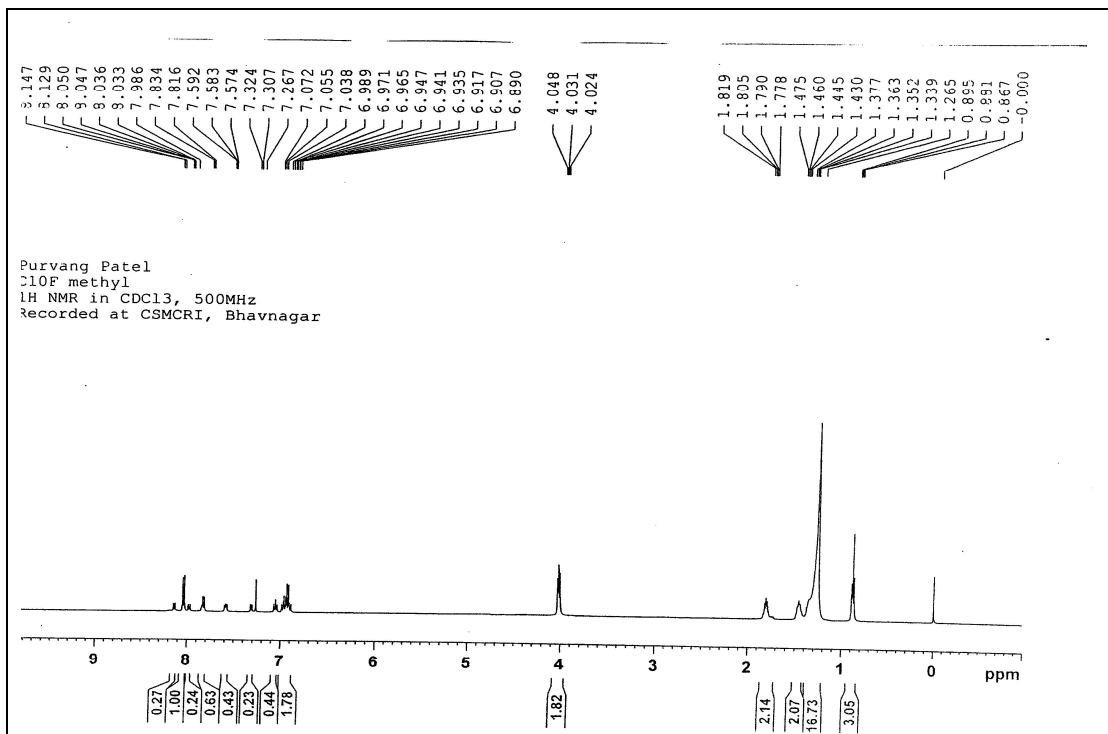


Figure 5.2 (a): ¹H NMR spectra of C10 homologue of series XI

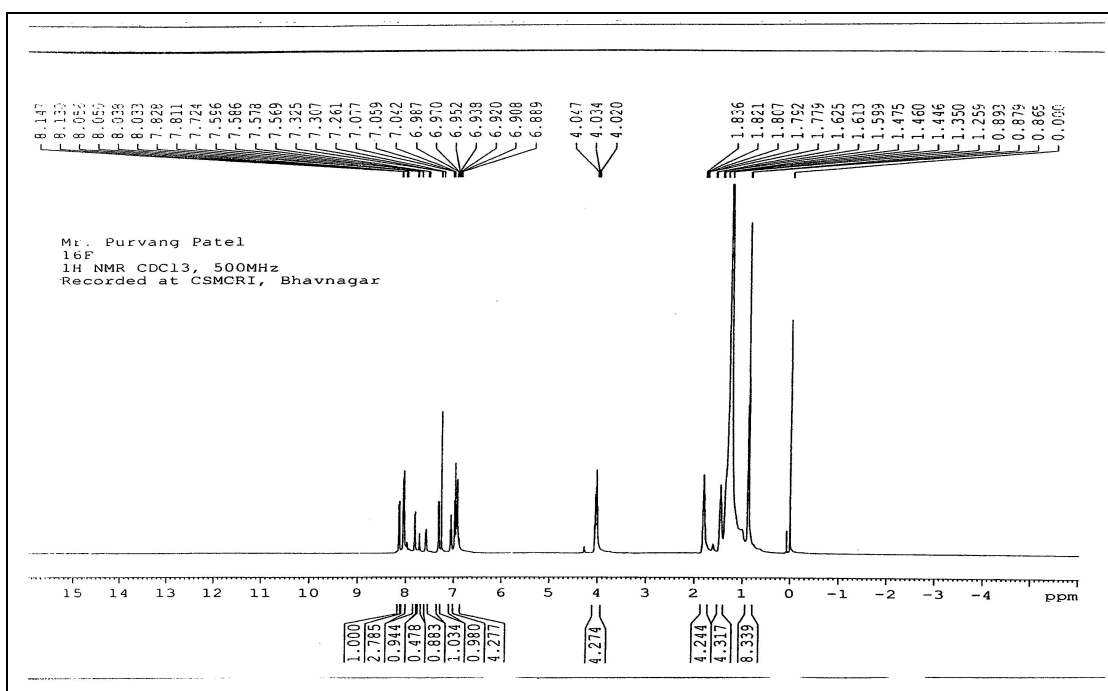


Figure 5.2 (b): ¹H NMR spectra of C16 homologue of series XI

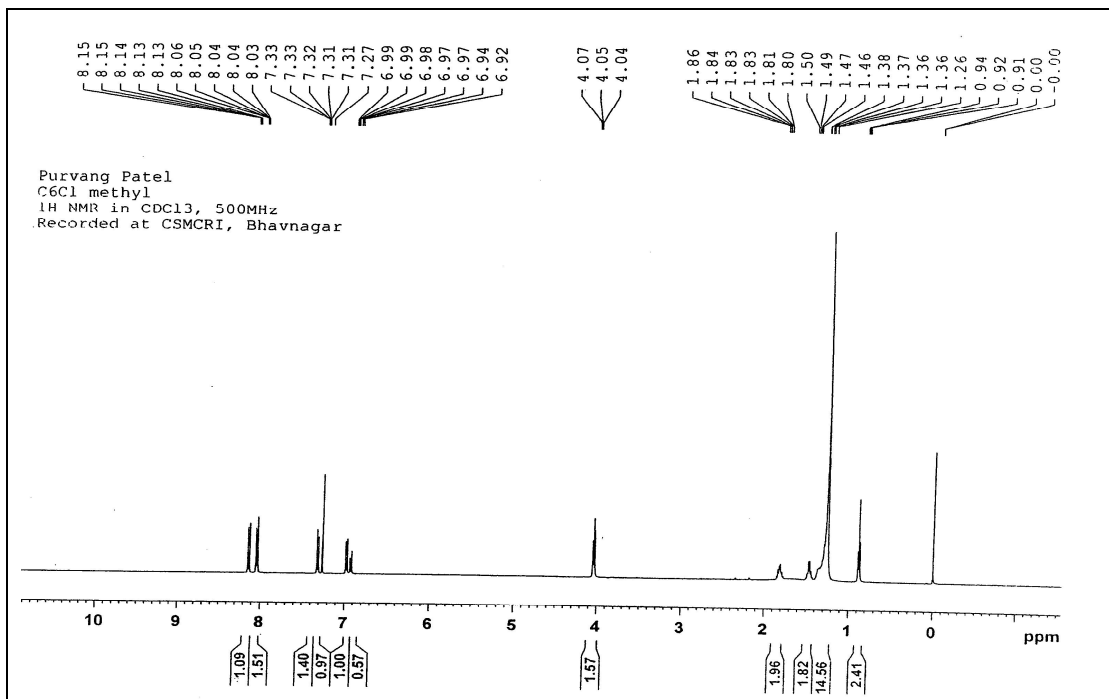


Figure 5.2 (c): ¹H NMR spectra of C6 homologue of series XII

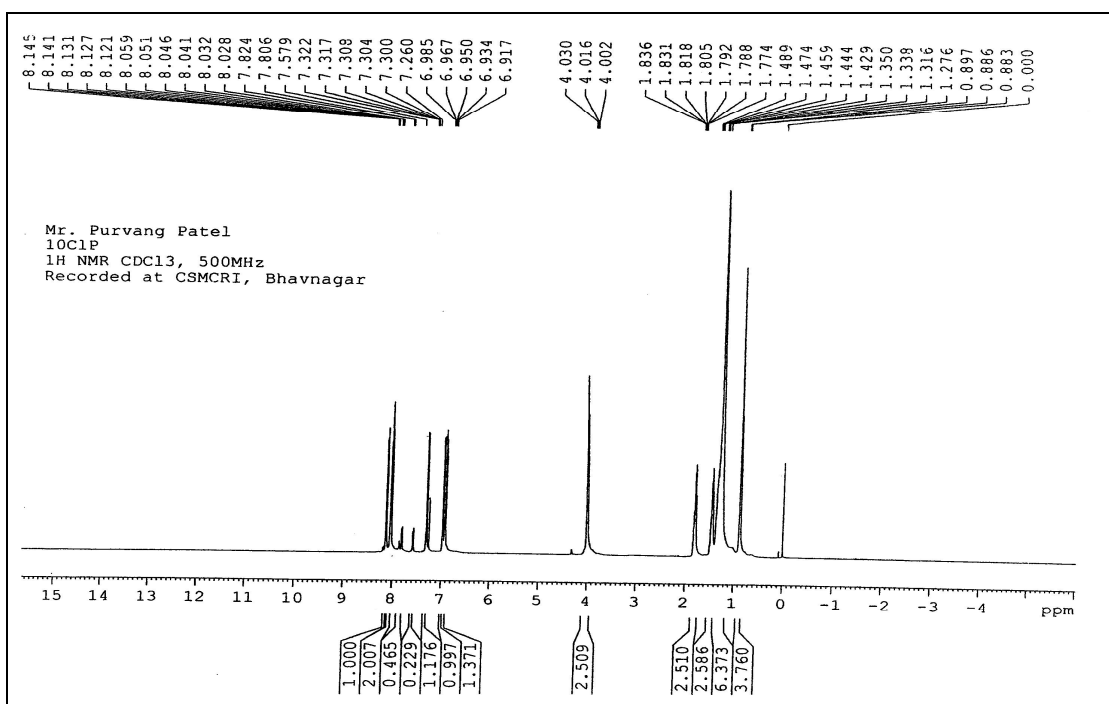


Figure 5.2 (d): ¹H NMR spectra of C10 homologue of series XII

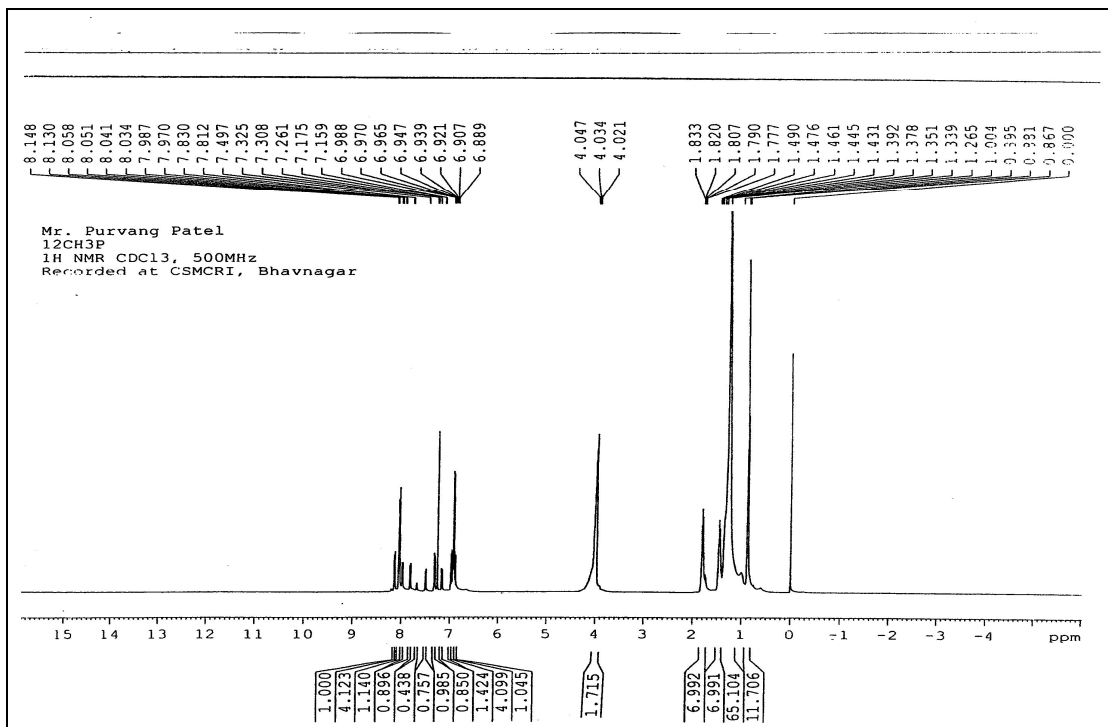


Figure 5.2 (e): ^1H NMR spectra of C12 homologue of series XIII

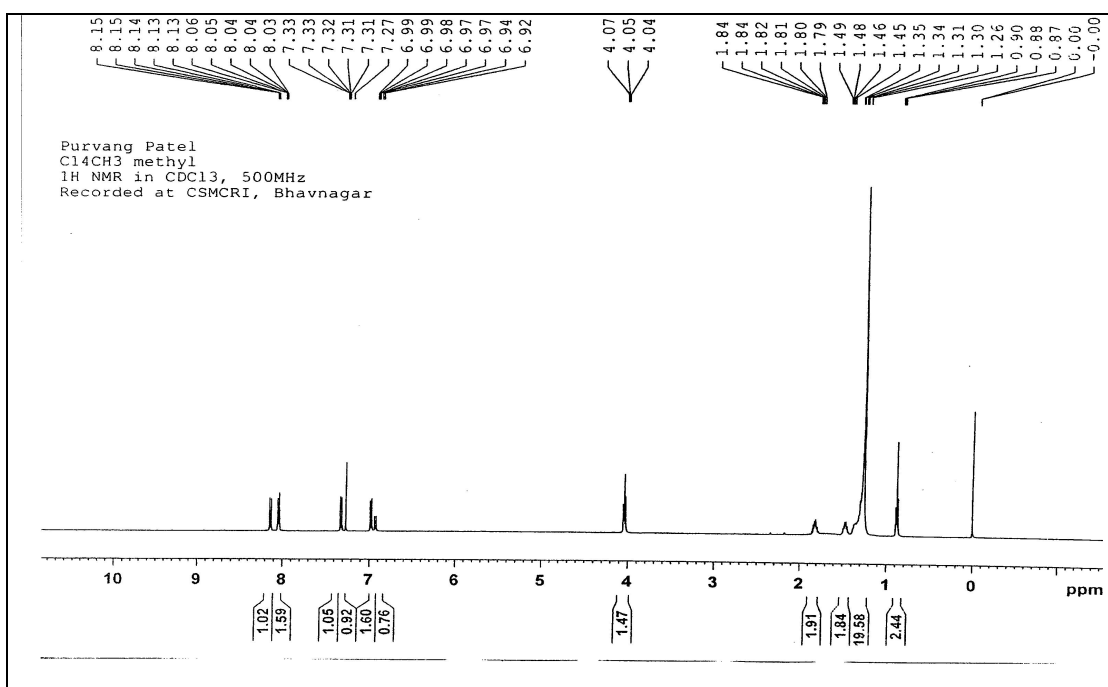


Figure 5.2 (f): ^1H NMR spectra of C14 homologue of series XIII

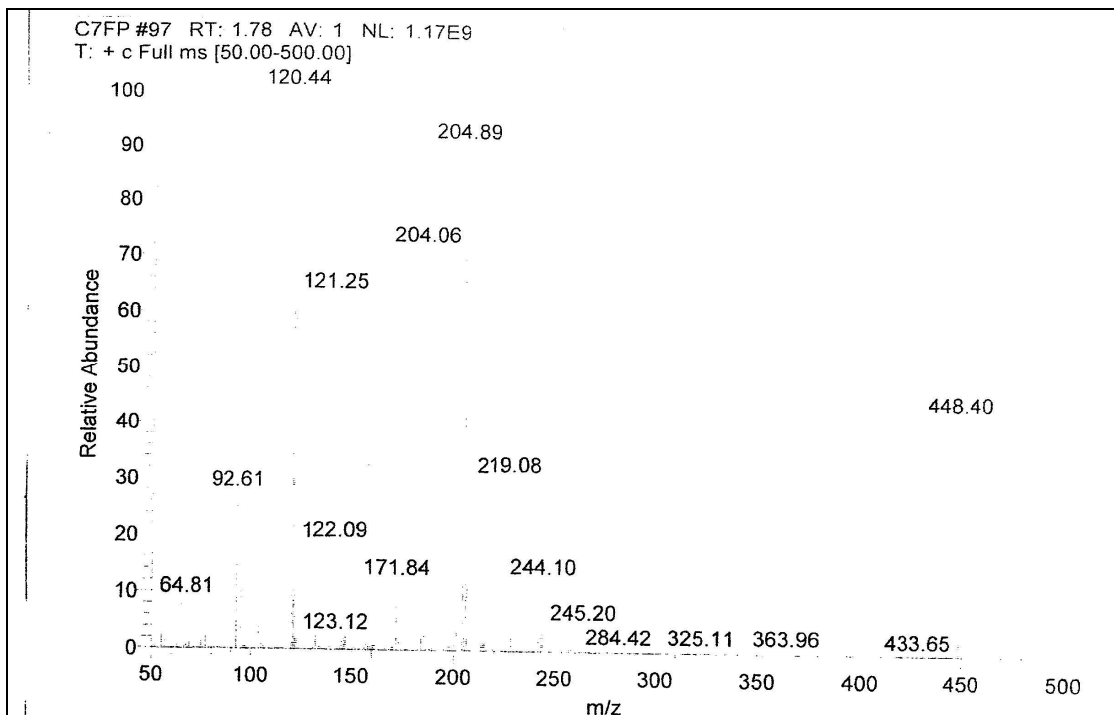


Figure 5.3 (a): Mass spectra of C7 homologue of series XI

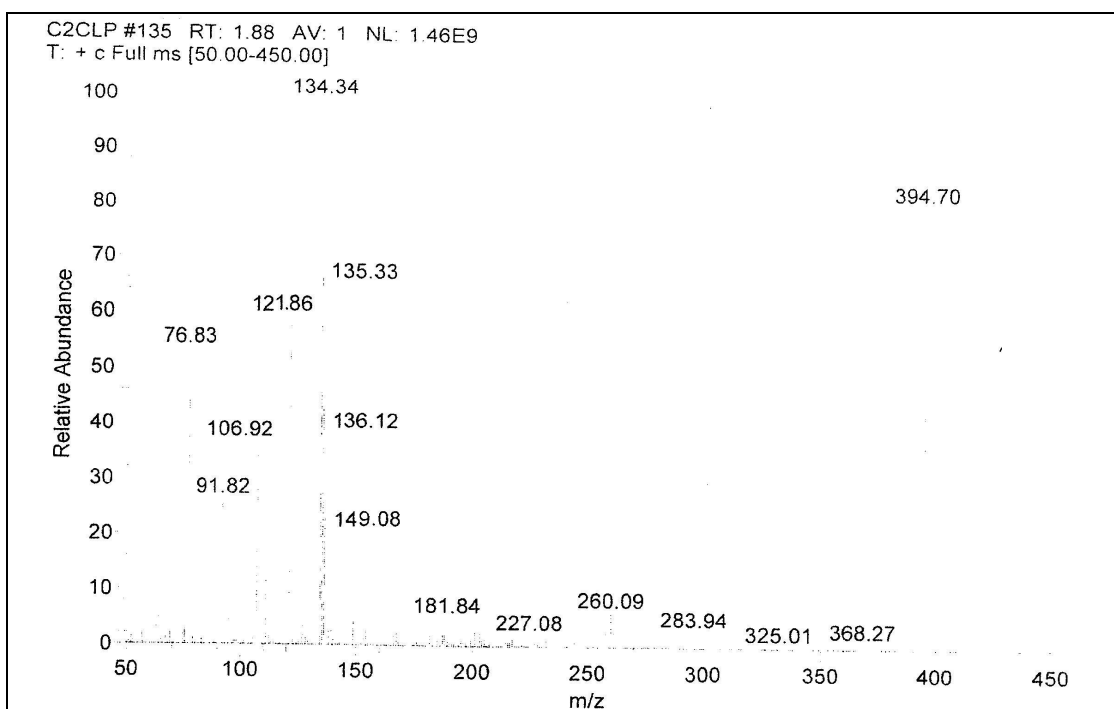


Figure 5.3 (b): Mass spectra of C2 homologue of series XII

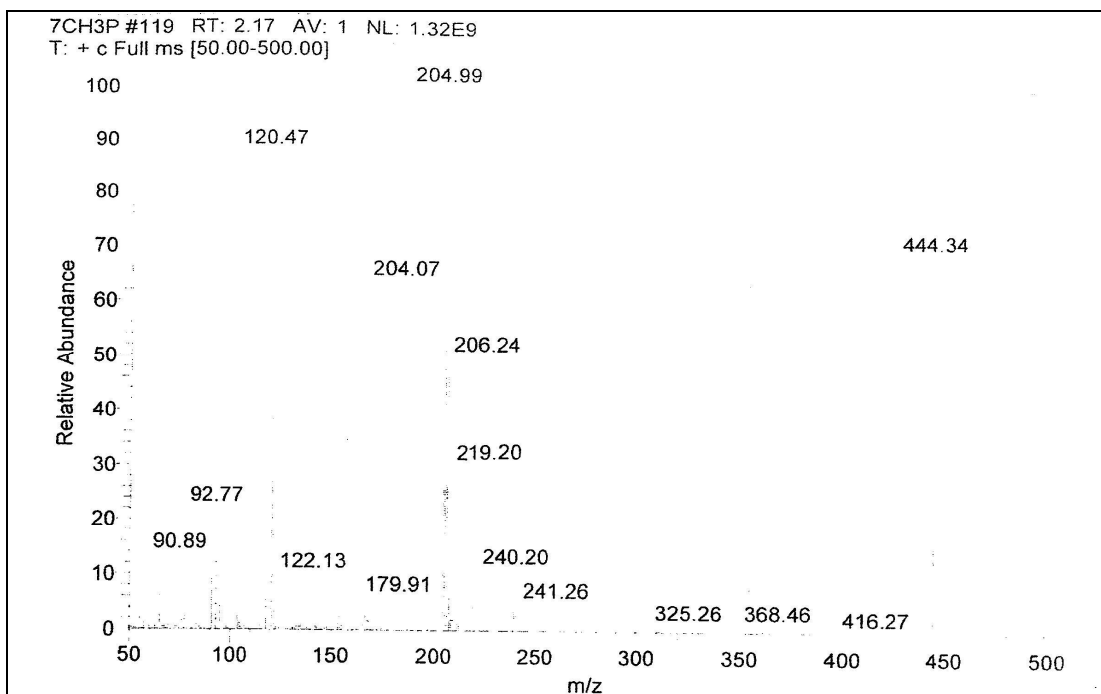


Figure 5.3 (c): Mass spectra of C7 homologue of series XIII

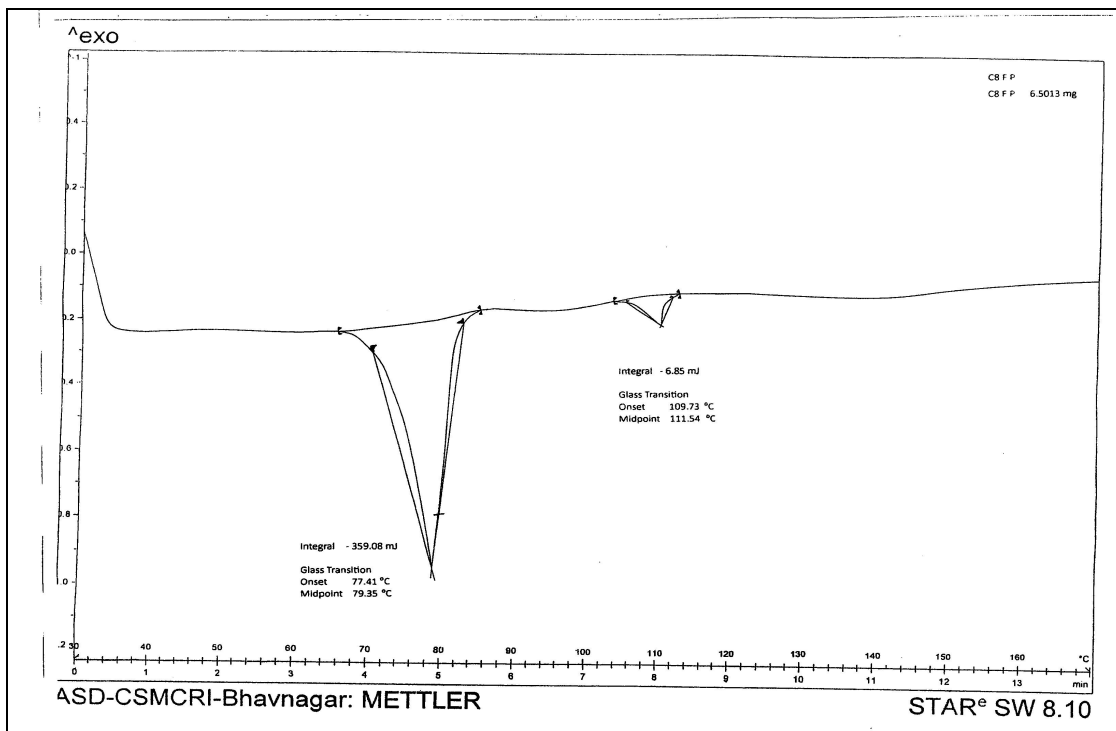


Figure 5.4 (a): DSC Thermogram of C8 homologue of series XI

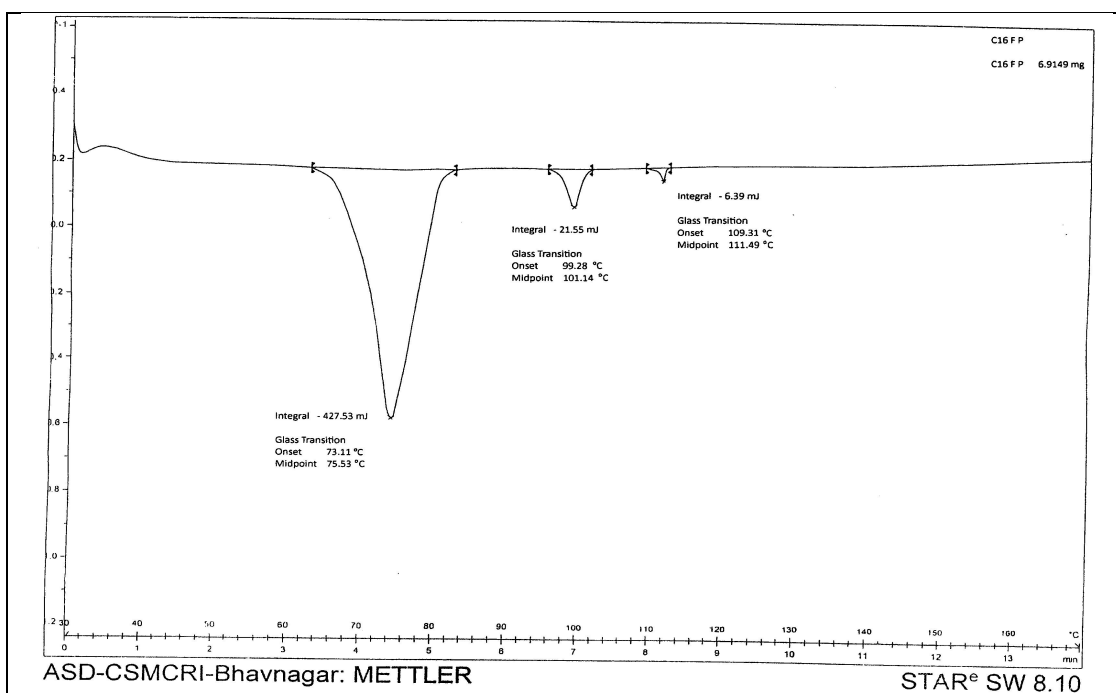


Figure 5.4 (b): DSC Thermogram of C16 homologue of series XI

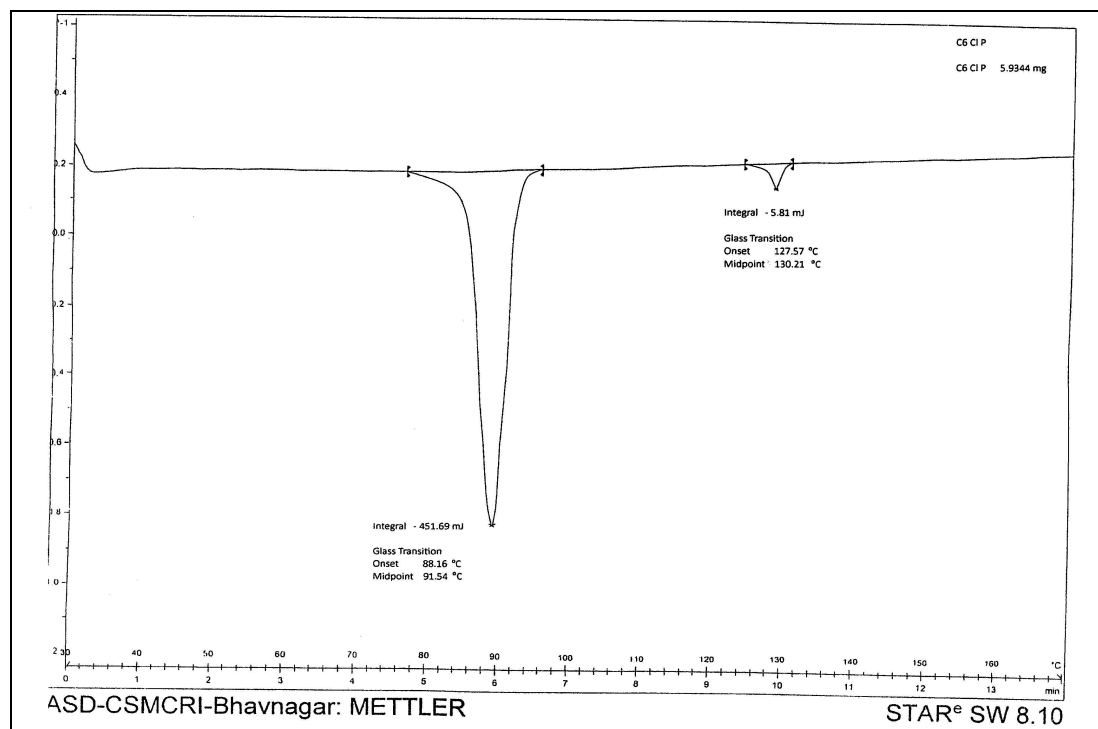


Figure 5.4 (c): DSC Thermogram of C6 homologue of series XII

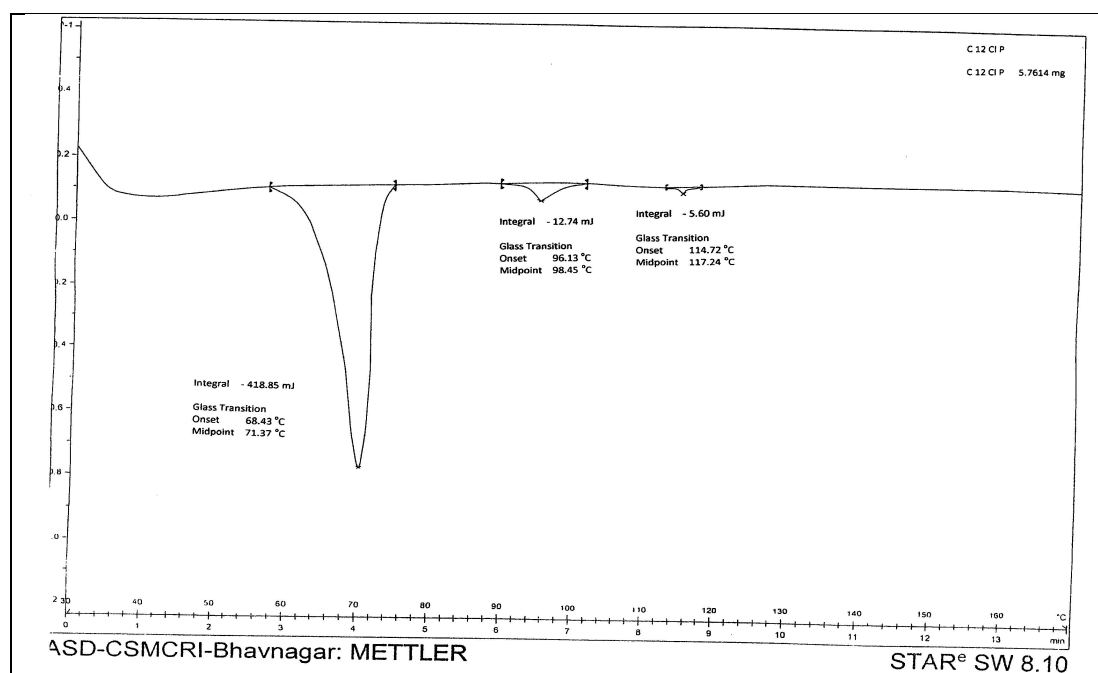


Figure 5.4 (d): DSC Thermogram of C12 homologue of series XII

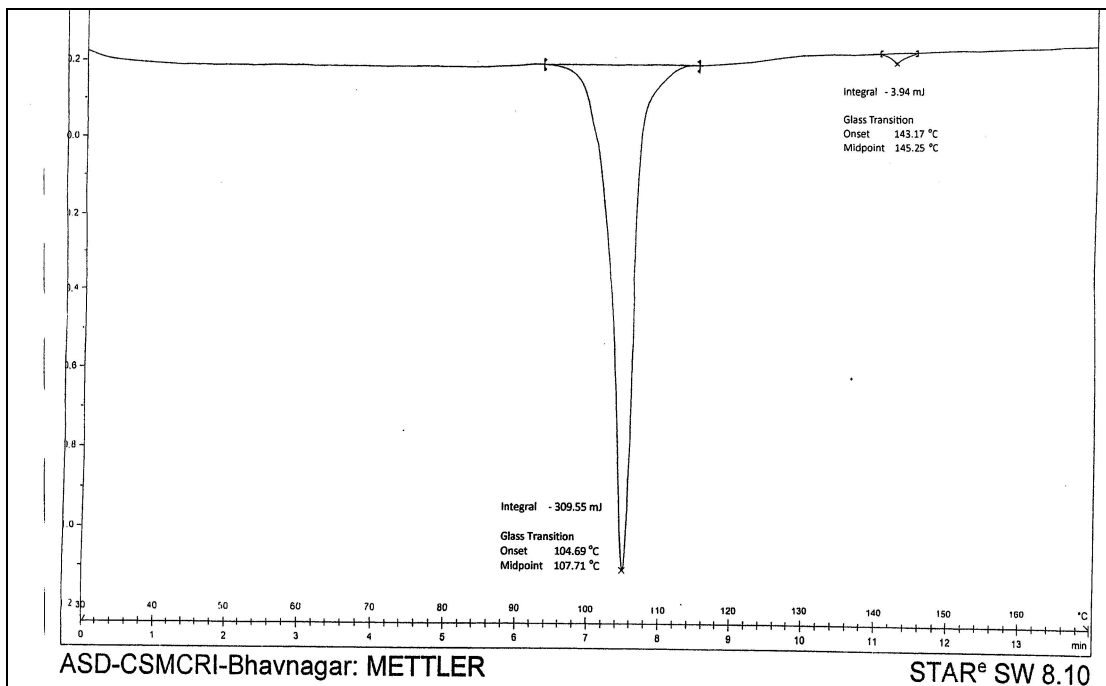


Figure 5.4 (e): DSC Thermogram of C5 homologue of series XIII

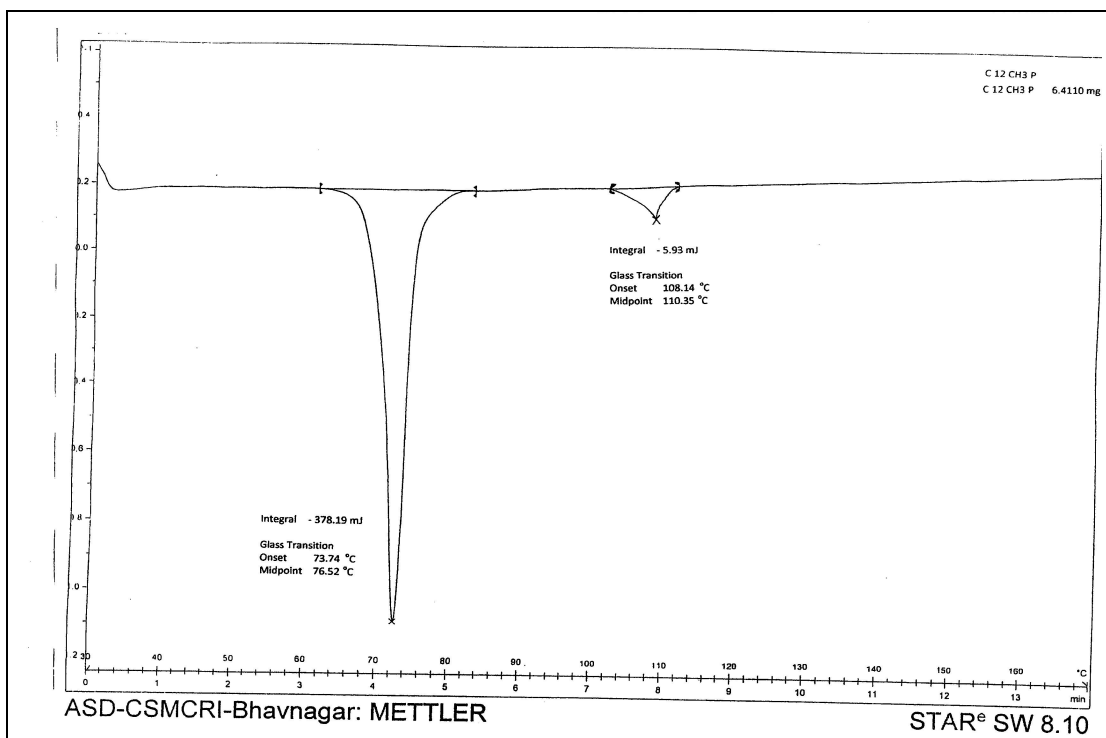


Figure 5.4 (f): DSC Thermogram of C12 homologue of series XIII

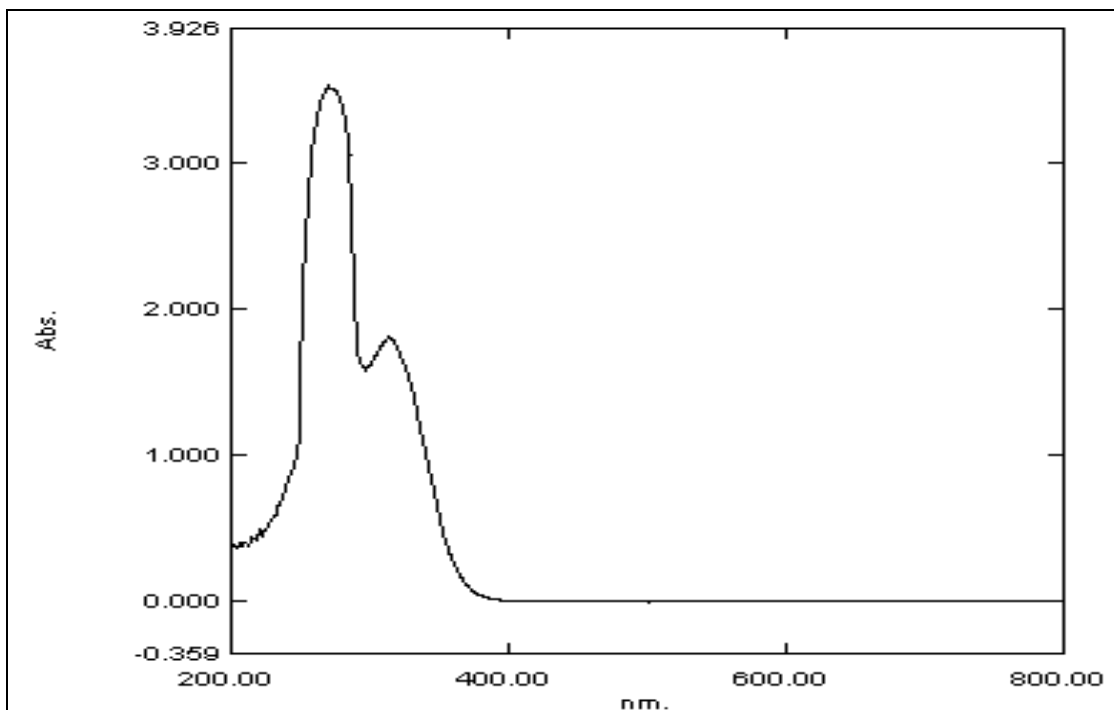


Figure 5.5 (a): UV spectra of C2 homologue of series XI

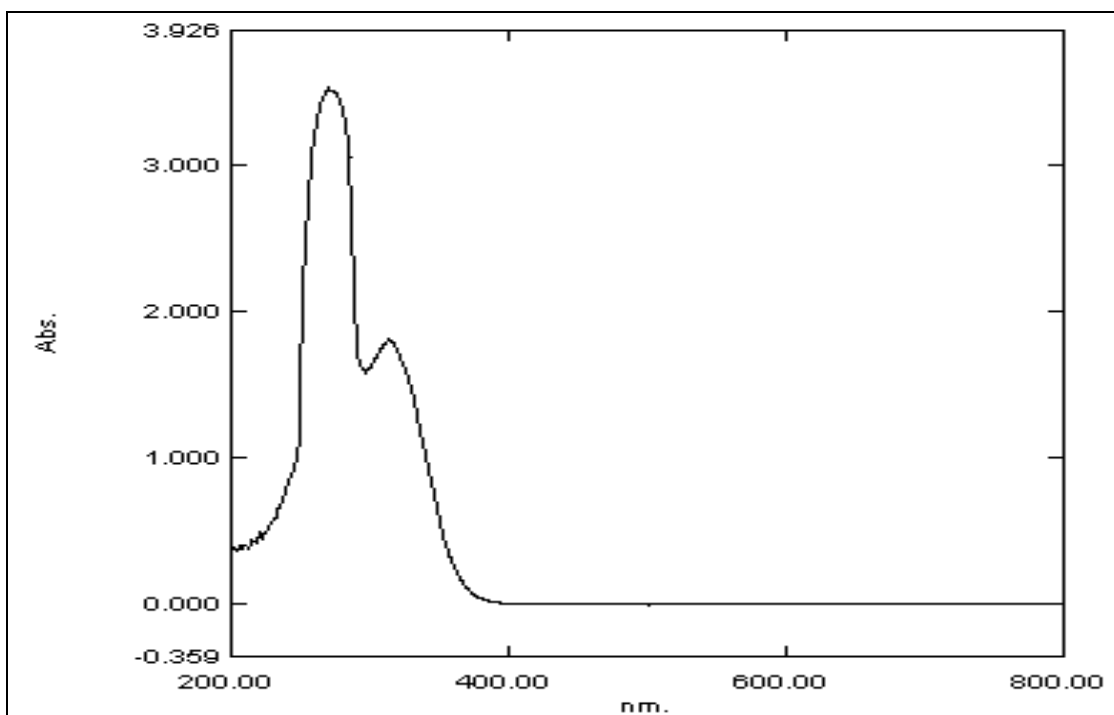


Figure 5.5 (b): UV spectra of C16 homologue of series XI

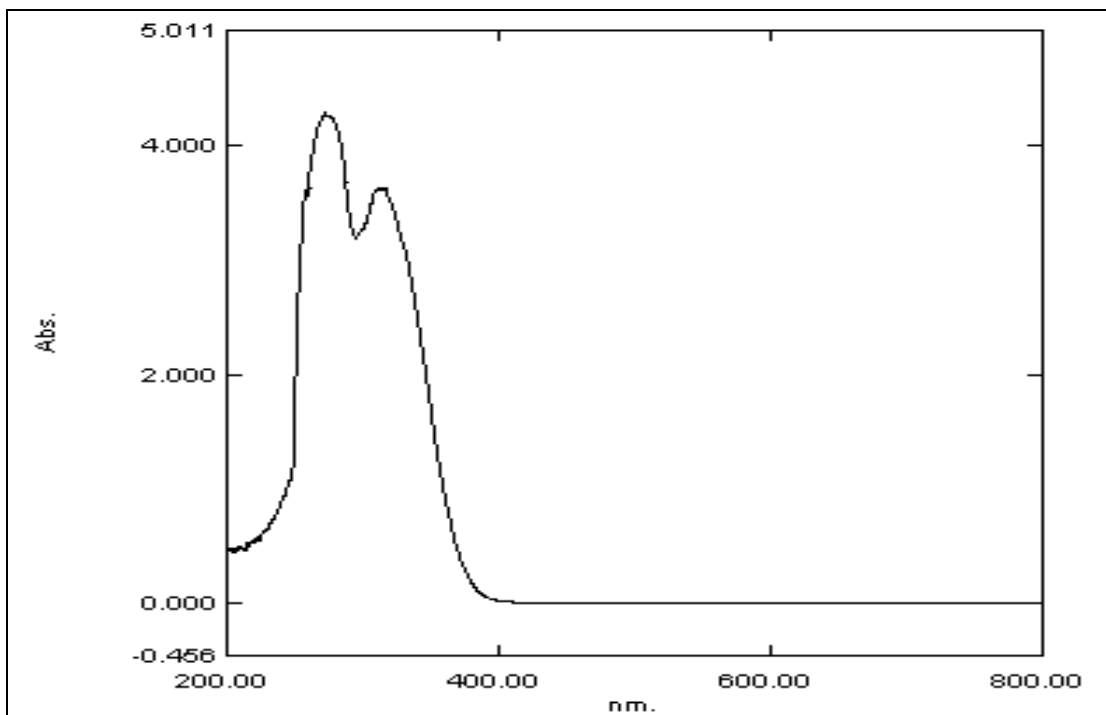


Figure 5.5 (c): UV spectra of C5 homologue of series XII

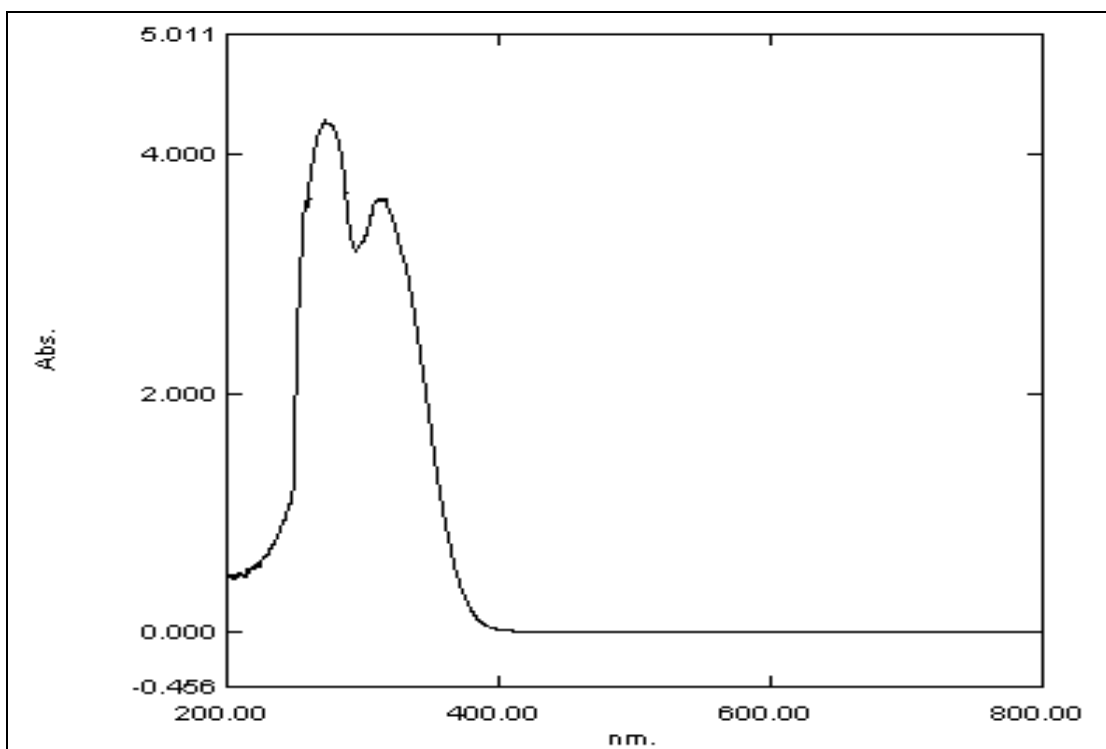


Figure 5.5 (d): UV spectra of C8 homologue of series XII

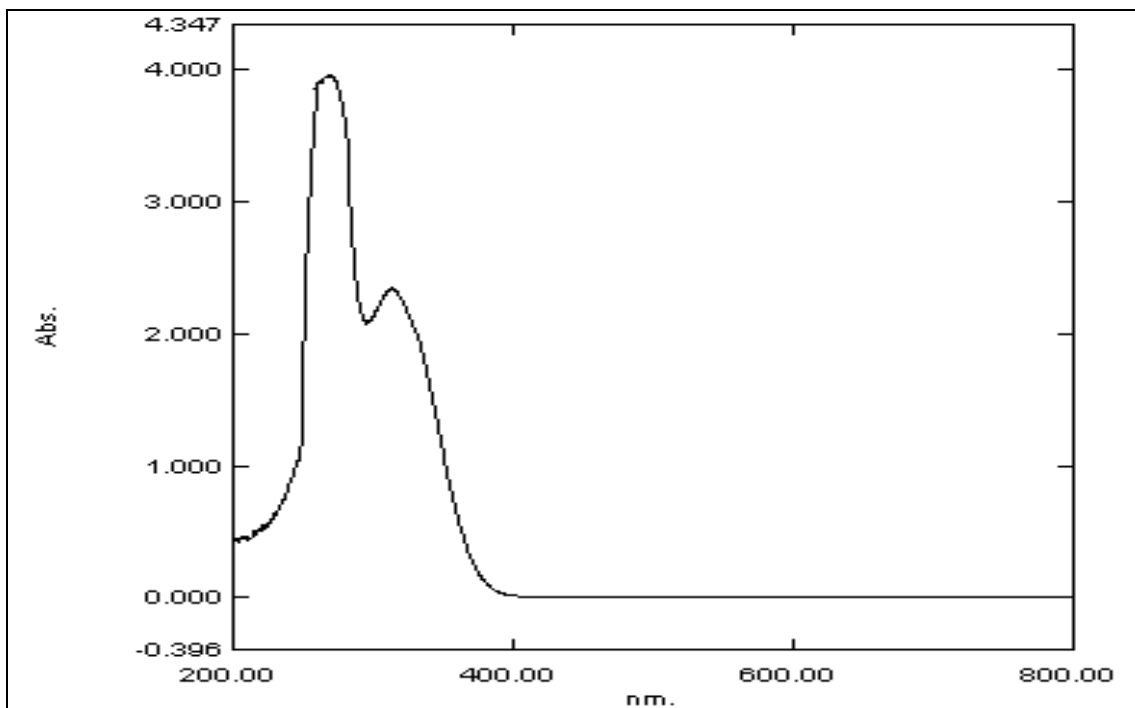


Figure 5.5 (e): UV spectra of C3 homologue of series XIII

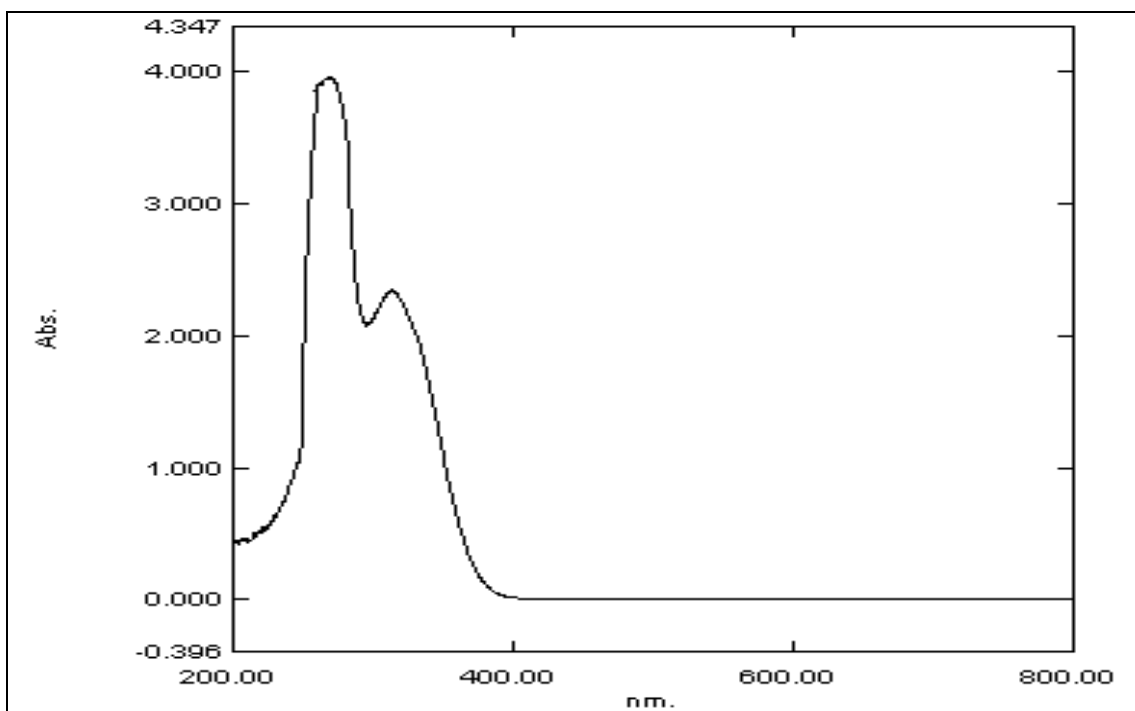
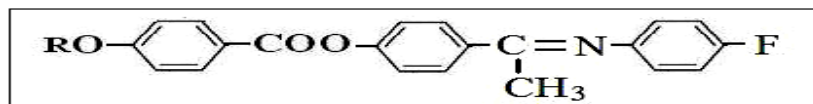


Figure 5.5 (f): UV spectra of C12 homologue of series XIII

5.3 Results and Discussion

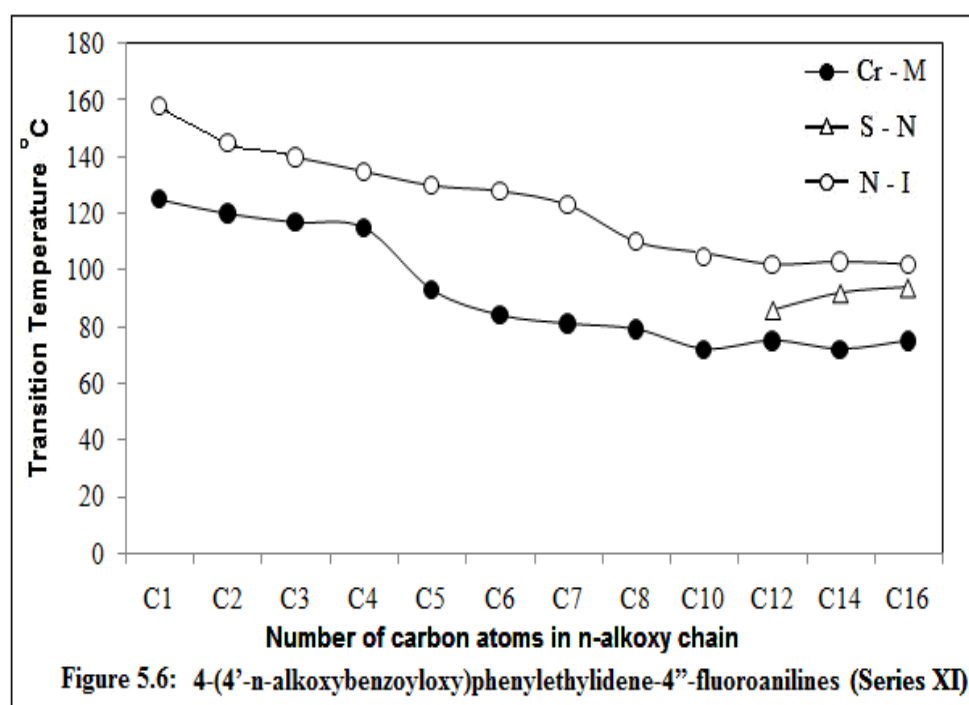
5.3.1 Series XI: 4-(4'-n-alkoxybenzoyloxy)phenylethylidene-4''-fluoroanilines

General molecular structure of series XI



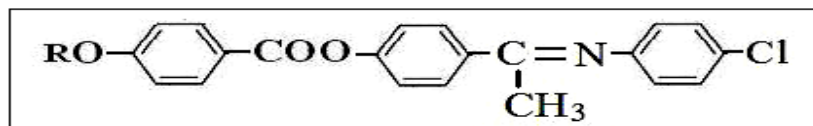
Where, R is C_nH_{2n+1} $n = 1$ to 8, 10, 12, 14 and 16

All the twelve homologues of the series XI are mesogens (Table 5.1); the nematic phase commences from the first methyl derivative and remains upto the last hexadecyl derivative while Smectic A phase commences from the dodecyl derivative and remains to be exhibited upto the last hexadecyl derivative synthesised. Figure 5.6 shows the plot of transition temperatures against number of carbon atoms in n-alkoxy chain; it indicates that N-I curve shows overall falling tendency as the series is ascended. No odd-even effect is observed in N-I curve. S-N curve between dodecyl and hexadecyl shows rising tendency as the series is ascended. The Cr-M transitions show overall falling tendency as the series is ascended. Nematic phase of the series shows threaded texture and the smectic phase shows focal conic fan-shaped texture of smectic A variety.



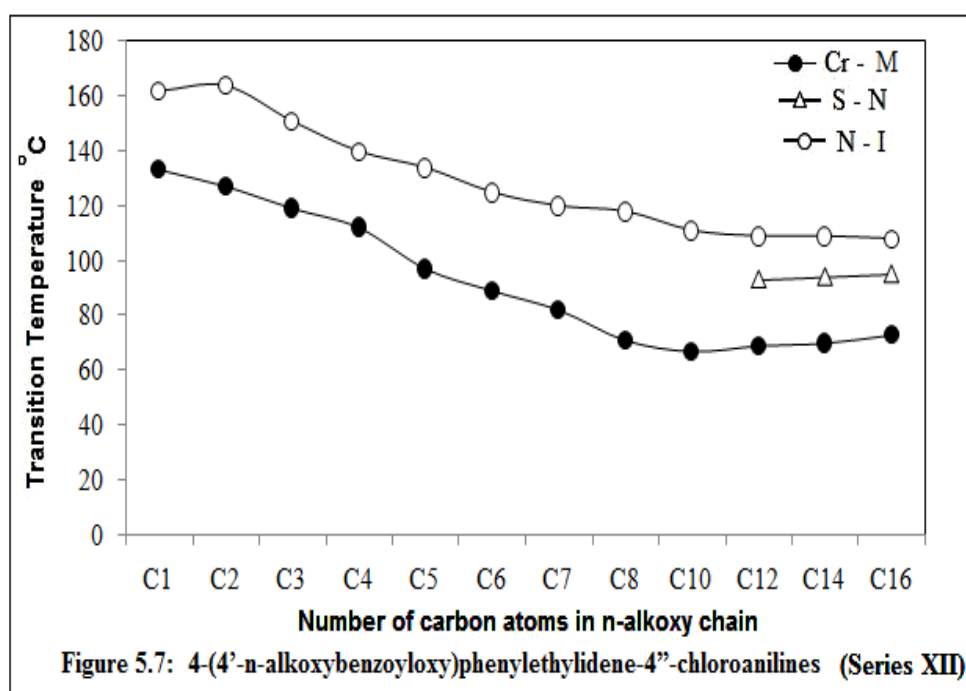
5.3.2 Series XII: 4-(4'-n-alkoxybenzoyloxy)phenylethylidene-4''-chloroanilines

General molecular structure of series XII



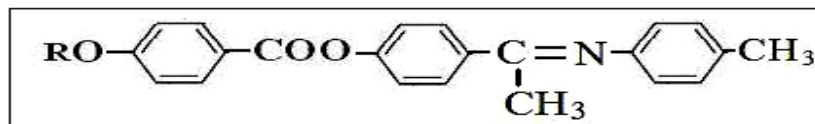
Where, R is C_nH_{2n+1} $n=1$ to 8, 10, 12, 14 and 16

All the twelve homologues of the series XII are mesogens (Table 5.5); the nematic phase commences from the first methyl derivative and remains up to the last hexadecyl derivative while Smectic A phase commences from the dodecyl derivative and remains to be exhibited up to the last hexadecyl derivative synthesised. Figure 5.7 shows the plot of transition temperatures against number of carbon atoms in n-alkoxy chain; it indicates that N-I curve shows overall falling tendency with slight increase at ethyl derivative as the series is ascended. No odd-even effect is observed in N-I curve. S-N curve between dodecyl and hexadecyl derivative shows rising tendency as the series is ascended. The Cr-M transitions show initially falling tendency upto decyl derivative and marginal rising tendency upto hexadecyl derivative as the series is ascended. Nematic phase of the series shows threaded texture and the smectic phase shows focal conic fan-shaped texture of smectic A variety.



5.3.3 Series XIII: 4-(4'-n-alkoxybenzoyloxy)phenylethylidene-4'-toluidines

General molecular structure of series XIII



Where, R is C_nH_{2n+1} $n=1$ to 8, 10, 12, 14 and 16

All the twelve homologues of the series XIII are mesogens (Table 5.9); the nematic phase commences from the first methyl derivative and remains exhibited upto the last hexadecyl derivative synthesised. Figure 5.8 shows the plot of transition temperatures against number of carbon atoms in n-alkoxy chain; it indicates that N-I curve shows overall falling tendency as the series is ascended. No odd-even effect is observed in N-I curve. The Cr-M transitions show initial rise from methyl to ethyl derivative and then a continuous fall upto hexadecyl derivative with a little steep fall from hexyl to heptyl derivative as the series is ascended. Nematic phase of the series shows threaded texture.

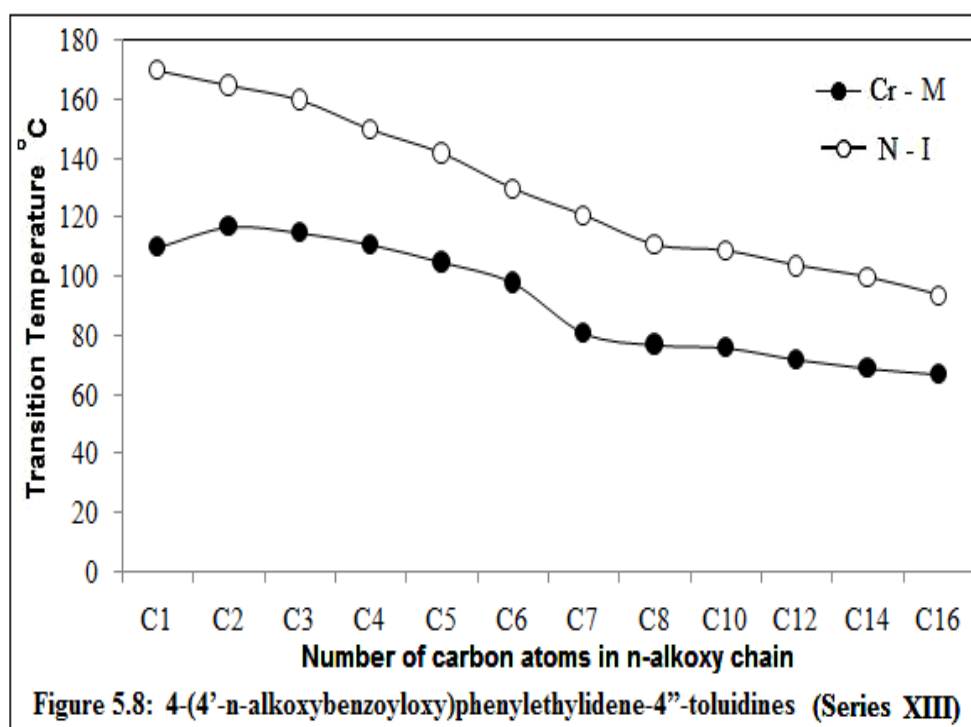


Table 5.13 and figure 5.9 show the average thermal stability for the homologous series. The average thermal stabilities of series XI, XII and XIII are compared with structurally related homologous series; scheme 5.2 gives the molecular structures of the series in comparison.

Table 5.13: Average thermal stability °C

Series	N-I	S-N	Commencement of smectic mesophase
XI	124.66 (C ₁ to C ₁₆)	91.00 (C ₁₂ to C ₁₆)	C ₁₂
XII	132.33 (C ₁ to C ₁₆)	100.66 (C ₁₂ to C ₁₆)	C ₁₂
XIII	130.75 (C ₁ to C ₁₆)	–	–
A	189.70 (C ₁ to C ₁₀)	116.80 (C ₈ to C ₁₆)	C ₈
B	195.90 (C ₁ to C ₁₂)	148.85 (C ₆ to C ₁₆)	C ₆
C	220.40 (C ₁ to C ₁₆)	104.50 (C ₇ to C ₁₆)	C ₇

Comparison of average thermal stabilities of all the three series (Table 5.13) shows that the N-I average thermal stability of series XII is higher than series XI and series XIII. The N-I average thermal stability of series XIII is higher than series XI. The S-N average thermal stability of series XII is higher than series XI.

All the structural features of the homologous series under comparison are same except the terminal group. Series XI has fluoro, series XII has chloro and series XIII has methyl terminal group. The N-I thermal stability of series XI is 124.66 °C, series XII is 132.33 °C and series XIII is 130.75 °C. Thus the nematic group efficiency for terminal group is Cl > CH₃ > F, which is in agreement with the order reported by Gray [83].

The series with terminal fluoro (series XI) and chloro (series XII) group only exhibit smectic mesophase and the S-N thermal stability of series XII is higher than series XI. It appears that the molecules of these homologues lie tilted to the planes of the smectic strata [349-350]. Thus, inducing the terminal dipoles due to C-Cl and C-F dispositions to act along the direction of the long axes of the molecules resulting into stronger predominance of lateral attractions which in turn enhance the S-N thermal stability.

Thus, the smectic group efficiency for terminal groups is $Cl > F$, which is in agreement with the order reported by Gray [83]. Here the series XIII does not exhibit smectic mesophase therefore its group efficiency order is not considered. The commencement of smectic mesophase in both the series XI and XII is at dodecyl derivative.

Comparing these presently synthesised homologous series XI, XII and XIII with structurally related series A[351], B[352] and C[353], it is seen that all the structural features of these series in comparison are same except one of the central bridge viz.

series XI, XII and XIII it is $\begin{array}{c} -C=N- \\ | \\ CH_3 \end{array}$ (ethylideneamino) and in series A, B and C the central bridge is $-N=N-$ (azo). The $-CH_3$ group in the ethylideneamino central linkage increases breadth of the molecule and causes disruption in the molecular packing, which reduces the transition temperatures and melting points as well as the N-I and S-N average thermal stabilities compared to the $-N=N-$ (azo) central linkage containing series A, B and C [332]. Therefore, series A, B and C have higher N-I and S-N average thermal stabilities than the corresponding series XI, XII and XIII respectively.

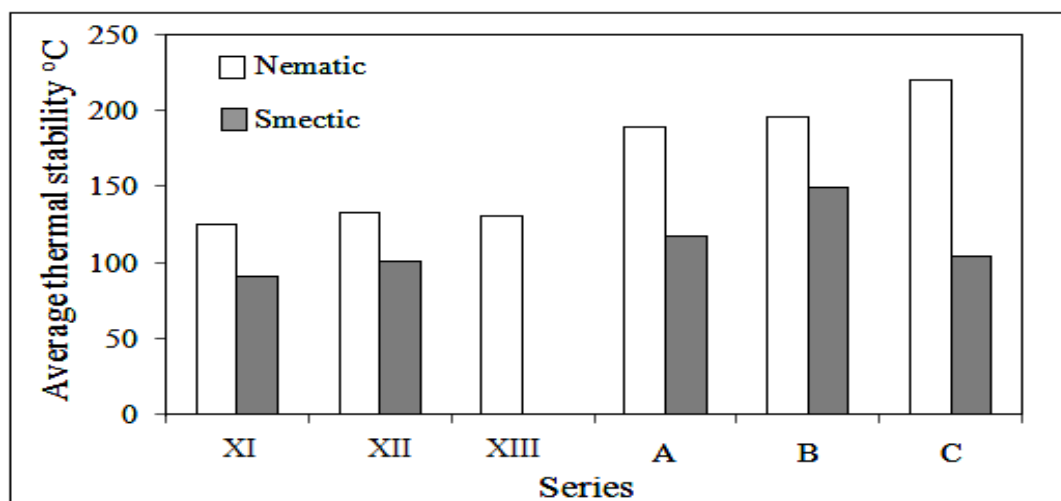
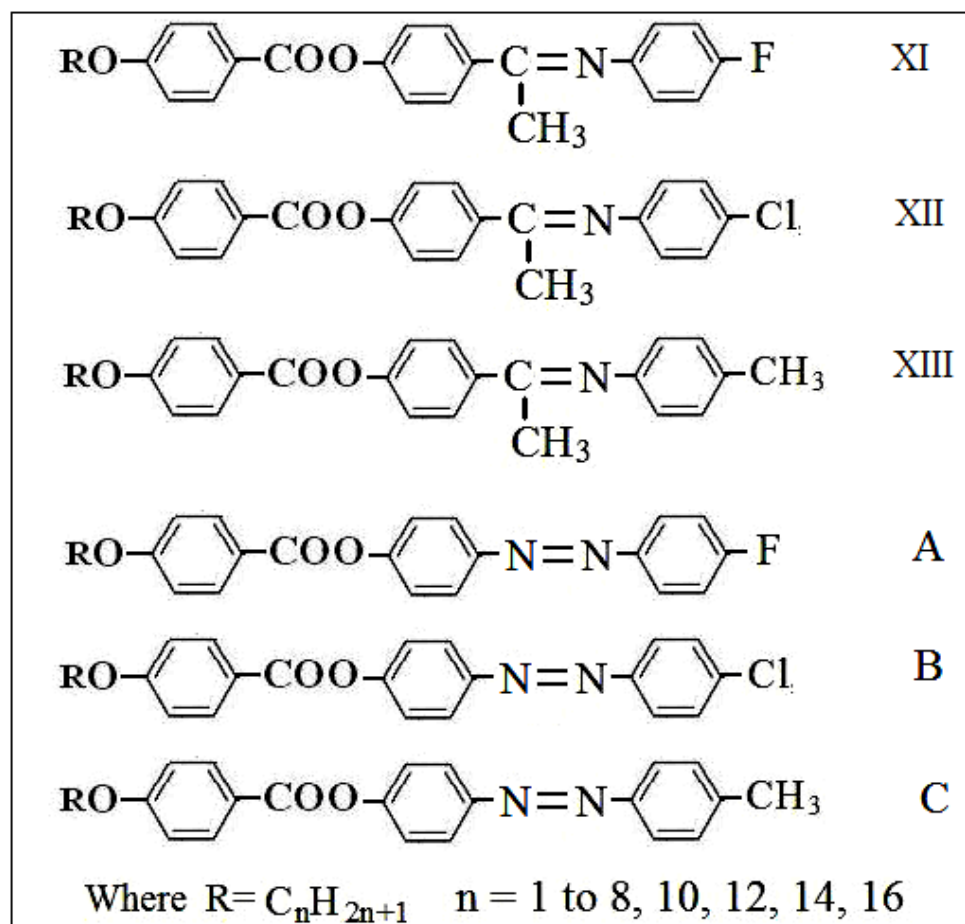
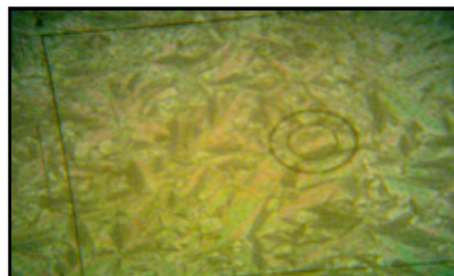


Figure 5.9: Average thermal stability for the series

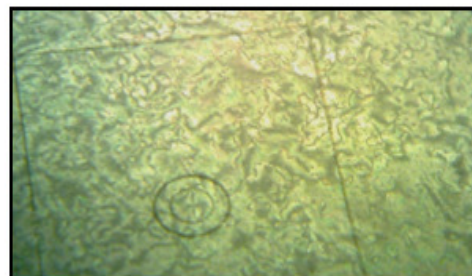


Scheme 5.2: Selected homologous series for comparison

Figure 5.10 shows the photomicrographs of the textures of representative derivatives.

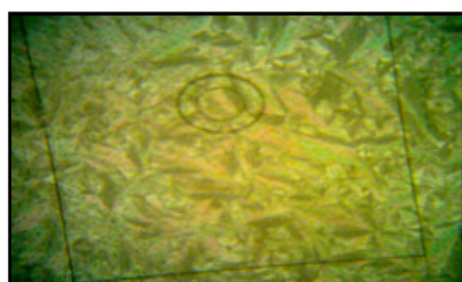


(a) Focal conic fan-shaped texture of smectic phase

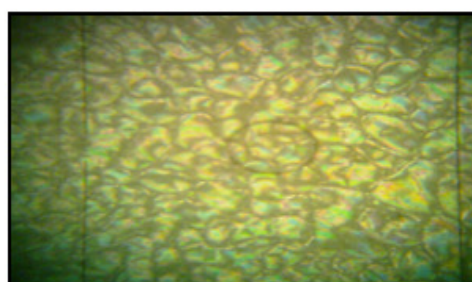


(b) Threaded texture of nematic phase

Photomicrographs of the textures of Tetradecyl homologue of series XI

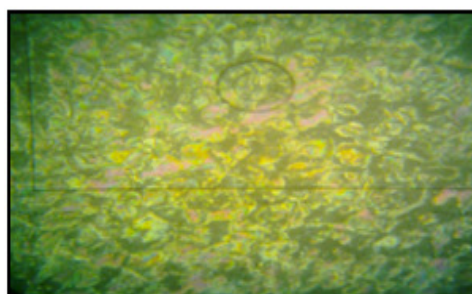


(c) Focal conic fan-shaped texture of smectic phase



(d) Threaded texture of nematic phase

Photomicrographs of the textures of Dodecyl homologue of series XII



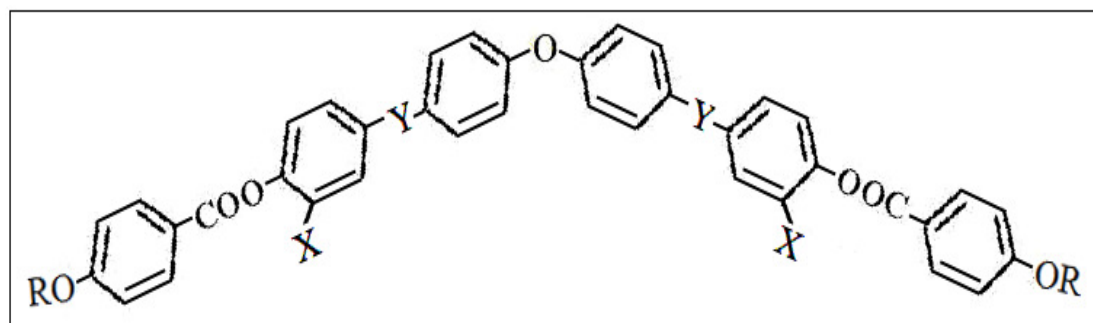
(e) Threaded texture of nematic phase

Photomicrographs of the textures of Butyl homologue of series XIII

Figure 5.10: Photomicrographs of the textures of the representative homologues

6.1 Introduction

Since chemical structure has been understood to have most significant effect on the mesophase formed by liquid crystalline compounds. It is observed that a molecule which possesses a linear structure along with two or more phenyl rings linked via stable central linkages seems to have an advantage in the formation of mesophases. Moreover, flexibility is also likely to have an important effect on the packing of the molecules [354]. However, quite a good number of novel compounds with non-linear structures having bent core have been found exhibiting liquid crystalline behavior [355-359]. Majority of bent shaped compounds containing five or seven phenyl rings [360-361]. Bent shaped compounds containing six phenyl rings are comparatively few [362-364]. Mesomorphic bent shaped derived from diphenylether moiety having six phenyl rings are reported [365]. Diphenylether moiety is first used by Vorlander in the field of liquid crystals [366]. In view of this two new homologous series of mesomorphic bent shaped derivatives having diphenylether moiety and six phenyl rings are synthesized; the effect of lateral methoxy group in the middle phenyl ring of the bent core molecules on the mesomorphism are studied by addition of the lateral methoxy group in the series XIV, moreover the effect of ethylideneamino central linkage on the mesomorphism in the bent core molecules are also studied in series XV. The study enables to understand the relationship between molecular structure and mesomorphic behavior in the bent core compounds. The general molecular structure of the series is



Where, R is C_nH_{2n+1} $n=1$ to 8, 10, 12, 14, 16

Series	X	Y
XIV	-OCH ₃	-CH=N-
XV	-H	-C=N- CH ₃

6.2 Experimental

6.2.1 Materials

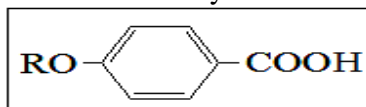
4-hydroxybenzoic acid, 4-hydroxyacetophenone, n-alkylhalides, thionylchloride, 4,4'-diaminodiphenylether, 3-methoxy-4-hydroxybenzaldehyde and all other chemicals are of Merck, SRL or Loba grade and used as received.

6.2.2 Synthesis

6.2.2.1 4,4'-Bis[4''-(4'''-n-alkoxybenzoyloxy)3''-methoxybenzylideneamino]-diphenylethers (Series XIV)

6.2.2.1.a 4-n-alkoxybenzoic acids

General molecular structure of 4-n-alkoxybenzoic acids

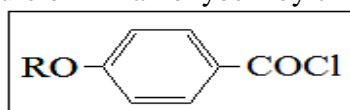


Where, R is C_nH_{2n+1} $n= 1$ to 8, 10, 12, 14 and 16

They are synthesized following the procedure reported in 3.2.2.1.a. [312]

6.2.2.1.b 4-n-alkoxybenzoylchlorides

General molecular structure of 4-n-alkoxybenzoylchlorides

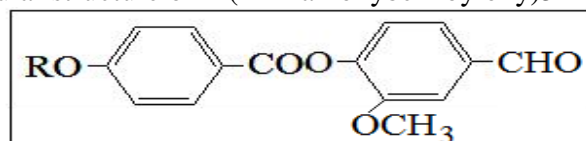


Where, R is C_nH_{2n+1} $n= 1$ to 8, 10, 12, 14 and 16

They are synthesized following the procedure reported in 3.2.2.1.b. [312]

6.2.2.1.c 4-(4'-n-alkoxybenzoyloxy)3-methoxybenzaldehydes

General molecular structure of 4-(4'-n-alkoxybenzoyloxy)3-methoxybenzaldehydes

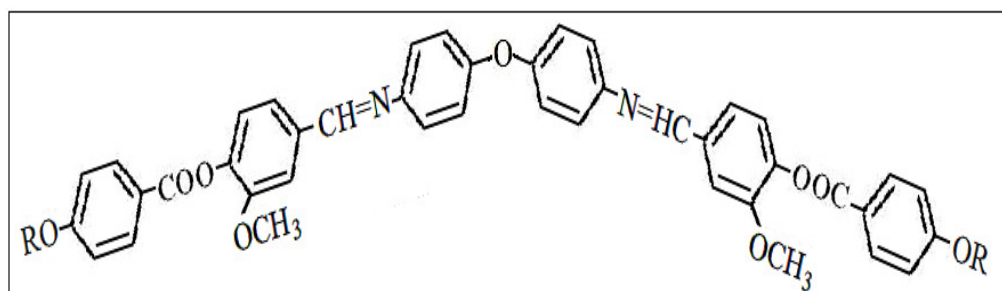


Where, R is C_nH_{2n+1} $n= 1$ to 8, 10, 12, 14 and 16

They are prepared by condensing the appropriate 4-n-alkoxybenzoylchlorides with 4-hydroxy-3-methoxybenzaldehyde following the similar method reported in step 3.2.2.1.d.

6.2.2.1.d 4,4'-Bis[4''-(4'''-n-alkoxybenzoyloxy)3''-methoxybenzylideneamino]-diphenylethers (Series XIV)

General molecular structure of 4,4'-Bis[4''-(4'''-n-alkoxybenzoyloxy)3''-methoxybenzylideneamino]-diphenylethers



Where, R is C_nH_{2n+1} $n= 1$ to 8, 10, 12, 14 and 16

They are synthesised by taking 0.002 mole of appropriate 4-(4'-n-alkoxybenzoyloxy)-3-methoxybenzaldehyde and 0.001 mole of 4,4'-diaminodiphenylethres following the similar method reported in step 4.2.2.1.c. The products are filtered, dried and recrystallized from acetone until constant transition temperatures are obtained. They are recorded in table 6.1. The elemental analysis of all the compounds are found to be satisfactory and are recorded in table 6.2.

6.2.2.2 4,4'-Bis[4''-(4'''-n-alkoxybenzoyloxy)phenylethylideneamino]-diphenyl-ethers (Series XV)

6.2.2.2.a 4-n-alkoxybenzoicacids

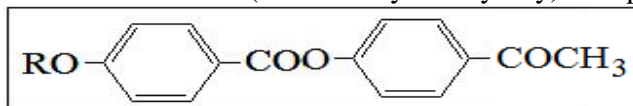
They are synthesized following the procedure reported in 3.2.2.1.a. [312]

6.2.2.2.b 4-n-alkoxybenzoylchlorides

They are synthesized following the procedure reported in 3.2.2.1.b. [312]

6.2.2.2.c 4-(4'-n-alkoxybenzoyloxy)acetophenones

General molecular structure of 4-(4'-n-alkoxybenzoyloxy)acetophenones

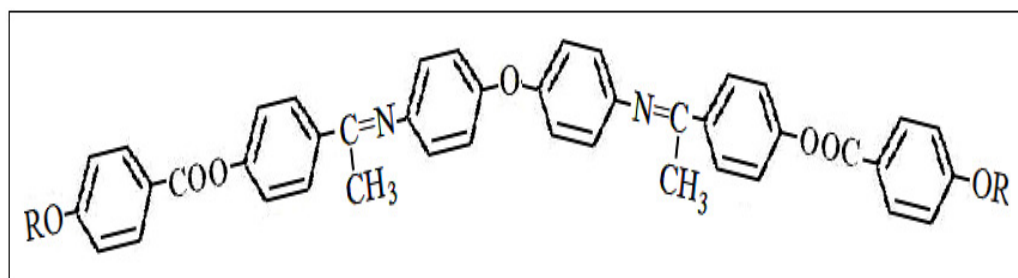


Where, R is C_nH_{2n+1} $n= 1$ to 8, 10, 12, 14 and 16

They are prepared by condensing the appropriate 4-n-alkoxybenzoylchlorides with 4-hydroxyacetophenone following the similar method reported in step 3.2.2.1.d.

6.2.2.2.d 4,4'-Bis[4''-(4'''-n-alkoxybenzoyloxy)phenylethylideneamino]-diphenyl-ethers (Series XV)

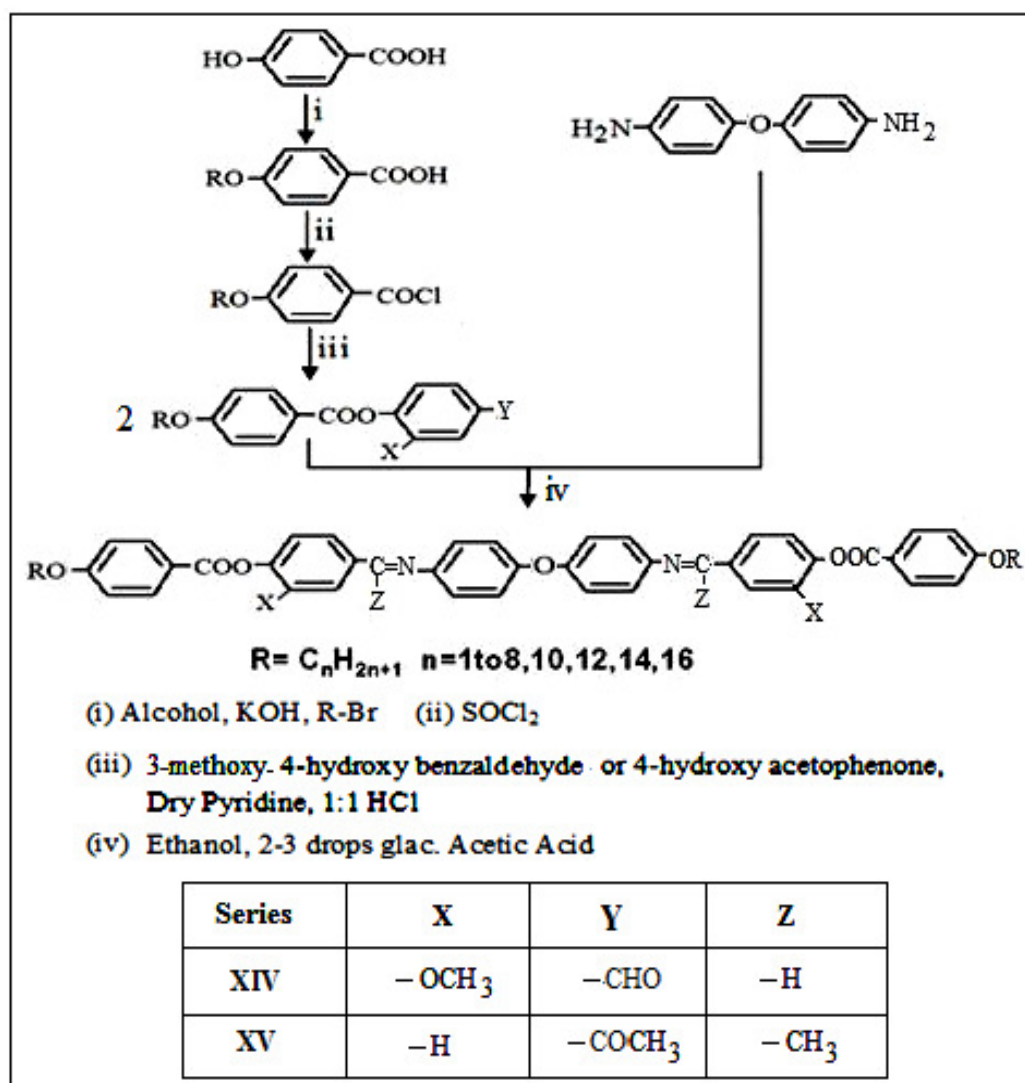
General molecular structure of 4,4'-Bis[4''-(4'''-n-alkoxybenzoyloxy)phenyl ethylideneamino]-diphenyl-ethers



Where, R is C_nH_{2n+1} $n= 1$ to 8, 10, 12, 14 and 16

They are synthesised by taking 0.002 mole of appropriate 4-(4'-n-alkoxybenzoyloxy)-acetophenone and 0.001 mole of 4,4'-diamino diphenyl ethres following the similar method reported in step 4.2.2.1.c. The products are filtered, dried and recrystallized from acetone until constant transition temperatures are obtained. They are recorded in table 6.5. The elemental analysis of all the compounds are found to be satisfactory and are recorded in table 6.6.

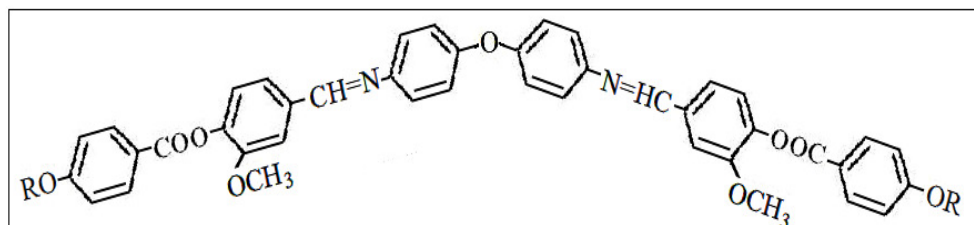
The synthetic route of series XIV and XV is shown in scheme 6.1.



Scheme 6.1: Synthetic route for series XIV and XV

6.2.3 Characterization

Elemental analysis of some of the representative compounds are performed on Perkin Elmer Series II 2400-CHN analyzer, Electronic spectra are recorded on a Shimadzu UV-2450 UV-visible spectrophotometer, IR spectra are recorded on a Perkin Elmer GX-FTIR, 1H NMR spectra are measured on a Bruker Avance II-500 spectrometer. Mass spectra are recorded on Thermoscientific DSQ II mass spectrometer. Transition temperatures and the textures of the mesophases are studied using Leitz Laborlux 12 POL polarizing microscope provided with a Kofler heating stage. DSC are performed on a Mettler Toledo Star SW 7.01.

Table 6.1: Transition temperatures: 4,4'-Bis[4''-(4'''-n-alkoxybenzoyloxy)3''-methoxybenzylideneamino]diphenylethers (Series XIV)

Homologue	Transition Temperatures °C	
	Nematic	Isotropic
Methyl	138	231
Ethyl	124	236
Propyl	126	228
Butyl	126	220
Pentyl	112	199
Hexyl	116	194
Heptyl	100	170
Octyl	107	146
Decyl	104	137
Dodecyl	91	128
Tetradecyl	89	114
Hexadecyl	90	100

Table 6.2: Elemental analysis

Homologue	Calculated			Found		
	C %	H %	N %	C %	H %	N %
Propyl	72.72	5.55	3.53	72.82	5.61	3.58
Octyl	74.67	6.86	3.00	74.78	6.69	3.05
Hexadecyl	76.81	8.30	2.42	76.97	8.51	2.49

FTIR (Nujol, KBr pellets, cm⁻¹)

Ethyl homologue: 2953, 2918, 1739 (-COO-), 1643, 1357, 1255, 1161 (-CH=N-), 1082 (-CH₂-O-), 943, 848, 758, 692

Dodecyl homologue: 2949, 2928, 1722 (-COO-), 1624, 1357, 1253, 1161 (-CH=N-), 1072 (-CH₂-O-), 939, 848, 758, 690

¹H NMR: (CDCl₃, 500 MHz, δ , ppm, standard TMS)

Hepxyl homologue: δ 0.9 (3H, t, -CH₃), 1.3-1.83 (m, alkyl chain), 3.99-4.05 (m, 6H, 2x -OCH₃ and 4H, 2x -OCH₂-CH₂), 6.67-8.14 (m, Ar-H), 8.46 (1H, S, 2x -CH=N-)

Decyl homologue: δ 0.9 (3H, t, -CH₃), 1.32-1.85 (m, alkyl chain), 3.85-3.93 (6H, t, 2x -OCH₃) 4.03-4.05 (4H, t, 2x -OCH₂-CH₂), 6.96-8.17 (m, Ar-H), 8.4 (1H, S, 2x -CH=N-)

Mass Spectra:

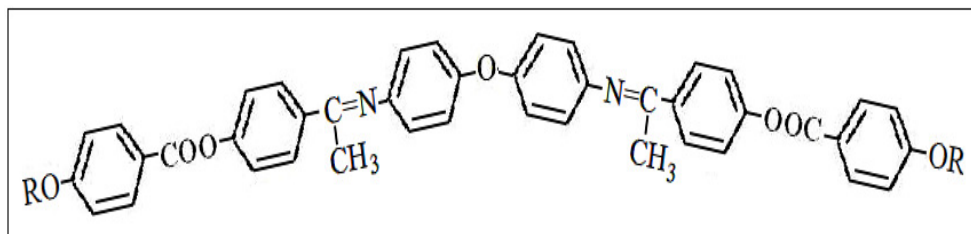
Hexyl homologue: MS m/z: 875 (M+1)

Table 6.3: DSC data

Series	Homologue	Transition Temperature °C	$\Delta H/Jg^{-1}$	$\Delta S/Jg^{-1}K^{-1}$
XIV	Pentyl	Cr-N 109	89.20	0.2340
		N-I 197	1.0850	0.0023
	Decyl	Cr-N 105	59.75	0.1645
		N-I 139	0.9070	0.0022

Table 6.4: UV data

Series	Homologue	UV λ max values nm (solvent- ethyl acetate)	
		$\pi \longrightarrow \pi^*$	$n \longrightarrow \pi^*$
XIV	Hexyl	269	367
	Dodecyl	269	367

Table 6.5: Transition temperatures: 4,4'-Bis[4''-(4'''-n-alkoxybenzoyloxy)phenyl ethylideneamino]diphenylethers (Series XV)

Homologue	Transition Temperatures °C	
	Nematic	Isotropic
R=n-alkyl group		
Methyl	127	210
Ethyl	112	195
Propyl	115	186
Butyl	99	175
Pentyl	109	177
Hexyl	100	145
Heptyl	89	122
Octyl	79	119
Decyl	80	114
Dodecyl	83	106
Tetradecyl	86	100
Hexadecyl	89	98

Table 6.6: Elemental analysis

Homologue	Calculated			Found		
	C %	H %	N %	C %	H %	N %
Ethyl	75.40	5.46	3.82	75.56	5.49	3.89
Dodecyl	78.26	7.90	2.76	78.20	7.96	2.73
Tetradecyl	78.65	8.23	2.62	78.61	8.38	2.66

FTIR (Nujol, KBr pellets, cm^{-1})

Butyl homologue: 2955, 2939, 1739 (-COO-), 1624, 1357, 1253, 1161 ($-\overset{\text{I}}{\text{C}}=\text{N}-$), 1082 (-CH₂-O-), 877, 758, 692.

Decyl homologue: 2935, 2924, 1732 (-COO-), 1629, 1359, 1255, 1161 ($-\overset{\text{I}}{\text{C}}=\text{N}-$), 1078 (-CH₂-O-), 889, 694.

¹H NMR: (CDCl₃, 500 MHz, δ , ppm, standard TMS)

Hexyl homologue: δ 0.93 (6H, t, 2x -CH₃), 1.26 (3H, s, -CH₃ of ethylideneamino), 1.48-1.85 (m, alkyl chain), 4.07 (4H, t, 2x -OCH₂-CH₂), 6.89-8.16 (m, Ar-H)

Heptyl homologue: δ 0.90 (6H, t, 2x -CH₃), 1.22 (3H, s, -CH₃ of ethylideneamino), 1.35-1.85 (m, alkyl chain), 4.0 (4H, t, 2x -OCH₂-CH₂), 6.98-8.13 (m, Ar-H)

Mass Spectra:

Hexyl homologue: MS m/z: 844 (M⁺)

Table 6.7: DSC data

Series	Homologue	Transition Temperature °C	$\Delta H/\text{Jg}^{-1}$	$\Delta S/\text{Jg}^{-1}\text{K}^{-1}$
XV	Hexyl	Cr-N 101	70.92	0.1885
		N-I 146	1.0154	0.0023
	Octyl	Cr-N 79	56.99	0.1613
		N-I 115	1.0401	0.0026

Table 6.8: UV data

Series	Homologue	UV λ max values nm (solvent- ethyl acetate)	
		$\pi \longrightarrow \pi^*$	$n \longrightarrow \pi^*$
XV	Butyl	265	362
	Hexyl	265	362

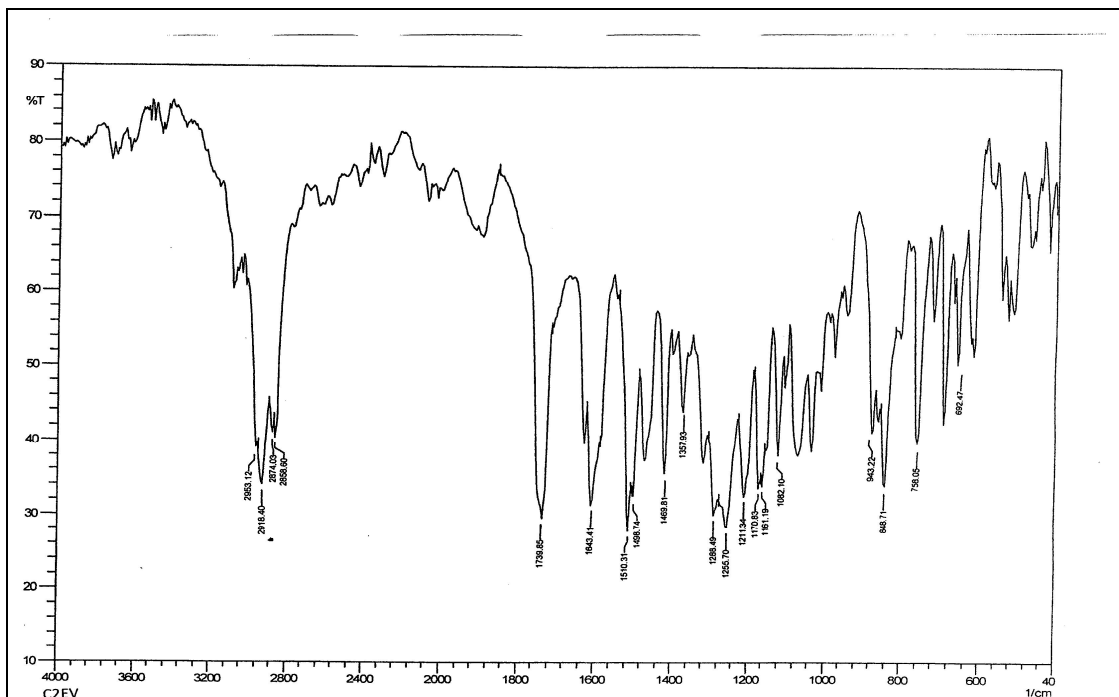


Figure 6.1 (a): IR spectra of C2 homologue of series XIV

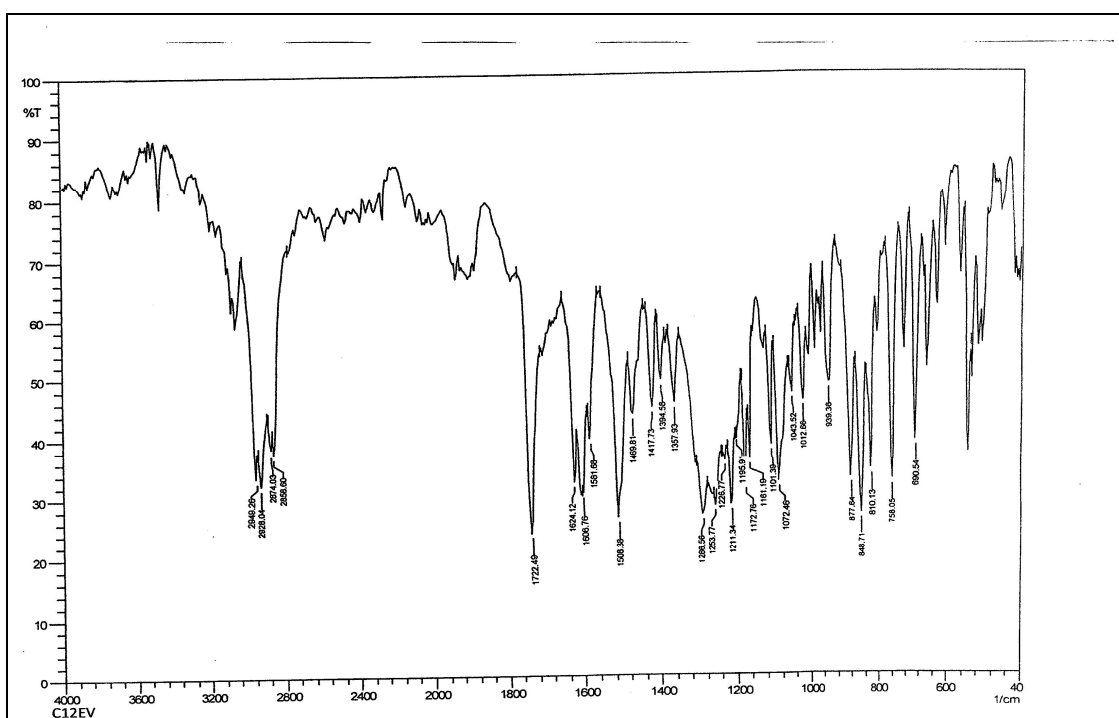


Figure 6.1 (b): IR spectra of C12 homologue of series XIV

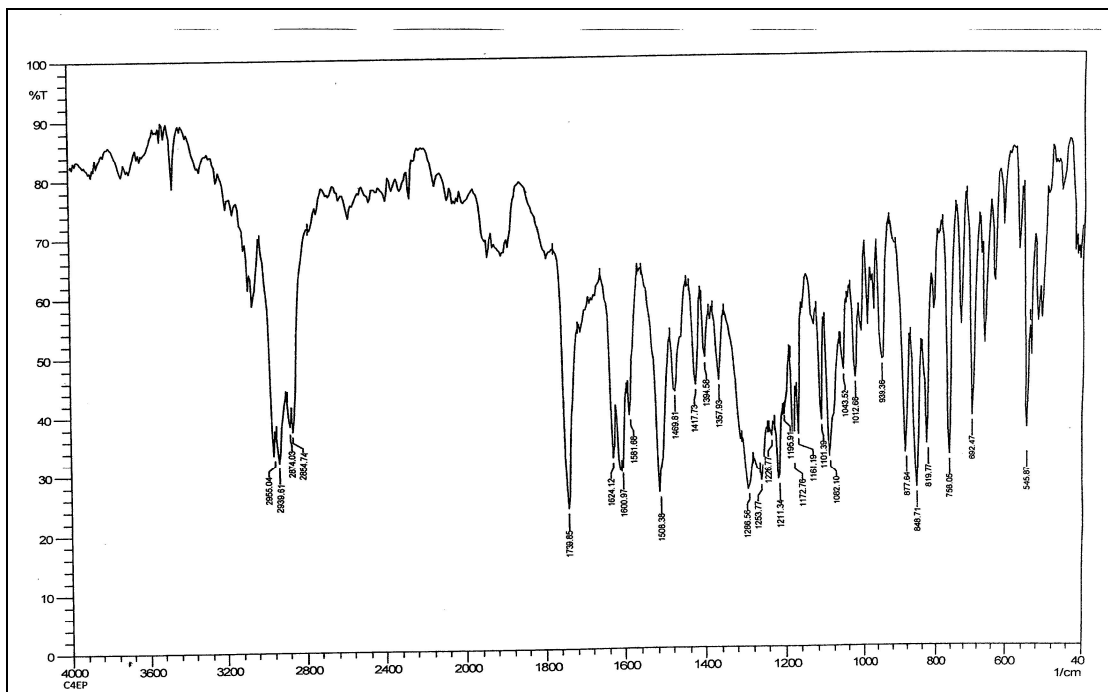


Figure 6.1 (c): IR spectra of C4 homologue of series XV

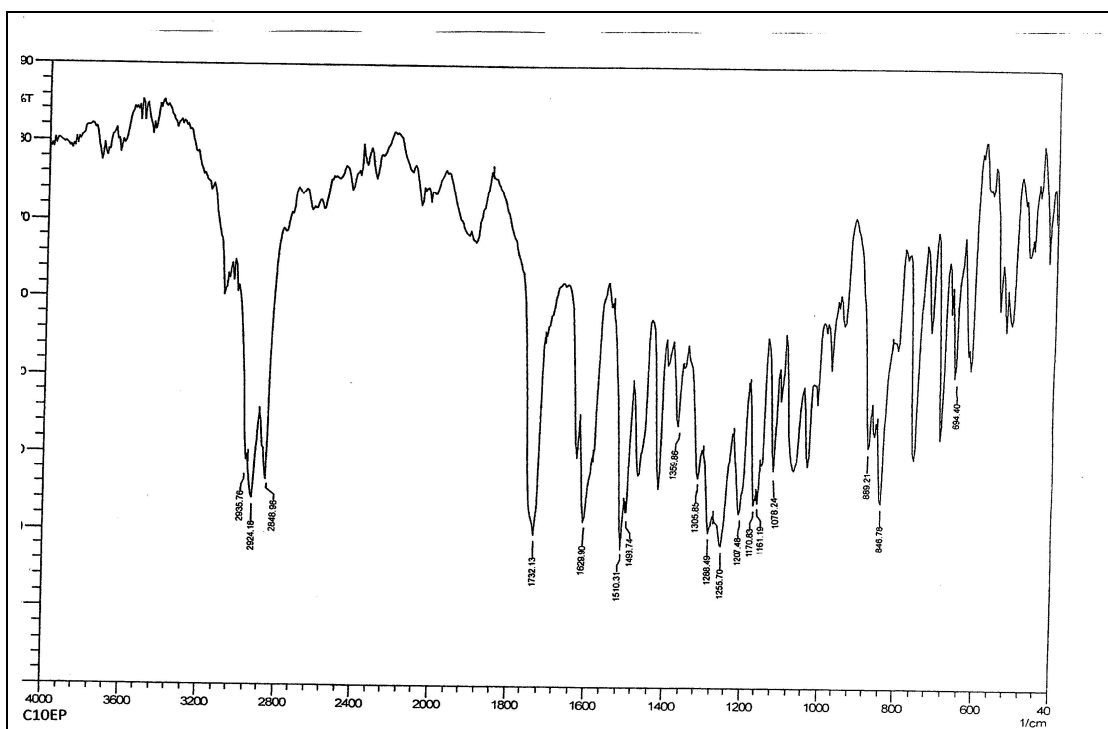
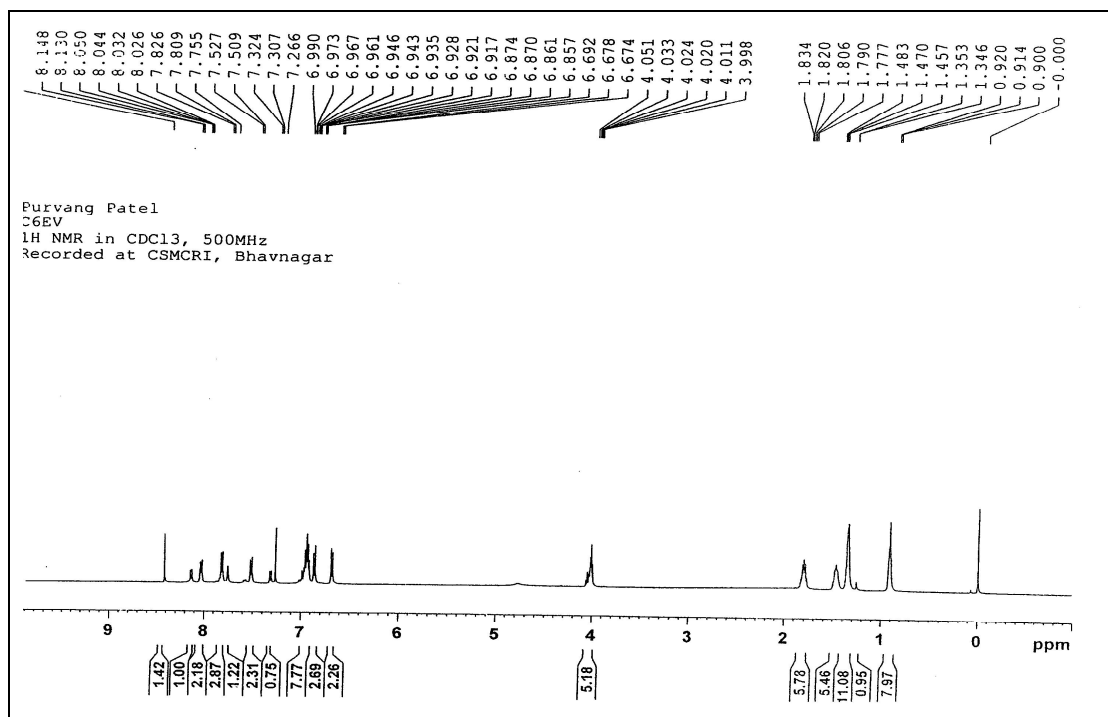
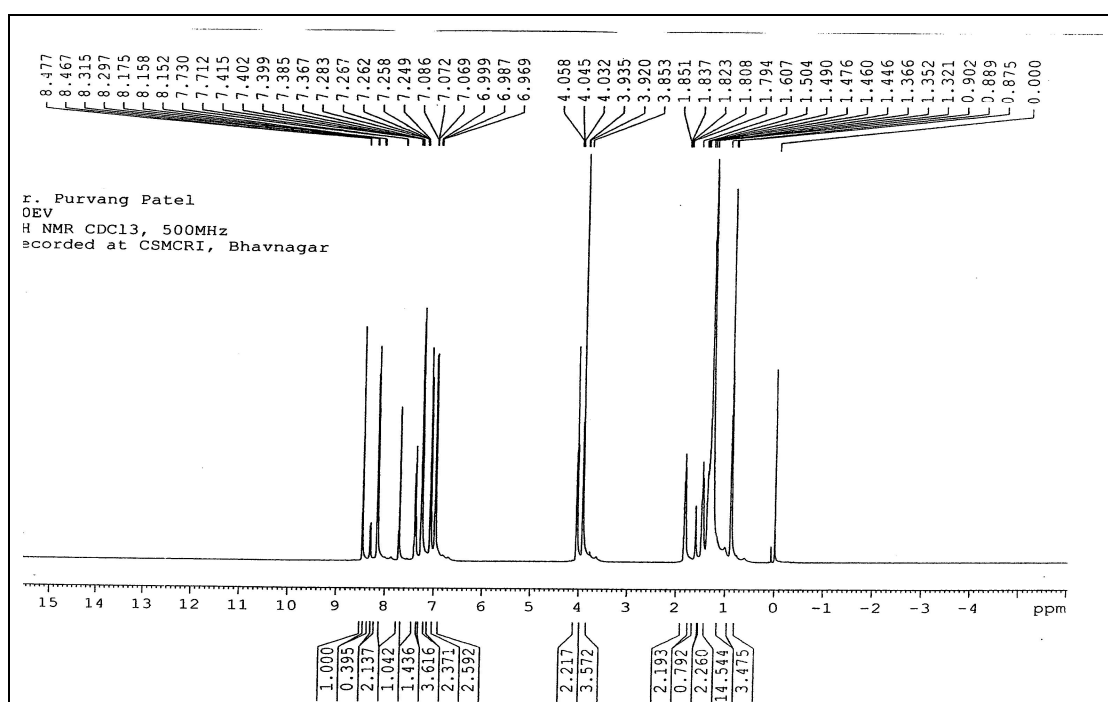
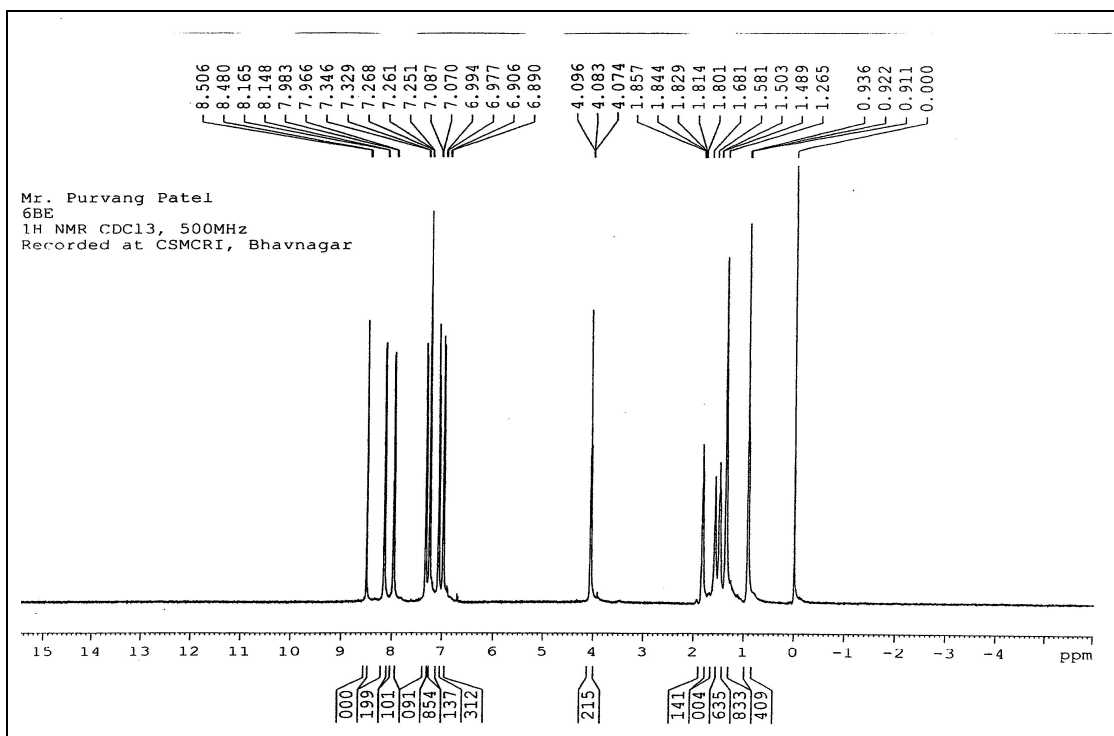
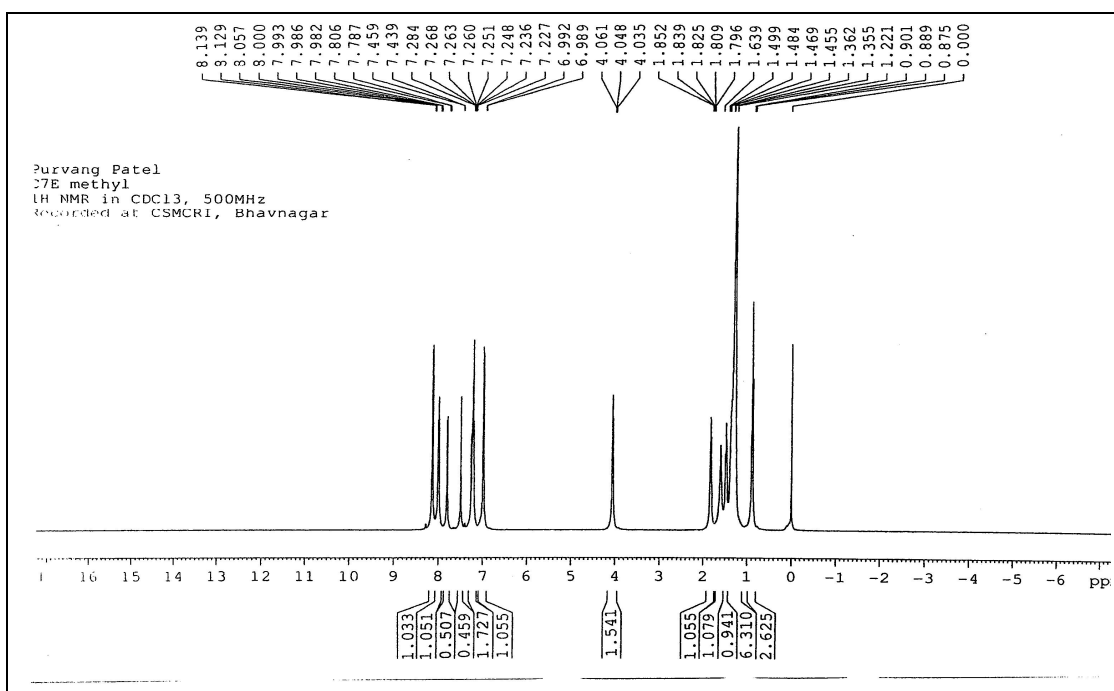


Figure 6.1 (d): IR spectra of C10 homologue of series XV

Figure 6.2 (a): ¹H NMR spectra of C6 homologue of series XIVFigure 6.2 (b): ¹H NMR spectra of C10 homologue of series XIV

Figure 6.2 (c): ^1H NMR spectra of C6 homologue of series XVFigure 6.2 (d): ^1H NMR spectra of C7 homologue of series XV

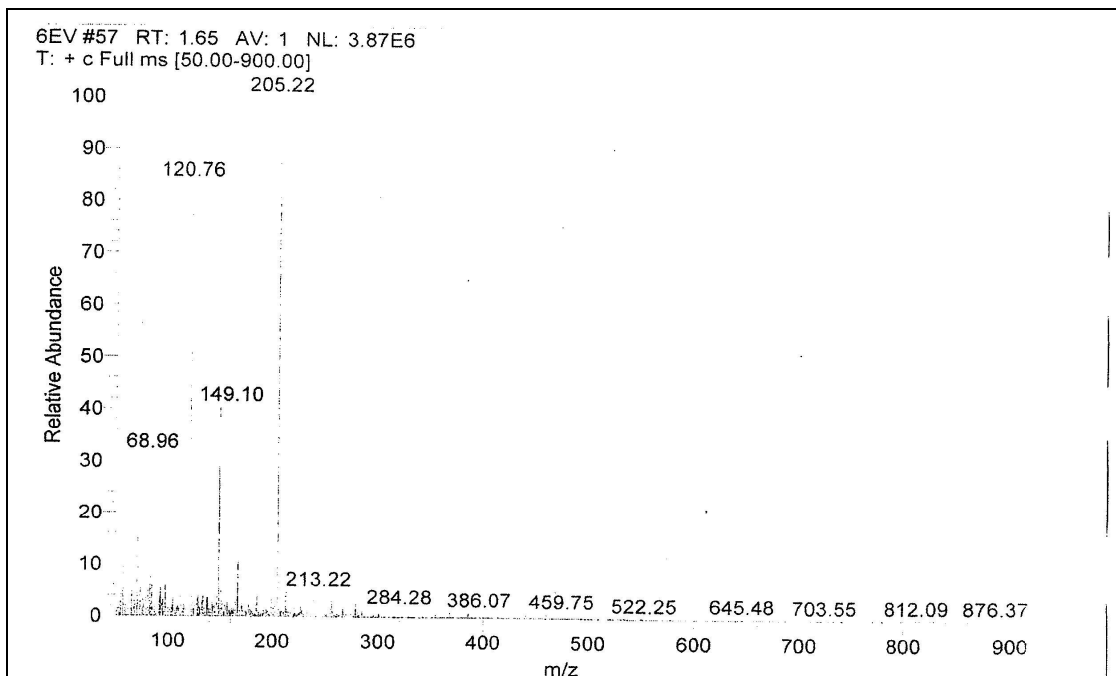


Figure 6.3 (a): Mass spectra of C6 homologue of series XIV

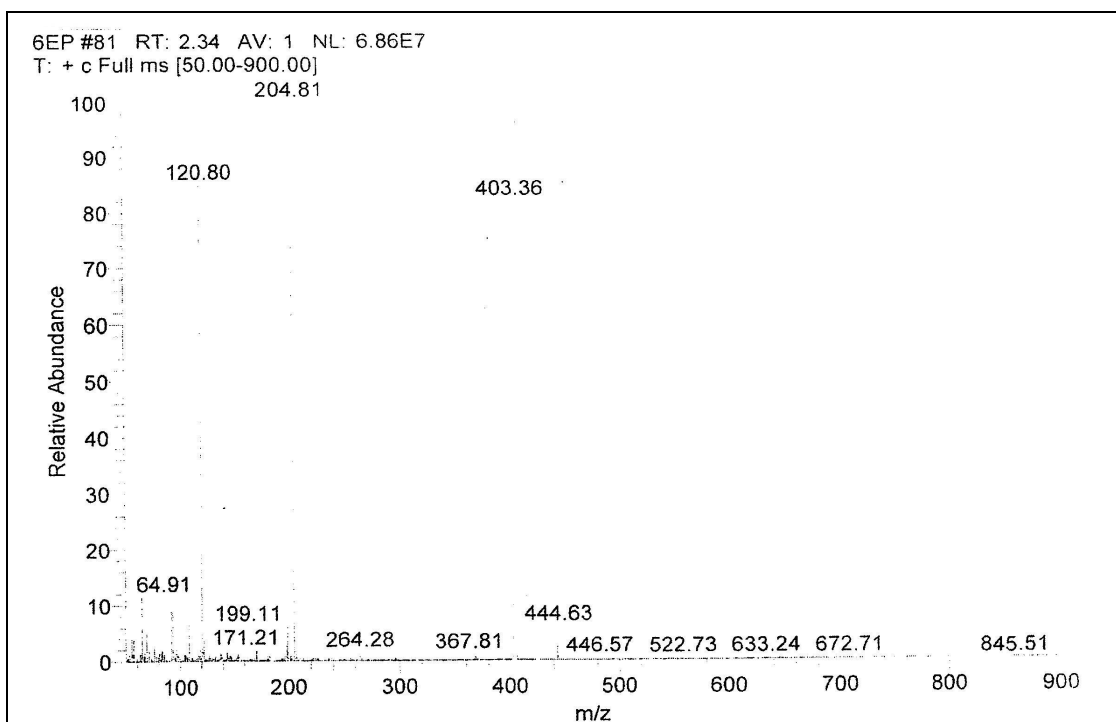


Figure 6.3 (b): Mass spectra of C6 homologue of series XV

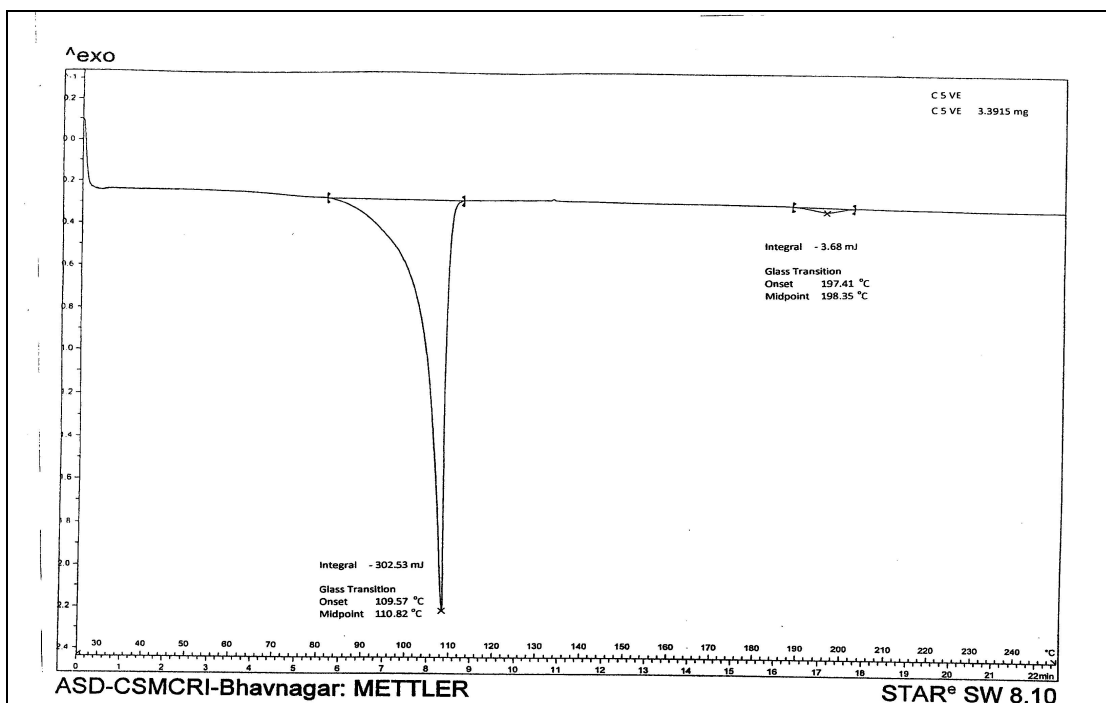


Figure 6.4 (a): DSC Thermogram of C5 homologue of series XIV

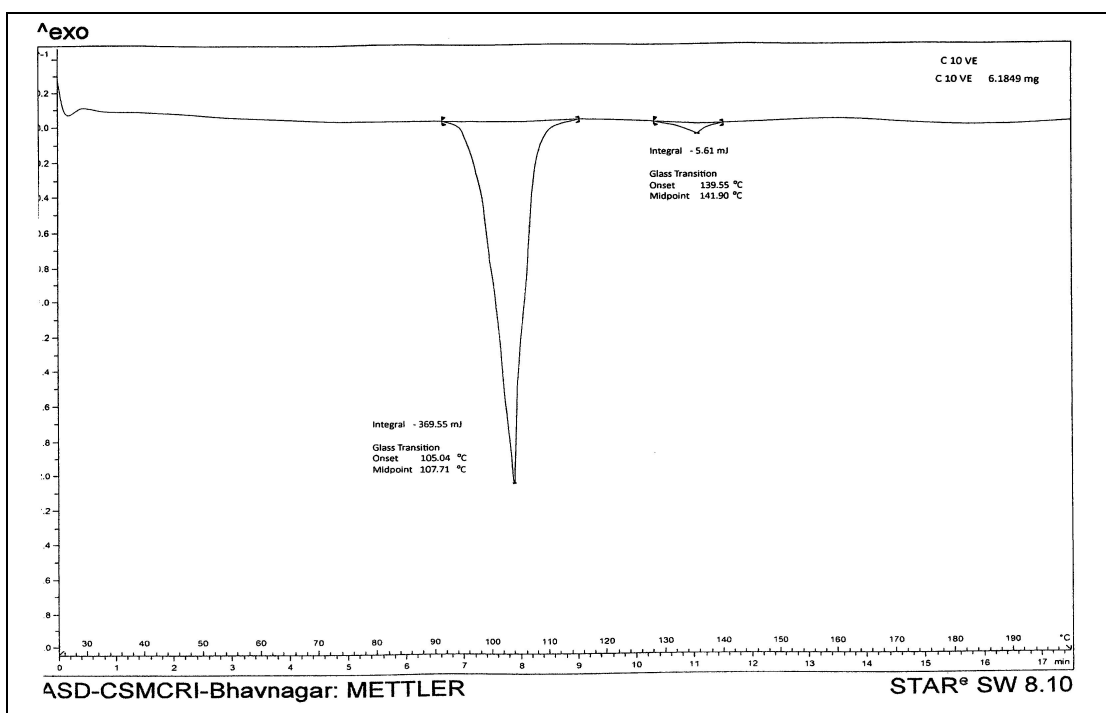


Figure 6.4 (b): DSC Thermogram of C10 homologue of series XIV

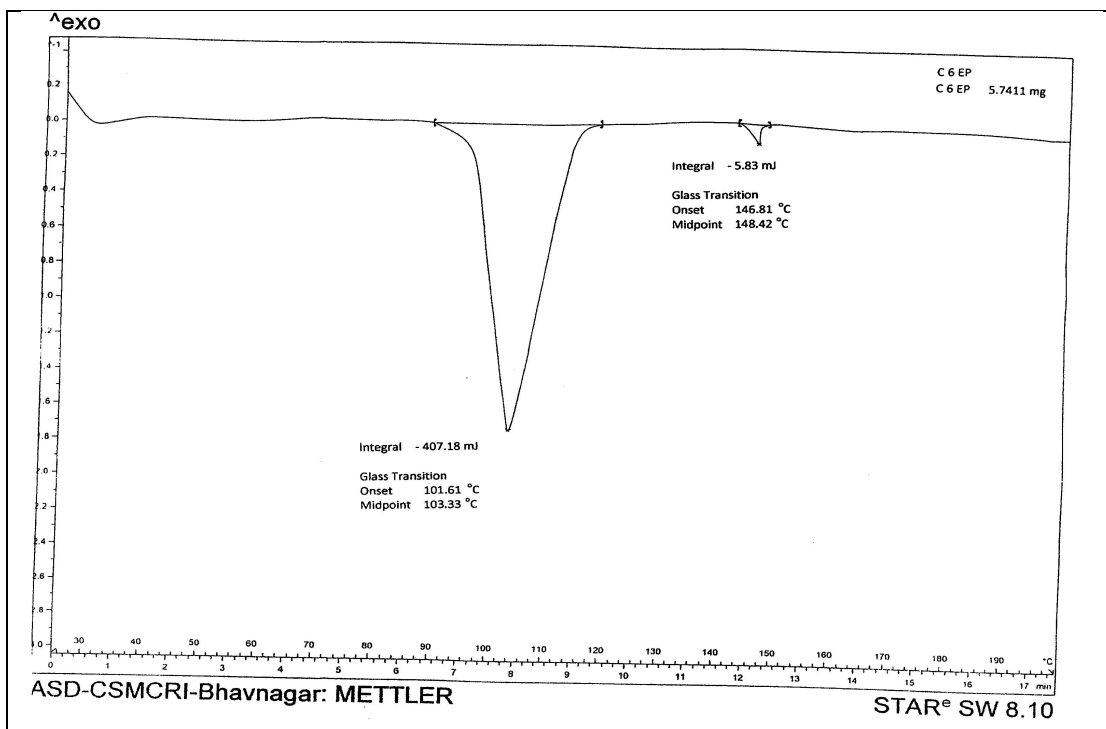


Figure 6.4 (c): DSC Thermogram of C6 homologue of series XV

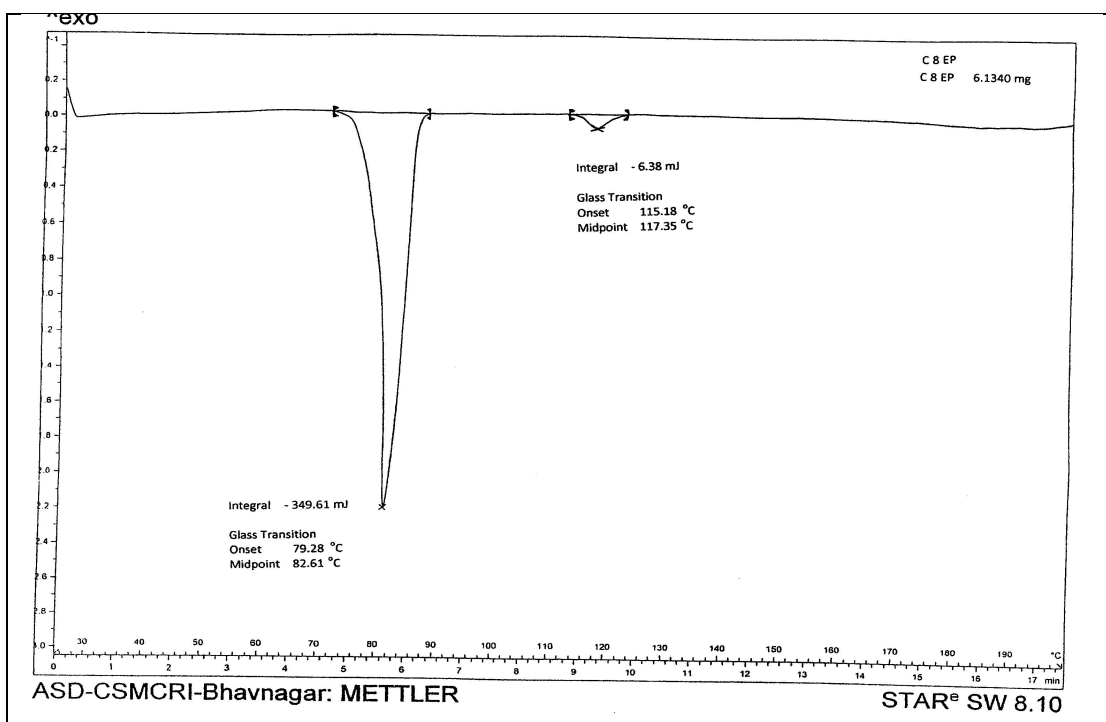


Figure 6.4 (d): DSC Thermogram of C8 homologue of series XV

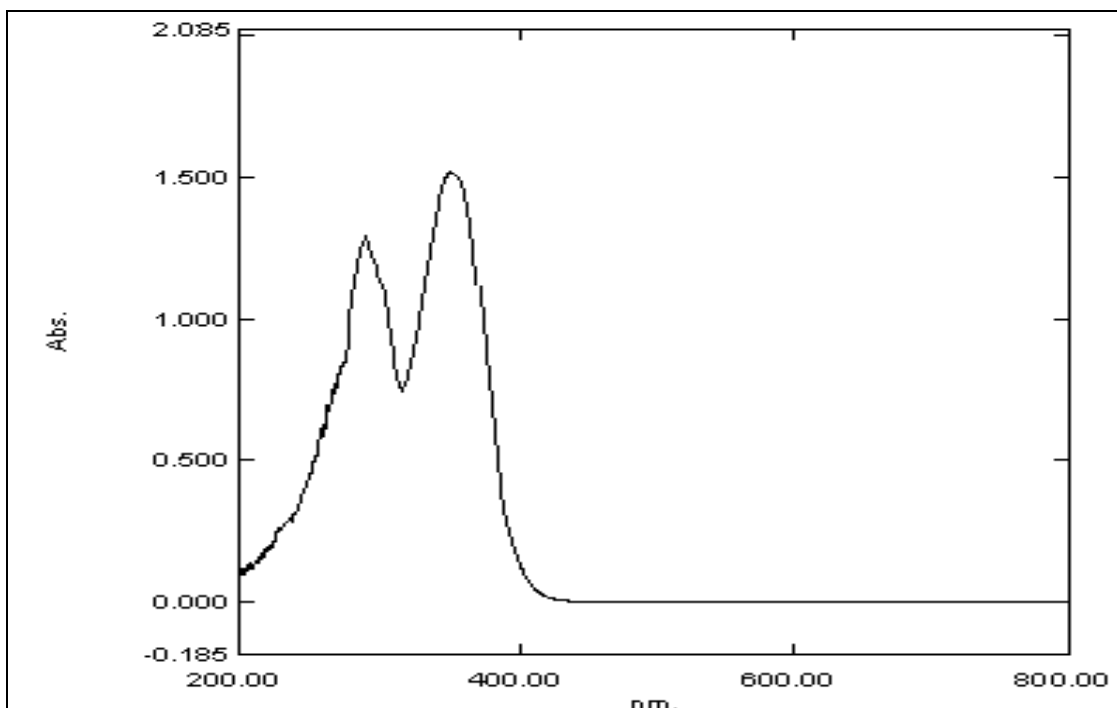


Figure 6.5 (a): UV spectra of C6 homologue of series XIV

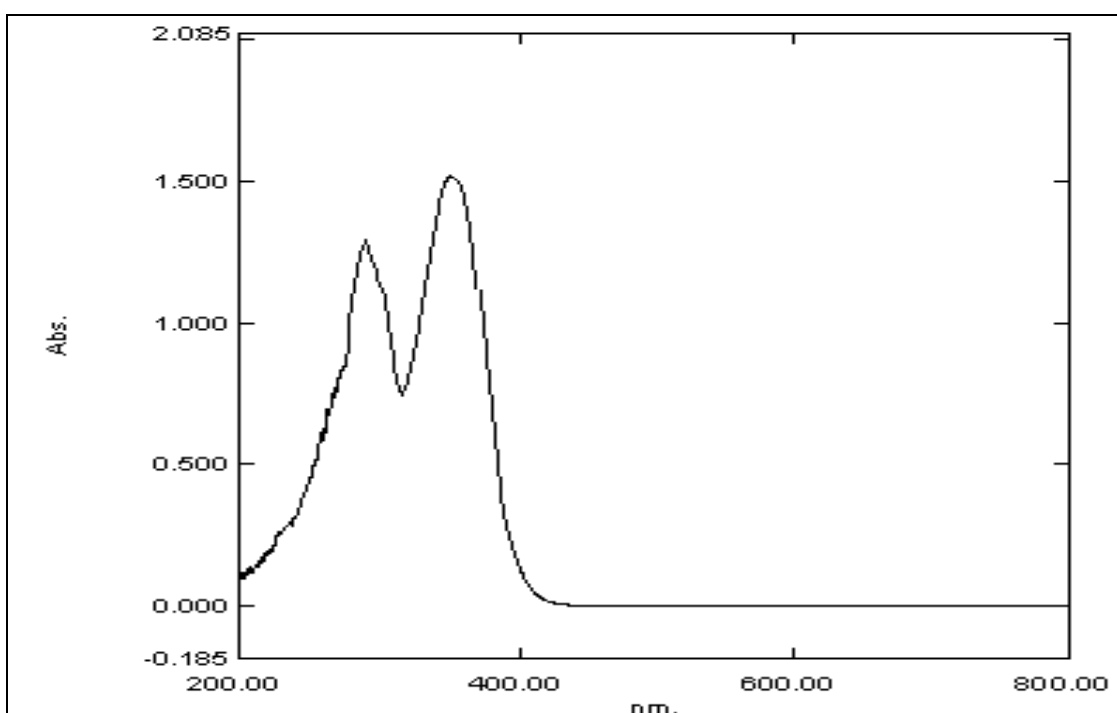


Figure 6.5 (b): UV spectra of C12 homologue of series XIV

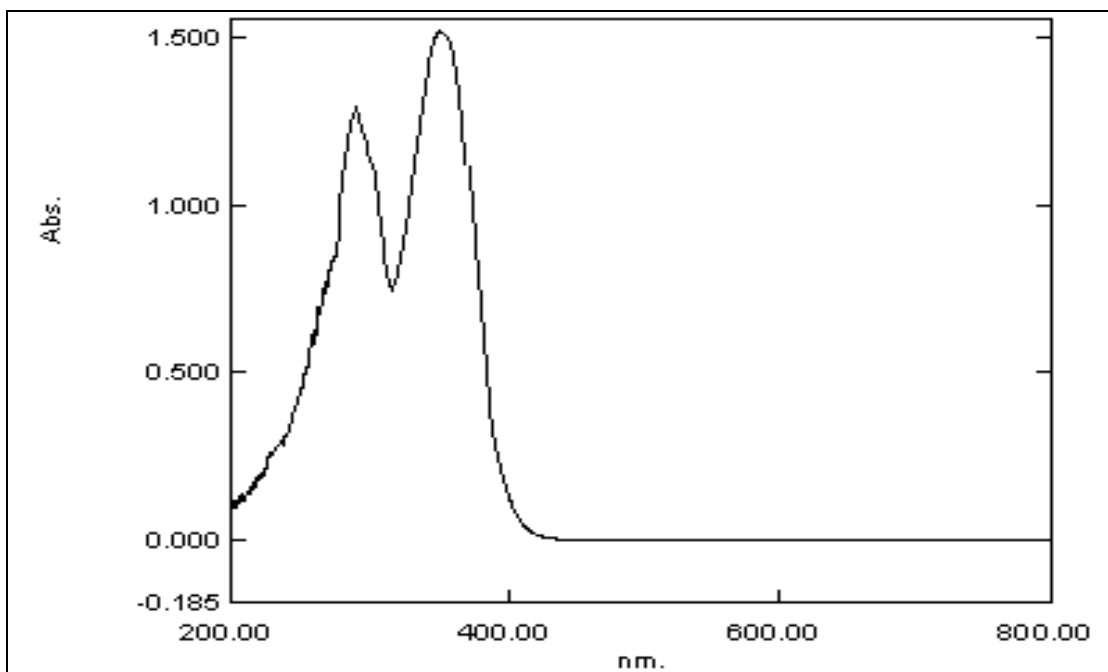


Figure 6.5 (c): UV spectra of C4 homologue of series XV

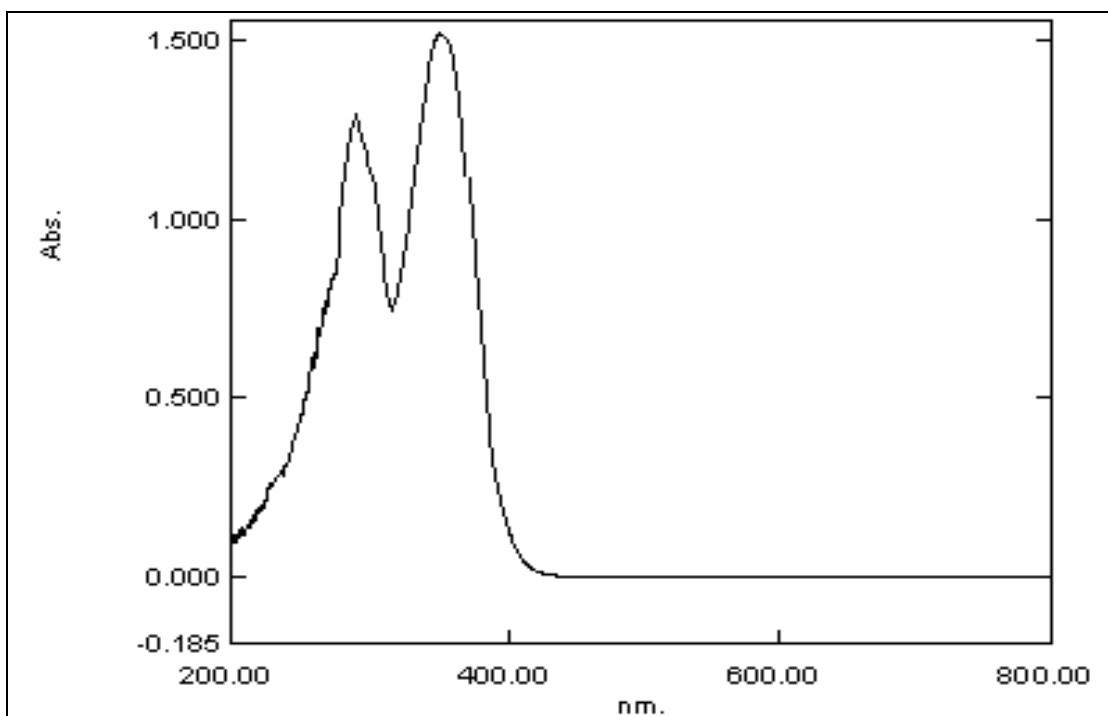
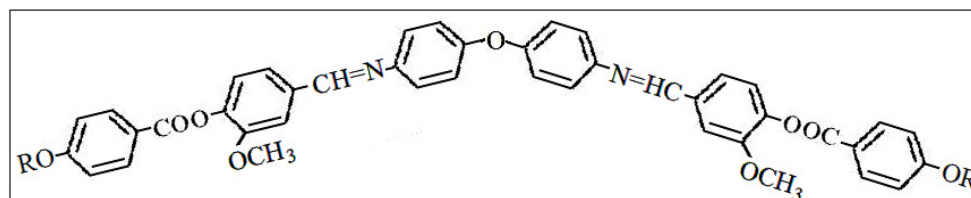


Figure 6.5 (d): UV spectra of C6 homologue of series XV

6.3 Results and Discussion

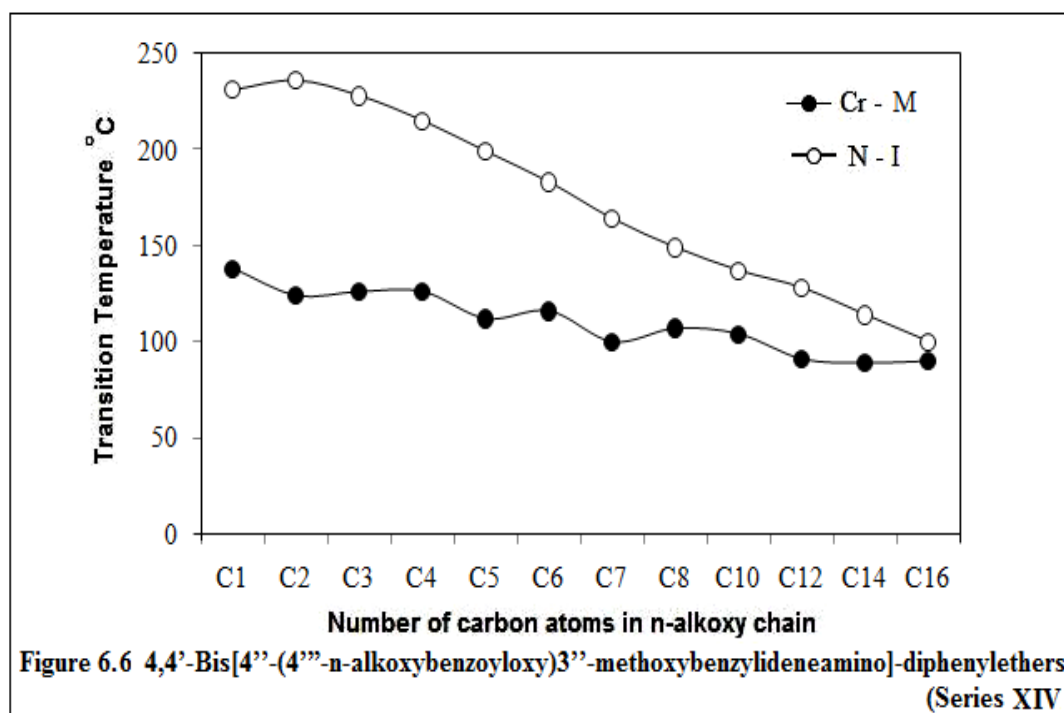
6.3.1 Series XIV: 4,4'-Bis[4''-(4'''-n-alkoxybenzoyloxy)3''-methoxybenzylideneamino]-diphenylethers

General molecular structure of series XIV



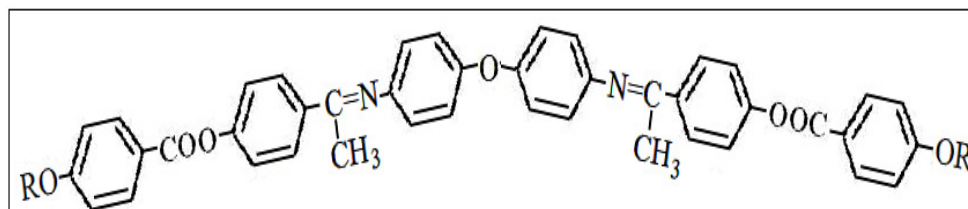
Where, R is C_nH_{2n+1} , $n=1$ to 8, 10, 12, 14, 16

All the twelve homologues of the series XIV are mesogens (Table 6.1); the nematic phase commences from the first methyl derivative and remains up to the last hexadecyl derivative synthesized. Figure 6.6 shows the plot of transition temperatures against number of carbon atoms in n-alkoxy chain; it indicates that N-I curve shows more or less steep falling tendency with a slight increase at ethyl derivative as the series is ascended. No odd-even effect is observed in N-I curve. The Cr-M transitions show an irregular pattern with overall falling tendency as the series is ascended. Nematic phase of the series shows marble texture.



6.3.2 Series XV: 4,4'-Bis[4''-(4'''-n-alkoxybenzoyloxy)phenylethylidene amino]-diphenylethers

General molecular structure of series XV



Where, R is C_nH_{2n+1} , $n = 1$ to 8, 10, 12, 14, 16

All the twelve homologues of the series XV are mesogens (Table 6.5); the nematic phase commences from the first methyl derivative and remains up to the last hexadecyl derivative synthesized. Figure 6.7 shows the plot of transition temperatures against number of carbon atoms in n-alkoxy chain; it indicates that N-I curve shows falling tendency. No odd-even effect is observed in N-I curve. The Cr-M transitions show overall falling tendency with slight increase at propyl and pentyl derivative as the series is ascended. Nematic phase of the series shows threaded texture.

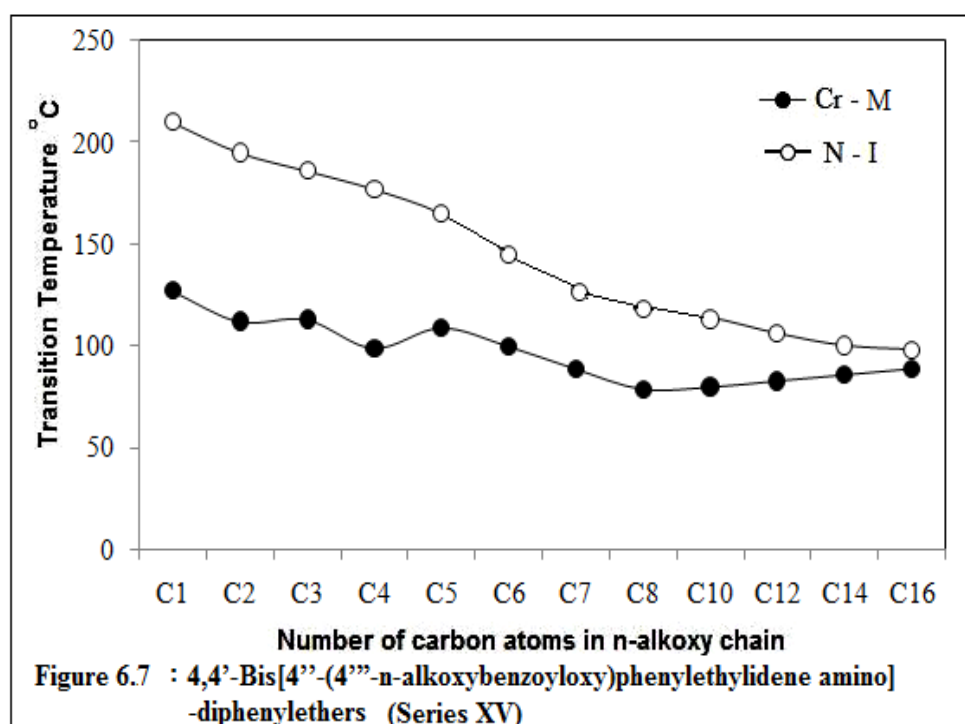


Figure 6.8 shows Energy minimized ball and stick model of methyl derivative of both the series XIV and XV. The average thermal stabilities of series XIV and XV are compared with structurally related homologous series; table 6.9 and figure 6.9 show the average thermal stabilities of the homologous series under comparison, whereas, scheme 6.2 gives the molecular structures of the series in comparison.

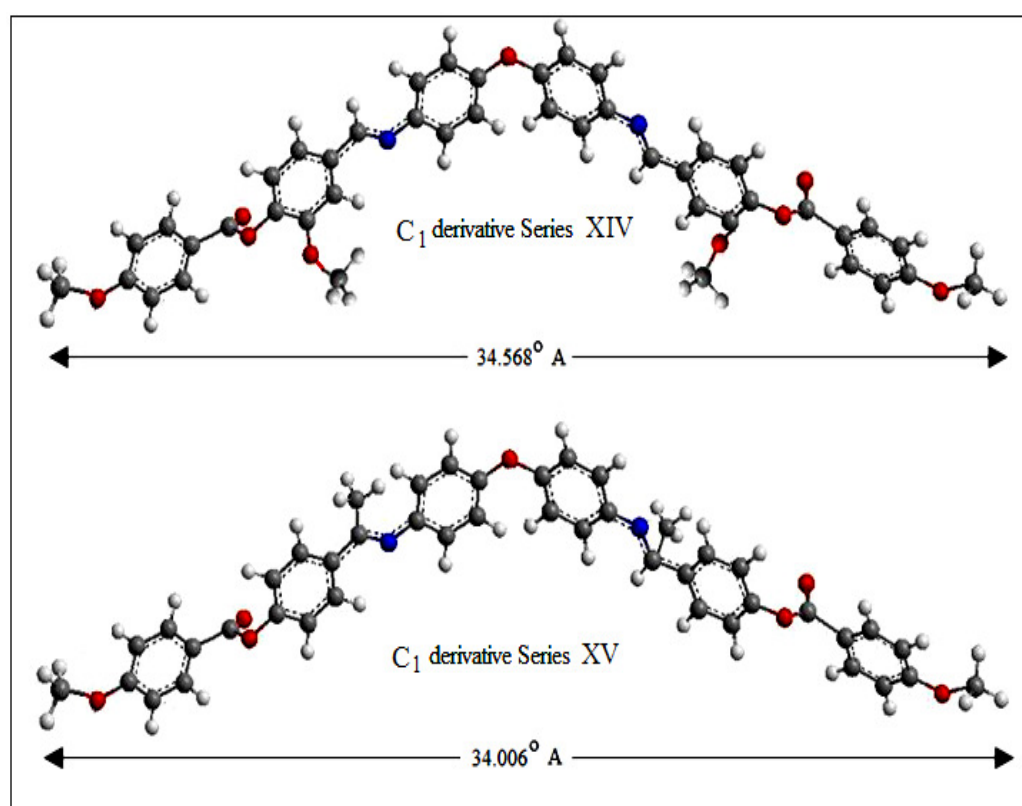


Figure 6.8: Energy minimized ball and stick model of methyl derivative -derived from CS Chem draw ultra 8.0 software.

Figure 6.8 shows the energy minimized ball and stick model of methyl derivative of series XIV and XV. The molecular length of methyl derivative of series XIV is 34.568°A and that of series XV is 34.006°A . In both the series XIV and XV the bond angle of Diphenylether moiety (Ph-O-Ph) is 109.5° which conforms the formation of bent molecule [365].

Table 6.9: Average thermal stability °C

Series	N-I	S-N	Commencement of smectic mesophase
XIV	173.66 (C ₁ to C ₁₆)	–	–
XV	145.33 (C ₁ to C ₁₆)	–	–
A	257.30 (C ₁ to C ₁₆)	253.25 (C ₁ to C ₄)	C ₁

Comparison of series XIV and XV with structurally related homologous series A shows that all the series in comparison are structurally more or less similar, consisting of six phenyl rings, ester central linkage and 'O' atom as central linking unit. Series XIV has lateral –OCH₃ group and has –CH=N– central linkage whereas series XV is laterally unsubstituted and has ethylideneamino central linkage is only the difference. Series A [365] is laterally unsubstituted and has –CH=N– central linkage. Comparison of average N-I thermal stability of both the series XIV and VX (Table 6.9) shows that the N-I stability of series XV is lower than that of series XIV by about 30°C. Here, the nature of lateral methoxy group (series XIV) and methyl group in ethylideneamino central linkage (series XV) has important implications on phase transition temperatures and average nematic thermal stability of the series. It seems that the broadening effect caused by ethylideneamino central linkage in series XV is more pronounced than the broadening effect caused by lateral –OCH₃ group in series XIV; therefore N-I stability of series XV is lower than that of series XIV. The average N-I thermal stability of series XIV is lower by about 102 °C than series A. This may be due to presence of lateral –OCH₃ group in series XIV, the length to breadth ratio of it increases than that of series A. The effect of lateral –OCH₃ group in the central benzene ring causes disruption in the molecular packing, which reduces the transition temperatures and melting points as well as decreases the average N-I thermal stability with absence of the smectic mesophase as compared to the laterally unsubstituted analogues series A [365]. The average N-I thermal stability of series XV is lower by about 131 °C than series A. This may be due to the replacement of the –H of –CH=N– linkage by –CH₃ group in series XV. –CH₃ group in ethylideneamino linkage of series XV plays an important role to effect their mesomorphic properties; here also the –CH₃

group in ethylideneamino linkage increases breadth of the molecule and causes disruption in the molecular packing. The broadening effect of the $-\text{CH}_3$ group of ethylideneamino linkage in series XV reduces the N-I thermal stability with absence of the smectic mesophase as compared to series A [332].

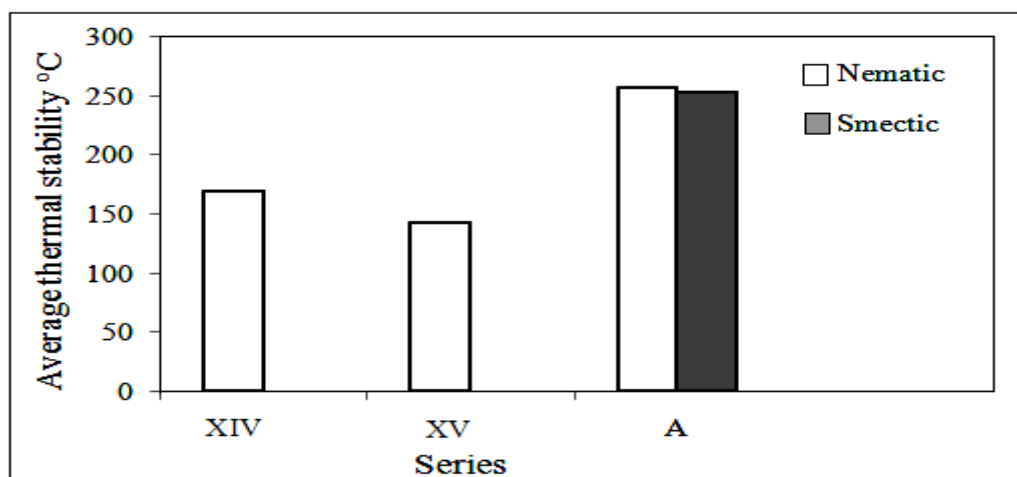
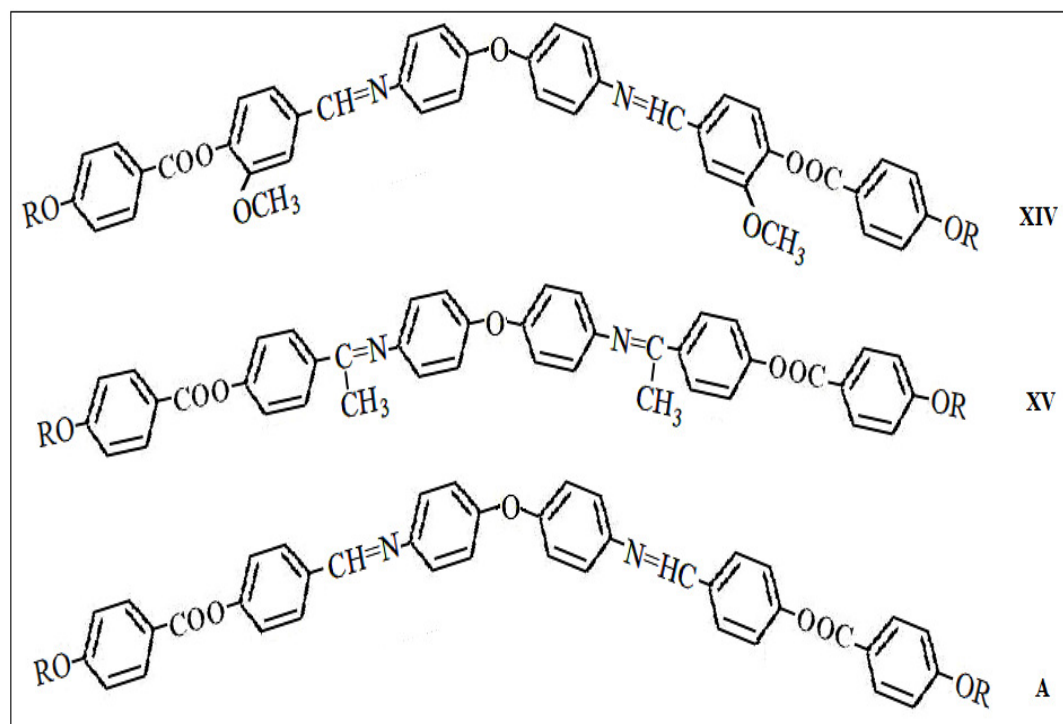


Figure 6.9: Average thermal stability for the series

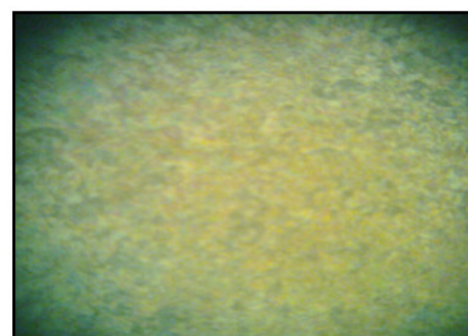


Scheme 6.2: Selected homologous series for comparison

Figure 6.10 shows the photomicrographs of the textures of representative compounds.

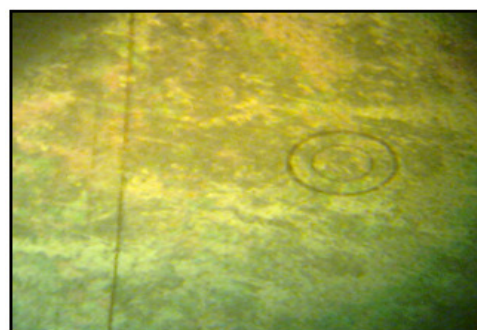


(a) Butyl homologue

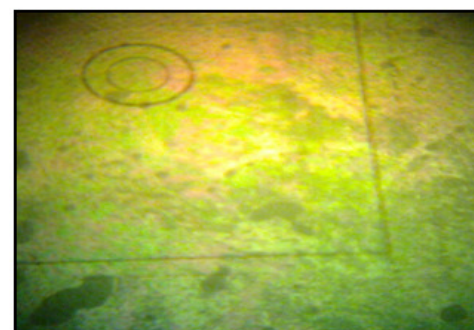


(b) Decyl homologue

Photomicrographs of marble texture of nematic phase of series XIV



(c) Pentyl homologue



(d) Octyl homologue

Photomicrographs of marble texture of nematic phase of series XV

Figure 6.10: Photomicrographs of the textures of the representative homologues

7.1 Introduction

Transition temperatures and mesophase ranges of individual mesogens may or may not undergo modifications in their mixture [367]. The trend of modifications, however, would become a characteristic by itself some times, if not always and therefore the study of mixtures of such compounds assumes importance. Emergences of the mesophase, increase or decrease of the mixed mesomorphic ranges and thermal stabilities and study of the factors which influence the modifications have received greater attention [368-370]. The binary mixtures of mesogens have provided better formulations for applications in different field [371]. Earlier studies [372-376] have suggested the formation of mesomorphism by mixing compounds where none, one or both compounds are mesogens. In a general sense, a binary system where one component is mesogen and another is non-mesogen [377], a series of mixed liquid crystals of the original variety of the liquid crystal component is expected to be formed over a range of temperature and concentration. Such binary systems are capable of throwing light on the extent to which a non-liquid crystalline component is causing hindrance to the exhibition of mixed mesophase on account of the difficulty in the packing of the molecules and weakening of the terminal and/or lateral attractions of the molecules. Continuous mixed mesomorphism is formed by binary mixtures of both mesomorphic components and a few have been reported giving rise to different textures [378-382].

In the present investigation, ten binary systems comprising of structurally dissimilar mesogens and non-mesogens have been prepared and their mesomorphic properties are studied. The components of the binary systems taken are

A1 4-(4'-n-butyloxybenzoyloxy)benzaldehyde (BBB) [331]

A2 4-methoxybenzylidene-4'-chloroaniline (MBCA) [383]

A3 4-methoxybenzylidene-4'-toluidine (MBT) [383]

A4 4-(4'-n-dodecyloxybenzoyloxy)naphthylazo-4''-fluorobenzene (DNFB)

B1 4-(4'-n-butyloxybenzoyloxy)phenylazo-4''-fluorobenzene (BPFB) [351]

B2 4-(4'-n-butyloxybenzoyloxy)benzylidene-4''-fluoroaniline (BBFA)

B3 4-(4'-n-heptyloxybenzoyloxy)phenylazo-4''-fluorobenzene (HPFB) [351]

B4 4-(4'-methoxybenzoyloxy)benzylidene-2''-aminopyridine (MBAP) [381]

7.2 Experimental

7.2.1 Materials

All the chemicals are of Merck, SRL or Loba grade and used as received.

7.2.2 Synthesis

7.2.2.1 Component A1

4-(4'-n-butyloxybenzoyloxy)benzaldehyde (BBB)

Component A1 is synthesized following the procedure reported in 4.2.3.2.

FTIR (Nujol, KBr pellets, cm^{-1}): 2953, 2939, 1729 (-COO-), 1680 (-CHO), 1600, 1253, 1066 (-CH₂-O-), 690

7.2.2.2 Component A2

4-methoxybenzylidene-4'-chloroaniline (MBCA)

Component A2 is synthesised by taking equimolar quantities of appropriate 4-methoxybenzaldehyde and 4-chloroaniline following the similar method reported in step 4.2.3.1.c.

FTIR (Nujol, KBr pellets, cm^{-1}): 2957, 2915, 1602, 1390, 1170 (-CH=N-), 1255, 1082 (-CH₂-O-), 692

7.2.2.3 Component A3

4-methoxybenzylidene-4'-toluidine (MBT)

Component A3 is synthesised by taking equimolar quantities of appropriate 4-methoxybenzaldehyde and 4-toluidine following the similar method reported in step 4.2.3.1.c.

FTIR (Nujol, KBr pellets, cm^{-1}): 2939, 2924, 1608, 1393, 1170 (-CH=N-), 1255, 1078 (-CH₂-O-), 694

7.2.2.4 Component A4

4-(4'-n-dodecyloxybenzoyloxy)naphylazo-4''-fluorobenzene (DNFB)

The component A4 is synthesized following the procedure reported in 3.2.3.6.

FTIR (Nujol, KBr pellets, cm^{-1}): 2950, 2926, 1733 (-COO-), 1606, 1359, 1170 (-N=N-), 1259, 1064 (-CH₂-O-), 690

7.2.2.5 Component B1

4-(4'-n-butyloxybenzoyloxy)phenylazo-4''-fluorobenzene (BPFB)

The component B1 is synthesized following the procedure reported in 3.2.3.1.

FTIR (Nujol, KBr pellets, cm^{-1}): 2958, 2920, 1729 (-COO-), 1597, 1496, 1389, 1199 (-N=N-), 1258, 1073 (-CH₂-O-), 969, 761, 692.

7.2.2.6 Component B2

4-(4'-n-butyloxybenzoyloxy)benzylidene-4''-fluoroaniline (BBFA)

The component B2 is synthesised by taking equimolar quantities of appropriate 4-(4'-n-butyloxybenzoyloxy)benzaldehyde and 4-fluoroaniline following the similar method reported in step 4.2.3.1.c.

FTIR (Nujol, KBr pellets, cm^{-1}): 2955, 2916, 1737 (-COO-), 1606, 1396, 1170 (-CH=N-), 1259, 1064 (-CH₂-O-), 694

7.2.2.7 Component B3

4-(4'-n-heptyloxybenzoyloxy)phenylazo-4''-fluorobenzene (HPFB)

The component B3 is synthesized following the procedure reported in 3.2.3.1.

FTIR (Nujol, KBr pellets, cm^{-1}): 2959, 2928, 1739 (-COO-), 1608, 1359, 1174 (-N=N-), 1255, 1062 (-CH₂-O-), 692

7.2.2.8 Component B4**4-(4'-methoxybenzoyloxy)benzylidene-2''-aminopyridine (MBAP)**

The component B4 is synthesised by taking equimolar quantities of appropriate 4-(4'-n-butyloxybenzoyloxy)benzaldehyde and 2-aminopyridine following the similar method reported in step 4.2.3.1.c.

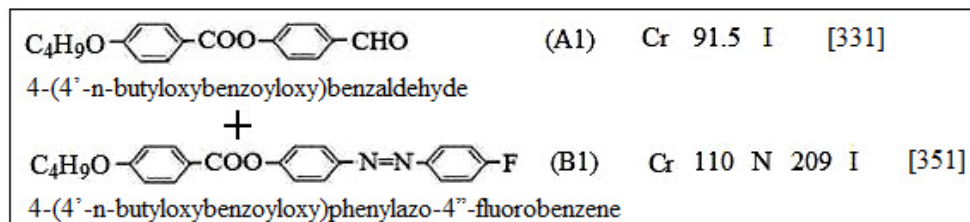
FTIR (Nujol, KBr pellets, cm^{-1}): 2954, 2918, 1734 (-COO-), 1602, 1392, 1172 (-CH=N-), 1255, 1069 (-CH₂-O-), 759

7.2.3 Preparation and study of binary mixtures

The components are weighted in known proportions and melted together in fusion tubes. They are thoroughly mixed in their melt to obtain a homogeneous mixture, after which they are cooled. This procedure is repeated three times. The solid obtained is finally ground and used for determining transition temperatures, by using a Leitz Laborlux 12 POL polarizing microscope fitted with a Kofler heating stage. Figure 7.11 shows the photomicrographs of the textures of the representative mixtures.

7.3 Type 1 Binary System [I to VI]

7.3.1 Binary System –I: BBB(A1) + BPFB(B1)



In this system (Table 7.1, Figure 7.1) the component A1 is non-mesogen (Cr 91.5 I) whereas B1 is nematogen (Cr 110 N 209 I) showing the nematic mesophase with marble texture. The phase diagram of this system shows that mixed nematic phase emerges in enantiotropic from with the addition of as low as 10.97 mole% of B1 into A1 and continues to be exhibited till the addition of 90.69 mole% of B1 into A1 and continues to be exhibited till the addition of 90.69 mole% of B1 into A1. The mixed nematic phase also shows marble texture. As the concentration of B1 increases the mixed mesophase range increases. Eutectic point is obtained at 47 °C at about 40.25 mole% of B1 and maximum mesophase range of 131 °C is observed at 90.69 mole% of B1. In this system N-I curve shows rising tendency, with steep increase from 70.10 mole% of B1 and then a fall of about 12 °C at 100 mole% of B1; thus N-I curve shows non-linear behavior. Some of the binary mixtures supercool up to about 40 °C.

Table 7.1: Binary system I: BBB (A1) + BPFB (B1)

Mole % B1	Transition Temperature °C	
	Nematic	Isotropic
0	-	91.5
10.97	58	85
20.92	60	98
30.77	59	118
40.25	47	132
50.60	58	151
60.73	60	151
70.10	80	175
80.46	82	210
90.69	90	221
100	110	209

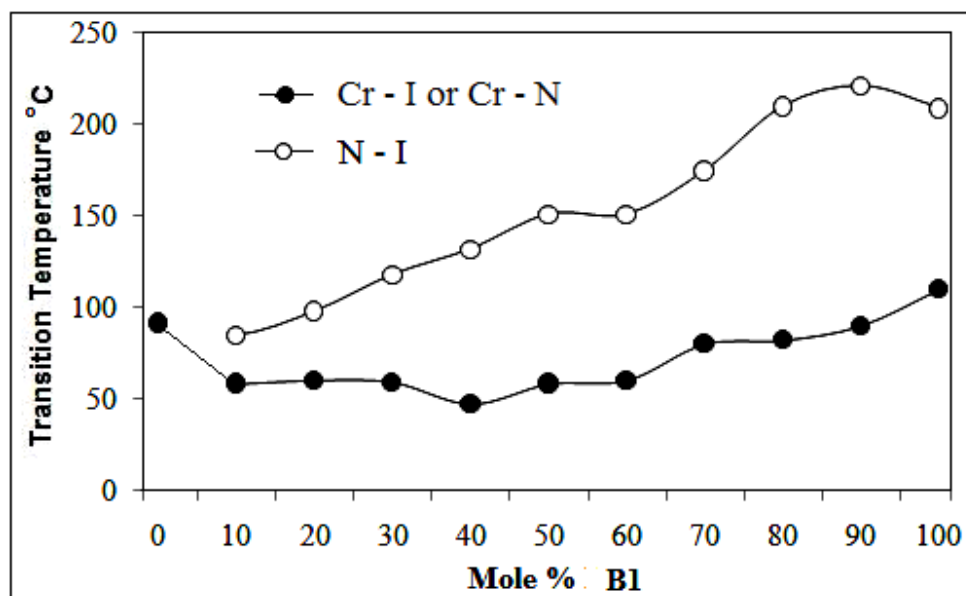
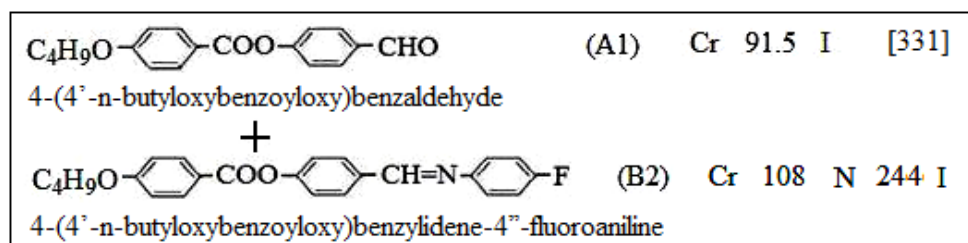


Figure 7.1: Phase diagram of Binary system I: BBB (A1) + BPFB (B1)

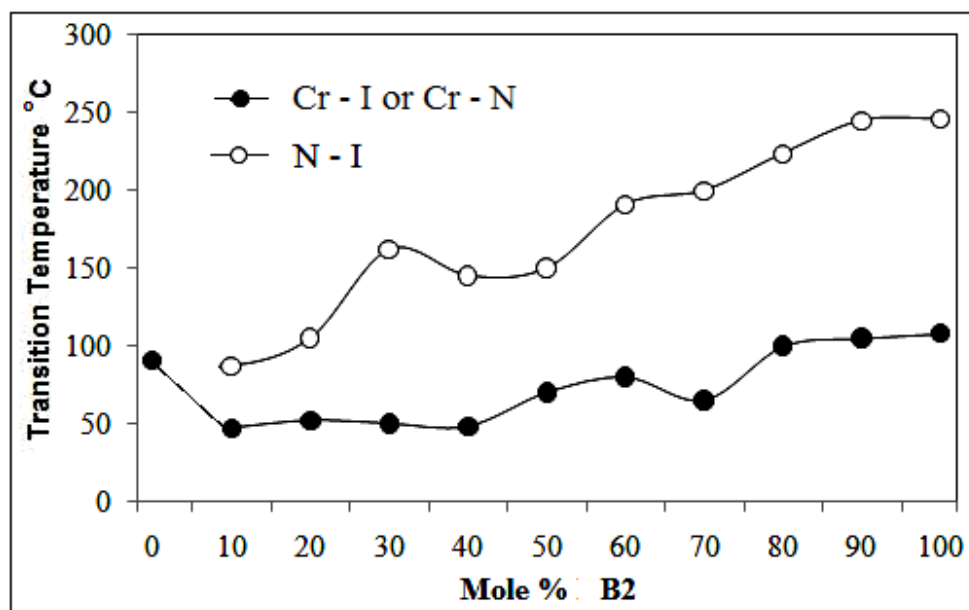
7.3.2 Binary System –II: BBB(A1) + BBFA(B2)



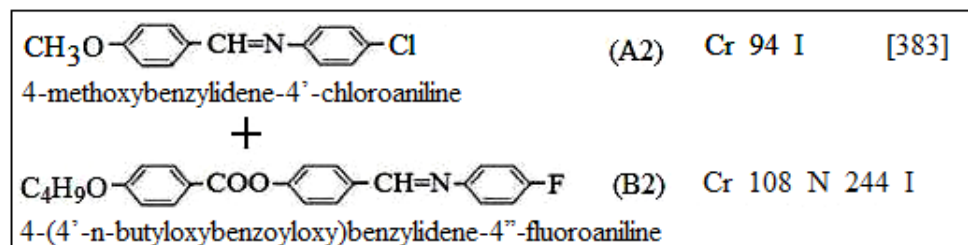
In this system (Table 7.2, Figure 7.2) the components A1 is non-mesogen (Cr 91.5 I) whereas B2 is nematogen (Cr 108 N 244 I) showing the nematic mesophase with marble texture. Here also the mixed nematic phase emerges in enantiotropic form by addition of as low as 10.54 mole% of B2 into A1 and continues to be exhibited till the addition of 90.57 mole% of B2 into A1. The mixed nematic phase also shows marble texture. As the concentration of B2 increases the mixed mesophase range increases. Eutectic point is obtained at 65 °C at about 69.94 mole % and maximum mesophase range of 140 °C is observed at 90.57 mole% of B2. In this system N-I curve shows rising tendency, with a jump at 30.25 mole% of B2; thus N-I curve shows non-linear behavior. Some of the binary mixtures supercool up to about 40 °C.

Table 7.2: Binary system II: BBB (A1) + BBFA (B2)

Mole % B2	Transition Temperature °C	
	Nematic	Isotropic
0	-	91.5
10.54	47	87
19.52	52	105
30.25	50	162
40.98	48	145
49.46	70	150
60.51	80	191
69.94	65	200
80.66	100	224
90.57	105	245
100	108	244

**Figure 7.2: Phase diagram of Binary system II: BBB (A1) + BBFA (B2)**

7.3.3 Binary System –III: MBCA(A2) + BBFA(B2)



This system (Table 7.3, Figure 7.3) consists of component A2 which is non-mesogen (Cr 94 I) and component B2 is nematogen (Cr 108 N 244 I) showing the nematic mesophase with marble texture. The mesogenic characteristic emerges in monotropic form with the addition of about as low as 8.93 mole% of B2 into A2 which becomes enantiotropic by addition of about 28.13 mole% of B2 into A2 and continues to be exhibited till the addition of 90.06 mole% of B2 into A2. The mixed nematic phase shows marble texture. As the concentration of B2 increases the mixed mesophase range increases. Eutectic point is obtained at 71 °C at about 39.71 mole% of B2 and maximum mesophase range of 109 °C is observed at 69.24 mole% of B2. In this system N-I curve shows non-linear behavior with overall rising tendency, with increase in concentration of B2. Some of the binary mixtures supercool up to about 50 °C.

Table 7.3: Binary system III: MBCA (A2) + BBFA (B2)

Mole % B2	Transition Temperature °C	
	Nematic	Isotropic
0	-	94
8.93	(79)	80
19.60	(75)	83
28.13	80	89
39.71	71	128
50.17	86	176
59.95	83	157
69.24	91	200
79.57	106	192
90.06	105	206
100	108	244

Values in parentheses indicates monotropic transitions

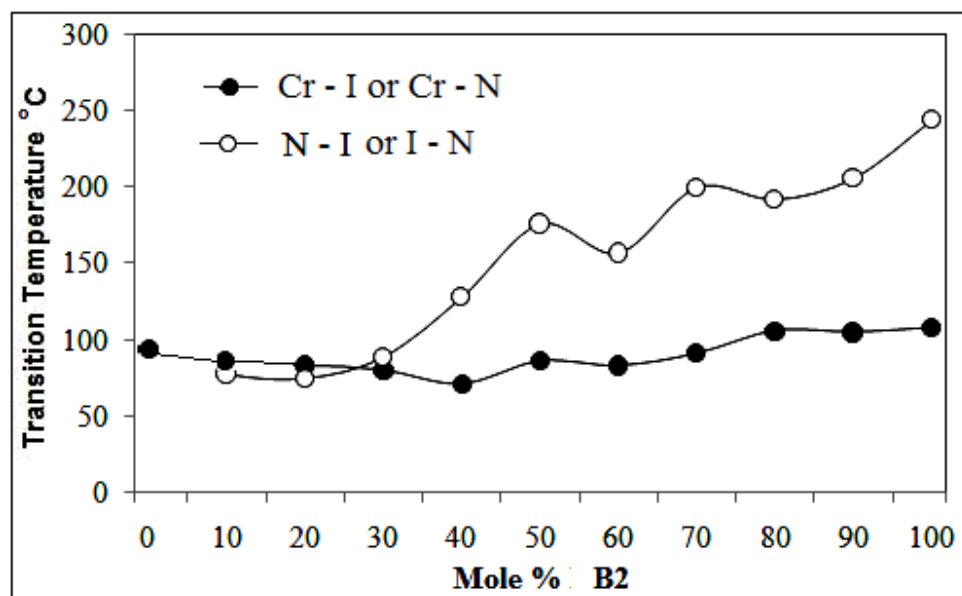
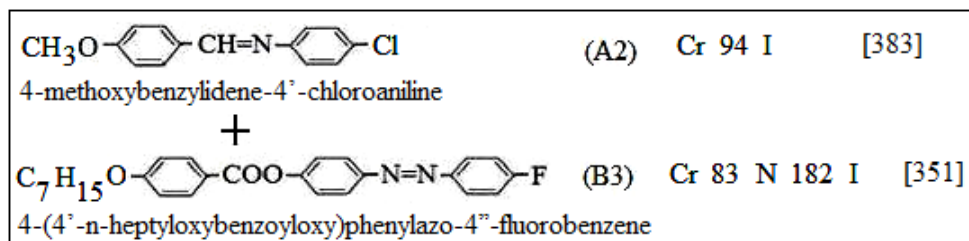


Figure 7.3: Phase diagram of Binary system III: MCBA (A2) + BBFA (B2)

7.3.4 Binary System -IV: MBCA(A2) + HPFB(B3)



Phase diagram of this system (Table 7.4, Figure 7.4) shows that nematic phase emerges as monotropic form with the addition of about as low as 19.34 mole% of nematogen B3 (Cr 83 N 182 I) into non-mesogen A2 (Cr 94 I). The monotropic nematic phase is transformed into enantiotropic form by addition of about 29.32 mole% of B3 into A2 and continuous to be exhibited till the addition of 89.08 mole% of B3 into A2. The mixed nematic phase shows threaded texture. As the concentration of B3 increases the mixed mesophase range increases. Eutectic point is obtained at 50 °C at about 69.22 mole% of B3 with maximum mesophase range of 72 °C is observed. In this system N-I curve shows non-linear behavior with overall rising tendency with increase in concentration of B3. Some of the binary mixtures supercool up to about 45 °C.

Mole % B3	Transition Temperature °C	
	Nematic	Isotropic
0	-	94
9.76	-	90
19.34	(38)	83
29.32	60	86
39.75	64	89
49.77	62	98
59.56	66	92
69.22	50	122
79.48	60	129
89.08	66	136
100	69	131

Values in parentheses indicates monotropic transitions

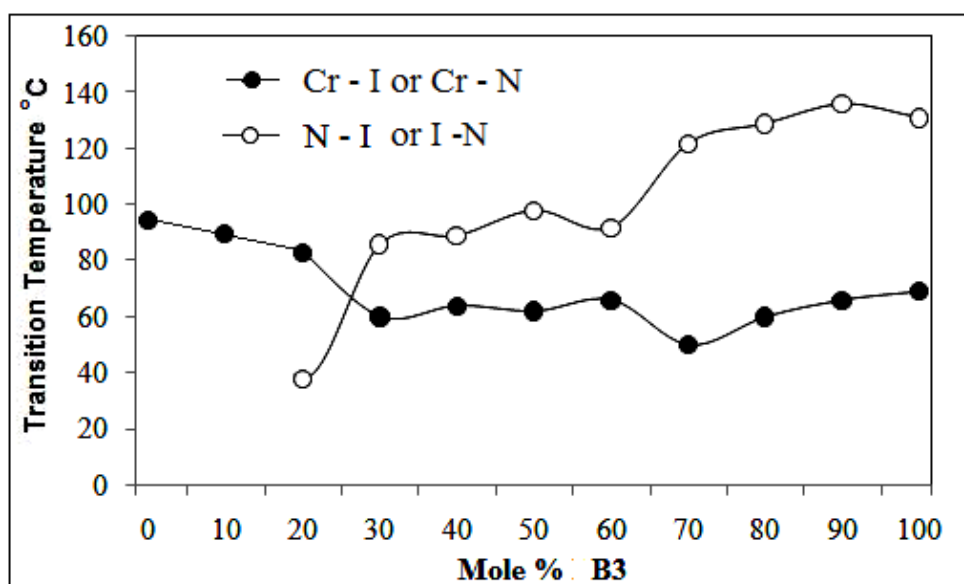
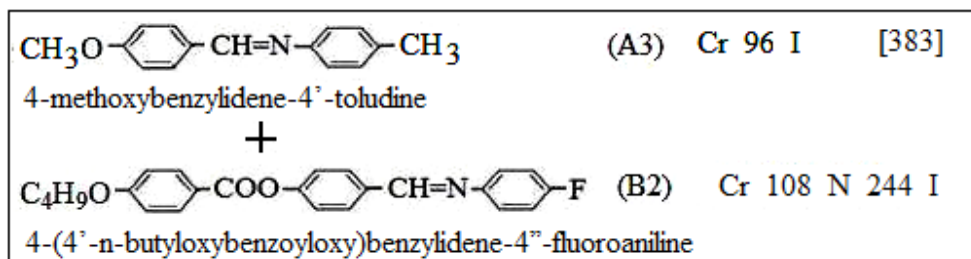


Figure 7.4: Phase diagram of Binary system IV: MBCA (A2) + HPFB (B3)

7.3.5 Binary System –V: MBT(A3) + BBFA(B2)



In this system (Table 7.5, Figure 7.5) component A3 is non-mesogen (Cr 96 I), whereas component B2 is nematogen (Cr 108 N 244 I) showing the nematic mesophase with marble texture. The non-mesogenic A3 is transformed into monotropic nematic phase by addition of about as low as 19.55 mole% of B2 into A3. The monotropic nematic phase is transformed into enantiotropic form by addition of about 29.03 mole% of B2 into A3 and continuous to be exhibited till the addition of 89.07 mole% of B2 into A3. The mixed nematic phase shows marble texture. As the concentration of B2 increases the mixed mesophase range increases. Eutectic point is obtained at 60 °C at about 59.25 mole% of B2 and maximum mesophase range of 126 °C is observed at 89.07 mole% of B2. In this system N-I curve shows non-linear behavior with steep rising tendency with increase in concentration of B2. Some of the binary mixtures supercool up to about 45 °C.

Table 7.5: Binary system V: MBT (A3) + BBFA (B2)

Mole % B2	Transition Temperature °C	
	Nematic	Isotropic
0	-	96
9.43	-	78
19.55	(54)	82
29.03	78	111
39.72	75	126
49.80	71	146
59.25	60	169
69.01	80	191
79.43	106	211
89.07	100	226
100	108	244

Values in parentheses indicates monotropic transitions

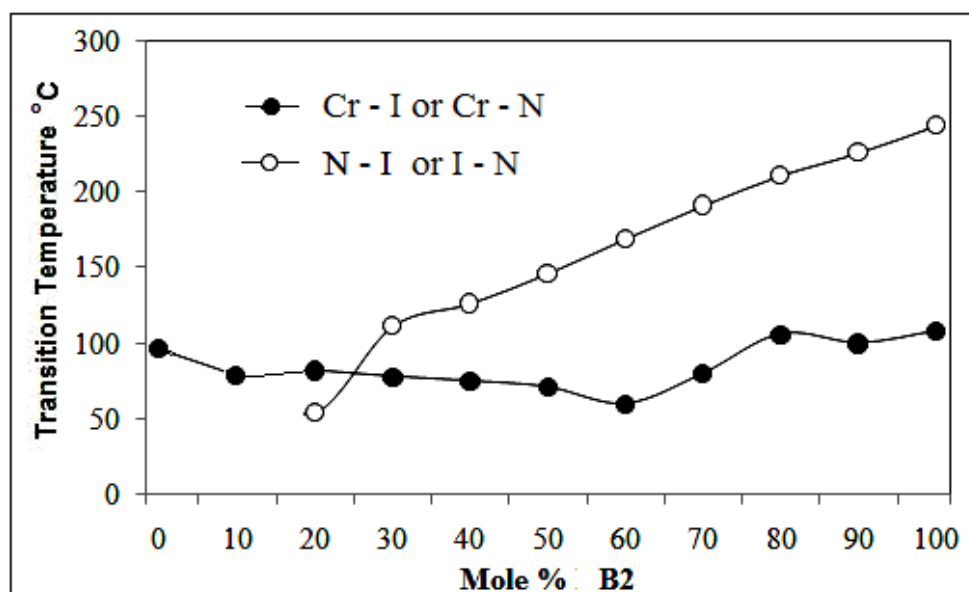
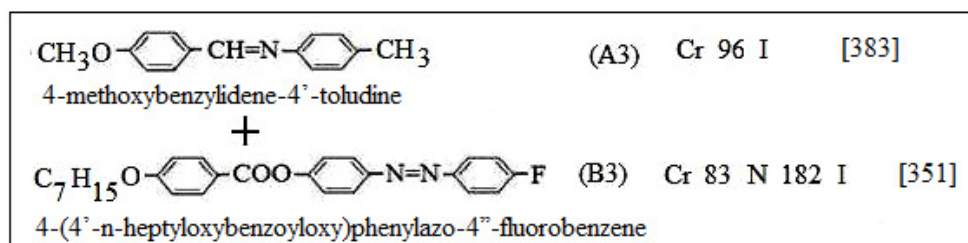


Figure 7.5: Phase diagram of Binary system V: MBT (A3) + BBFA (B2)

7.3.6 Binary System –VI: MBT(A3) + HPFB(B3)

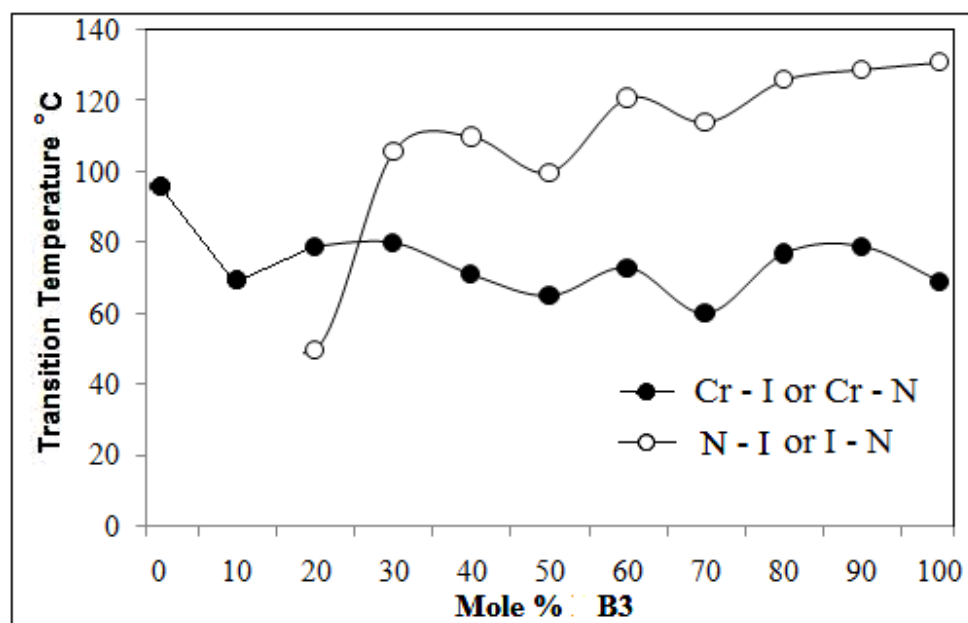


In this system (Table 7.6, Figure 7.6) component A3 is non-mesogen (Cr 96 I), whereas component B3 is nematogen (Cr 83 N 182 I) showing the nematic mesophase with marble texture. The non-mesogenic A3 is transformed into monotropic nematic phase by addition of about as low as 8.96 mole% of B3 into A3. The monotropic nematic phase is transformed into enantiotropic form by addition of about 59.15 mole% of B3 into A3 and continuous to be exhibited till the addition of 89.84 mole% of B3 into A3. The mixed nematic phase shows marble texture. As the concentration of B3 increases the mixed mesophase range increases. Eutectic point is obtained at 60 °C at about 68.83 mole% of B3 and maximum mesophase range of 54 °C is also observed at 68.83 mole% of B3. In this system N-I curve shows non-linear behavior with zig-zag tendency with increase in concentration of B3. Some of the binary mixtures supercool up to about 50 °C.

Table 7.6: Binary system VI: MBT (A3) + HPFB (B3)

Mole % B3	Transition Temperature °C	
	Nematic	Isotropic
0	-	96
8.96	-	70
20.51	(50)	79
29.13	80	106
38.77	71	110
50.26	65	100
59.15	73	121
68.83	60	114
79.42	77	126
89.84	79	129
100	69	131

Values in parentheses indicates monotropic transitions

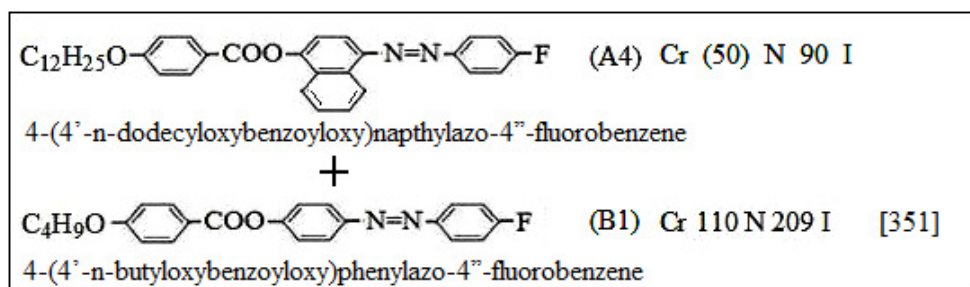
**Figure 7.6:** Phase diagram of Binary system VI: MBT (A3) + HPFB (B3)

7.3.7 Conclusion

The binary systems I to VI are composed of non-mesogenic components A1, A2 and A3 while the second components are mesogenic B1, B2 and B3. In the binary systems with the non-mesogen as one of the components, the nematic phase emerges either in monotropic or enantiotropic form with the addition of as low as 10 to 20 mole% of the non-mesogenic component in the mixture. The N-I curve shows non-linear behavior. Some of the binary mixtures supercool up to about 45 °C.

7.4 Type 2 Binary System [VII and VIII]

7.4.1 Binary System –VII: DNFB(A4) + BPFB(B1)



In this system (Table 7.7, Figure 7.7) both the components A4 and B1 are mesogenic in nature; A4 is monotropic nematogen (Cr (50) N 90 I) whereas B1 is enantiotropic nematogen (Cr 110 N 209 I); the nematic mesophase shows schlieren texture in A4 whereas marble texture in B1. The monotropic nematic phase of A4 is transformed into enantiotropic nematic phase by addition of as low as 11.06 mole% of B1 into A4 and continues to be exhibited till the addition of 90.79 mole% of B1 into A4. The mixed nematic phase shows schlieren texture. As the concentration of B1 increases the mixed mesophase range is increases. Eutectic point is obtained at 79 °C at about 71.40 mole % of B1 and maximum mesophase range of 121 °C is observed at 90.79 mole% of B1. In this system N-I curve is continuous and shows rising tendency, with slight increase at 90.79 mole% of B1; thus N-I curve shows non-linear behavior. Some of the binary mixtures supercool up to about 50 °C.

Table 7.7: Binary system VII: DNFB (A4) + BPFB (B1)

Mole % B1	Transition Temperature °C	
	Nematic	Isotropic
0	(50)	90
11.06	68	98
20.76	71	106
30.18	75	114
40.43	90	130
50.47	95	145
60.83	96	159
71.40	79	170
80.47	109	184
90.79	89	210
100	110	209

Values in parentheses indicates monotropic transitions

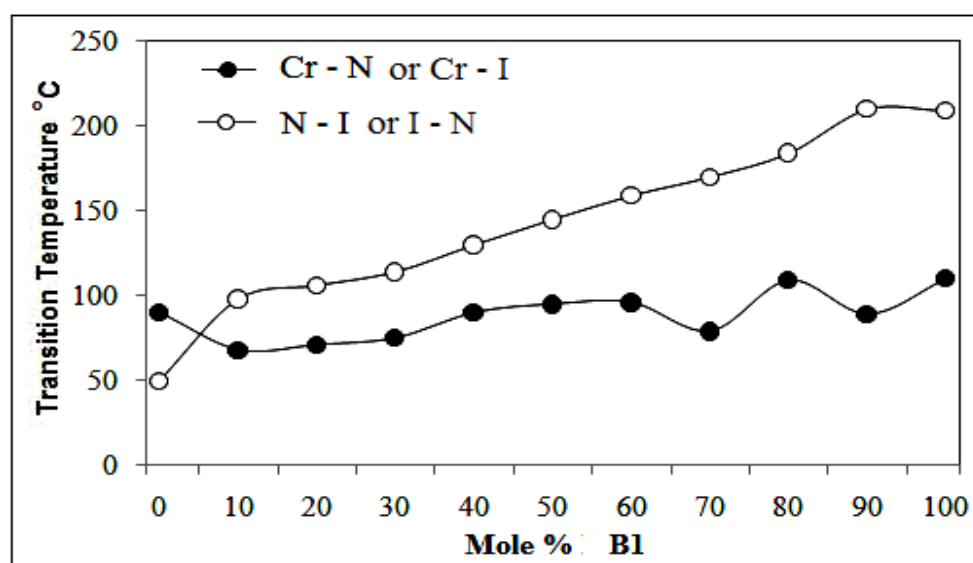
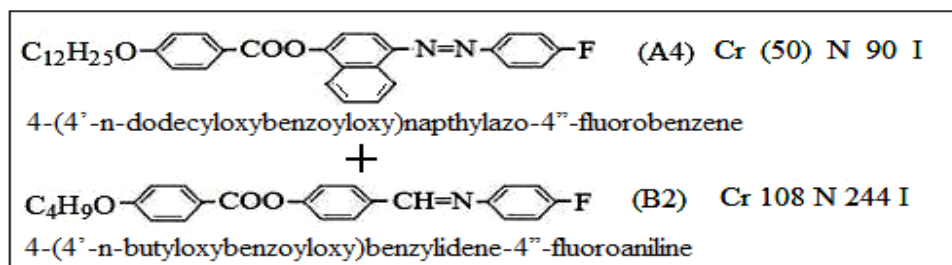


Figure 7.7: Phase diagram of Binary system VII: DNFB (A4) + BPFB (B1)

7.4.2 Binary System –VIII: DNFB(A4) + BBFA(B2)



In this system (Table 7.8, Figure 7.8) both the components A4 and B2 are mesogenic in nature; A4 is monotropic nematogen (Cr (50) N 90 I) whereas component B2 is enantiotropic nematogen (Cr 108 N 244 I); the nematic mesophase shows schlieren texture in A4 whereas marble texture in B2. The monotropic nematic phase of A4 is transformed into enantiotropic nematic phase by addition of as low as 10.92 mole% of B2 into A4 and continues to be exhibited till the addition of 90.94 mole% of B2 into A4. The mixed nematic phase also shows schlieren texture. As the concentration of B2 increases the mixed mesophase range is increases. No sharp eutectic point is obtained and maximum mesophase range of 81 °C is observed at 80.16 mole% of B2. In this system N-I curve shows rising tendency with steep rise from 80.16 mole% of B2; thus N-I curve shows non-linear behavior. Some of the binary mixtures supercool up to about 50 °C.

Table 7.8: Binary system VIII: DNFB (A4) + BBFA (B2)

Mole % B2	Transition Temperature °C	
	Nematic	Isotropic
0	(50)	90
10.92	64	89
21.52	66	86
30.78	82	104
40.85	90	118
51.27	92	118
60.44	88	135
70.78	106	173
80.16	99	180
90.94	110	225
100	108	244

Values in parentheses indicates monotropic transitions

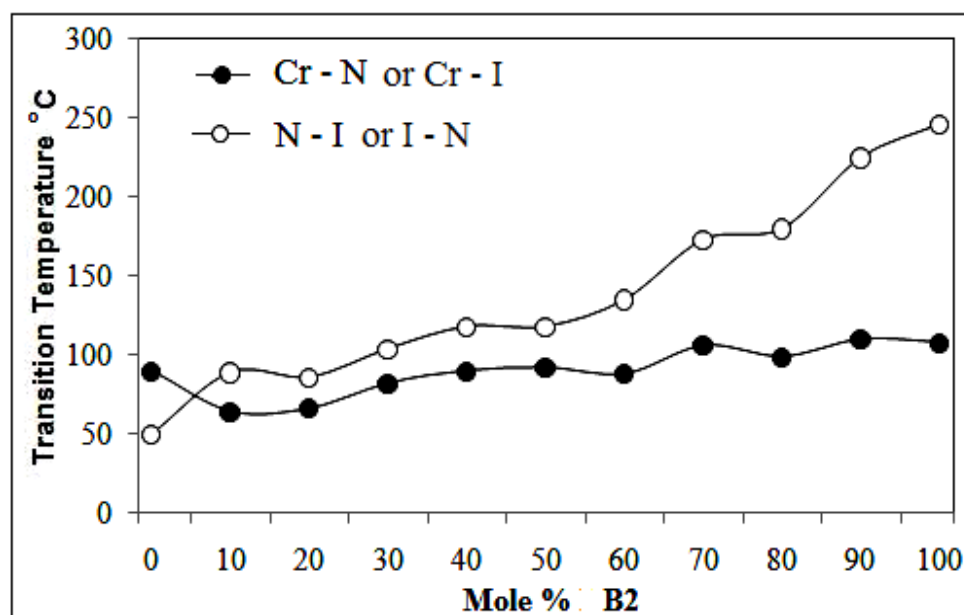


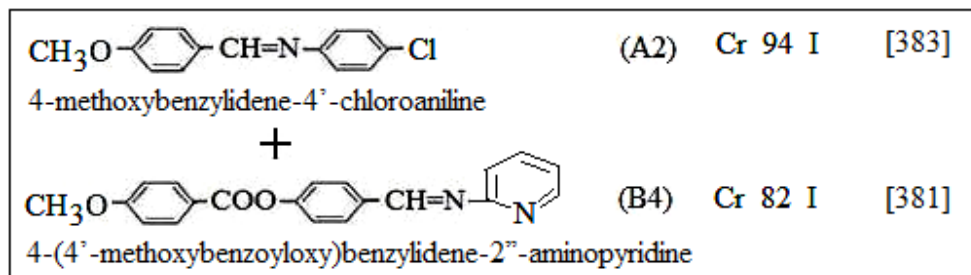
Figure 7.8: Phase diagram of Binary system VIII: DNFB (A4) + BBFA (B2)

7.4.3 Conclusion

The binary systems VII to VIII are composed of monotropic nematogen A4 and enantiotropic nematogen B1 and B2. This study shows that the monotropic nematogen are transformed into enantiotropic mixed nematic phase by addition of as low as about 10 mole% of enantiotropic nematogen in the mixture. The N-I curve shows non-linear behavior. Some of the binary mixtures supercool up to about 50 °C.

7.5 Type 3 Binary System [IX and X]

7.5.1 Binary System –IX: MBCA(A2) + MBAP(B4)



In this system (Table 7.9, Figure 7.9) both the components A2 (Cr 94 I) and B4 (Cr 82 I) are non-mesogenic in nature. The mesogenic characteristic commences in monotropic nematic form with the addition of as low as 9.28 mole% of B4 into A2; with addition of 19.64 mole% of B4 into A3 the monotropic nematic phase becomes enantiotropic in nature, which persists to remain in enantiotropic form till addition of 79.95 mole% of B4 into A3. No sharp eutectic point is obtained; maximum mesophase range of 85 °C is observed at 49.47 mole% of B4. In this system I-N curve shows rising tendency from 9.28 mole% of B4 and it merges with the rising N-I curve at 19.64 mole% of B4. The N-I curve rises upto 49.47 mole% of B4 and then shows falling tendency upto 79.95 mole% of B4; the curve then again merges with falling I-N curve at 89.18 mole% of B4. The N-I curve deviates from linearity. The mixed nematic phase shows threaded texture.

Table 7.9: Binary system IX: MBCA (A2) + MBAP (B4)

Mole % B4	Transition Temperature °C	
	Nematic	Isotropic
0	-	94
9.28	(43)	54
19.64	72	100
28.35	67	106
39.81	71	123
49.47	90	175
59.55	81	129
68.67	83	126
79.95	64	78
89.18	(46)	62
100	-	82

Values in parentheses indicates monotropic transitions

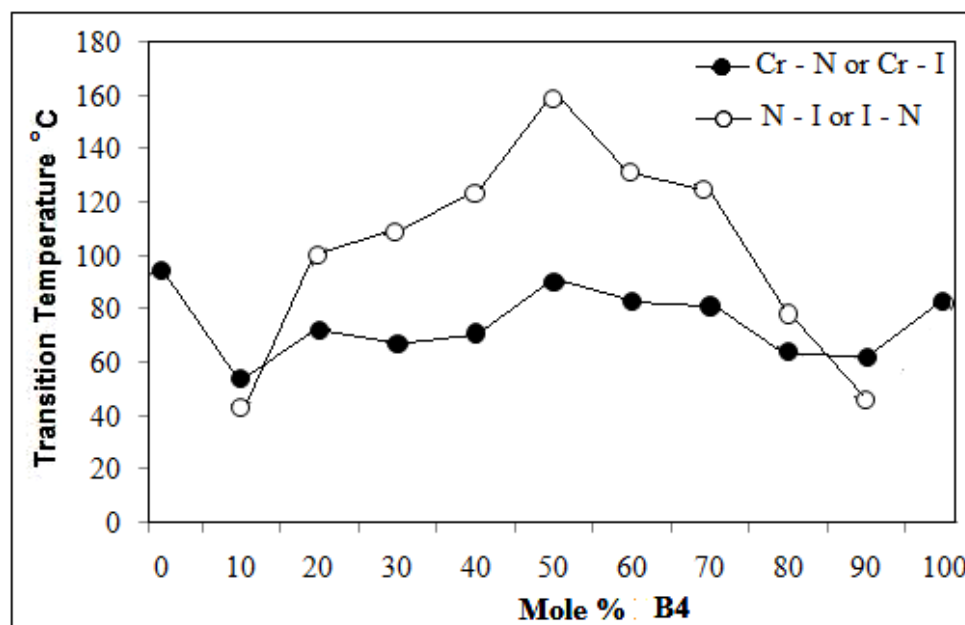
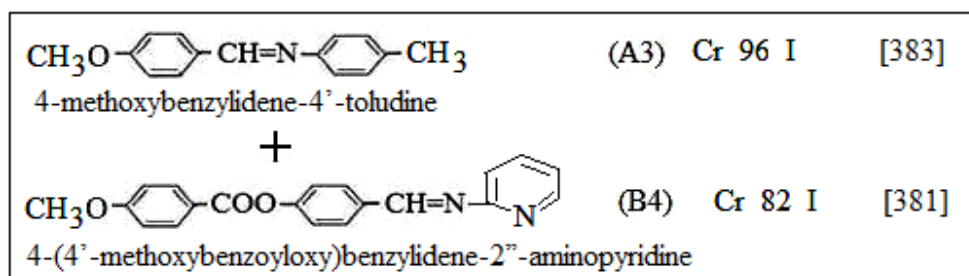


Figure 7.9: Phase diagram of Binary system IX: MBCA (A2) + MBAP (B4)

7.5.2 Binary System -X: MBT(A3) + MBAP(B4)



In this system (Table 7.10, Figure 7.10) both the components A3 (Cr 96 I) and B4 (Cr 82 I) are non-mesogenic in nature. The mesogenic characteristic commences in monotropic nematic form with the addition of as low as 8.69 mole% of B4 into A3; with addition of 19.31 mole% of B4 into A3 the monotropic nematic mesophase becomes enantiotropic in nature, which persist to remain till addition of 78.48 mole% of B4 into A3. No sharp eutectic point is obtained; maximum mesophase range of 114 °C is observed at 59.82 mole% of B4. In this system I-N curve shows rising tendency from 8.69 mole% of B4 and it merges with the rising N-I curve at 19.31 mole% of B4. The N-I curve rises upto 49.33 mole% of B4 and then shows steep falling tendency upto 69.12 mole% of B4; the curve then again merges with I-N curve at

78.48 mole% of B4. Again the I-N curve rises from 78.48 mole% to 89.10 mole% of B4. The N-I curve deviates from linearity. The mixed nematic phase shows marble texture.

Table 7.10: Binary system X: MBT (A3) + MBAP (B4)

Mole % B4	Transition Temperature °C	
	Nematic	Isotropic
0	-	96
8.69	(39)	81
19.31	80	134
29.90	78	150
39.58	105	209
49.33	114	218
59.82	124	210
69.12	82	110
78.48	(56)	76
89.10	(62)	73
100	-	82

Values in parentheses indicates monotropic transitions

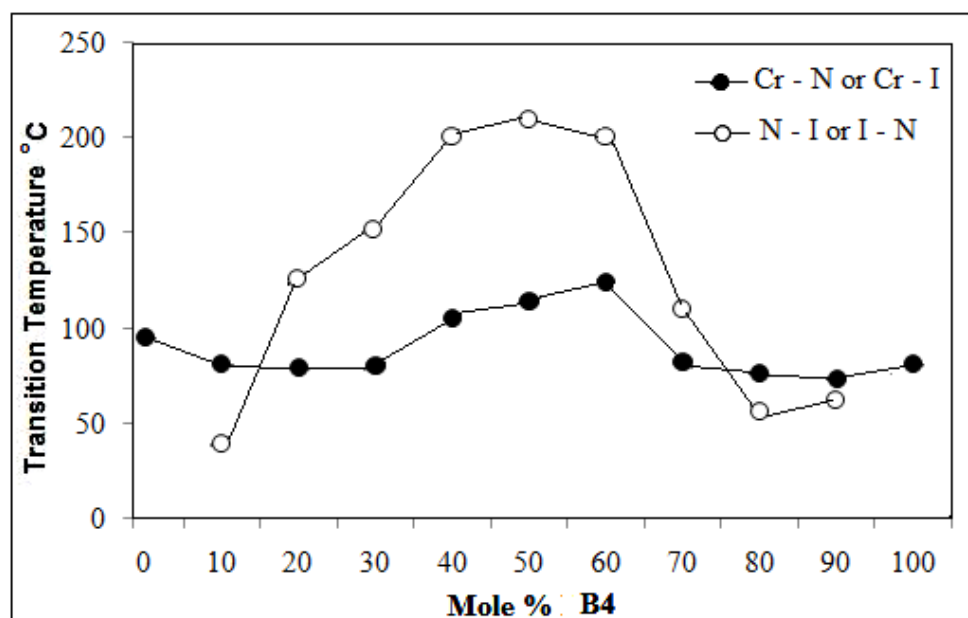
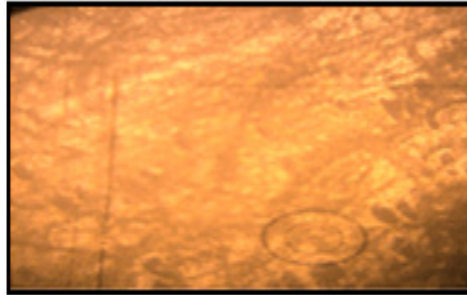


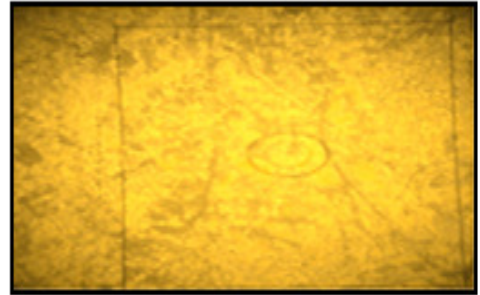
Figure 7.10: Phase Diagram of Binary system X: MBT (A3) + MBAP (B4)

7.5.3 Conclusion

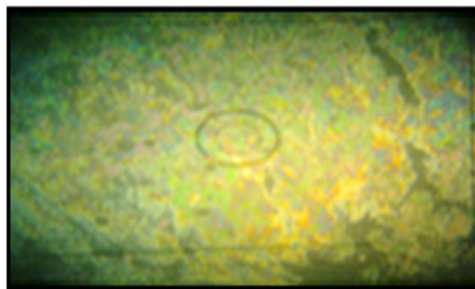
The binary systems IX to X are composed of non-mesogens A2, A3 and B4. The study shows that the nematic mesophase emerges into monotropic form with the addition of about 10 mole% of B4 into A2 and as well as A3 respectively and then it transformed into enantiotropic form with the addition of about 20 mole% of B4 into A2 and as well as A3 respectively. The N-I curve shows non-linear behavior.



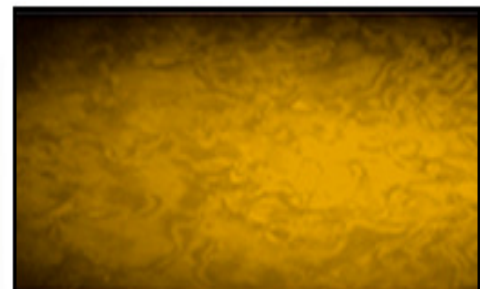
(a) Marble texture of nematic phase
Binary system I (40.25 mole%)



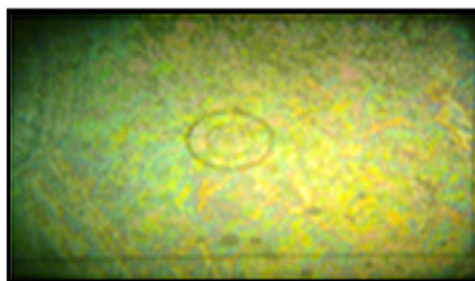
(b) Marble texture of nematic phase
Binary system II (59.02 mole%)



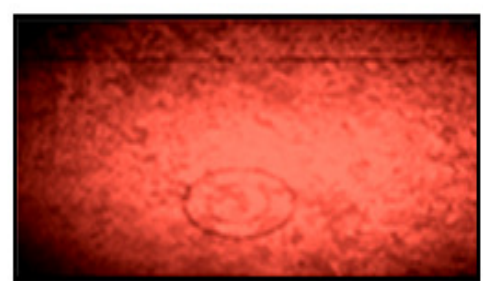
(c) Marble texture of nematic phase
Binary system III (69.24 mole%)



(d) Threaded texture of nematic phase
Binary system IV (39.75 mole%)



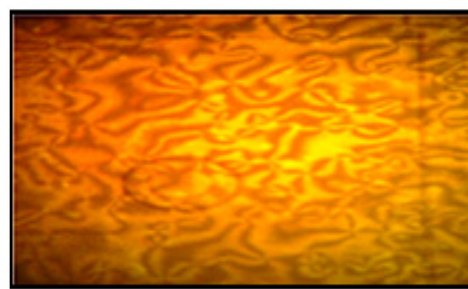
(e) Marble texture of nematic phase
Binary system V (79.43 mole%)



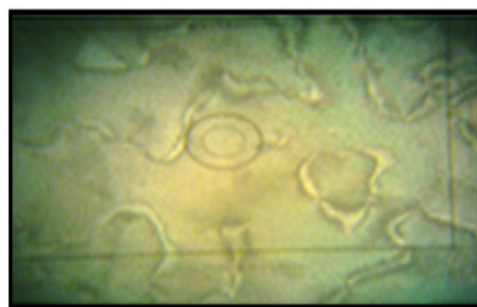
(f) Marble texture of nematic phase
Binary system VI (20.51 mole%)



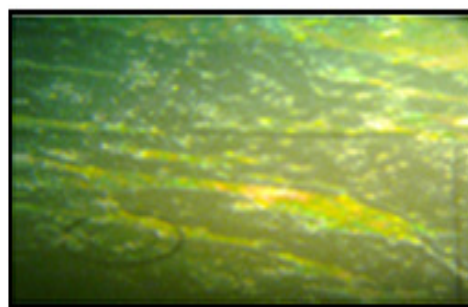
(g) Schlieren texture of nematic phase
Binary system VII (69.82 mole%)



(h) Schlieren texture of nematic phase
Binary system VIII (78.48 mole%)



(i) Threaded texture of nematic phase
Binary system IX (28.35 mole%)



(j) Marble texture of nematic phase
Binary system X (89.10 mole%)

Figure 7.11: Photomicrographs of the textures of the representative mixtures.

References

- 1 Reinizer, F., *Monatsh*, Vol. 9, 421 (1888).
- 2 Lehmann, O., *Z. Phys. Chem. (Leipzig)*, Vol. 4, 462 (1889).
- 3 Gattermann, L. and Ritschke, A., *Ber.*, Vol. 23, 1738 (1890).
- 4 Vorlander, D., *Kristallinisch flussige substanzen*, Vol. 12, 9-10 Heft, F., Enke, Stuttgart (1908).
- 5 Friedel, G., *Ann. Phys. (Paris)*, Vol. 18, 273 (1922).
- 6 Friedel, G. and Friedel, E., *Z. Krist*, Vol. 79, 1 (1931).
- 7 Brown, G. H. and Shaw, W. G., *Chem. Rev.*, Vol. 57, 1052 (1957).
- 8 Gray, G. W., *Liquid Crystals and Plastic Crystals*, Ellis Horwood Ltd., Chichester, England, Vol.1, p. 10, 103, 111, 116, 122, 125, 127,130, 137 (1974).
- 9 Coates, D. *Liquid Crystals, Applications and Uses*, (Eds: Bahadur, B.), Vol. 1, p. 91-137 (1990).
- 10 Herrmann, K., *Trans. Faraday Soc.*, Vol. 29, 972 (1933).
- 11 Saupe, A., *Liquid Crystals and Plastic Crystals*, Vol. 1, Gray, (Eds: G. W and Winsor, P. A.), Ellis Horwood Ltd., Chichester, England, p. 20 (1974).
- 12 Sackman, H. and Demus, D., *Mol. Cryst. Liq. Cryst.*, Vol. 21, 239 (1973); *Mol. Cryst.*, Vol. 2, 81 (1967); *Z. Phys. Chem.*, Vol. 222, 127 and 143 (1963).
- 13 de Vries, A., *Mol. Cryst. Liq. Cryst.*, Vol. 20, 119 (1973).
- 14 de Vries, A., *Mol. Cryst. Liq. Cryst.*, Vol. 24, 337 (1973).
- 15 Levelut, A., Germain, C., Keller, P., Liebert, L. and Billard, J., *J. de. P. Phys. (Paris)*, Vol. 44, 623 (1983).
- 16 Bennemann, D., Heppke, G., Levelut, A. M. and Lotzsch, D., *Mol. Cryst. Liq. Cryst.*, Vol. 260, 351 (1995).
- 17 Bennemann, D., Heppke, G. and Lotzsch, D., Presented at the sixteenth International conference on Liquid Crystals, Kent, Ohio, U.S.A., Abst No. B, 2006, 115 (1996).
- 18 de Vries A., *Mol. Cryst. Liq. Cryst.*, Vol. 10, 31 (1970).
- 19 Bose, E., *Phys. Z.*, Vol. 10, 230 (1909).
- 20 Zimmer, J. E. and White, J. L., *Mol. Cryst. Liq. Cryst.*, Vol. 38, 177 (1977).

-
- 21 Gasparoux, H., *Mol. Cryst. Liq. Cryst.*, Vol. 63, 231 (1981).
- 22 Tinh, N. H., Destrade, C. and Gasparoux, H., *Mol. Cryst. Liq. Cryst.*, Vol. 72, 247-253 (1982).
- 23 Arora, S. L., Muhoray, P. P., Vora, R. A., David, D. J. and Dasgupta, A. M., *Liq. Cryst.*, Vol. 5, No. 1, 133-140 (1989).
- 24 Harwood, S. M., Toyne, K. J., Goodby, J. W. and Parsley, M., *Mol. Cryst. Liq. Cryst.*, Vol. 332, 485-495 (1999).
- 25 Harwood, S. M., Toyne, K. J., Goodby, J. W., Parsley, M., and Gray, G. W., *Liq. Cryst.*, Vol. 27, No. 4, 443-449 (2000).
- 26 Dave, J. S. and Kurian, G., *Mol. Cryst. Liq. Cryst.*, Vol. 24, 347-355 (1973).
- 27 Hur, S. T., Gim, M. J., Yoo, H. J., Choi, S. W. and Takezoe, H., *Soft Matter*, Vol. 7, 8800 (2011).
- 28 Yeap, G. Y., Hng, T. C., Ito, M. M., Mohmood, W. A. K., Takeuchi, D. and Osakada, K., *Mol. Cryst. Liq. Cryst.*, Vol. 515, 215-229 (2009).
- 29 Crooker, P. P., *Liq. Cryst.*, Vol. 5, 751 (1989).
- 30 Keyes, P.H., *Mater. Res. Bull.*, Vol. 16, 32 (1991).
- 31 Crooker, P. P., *Chirality in Liquid Crystals*, (Eds: Kitzerow, H.S. and Bahr, C.), Springer, New York, pp. 186-222 (2001).
- 32 Kitzerow, H. S. and Crooker, P. P., *Phys. Rev. Lett.*, Vol. 67, 2151 (1991).
- 33 Lee, M., Hur, S. T., Higuchi, H., Song, K., Choi, S. W. and Kikuch, H., *J. Mater. Chem.*, Vol. 20, 5813 (2010).
- 34 Renn, S. R. and Lubensky, T. C., *Phys. Rev. A*, Vol. 38, 2132(1988).
- 35 Goodby, J.W., Waugh, M. A., Stein, S. M., Chin, E., Pindak, R., Patel, J. S., *J. Am. Chem. Soc.*, Vol. 111, 8119 (1989).
- 36 Srajer, G., Pindak, R., Waugh, M. A., Goodby, J. W. and Patel, J. S., *Phys. Rev. Lett.*, Vol. 64, 1545 (1990),
- 37 Nagappa, M. J., Hanumantha, N. R. and Alapati, P. R., *Mol. Cryst. Liq. Cryst.*, Vol. 304, 409 (1997).
- 38 Govindaiah, T. N., Nagappa, P. M., Mahadava, S. J. and Sreepad, H. R., *Mol. Cryst. Liq. Cryst.*, Vol. 548, 120-125 (2011).
- 39 Kasthuraiah, N., Sadashiva, B. K., Nguyen, H. T., Rouillon, J. C. and Isaert, N., *Ferroelectrics*, Vol. 243, 37-47 (2000).
-

-
- 40 Pandey, V. S., Dhar, R., Singh, A. K., Achalkumar, A. S. and Yelamaggad, C. V., *Phase Transitions*, Vol. 83, No. 12, 1049-1058 (2010).
- 41 Meier, J. G., Rudquist, P., Petrenko, A. S., Goodby, J. W. and Lagerwall, S. T., *Liq. Cryst.*, Vol. 29, No. 2, 179-189 (2002).
- 42 Yelamaggad, C. V., Bonde, N. L., Achalkumar, A. S., Rao, D. S. S., Prasad, S. K., and Prajapati, A. K., *Chem. Mater.*, Vol. 19, 2463-2472 (2007).
- 43 Arora, S. L., Ferguson, J. L. and Saupe, A., *Mol. Cryst. Liq. Cryst.*, Vol. 10, 243 (1970).
- 44 Helfrich, W. and Oh, C. S., *Mol. Cryst. Liq. Cryst.*, Vol. 14, 289 (1971).
- 45 Goodby, J. W., Toyne, K. J., Hird, M., Styring, P., Lewis, R. A., Beer, A., Dong, C. C., Glendenning, M. E., Jones, J. C., Lymer, K. P., Slaney, A. J., Minter, V., Chan, L. K., *Mol. Cryst. Liq. Cryst.*, Vol. 346, 169-182 (2000).
- 46 Hird, M., Goodby, J. W., Toyne, K. J., *Mol. Cryst. Liq. Cryst.*, Vol. 360, 1-15 (2001).
- 47 Futterer, T., Heppke, G., Lotzsch, D., Moro, D., Goodby, J. W., Tuffin, R. P., *Liq. Cryst.*, Vol. 29, No. 9, 1161-1167 (2002).
- 48 Mills, J. T., Gleeson, H. F., Goodby, J. W., Hird, M., Seed, A., Styring, P., *Mol. Cryst. Liq. Cryst.*, Vol. 330, 449-456 (1999).
- 49 Shtykov, N. M., Vij, J. K., Lewis, R. A., Hird, M., Goodby, J. W., *Liq. Cryst.*, Vol. 28, No. 11, 1699-1704 (2001).
- 50 Stipetic, A. I., Goodby, J. W., Hird, M., Raoul, Y. M., Gleeson, H. F., *Liq. Cryst.*, Vol. 33, No. 7, 819-828 (2006).
- 51 Chandrasekhar, S., Sadashiva, B. K. and Suresh, K. A., *Pramana*, Vol. 9, 471 (1977).
- 52 Boden, N., Bushby, R. J., Liu, Q. and Lozman, O. R., *J. Mater. Chem.*, Vol. 11, 1612-1617 (2001).
- 53 Varshney, S. K., Nagayama, H., Prasad, V. and Takezoe, H., *Liq. Cryst.*, Vol. 38, No. 10, 1321-1329 (2011).
- 54 Mahlstedt, S., Janietz, D., Stracke, A. and Wendorff, J. H., *Chem. Comm.*, No. 1, 15 (2000).
- 55 Kaller, M., Staffeld, P., Haug, R., Frey, W., Giesselmann, F. and Laschat, S., *Liq. Cryst.*, Vol. 38, No. 5, 531-553 (2011).
-

-
- 56 Zhang, C., PU, J., WU, H., Cheng, S., Zhand, R., Zhang, A. and Zhang, M., *Mol. Cryst. Liq. Cryst.*, Vol. 542, 99-105 (2011).
- 57 Bisoyi, H. K., Srinivasa H. T., and Kumar, S., *Beilstein J. Org. Chem.*, Vol. 5, No. 52, (2009).
- 58 Majumdar, K. C., Roy, N. D. B. and Bhaumik, A., *Mol. Cryst. Liq. Cryst.*, Vol. 548, 164-171 (2011).
- 59 Liao, Y. T., Zhao, K. Q., Wang, L., Hu, P. and Wang, B. Q., *Mol. Cryst. Liq. Cryst.*, Vol. 542, 75-83 (2011).
- 60 Kumar, S., Varshney, S. K. and Chauhan, D. *Mol. Cryst. Liq. Cryst.*, Vol. 396, 241-250 (2003).
- 61 Kumar, S., *Liq. Cryst.*, Vol. 31, 1037-1059 (2004).
- 62 Barbera, J., Godoy, M. A., Hidalgo, P. I., Para, M. L., Ulloa, J. A. and Vergara, J. M., *Liq. Cryst.*, Vol. 38, No. 6, 679-688 (2011).
- 63 Hermann, S. O., Wendorff, J. H., Ringsdorf, H., and Tschirner, P., *Makromol. Chem. Rapid. Commun.*, Vol. 7, 791 (1986).
- 64 Haristoy, D., Mery, S., Heinrich, B., Mager, L., Nicoud, J. F. and Guillon, D., *Liq. Cryst.*, Vol. 27, No. 3, 321-328 (2000).
- 65 Lehmann, O., *Ann. Phys.*, (3) 56, 771 (1895); 21, 181 (1906).
- 66 Hartshorne, N. H. and Stuart. A., *Crystals and Polarising Microscope*, 4th ed., p. 543, Edward Pub. Ltd., London (1970).
- 67 Song, C. A., Litt, M. H., Mano's-Zloczower, I., *Macromolecules*, Vol. 25 (8), 2166-2169 (1992).
- 68 Oliveira, D. A., Palangana, A. J. and Amaral, L. Q., *Mol. Cryst. Liq. Cryst.*, Vol. 547, 195-200 (2011).
- 69 Nesrullajev, A., Okcan, M., Kazanci, N., *J. Mol. Liq.*, Vol. 108/1-3, 313-332 (2003).
- 70 Vijayaraghavan, D., *Mol. Cryst. Liq. Cryst.*, Vol. 547, 189-194 (2011).
- 71 Olga, V., Vlada, P., Marina, K., Valentina, P. and Longin, L., *Mol. Cryst. Liq. Cryst.*, Vol. 547, 155-163 (2011).
- 72 Gray. G. W., *Liquid Crystals and Plastic Crystals*, Vol. 1, Eds Gray, G. W. and Winsor, P. A., Ellis Harwood Ltd., Chichester, England (1974).
-

-
- 73 Gray. G. W. and Mosley. A., *Mol. Cryst. Liq. Cryst.*, Vol. 37, 213-231 (1976).
- 74 Weissflog, W., Wegeleben, A and Demus, D., Presented at the 9th International Liquid Crystal Conference, Bangalore, India, Dec. (1982).
- 75 Demus, D., *Mol. Cryst. Liq. Cryst.*, Vol. 165, 45-84 (1988).
- 76 Weissflog, W., Demus, D., Selbmann, C. and Hause, A., Presented at the 10th International Liquid Crystal Conference, York, U.K., July (1984).
- 77 Weissflog, W., Wegeleben, A and Demus, D., *Mater. Chem. Phys.*, Vol. 12 No. 5, 461 (1985).
- 78 Gray. G. W., *Molecular Structure and the Properties of Liquid Crystals*, Academic Press, London, pp. 207-224 (1962).
- 79 Sadashiva, B. K., *Mol. Cryst. Liq. Cryst.*, Vol. 53, 253 (1979).
- 80 Dave, J. S., Menon, M. R. and Patel, P. R., *Mol. Cryst. Liq. Cryst.*, Vol. 378, 1-11 (2002).
- 81 Coates, D., *Liq. Cryst.*, Vol. 2, No. 1, 63 (1987).
- 82 Gray, G. W. and Harrison, K. J., *Mol. Cryst. Liq. Cryst.*, Vol. 13, 37 (1971); Vol. 22, 99 (1971).
- 83 G. W. Gray, *Liquid Crystals and Plastic Crystals*, Ellis Horwood Limited, Chichester, England, Vol. 1, pp. 124,125 (1974).
- 84 Gray, G. W. *Liquid Crystals and Plastic Crystals*, Ellis Horwood Limited, Chichester, England, Vol. 1, pp. 125,126 (1974).
- 85 Gallardo, V. and Muller, H. J., *Mol. Cryst. Liq. Cryst.*, Vol. 102, 13 (1984).
- 86 Dixit, S. and Vora, R. A., *Mol. Cryst. Liq. Cryst.*, Vol. 501, 43-52 (2009).
- 87 Matharu, A. S. and Asman, D. C., *Liq. Cryst.*, Vol. 34, 1317-1336 (2007).
- 88 Prajapati, A. K., *Liq. Cryst.*, Vol. 27, 1017-1020 (2000).
- 89 Weissflog, W. and Demus, D., *Liq. Cryst.*, Vol. 3, 278 (1988).
- 91 Matsunaga, Y., Mukougava, T. and Saito, Y., *Mol. Cryst. Liq. Cryst.*, Vol. 317, 237-243 (1998).
-

-
- 92 Jiang, Y., Lu, L., Chen, P., Chen, X., Li, J. and An, Z., *Liq. Cryst.*, Vol. 39, No. 8, 957-963 (2012).
- 93 Weissflog, W., Diele, S. and Demus, D., *Mol. Cryst. Liq. Cryst.*, Vol. 191, 9-15 (1990).
- 94 Branch, S. J., Hyron, D. J., Gray, G. W., Ibboston, A. and Worrall, B. M., *J. Chem. Soc.*, 3279 (1964).
- 95 Branch, S. J., Gray, G. W., Ibboston, A. and Worrall, B. M., *J. Chem. Soc.*, 2246 (1963).
- 96 Ho, M. S., Fung, B. M. and Bayle, J. P., *Mol. Cryst. Liq. Cryst.*, Vol. 225, 383 (1993).
- 97 Weissflog, W., Diele, S. and Demus, D., *Mol. Cryst. Liq. Cryst.*, Vol. 191, 9-15 (1990).
- 98 Gray, G. W. *Liquid Crystals and Plastic Crystals*, Ellis Horwood Limited, Chichester, England, Vol. 1, pp. 127 (1974).
- 99 Vorlander, D., *Ber.*, Vol. 62, 2831 (1929).
- 100 Pelz, G., Diele, S. and Weissflog, W., *Adv. Mater.*, Vol. 11, 707(1998).
- 101 Niori, T., Sekine, T., Watanabe, J., Furukawa, T. and Takezoe, H., *J. Mater. Chem.*, Vol. 6, 1231 (1996).
- 102 Sekine, T., Niori, T., Watanabe, J., Furukawa, T., Choi, S.W. and Takezoe, H., *J. Mater. Chem.*, Vol. 7, 1307 (1997).
- 103 Majumdar, K.C., Pal, N. and Rao, N.V.S., *Liq. Cryst.*, Vol. 33, No. 5, 531-535 (2006).
- 104 Yelamagad, C. V., Shashikala, I., Rao, D. S. S., Prasada, S. K., *Liq. Cryst.*, Vol. 31, No. 7, 1027-1036 (2004).
- 105 Yanga, P. J., Lina, H.C., *Liq. Cryst.*, Vol. 33, No. 5, 587-603 (2006).
- 106 Prajapati, A. K. and Modi, V., *Liq. Cryst.*, Vol. 37, No. 4, 407-415 (2010).
- 107 Mathews, M., Kang, S., Kumar, S., Li, Q., *Liq. Cryst.*, Vol. 38, No. 1, 31-40 (2011).
- 108 Reddy, R. A. and Sadashiva, B. K., *Liq. Cryst.*, Vol. 27, No. 12, 1613-1623 (2000).
-

-
- 109 Sadashiva, B. K., Raghunathan, V. A. and Pratibha, R., *Ferroelectrics*, Vol. 243, 249-260 (2000).
- 110 Wirth, I., Diele, S., Ermin, A., Pelz, G., Grande, S., Kovalenko, I., Pancenko, N. and Weissflog, W., *J. Mater. Chem.*, Vol. 11, 1642-1650 (2001).
- 111 Sadashiva, B. K., Murthy, H. N. S. and Dhara, S., *Liq. Cryst.*, Vol. 28, No.3, 483-487 (2001).
- 112 Weissflog, W., Nadası, H., Dunemann, U., Pelz, G., Diele, S., Eremin, A. and Kresse, H., *J. Mater. Chem.*, Vol. 11, 2748-2758 (2001).
- 113 Thisayukta, J., Nakayama, Y., Kawauchi, S., Takezoe, H. and Watanabe, J., *J. Am. Chem. Soc.*, 122, 7441-7448 (2000).
- 114 Shen, D., Pegenau, A., Diele, S., Wirth, I. and Tschierske, C., *J. Am. Chem. Soc.*, Vol. 122, 1593-1601 (2000).
- 115 Shen, D., Diele, S., Pelz, G., Wirth, I. and Tschierske, C., *J. Mater. Chem.*, Vol. 9, 661-672 (1999).
- 116 Karamysheva, L. A., Torogova, S. I. and Agafonova, I. F., *Liq. Cryst.*, Vol. 27, No. 3, 393-405 (2000).
- 117 Semmler, K. J. K., Dingermans, T. D. and Samulski, E. T., *Liq. Cryst.*, Vol. 24, No. 6, 799-803 (1998).
- 118 Imrie, C.T., Henderson, P.A., *Chem. Soc. Rev.*, Vol. 36, 2096-2124 (2007).
- 119 Imrie, C.T., Henderson, P.A. and Yeap, G.Y., *Liq. Cryst.*, Vol. 36, No. 6-7, 755-777 (2009).
- 120 Chiellini, E. and Laus, M., *Main chain liquid crystalline semiflexible polymers.*, *Handbook of Liquid Crystals*, Demus, D., Goodby, J., Gray, G. W., Spiess, H. W. and Vill, V. (Eds.), Wiley-VCH: Weinheim, Vol. 3, Chapter II, p. 93 (1998).
- 121 D. Vorlander, *Z. Phys. Chem.*, Vol. 126, 449 (1927).
- 122 L. Marin, A. Zabolica and M. Sava, *Liq. Cryst.*, Vol. 38, 433-440 (2011).
-

-
- 123 Bisoyi, H. K. and Kumar, S., *Phase Transitions*, Vol. 79, No. 4-5, 285-292 (2006).
- 124 Noji, A. and Yoshizawa, A., *Liq. Cryst.*, Vol. 38, No. 4, 451-459 (2011).
- 125 Weissflog, W., Lischka, C., Diele, S., Wirth, I. and Pelzl, G., *Liq. Cryst.*, Vol. 27, No. 1, 43-50 (2000).
- 126 Dantlgraber, G., Diele, S. and Tschierske, C., *Chem. Commun.*, 2768 (2002).
- 127 Kosata, B., Tamba, M. G., Baumeister, U., Pelzl, K., Diele, S., Pelzl, G., Galli, G., Samaritani, S., Agina, E. V., Boiko, N. I., Shibave, V. P. and Weissflog, W., *Chem. Mater.*, Vol. 18, 691-701 (2006).
- 128 Kołpaczynska, M., Madrak, K., Mieczkowski, J., Gorecka, E. and Pocięcha, D., *Liq. Cryst.*, Vol. 38, No. 2, 149-154 (2011).
- 129 Prajapati, A. K., Varia, M. C. and Sahoo, S. P., *Liq. Cryst.*, Vol. 38, No. 7, 861-869 (2011).
- 130 Prajapati, A. K., Varia, M. C. and Sahoo, S. P., *Phase Transitions*, Vol. 84, No. 4, 325-342 (2011).
- 131 Prasad, V., Roy, A., Nagaveni, N.G. and Gayathri, K., *Liq. Cryst.*, Vol. 38, No. 10, 1301-1314 (2011).
- 132 Majumdar, K.C., Ghosh, T., Rao, D. S. S., and Prasad, S. K., *Liq. Cryst.*, Vol. 38, No. 10, 1269-1277 (2011).
- 133 Yoshizawa, A., Nakata, M., and Yamaguchi, A., *Liq. Cryst.*, Vol. 33, No. 5, 605-609 (2006)
- 134 Marcelis, A. T. M., Koudijs, A., and Sudholter, E. J. R., *Mol. Cryst. Liq. Cryst.*, Vol. 330, 45-52 (1999).
- 135 Yelamaggad, C. V., Anitha, N. S., Hiremath, U. S., Rao, D. S., and Prasad, S. K., *Liq. Cryst.*, Vol. 28, No. 10, 1581-1583 (2001).
- 136 Yeap, G. Y., Hng, T. C., Mahmood, W. A. K., Gorecka, E., Takeuchi, D. and Osakada, K., *Mol. Cryst. Liq. Cryst.*, Vol. 506, 109-133 (2009).
-

-
- 137 Henderson, P.A. and Imrie, C.T., *Liq. Cryst.*, Vol. 32, No. 6, 673-682 (2005).
- 138 Donaldson, T., Henderson, P. A., Achard, M. F. and Imrie, C. T., *Liq. Cryst.*, Vol. 38, No. 10, 1331-1339 (2011).
- 139 Imrie, C.T. and Luckhurst, G.R., *J. mater. Chem.*, Vol. 8, 1339-1343 (1998).
- 140 Henderson, P.A. and Imrie, C. T., *Liq. Cryst.*, Vol. 32, No. 6, 673-682 (2005)
- 141 Achalkumar, A. S., Hiremath, U. S., Rao, D. S. S. and Yelamaggad, C. V. *Liq. Cryst.*, Vol. 38, No. 11-12, 1563-1589 (2011).
- 142 Itahara, T., and Tamura, H., *Mol. Cryst. Liq. Cryst.*, Vol. 474, 17-27 (2007).
- 143 Yelamaggad, C. V., Nagamani, S. A., Hiremath, U. S., Rao, D. S. S., and Prasad, S. K., *Liq. Cryst.*, Vol. 29, 231 (2002).
- 144 Henderson, P. A., and Imrie, C. T., *Macromolecules*, Vol. 38, 3307 (2005).
- 145 Henderson, P. A., Inkster, R. T., Seddon, J. M. and Imrie, C. T., *J. Mater. Chem.*, Vol. 11, 2722-2731 (2001).
- 146 Emsley, J. E., Luckhurst, G. R., Shilstone, G. N. and Sage, I., *Mol. Cryst. Liq. Cryst. Lett.*, Vol. 102, 223 (1984).
- 147 Imrie, C. T., and Luckhurst, G. R., *Liquid crystal dimers and oligomers. Handbook of Liquid Crystals*. Demus, D., Goodby, J., Gray, W. G., Spiess, H. W., and Vill, V. (Eds.), Wiley-VCH: Weinheim, Vol. 2B, Chapter X, p. 801 (1998).
- 148 Imrie, C.T., Stewart, D., Remy, C., Christie, D.W., Hamley, I.W., Harding, R., *J. Mater. Chem.*, Vol. 9, 2321-2325 (1998).
- 149 Donaldson, T., Henderson, P.A., Achard, M.F., Imrie, C.T., *J. Mater. Chem.*, 10935-10941 (2011).
- 150 Oster, G., *J. Gen. Physiology*, Vol. 33, 445 (1950).
- 151 Robinson, C., *Tetrahedron*, Vol. 13, 219 (1961).
- 152 Finkelmann, H., *Polymer Liquid Crystals*, Edts. Ciferri, A., Krigbaum, W. R. and Meyer, R. B., Academic Press, New York, pp. 35, 36, 39, 53 (1982).
- 153 Ober, Christopher, K., Bluhm, L. Terry., *Thermotropic Liquid Crystals*, current Topics in Polymer Science, Vol. I, Hunser Publishers (1987).
-

-
- 154 Demus, D., *Liq. Cryst.*, Vol. 5, 75 (1989); Hopken, J., Pugh, C., Richtering, W. and Moller, M., *Makromol. Chem.*, Vol. 189, 911 (1988).
- 155 Percec, V. and Yourd, R., *Macromolecules*, Vol. 21, 3379 (1988).
- 156 Bacilieri, A., Caruso, U., Panunzi, B., Roviello, A. and Sirigu, A., *Polymer*, Vol. 41, 6423-6430 (2000).
- 157 Shen, Y, Chen, E.Q., Ye, C., Zhang, H.L, Wu, P.Y, Noda, and Zhou, Q.F., *J. Phys. Chem. Part B*, Vol. 109, 6089-6095 (2005).
- 158 Konga, X., Hea, Z., Gopeeb, H. and Cammidge, A. N., *Liq. Cryst.*, Vol. 38, No. 8, 943-955 (2011).
- 159 Uekusa, T., Nagano, S., and Seki, T., *Langmuir*, Vol. 23, 4642 (2007).
- 160 Blumstein, A. and Hus, E. C., *Liquid Crystalline Order in Polymers*, ed. Blumstein, A., Academic Press, New York (1982).
- 161 Cifferri, A., Krigbaum, W. R. and Mayer, R. B., *Polymeric Liquid Crystals*, Academic Press, New York (1982).
- 162 Henriquez, C. M. G., Bustamante, E. A. S., Gordillo, D. A. W. and Haase, W., *Liq. Cryst.*, Vol. 36, No. 5, 541-547 (2009).
- 163 He, X. Z., Zhang, B. Y., Ma, W. W., Zhang, L. and My, Q., *Liq. Cryst.*, Vol. 36, No. 8, 847-854 (2009).
- 164 Keith, C., Reddy, R. A. and Tschierske, C., *Chem. Commun.*, 871 (2005).
- 165 Patel, P. R. and Dave, J. S., *Liq. Cryst.*, Vol. 30, No. 6, 691-696 (2003).
- 166 Kondo, M., Takemoto, M., Matsuda, T., Fukae, R. and Kawatsuki, N., *Mol. Cryst. Liq. Cryst.*, Vol. 550, 98-104 (2011).
- 167 Gu, H. D., Chen, L., Yan, J. X., *Liq. Cryst.*, Vol. 36, 1319-1327 (2009).
- 168 Bubnov, A., Kaspar, M., Sedlakov, Z., *Phase Transitions*, Vol. 83, No. 1, 16-27 (2010).
- 169 Craig, A. A. and Imrie, C. T., *Polymer*, Vol. 38, No. 19, 4951 (1997).
- 170 Chauhan, B. C., Gade, R. M., Menon, M. and Jejurkar, C. R., *Phosphorous, Sulphur and Silicon*, Vol. 150-151, 277-285 (1999).
- 171 Serano, J. L. (Editor), *Metallomesogens*, VCH Weinheim (1996).
-

-
- 172 Vorlander, D., *Ber. Disch. Ges.*, Vol. 43, 3120 (1910).
- 173 Pucci, D., *Liq. Cryst.*, Vol. 38, No. 11-12, 1451-1465 (2011).
- 174 Espinet, P., Esteruelas, M. A., Ora, L. A., Serrano, J. L. and Sola, E., *Coord. Chem. Rev.*, Vol. 117, 215 (1992).
- 175 Barbera, J., Gimenez, R., Gimeno, N., Marcos, M., Pina, M.D.C. and Serrano, J. L., *Liq. Cryst.*, Vol. 30, 651 (2003).
- 176 Date, R. W. and Bruce, D. W., *Liq. Cryst.*, Vol. 31, 1435 (2004).
- 177 Miyajma, N. H., Sekiuchi, T., Yamazaki, W. and Sasaki, T., *Mol. Cryst. and Liq. Cryst.*, Vol. 286, 311-316 (1996).
- 178 Prajapati, A. K. and Bonde, N., *Liq. Cryst.*, Vol. 33, 1189-1197 (2006).
- 179 Bruce, D. W., Dunmur, D. A., Maitlis, P. M., Styring, P., Esteruelas, M. A., Ora, L. A., Ros, M. B., Serrano, J. L. and Sola, E., *Chem. Mater.*, Vol. 1, 479 (1989).
- 180 Esteruelas, M. A., Sola, E., Ora, L. A., Ros, M. B., Macros, M. and Serrano, J. L., *J. Organomet. Chem.*, Vol. 387, 103 (1990).
- 181 Bhatt. J., Fung, B. M., Nicholas, K. M. and Poon, C. D., *Chem. Commun.*, 1439 (1998).
- 182 Gao, Y., and Shreeve, J. M., *J. Inorg. and Organometallic Polymers and Materials*, Vol. 17, No. 1, 19-36 (2007).
- 183 Jejurkar, C. R., Dave, J. S., Patel, P. R. and Menon, M. R., *Mol. Cryst. Liq. Cryst.*, Vol. 364, 753-758 (2001).
- 184 Patel, D., Bhattacharya, P. K., Patel, P. and Dave, J. S., *Mol. Cryst. Liq. Cryst.*, Vol. 403, 33-47 (2003).
- 185 Circu, V. and Dumitrascu, F., *Mol. Cryst. Liq. Cryst.*, Vol. 534, 41-49 (2011).
- 186 Bhattacharjee, C. R., Das, G. and Mondal, P., *Liq. Cryst.*, Vol. 38, No. 4, 441- 449 (2011).
- 187 Singh, A. K, Kumari, S., Kumar, K. R., Sridhar, B. and Rao, T. R., *Polyhedron*, Vol. 27, 181-186 (2008).
- 188 Sasaki, I., Vender, L., Sournia S. A., and Lacroix, P. G., *Eur. J. Inorg. Chem.*, 3294-3302 (2006).
- 189 Wang, C. H., Wang, Y. J., Hu, H. M., Lee, G. H. and Lai, C.K., *Tetrahedron*, Vol. 64, 4939-4948 (2008).
-

-
- 190 Gurol, I. and Ahsen, V., *Mol. Cryst. Liq. Cryst.*, Vol. 442,103-118, (2005).
- 191 Singh, S. K., Vikram, K. and Singh, B., *Liq. Cryst.*, Vol. 38, No. 9, 1117-1129 (2011).
- 192 Majumdar, K. C., Ghosh, T. and Shyam, P. K., *Liq. Cryst.*, Vol. 38, No. 5, 567-573 (2011).
- 193 Tamman, G., *Ann. Physik.*, 4, 524 (1901); 8, 103 (1902); 19, 421 (1906).
- 194 Lehmann, O., *Die Flussige Kristalle*, Leipzig (1904).
- 195 Kleman, M., *Advances in Liquid Crystals*, Vol.1, Edt. Brown, G. H., Academic Press, London, 267 (1975).
- 196 Lagerwall, S. T. and Stebler, B., International Liquid Crystal Conference, Bangalore, India, Dec. (1979), Liquid Crystals Editor, S. Chandrasekhar, Heyden-Verlay, 223 (1980).
- 197 Schenk, R., *Z. Phys. Chem.*, Vol. 25, 337 (1898).
- 198 Schenk, R. and Schneider, F., *Z. Phys. Chem.*, Vol. 29, 546 (1899).
- 199 Dave, J. S. and Dewar, M. J. S., *J. Chem. Soc.*, 4616, 4505 (1955).
- 200 Dave, J. S. and Lohar, J. M., *Proc. Nat. Acad. Sc.*, India, 29A, Part I, 35 (1960); *Chem. Ind. (London)* 597 (1959); *Indian J. Chem.*, Vol. 4, 386 (1966); *J. Chem. Soc.(A)*, 1473 (1967).
- 201 Dave, J. S. and Vasanth, K. L., *Ind. J. Chem.*, Vol. 7, 498 (1969); *Mol. Cryst*; Vol. 2, 125 (1966); *Pramana Suppl.*, No. 1, 415 (1975).
- 202 Lohar, J. M. and Shah, D. S., *Mol. Cryst. Liq. Cryst.*, Vol. 28, 293 (1975).
- 203 Lohar, J. M. and Patel, G. H., *Curr. Sci.*, Vol. 44, No. 24 (1975).
- 204 Lohar, J. M. and Mashru, U., *J. Ind. Chem. Soc.*, L. VIII (1980); Lohar, J. M. and Mashru, U., *Liquid Crystal*, Editor, S. Chandrasekhar, Heyden-Verlay., 543 (1980).
- 205 Lohar, J. M. and Dave, J. S., *Mol. Cryst. Liq. Cryst.*, Vol. 103, 181 (1983).
- 206 Dave, J. S. and Menon, M. R., *J. Ind. Chem. Soc.*, Vol. 74, 809 (1997).
-

-
- 207 Dave, J. S., Menon, M. R. and Patel, P. R., *Mol. Cryst. Liq. Cryst.*, Vol. 365, 581-591 (2001).
- 208 Mahajan, R., Nandedkar, H., Vora, A. and Patel, P., *Mol. Cryst. Liq. Cryst.*, Vol. 368, 687-696 (2001).
- 209 Parmar, C. M., Dave, J. S. and Dhake, K. P., *Mol. Cryst. Liq. Cryst.*, Vol. 213, 51-56 (1992).
- 210 Lio, C. T., Wu, Z. L., Wu, N. C., Liu, T. Y., Jiang, M. H., Zou, S. F. and Lee, J. Y., *Mol. Cryst. Liq. Cryst.*, Vol. 533, 3-5 (2010).
- 211 Vora, R. A. and Dixit, N., *Mol. Cryst. Liq. Cryst.*, Vol. 104, 249-256 (1984).
- 212 Dave, J. S., Patel, P. R. and Vasanth, K. L., *Mol. Cryst. Liq. Cryst.*, Vol. 8, 93-100 (1969).
- 213 Bogojawlensky, A. D. and Winogradow. N., *Z. Phys. Chem.*, 60, 433 (1907); 64, 229(1908).
- 214 Walter, R., *Ber. Dtech. Chem. Ges.*, Vol. 58, 2303 (1925).
- 215 Dewar, M. J. S. and Goldberg, R. S., *J. Am. Chem. Soc.*, Vol. 92, 1582 (1970).
- 216 de. Kock, A.C., *Zeit. Physik. Chem.*, Vol. 48, 129 (1904).
- 217 Richter, L., Sharma, N. K., Skubatz, R., Demus, D. and Sackman, H., *Mol. Cryst.*, Vol. 80, 195-209 (1982).
- 218 Madhusudana, N. V., *Liq. Cryst.*, Vol. 36, No. 10-11, 1173-1184 (2009).
- 219 Van der Lingen, J. S., *Chem. Ber.*, Vol. 15, 913 (1913).
- 220 Huckel, B., *Phys Z.*, Vol. 22, 561 (1921).
- 221 Haldar, S., Mandal, P. K., Prathap, S. J., Row, T. N. G. and Dabrowski, R., *Mol. Cryst. Liq. Cryst.*, Vol. 503, 99-111 (2009).
- 222 Yang, I. K. and Liu, C. Y., *Mol. Cryst. Liq. Cryst.*, Vol. 503, 32-44 (2009).
- 223 Iida, A. and Takanishi, Y., *Liq. Cryst.*, Vol. 34, No. 11, 1285-1290 (2007).
- 224 Tanaka, Y., Kishi, R. and Ichijo, H., *Mol. Cryst. Liq. Cryst.*, Vol. 348, 179-186 (2000).
-

-
- 225 Cifelli, M., Domenici, V., Marini, A. and Veracini, C. A., *Liq. Cryst.*, Vol. 27, No. 11, 1473-1479 (2000).
- 226 Lippmann, H., *Ann. Physik.*, Vol. 2, 287 (1958).
- 227 Lippmann, H. and Weber, K. H., *Ann. Physik.*, Vol. 20, 265 (1957).
- 228 Saupe, A. and Englert, B., *Phys. Rev. Lett.*, Vol. 11, 462 (1963).
- 229 Sun, H., Shun, W. and Fung, B. M., *Liq. Cryst.*, Vol. 27, 1473-1479 (2000).
- 230 Khoo, I. C., Ding, J., Diaz, A., Zhang, Y. and Chen, K., *Mol. Cryst. Liq. Cryst.*, Vol. 375, 33-44 (2002).
- 231 Schafer, W., Uhlig, G., Zschke, H., Demus, D., Diele, S., Kresse, H., Ernst, S. and Welder, W., *Mol. Cryst. Liq. Cryst.*, Vol. 191, 269-276 (1990).
- 232 Dewar, M. J. S. and Schroeder, J. P., *J. Am. Chem. Soc.*, Vol. 86, 5235 (1964).
- 233 Kelker, H., Ber, Busenger, *Physik. Chem.*, Vol. 67, 698; *Z. Anal. Chem.*, Vol. 198, 254 (1963).
- 234 Taylor, P. J., and Shermann, P. L., *J. Liq. Chromatogr.*, Vol. 2, 1271 (1970).
- 235 Janini, G. M., *Adv. Chromatogr.*, Vol. 17, 231 (1979).
- 236 Witkiewicz, Z., *Prezem, Chem.*, Vol. 58, No. 8, 407 (1979).
- 237 Dunmur David, *Physical Properties of Liquid Crystals*, ed. by Demus, D., Wiley-VCH, Verlag Gmbh, Weinheim, Germany, pp. 113 (1999).
- 238 Palffy-Muhoray P., *Physical Properties of Liquid Crystals*, ed. by Demus, D., Wiley-VCH, Verlag Gmbh, Weinheim, Germany, pp. 467-479 (1999).
- 239 Demus, D., Goodby, J., Gray, G. W., *Physical Properties of Liquid Crystals*, ed. by Demus, D., Wiley-VCH, Verlag Gmbh, Weinheim, Germany, pp. 503 (1999).
- 240 Virchow, R., *Virchow's Arch. Pathol. Anat. U. Physiol*, Vol. 6, 562 (1854).
- 241 Bernal, J. D. and Faukuchen, I. J., *Gen. Phys.*, Vol. 25, 147 (1941).
- 242 Stewart, G. T., *Nature*, Vol. 183, 873 (1959).
-

-
- 243 Stewart, G. T., in *Liquid Crystals*, Brown, G. H., Dienes, G. J., Labes, M. M., *Proceedings of the International Conference on Liquid Crystals*, Kent State University, August 16-20, Gordon and Breach, Science Publishers, New York, pp. 243 (1965).
- 244 Stewart, G.T., *Liq. Cryst.*, Vol. 30, 541–557 (2003).
- 245 Hamley, I.W., *Soft Matter*, Vol. 6, 1863–1871 (2010).
- 246 Jewell, S. A., *Liq. Cryst.*, Vol. 38, 1699-1714 (2011).
- 247 Xu, X., Xu, M., Jones, O. D., Chen, X., Li, Y., Yan, G., Pan, Y., Davis, H. G., Xu, Y., Bryant, J. L., Zheng, S. and Anthony, D. D., *Mol. Cryst. Liq. Cryst.*, Vol. 547, 1854-1862 (2011).
- 248 Woltman, S.J., Jay, G.D. and Crawford, G.P., *Nat. Mater.*, Vol. 6, 929–938 (2007).
- 249 Livolant, F. *Physica A* , Vol. 176, 117–137 (1991).
- 250 Strzelecka, T.E., Davidson, M.W. and Rill, R.L., *Nature*, Vol. 331, 457–460 (1988).
- 251 Bouligand, Y. and Norris, V., *Biochimie*, Vol. 83, 187–192 (2001).
- 252 Neville, A.C. and Luke, B.M., *J. Cell Sci.*, Vol. 8, 93–109 (1971).
- 253 Knight, D.P. and Vollrath, F., *Proc. R. Soc. London, Ser. B*, Vol. 266, 519–523 (1999).
- 254 Geelhaar, T., *Liq. Cryst.*, Vol. 24, No. 1, 91 (1998).
- 255 Gray, G. W., Harrison, K. J., GB-B 1433130 (1972).
- 256 Gray, G. W., Harrison, K. J. and Nash, J. A., *Electron. Lett.*, 9 (1973).
- 257 Eidenschink, R., Krause, J. and Pohl, L., DE-B 26366844 (1976).
- 258 Eidenschink, R., Erdmann, D., Krause, J. and Pohl, L., *Angew. Chem.*, Vol. 89, 880 (1977).
- 259 Schad, H. and Osman, M. A., *J. Chem. Phys.*, Vol. 75, 880 (1981).
- 260 Kurmeier, H. A. Scheuble, B., Poetsch, E. and Finkenzeller, EP-B 0334911 (1988).
- 261 Matsumoto, T., Fukuda, A., Johno, M., Motoyama, Y., Yui, T., Seomum, S. and Yamashita, M., *J. Mater. Chem.*, Vol. 9, 2051 (1999).
-

-
- 262 Modlinska, A., Dardas, D., Jadzyn, J. and Bauman, D., *Mol. Cryst. Liq. Cryst.*, Vol. 542, 550-558 (2011).
- 263 Yang, Y.G., Chen, H., Tang, G., and Wen, J. X., *Liq. Cryst.*, Vol. 29, 255 (2002).
- 264 Takatsu, H., *Mol. Cryst. Liq. Cryst.*, Vol. 458, 17 (2006).
- 265 Czub, J., Dabrowski, R., and Urban, S., *Phase Transitions*, Vol. 80, 638 (2007).
- 266 Kim, H. S., Shin, S. H., Nam, C., Yoo, D. K., Lee, H. M., Lee, K. H. and Jun, M. C., *Mol. Cryst. Liq. Cryst.*, Vol. 550, 128-133 (2011).
- 267 Gray, G.W., *Liquid Crystals and Plastic Crystals*, Vol. 1., Gray, G. W. and Winsor, P. A., Eds., Ellis Harwood Ltd., Chichester, England, pp. 103, 116, 123, 125, 127, 130, 137, 327 (1974).
- 268 Manaranche, J. C., *J. Phys, D.*, Vol. 5, 1120-1122 (1972).
- 269 Riza, N. A. and Dejule, M. C., *Inst., Phys. Conf.*, No. 139, 231 (1995).
- 270 Sage, I., *Liquid Crystals- Applications and Uses*, Vol. 3 edited by Bahadur, B., World Scientific, Singapore, 330 (1992).
- 271 Mc. Donnell, D. G. *Thermotropic Liquid Crystals*, eds Gray, G. W., John Wiley and Sons, Chichester, pp. 130 (1987).
- 272 Janini, G. M., Johnston, K. and Zieliaski, Jr., W. L., *Anal. Chem.*, Vol. 47, 670 (1975).
- 273 Luffer, D. R., Ecking, W. and Novothy, M., *J. Chromatogr.*, Vol. 505, 79-97 (1990).
- 274 Martire, D. E., Nikolic, A. and Vasanth K.L., *J. Chromatogr.*, Vol. 178, 401 (1979).
- 275 Janini, G. M., and Ubeid, M. T., *J. Chromatogr.*, Vol. 236, 329-337 (1982).
- 276 Yan, C. and Martire, D. E., *J. Anal. Chem.*, Vol. 64, 1246 (1992).
- 277 Zieliaski, Jr., W. L., *J. Chromatogr.*, Vol. 186, 237-247 (1979).
- 278 Saupe, A., *Mol. Cryst. Liq. Cryst.*, Vol. 16, 87 (1972).
-

-
- 279 Pohl, L., *Topics in Physical Chemistry*, Vol. 3, *Liquid Crystals*: ed. Stegemeyer, H., Springer, New York, pp. 173 (1991).
- 280 Leigh, W. J., *Liquid Crystals - Applications and uses*, Vol. 2, Ed., Bahadur, B., World scientific Singapore pp. 357 (1991).
- 281 Weiss, R. G., *Photochemistry in organized and constrained Media*,: Ed. Ramamurthy, V., VCH, Weinheim, pp. 603 (1991).
- 282 Percrc, V., Jonsson, H. and Tomazas, D., *Polymer Organized Media*, Ed. Paleo, C., Gordon and Breach, Philadelphia, pp. 1 (1992).
- 283 Stephanie, K., Hiroshi, M. and Tadahiko, T., "High- Performance Fibers" in *Ullmann's Encyclopedia of Industrial Chemistry*, Wiley-VCH, Weinheim (2002).
- 284 Seed, A. J., Cross, G. J., Toyne, K. J. and Goodby, J. W., *Liq. Cryst.*, Vol. 30, No. 9, 1089-1107 (2003).
- 285 Seed, A. J., Toyne, K. J., and Goodby, J. W., *J. Mater. Chem.*, Vol. 5, 653 (1995).
- 286 Seed, A. J., Toyne, K. J., Goodby, J. W., and Hird, M., *J. Mater. Chem.*, Vol. 10, 2069 (2000).
- 287 Mori, H., Itoh, Y., Nishiura, Y., Nakamura, T., and Shinagawa, Y., *Jpn. J. Appl. Phys.*, Vol. 36, 143-147 (1997).
- 288 Sasaki, T., Ikeda, T., and Ichimura, K., *Macromolecules*, Vol. 25, 3807-3811 (1992).
- 289 Sung, J-H., Hirano, S., Tsutsumi, O., Kanazawa, A., Shiono, T., and Ikeda, T., *Chem. Mater.*, Vol. 14, 385-391 (2002).
- 290 S. Kumar, *Current Science*, Vol. 82, No. 3, 256-257 (2002).
- 291 Chandrasekhar, S. in *Hand Book of Liquid Crystals*, eds. Demus, D., Wiley-VCH, Weinheim, Vol. 2-B, Chapter VIII (1998).
- 292 Schouten, P. G., *J. Am. Chem. Soc.*, Vol. 116, 6880 (1994).
- 293 Wazynska, B., and Okowiak, J., *Tribology Letters*, Vol. 24, 1-5 (2006).
-

-
- 294 Eidenschink, R., and Hager, A. M., *Mol. Cryst. Liq. Cryst.*, Vol. 304, 513-517 (1997).
- 295 Wazynska, B., Tykarska, M. and Chinalska, J. O., *Mol. Cryst. Liq. Cryst.*, Vol. 542, 735-742 (2011).
- 296 Gray, G. W., *Molecular Structure and the Properties of Liquid Crystals*. Academic Press, London and New York (1962).
- 297 Patel, P. R. and Dave, J. S., *Liq. Cryst.*, Vol.33, No.9, 1065-1076 (2006).
- 298 Dave, J. S., Menon, M. R. and Patel, P. R., *Mol. Cryst. Liq. Cryst.*, Vol. 378, 1-11 (2002).
- 299 Thaker, B. T., Dhimar, Y. T., Patel, B. S., Solanki, D. B., Patel, N. B., Chotani, N. J. and Kanojiya, J. B., *Mol. Cryst. Liq. Cryst.*, Vol. 548, 172- 191 (2011).
- 300 Thaker, B. T., and Kanojiya, J. B., *Liq. Cryst.*, Vol. 38, No. 8, 1035- 1055 (2011).
- 301 Gray, G. W., *Liquid Crystals and Plastic Crystals*, Ellis Horwood Limited, Chichester, England, Vol. 1, p. 130-131 (1974).
- 302 Bezborodov, V. S., Perrov, V. F., *Liq. Cryst.*, Vol. 23, No. 6, 771- 788 (1997).
- 303 Bristol, D. W. and Schroeder, J. P., *J. Org. Chem.*, Vol. 39, No. 21, 3138-3141 (1974).
- 304 Vora, R. A., Prajapati, A. K., Kevat, J. B. and Raina, K. K., *Liq. Cryst.*, Vol. 28, No. 7, 983- 989 (2001).
- 305 Jadav, N. D., Prajapati, A. K. and Prajapati, B. A., *Mol. Cryst. Liq. Cryst.*, Vol. 399, 53-60 (2003).
- 306 Thaker, B. T., Patel, D. M. and Tandel, P. K., *Ind. J. Chem.*, Vol. 46-B, 1020-1024 (2007).
- 307 Vora, R. A. and Dixit, N., *Mol. Cryst. Liq. Cryst.*, Vol. 67, 193-198 (1981).
- 308 Thaker, B. T., Kanojiya, J. B. and Tandel, R. S., *Mol. Cryst. Liq. Cryst.*, Vol. 528, 120-137 (2010).
- 309 Thaker, B. T., and Tandel, P. K., *Mol. Cryst. Liq. Cryst.*, Vol. 451, 127-138 (2006).
-

-
- 310 Gray, G. W. and Jones, B., *J. Chem. Soc.*, 4179 (1953), 678, 683, 1467 (1954), 236 (1955).
- 311 Jones, B., *J. Chem. Soc.*, 1874 (1935).
- 312 Dave, J. S. and Vora, R. A., *Liquid Crystals and Ordered Fluids*, eds. Johnson, J. F. and Porter, R. S., Plenum Press, New York, pp. 477 (1970).
- 313 *Vogel's Textbook of Practical Organic Chemistry*. IVth Edn, Revised by Furniss, B. S., Hannford, A. J., Smith, P. W. G. and Tatchell, A. R., Revisors: Longman Singapore Publishers Pvt. Ltd., 563-649 (1989).
- 314 Gray, G. W., *Liquid Crystals and Plastic Crystals*, Ellis Horwood Limited, Chichester, England, Vol. 1, Chapter 4, p. 136-137 (1974).
- 315 Doshi, A. V. and Makwana, N. G., *Mol. Cryst. Liq. Cryst.*, Vol. 548, 220-227 (2011).
- 316 Doshi, A. V. and Makwana, N. G., *Der Pharma Chemica*, Vol. 3, No. 2, 433-439 (2011).
- 317 Dave, J. S., Kurian, G., Patel, N. R. and Prajapati, A. P., *Mol. Cryst. Liq. Cryst.*, Vol. 112, 311-317 (1984).
- 318 Gray, G. W., *Liquid Crystals and Plastic Crystals*, Ellis Horwood Limited, Chichester, England, Vol. 1, p. 110-111 (1974).
- 319 Nguyen, H., Zanna, T. and Duboisj, C. *Mol. Cryst. Liq. Cryst.*, Vol. 53, 43-54 (1979).
- 320 Thaker, B. T., Patel, P. H., Vansadiya, A. D. and Kanojiya, J. B., *Mol. Cryst. Liq. Cryst.*, Vol. 515, 135-147 (2009).
- 321 Chudgar, N. K. and Shah, S. N., *Liq. Cryst.*, Vol. 4, No. 6, 661-668 (1989).
- 322 Yeap, G. Y., Susanti, I., Teoh, B. S., Mahmood, W. A. K. and Harrison, W. T. A., *Mol. Cryst. Liq. Cryst.*, Vol. 442, 133-146 (2005).
- 323 Thaker, B. T., Patel, D. M., Tandel, P. K., Jesani, M. S., Vyas, C. J. and Vansadiya, A. D., *Phase Transitions*, Vol. 78, No. 6, 521-527 (2005).
- 324 Thaker, B. T., Vansadiya, A. D. and Patel, P. H., *Mol. Cryst. Liq. Cryst.*, Vol. 479, 95-110 (2007).
-

-
- 325 Vora, R. A. and Gupta, R., *Mol. Cryst. Liq. Cryst.*, Vol. 91, 45-52 (1983).
- 326 Gallardo, H. and Favarin, I., *Liq. Cryst.*, Vol. 13, No. 1, 115-125 (1993).
- 327 Petrov, V. F. and Pavluchenko, A. I., *Mol. Cryst. Liq. Cryst.*, Vol. 393, 1-13 (2003).
- 328 Gray, G. W. and Jones, B., *J. Chem. Soc.*, 1467, (1954).
- 329 Stoermer, R. and Wodarg, F., *Chem. Berg.*, 61B, 2323, (1928).
- 330 *Vogel's Textbook of Practical Organic Chemistry*. IVth Edn, Revised by Furniss, B. S., Hannford, A. J., Smith, P. W. G. and Tatchell, A.R., Revisors: Longman Singapore Publishers Pvt. Ltd., pp. 1034, (1989).
- 331 Dave, J. S. and Kurian, G., *J. of Physics*, Vol. 36, C-1, 403-407 (1975).
- 332 Gray, G. W., *Liquid Crystals and Plastic Crystals*, Ellis Horwood Limited, Chichester, England, Vol. 1, pp. 137, (1974).
- 333 Dave, J. S., Menon, M. R. and Patel, P. R., *Mol. Cryst. Liq. Cryst.*, Vol. 364, 575-587 (2001).
- 334 Essid, S., Rihab, Z. and Nguyen, H. T., *Liq. Cryst.*, Vol. 39, No. 7, 865-872 (2012).
- 335 Chudgar, N. K., Shah, S. N., *Liq. Cryst.*, Vol. 4, No. 6, 661-668 (1989).
- 336 Duan, M., Okamoto, H., Petrov, V. F. and Takenaka, S., *Mol. Cryst. Liq. Cryst.*, Vol. 326, 357-367 (1999).
- 337 Patel, R. B. and Patel, V. R., *Mol. Cryst. Liq. Cryst.*, Vol. 552, 3-9 (2012).
- 338 Thaker, B. T. and Kanojiya, J. B., *Mol. Cryst. Liq. Cryst.*, Vol. 542, 606-620 (2011).
- 339 Patel, P. R. and Dave, J. S., *Liq. Cryst.*, Vol. 33, No. 9, 1065-1076 (2006).
- 340 Dave, J. S., Menon, M. R. and Patel, P. R., *Mol. Cryst. Liq. Cryst.*, Vol. 378, 1-11 (2002).
- 341 Dave, J. S. and Dhake, K. P., *Bull. Chem. Soc. Jpn.*, Vol. 65, 559-561 (1992).
- 342 Wei, Q., Yang, H. and Wang, Y., *Mol. Cryst. Liq. Cryst.*, Vol. 487, 31-38 (2008).
-

-
- 343 Mori, A., Hashimoto, M. and Ujiie, S., *Liq. Cryst.*, Vol. 38, No. 2, 263-276 (2011).
- 344 Chauhan, B. C. and Doshi, A. V., *Mol. Cryst. Liq. Cryst.*, Vol. 552, 16-23 (2012).
- 345 Thaker, B. T., Solanki, D. B., Patel, B. S., Vansadiya, A. D. and Dhimmarr, Y. T., *Mol. Cryst. Liq. Cryst.*, Vol. 552, 134-146 (2012).
- 346 Thaker, B. T., Patel, P. H., Vansadiya, A. D. and Kanojiya, J. B., *Mol. Cryst. Liq. Cryst.*, Vol. 515, 135-147 (2009).
- 347 Vora, R. A. and Prajapati, A. K., *Mol. Cryst. Liq. Cryst.*, Vol. 332, 329-338 (1999).
- 348 Thaker, B. T., and Patel, P. H., *Mol. Cryst. Liq. Cryst.*, Vol. 509, 173-185 (2009).
- 349 Gray, G. W., *Molecular Structure and the Properties of Liquid Crystals*. Academic Press, London and New York, pp. 172-173 (1962).
- 350 Dave, J. S., Ph. D. Thesis, M. S. University of Baroda, pp. 230 (1981).
- 351 Dave, J. S., Upasani, C. B. and Patel, P. D., *Mol. Cryst. Liq. Cryst.*, Vol. 533, 73-81 (2010).
- 352 Bhoya, U. C. and Doshi, A. V., *Journal of Institution of Chemists (India)*, Vol. 72, Part 1, 15-20 (2000).
- 353 Doshi, A. V. and Ganatra, K. J., *Proc. Indian Acad. Sci. (Chem. Sci.)*, Vol. 11 I, No. 4, 563-568 (1999).
- 354 Thisayukta, J., Nakayama, Y. and Watanabe, J., *Liq. Cryst.*, Vol. 27, No. 9, 1129-1135 (2000).
- 355 Prajapati, A. K. and Modi, V., *Liq. Cryst.*, Vol. 38, No. 2, 191-199 (2011).
- 356 Archer, P. and Dierking, I., *Liq. Cryst.*, Vol. 33, No. 3, 257-265 (2006).
- 357 Reddy, R. A. and Sadashiva, B. K., *J. Mater. Chem.*, Vol. 12, 2627-2632 (2002).
- 358 Majumdar, K. C., Ghosh, T. and Chakravorty, S., *Mol. Cryst. Liq. Cryst.*, Vol. 533, 63-72 (2010).
- 359 Prajapati, A. K. and Modi, V., *Phase Transitions*, Vol. 83, 634-649 (2010).
-

-
- 360 Sadashiva, B. K., Reddy, R. A., Pratibha, R. and Madhusudana, N. V., *J. Mater. Chem.*, Vol. 12, 943-950 (2002).
- 361 Kohout, M., Savoboda, J., Novotna, V. and Pociеча, D., *Liq. Cryst.*, Vol. 38, No. 9, 1099-1110 (2011).
- 362 Matsunaga, Y., *Mol. Cryst. Liq. Cryst.*, Vol. 350, 87-92 (2000).
- 363 Matsunaga, Y. and Yuri, T., *Mol. Cryst. Liq. Cryst.*, Vol. 237, 145-150 (1993).
- 364 Mahajan, R., Nandedkar, H. and Vora, R. A., *Liq. Cryst.*, Vol. 31, No. 2, 161-167 (2004).
- 365 Kuboshita, M., Matsunaga, Y. and Miyauchi, T., *Mol. Cryst. Liq. Cryst.*, Vol. 264, 145-153 (1995).
- 366 Vorlander, D., *Z. Angew. Chem.*, Vol. 35, 249 (1922).
- 367 Dave, J. S., Menon, M. R. and Patel, P. R., *Proc. Indian. Acad. Sci.*, Vol. 114, No. 3, 213-221 (2002).
- 368 Gupta, R. and Vora, R. A., *Mol. Cryst. Liq. Cryst.*, Vol. 106, 147-159 (1984).
- 369 Vora, R. A., Gupta, R. and Patel, K., *Mol. Cryst. Liq. Cryst.*, Vol. 209, 251-263 (1991).
- 370 Prajapati, A. K., Patel, N. S. and Lad, V. G., *Mol. Cryst. Liq. Cryst.*, Vol. 348, 41-51 (2000).
- 371 Hird, M., Goodby, J. W. and Toyne, K. J., *Mol. Cryst. Liq. Cryst.*, Vol. 360, 1-15 (2001).
- 372 Hsu, E. C. H. and Johnson, J. F., *Mol. Cryst. Liq. Cryst.*, Vol. 25, 145-151 (1974).
- 373 Vora, R. A. and Rajput, S. J., *Mol. Cryst. Liq. Cryst.*, Vol. 209, 265-277 (1991).
- 374 Dave, J. S., Menon, M. R. and Patel, P. R., *Mol. Cryst. Liq. Cryst.*, Vol. 365, 581-591 (2001).
- 375 Vora, R. A. and Dixit, N., *Mol. Cryst. Liq. Cryst.*, Vol. 104, 249-256 (1984).
-

-
- 376 Doshi, A. V., Odedara, D. A. and Patel, R. B., *Mol. Cryst. Liq. Cryst.*, Vol. 552, 97-103 (2012).
- 377 Dave, J. S., Ph. D. Thesis, M. S. University of Baroda (1981)
- 378 Lohar, J. M. and Dave, J. S., *Mol. Cryst. Liq. Cryst.*, Vol. 103, 181-192 (1983).
- 379 Parmar, C. M., Dave, J. S. and Dhake, K. P., *Mol. Cryst. Liq. Cryst.*, Vol. 213, 51 (1992).
- 380 Sarkar, S. D., Chaudhury, B. and Dash, M. K., *Phase Transitions*, Vol. 85, No.1-2, 85-95 (2012).
- 381 Menon, M. R., Ph. D. Thesis, M. S. University of Baroda (1999).
- 382 Patel, P. R., Ph. D. Thesis, M. S. University of Baroda (2003).
- 383 Bertleff, V., Dissertation Halle (1908).

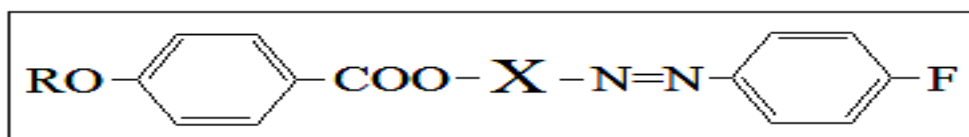
Liquid crystals are special materials in terms of their unique combination of factors namely flow properties of liquids and anisotropic properties of solids. This aspect of liquid crystals makes them intrinsically interesting and ripe for technical applications. The ever widening liquid crystal activity has given rise to wider vista of new thinking; in turn creating a necessity of continued efforts for their basic study. Consequently, drive in search of new compounds have encouraged chemists to explore structural variations in liquid crystalline compounds, both, to understand the effect of chemical constitution and for different application oriented studies.

Keeping this in view, fifteen homologous series, each comprising of twelve compounds, with special structural features have been synthesized to study the effect of structural variations on liquid crystalline properties of the mesogenic systems. The influence of different aromatic rings, central linkages, lateral and terminal substitutions has been investigated. Characterization of some of the homologues by elemental analysis, IR, NMR, Mass, UV-visible and DSC has been carried out. Transition temperatures and the textures of the mesophases are studied using Leitz Laborlux 12 POL polarizing microscope fitted with a Kofler heating stage.

Mesogenic homologous series having terminal fluoro group

A number of homologous series with ester and azo central linkages have been synthesized having different terminal groups. Introduction of lateral substitution makes molecules broad and plays an effective role in variation in mesogenic properties of mesogenic compounds. Similarly introduction of naphthalene ring in mesogenic homologues also makes molecules broad and plays an important role in variation in their mesomorphic properties.

Five homologous series having ester and azo central linkages with different lateral substituents and one series having central naphthalene moiety with terminal fluoro group are synthesized to investigate the effect of lateral substituents and central naphthalene moiety on fluoro liquid crystalline compounds (figure 1).



Where, R is C_nH_{2n+1} , $n=1$ to 8, 10, 12, 14, 16

Series	I	II	III	IV	V	VI
X						

Figure 1

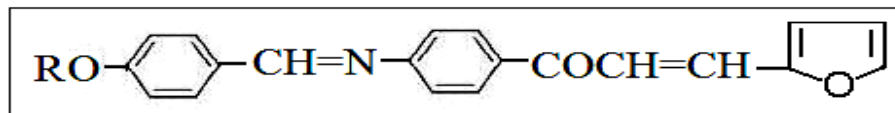
- I** 4-(4'-n-alkoxybenzoyloxy)phenylazo-4''-fluorobenzenes
II 4-(4'-n-alkoxybenzoyloxy)3-chlorophenylazo-4''-fluorobenzenes
III 4-(4'-n-alkoxybenzoyloxy)3-methylphenylazo-4''-fluorobenzenes
IV 4-(4'-n-alkoxybenzoyloxy)2-chlorophenylazo-4''-fluorobenzenes
V 4-(4'-n-alkoxybenzoyloxy)2-methylphenylazo-4''-fluorobenzenes
VI 4-(4'-n-alkoxybenzoyloxy)naphthylazo-4''-fluorobenzenes

All the twelve homologues of each of these series are mesogenic in nature. Series I to IV show both smectic C and nematic phase while series V and VI show only nematic phase. Smectic phase of series I to IV shows schlieren texture of the smectic C variety. Nematic phase of series I to V shows marble texture whereas that of series VI shows schlieren texture.

Mesogens having heterocyclic furfural moiety and chalcone as one of the central linkages

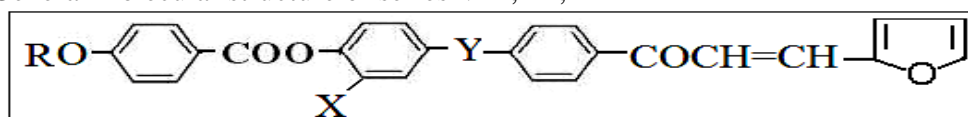
It has been observed that chalcone central linkage is comparatively less conducive to mesomorphism as compared to azomethine, azo and ester central linkages due to the non linearity and angle strain arising from the keto group; however, when chalcone linkage is present with other central linkages it becomes conducive to mesomorphism. Liquid crystalline derivatives having heterocyclic moieties with chalcone as one of the central linkages are comparatively less explored. In view of this four homologous series (VII to X) are synthesized consisting of furfural moiety and chalcone as one of the central linkages along with other central linkages. Molecular structures of the homologous series (VII to X) are given in figure 2.

General molecular structure of series VII



Where, R is C_nH_{2n+1} , $n=1$ to 8, 10, 12, 14, 16

General molecular structure of series VIII, IX, X



Where, R is C_nH_{2n+1} , $n=1$ to 8, 10, 12, 14, 16

Series	X	Y
VIII	-H	-CH=N-
IX	-OCH ₃	-CH=N-
X	-H	-C=N- CH ₃

Figure 2

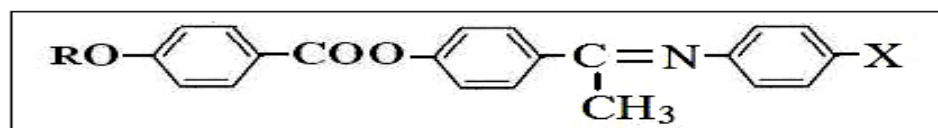
- VII** 1-(4-(4'-n-alkoxybenzylideneamino)phenyl)-3-(furan-2-yl)-prop-2-en-1-ones
- VIII** 1-(4-(4'-(4''-n-alkoxybenzoyloxy)benzylideneamino)-phenyl)-3-(furan-2-yl)-prop-2-en-1-ones
- IX** 1-(4-(4'-(4''-n-alkoxybenzoyloxy)2'-methoxybenzylideneamino)-phenyl)-3-(furan-2-yl)-prop-2-en-1-ones
- X** 1-(4-(4'-(4''-n-alkoxybenzoyloxy)phenylethylideneamino)-phenyl)-3-(furan-2-yl)-prop-2-en-1-ones

First three members of series VII are non-mesogenic in nature whereas C_4 to C_{16} members are monotropic nematogens. All the twelve homologues of series VIII and IX are mesogens. Series VIII shows both nematic and smectic mesophases while series IX exhibits only nematic mesophase. First three members of series X are non-mesogens, C_4 to C_5 members are monotropic nematogens whereas C_6 to C_{16} members are nematogens. Nematic phase of series shows threaded/ marble texture whereas smectic mesophase of series shows schliere texture of smectic C variety.

Mesogenic homologous series having ester and ethylideneamino central linkages

Liquid crystalline compounds with different central linkages and terminal groups are known; however, mesogens having ethylideneamino central linkage are comparatively less explored. Three new homologous series (XI-XIII) with ester and ethylideneamino central linkages and fluoro, chloro and methyl terminal groups respectively are synthesised (figure 3) and their mesomorphic properties are studied.

General molecular structure of series XI-XIII



Where, R is C_nH_{2n+1} , $n=1$ to 8, 10, 12, 14, 16 $X= -F, -Cl, -CH_3$

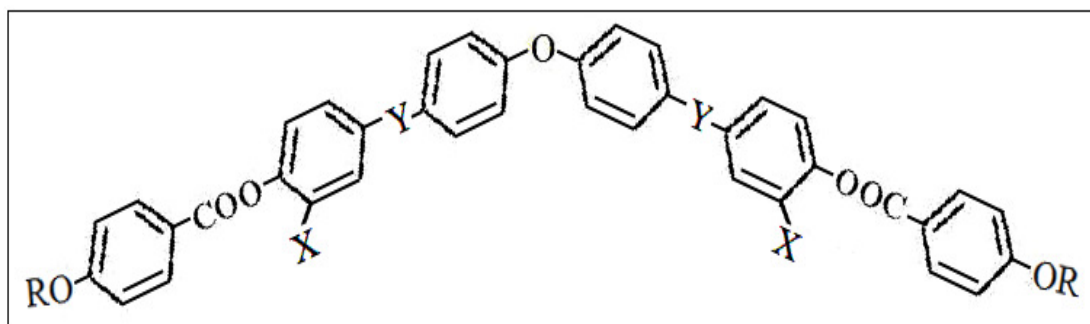
Figure 3

- XI** 4-(4'-n-alkoxybenzoyloxy)phenylethylidene-4''-fluoroanilines
- XII** 4-(4'-n-alkoxybenzoyloxy)phenylethylidene-4''-chloroanilines
- XIII** 4-(4'-n-alkoxybenzoyloxy)phenylethylidene-4''-toluidines

All the twelve homologues of each of the series are mesogenic in nature. Series XI and XII show both the smectic and nematic phase, whereas all the derivatives of series XIII are nematogenic in nature. The nematic phase of all the series show threaded texture, whereas smectic phase shows focal conic fan shaped texture of smectic A variety.

Bent-shaped mesogens derived from Diphenylether moiety

Since chemical structure has been understood to have most significant effect on the mesophase formed by liquid crystalline compounds. It is observed that a molecule which possesses a linear structure along with two or more phenyl rings linked via stable central linkages seems to have an advantage in the formation of mesophases. However, quite a good number of novel compounds with non-linear structures having bent core have been found exhibiting liquid crystalline behavior. In view of this two new homologous series with bent core are synthesized and their mesomorphic properties are studied (figure 4).



Where, R is C_nH_{2n+1} , $n=1$ to 8, 10, 12, 14, 16

Series	X	Y
XIV	$-OCH_3$	$-CH=N-$
XV	$-H$	$\begin{array}{c} -C=N- \\ \\ CH_3 \end{array}$

Figure 4

XIV 4,4'-Bis-[4''-(4'''-n-alkoxybenzoyloxy)3''-methoxybenzylideneamino]-diphenylethers

XV 4,4'-Bis-[4''-(4'''-n-alkoxybenzoyloxy)phenylethylideneamino]-diphenylethers

All the twelve homologues of both the series (XIV and XV) are mesogenic in nature and exhibit only nematic mesophase. Nematic phase of the series shows marble texture. The effects of lateral methoxy group and central linkages on mesomorphism are studied.

Mixed mesomorphism

Binary mixtures are necessary to lower the transition temperatures, broaden the available temperature range of mesophases and tailor the physical properties to find their possible applications. In the present investigation, ten binary systems of structurally dissimilar components are studied (figure 5) to evaluate the effect on mixed mesomorphism due to the variations in the structural characteristics of the components.

The components of the binary systems taken are:

A1 4-(4'-n-butyloxybenzoyloxy)benzaldehyde (BBB)

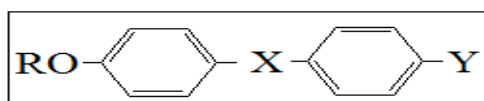
A2 4-methoxybenzylidene-4'-chloroaniline (MBCA)

A3 4-methoxybenzylidene-4'-toluidine (MBT)

A4 4-(4'-n-dodecyloxybenzoyloxy)naphthylazo-4''-fluorobenzene (DNFB)

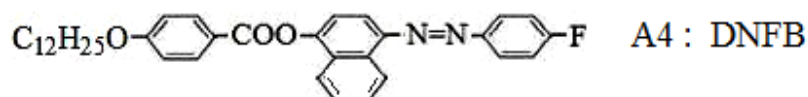
- B1** 4-(4'-n-butyloxybenzoyloxy)phenylazo-4''-fluorobenzene (BPFB)
B2 4-(4'-n-butyloxybenzoyloxy)benzylidene-4''-fluoroaniline (BBFA)
B3 4-(4'-n-heptyloxybenzoyloxy)phenylazo-4''-fluorobenzene (HPFB)
B4 4-(4'-methoxybenzoyloxy)benzylidene-2''-aminopyridine (MBAP)

General molecular structure of component A1 to A3

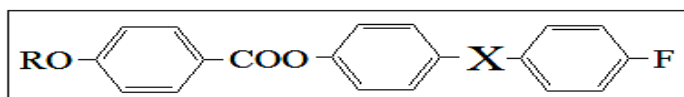


- Where, R is C_nH_{2n+1}
- A1 : BBB; $n=4$, X= -COO-, Y= -CHO
 A2 : MBCA; $n=1$, X= -CH=N-, Y= -Cl
 A3 : MBT; $n=1$, X= -CH=N-, Y= -CH₃

Molecular structure of component A4



General molecular structure of component B1 to B4



- Where, R is C_nH_{2n+1}
- B1 : BPFB; $n=4$, X= -N=N-
 B2 : BBFA; $n=4$, X= -CH=N-
 B3 : HPFB; $n=7$, X= -N=N-

Molecular structure of component B4

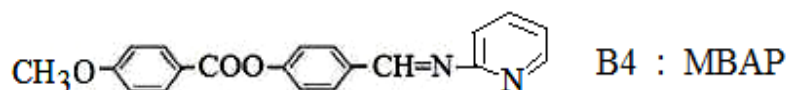


Figure 5

The binary systems studied are:

Type 1

Binary System	First Component	Second Component
I	A1 (BBB)	B1 (BPFB)
II	A1 (BBB)	B2 (BBFA)
III	A2 (MBCA)	B2 (BBFA)
IV	A2 (MBCA)	B3 (HPFB)
V	A3 (MBT)	B2 (BBFA)
VI	A3 (MBT)	B3 (HPFB)

Type 2

Binary System	First Component	Second Component
VII	A4 (DNFB)	B1 (BPFB)
VIII	A4 (DNFB)	B2 (BBFA)

Type 3

Binary System	First Component	Second Component
IX	A2 (MBCA)	B4 (MBAP)
X	A3 (MBT)	B4 (MBAP)

As the molecular geometry of the components in the mixtures differ, the N-I transition curves deviate from the linear nature. In the binary systems with the non-mesogen as one of the components, the nematic phase emerges either in monotropic or enantiotropic form with the addition of as low as 10 to 20 mole% of the non-mesogenic component in the mixture. It is observed that all the binary mixtures exhibit good mixed mesophase range which is more than the mesophase range of individual components. Some of the mixtures show supercooling below 45° C.

The present studies have provided host of novel liquid crystalline compounds with different molecular structures and vast variations in their mesomorphic properties. The study of binary mixtures with structurally dissimilar mesogens also throws immense light on mixed mesomorphism and their potential for applications in nonlinear optics and electro-optic display devices.

List of Presentation

1. **“Synthesis and Mesomorphic Characteristics of a New Mesogenic Homologous Series with terminal Fluoro group”** presented at National Conference on Green Chemistry, 6th – 8th February, 2009 at Department of Chemistry, Veer Narmad South Gujarat University, Surat.
2. **“Synthesis and Mesomorphic Characteristics of Mesogens with lateral Chloro group”** presented at 16th National Conference on Liquid Crystals, 26th - 28th October, 2009 at University of Lucknow, Lucknow.
3. **“Synthesis and Mesomorphic Characteristics of Mesogens with lateral Methyl group”** presented at Sixth All Gujarat Research Scholars’ Meet, 31st January, 2010 at Department of Chemistry, Faculty of Science, M.S.University of Baroda, Vadodara.
4. **“Synthesis and Mesomorphic Characteristics of Furfural derivatives with central chalcone and azomethane linkages”** presented at XXIV- Gujarat Science Congress 2010, 21st March, 2010 at Gujarat University, Ahmedabad.
5. **“Mesogenic azo esters with terminal fluoro and lateral chloro group”** presented at 17th National Conference on Liquid Crystals, 15th - 17th November, 2010 at Department of Chemistry, Veer Narmad South Gujarat University, Surat.
6. **“Synthesis and Mesomorphic Characteristics of fluoro aniline derivatives with different lateral groups”** presented at Soft Matter Chemistry Workshop, 9th-11th November, 2011 at Raman Research Institute, Bangalore.
7. **“Mesomorphic characterization of naphthyl azo-esters with terminal fluoro group”** presented at Regional Science Congress, September 15th-16th, 2012 at The M. S. University of Baroda, Vadodara.

Special Achievement**First Prize Winner**

“Synthesis and Mesomorphic Characteristics of Mesogens with lateral Methyl group” presented at Sixth All Gujarat Research Scholars’ Meet, 31st January, 2010 at Department of Chemistry, Faculty of Science, M.S.University of Baroda, Vadodara.

Research Publications

1. **“Effect of lateral substitution on mesogenic properties of fluoroaniline derivatives”** Jayrang S. Dave, C. B. Upasani and Purvang D. Patel, Journal of Molecular Crystals Liquid Crystals (Taylor & Francis), Vol. 533, pp. 73-81 (2010).
2. **“Synthesis and mesomorphic characteristics of fluoroaniline Derivatives with different lateral groups”** Jayrang S. Dave, Purvang D. Patel and Himanshu S. Bhatt, Journal of Molecular Crystals Liquid Crystals (Taylor & Francis), Vol. 562, pp. 76-84 (2012).
3. **“Liquid crystalline behavior of binary mixtures of structurally dissimilar mesogens and non-mesogens”** Jayrang S. Dave, Purvang D. Patel and Himanshu S. Bhatt (Communicated for publication).

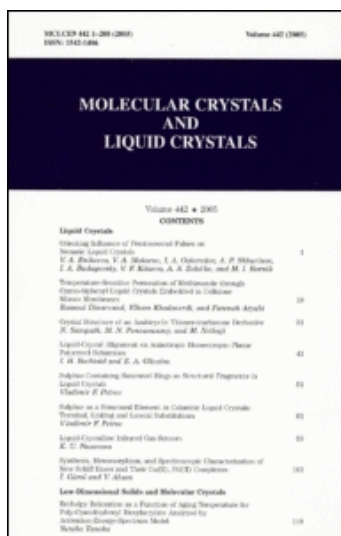
This article was downloaded by: [INFLIBNET India Order]

On: 15 December 2010

Access details: Access Details: [subscription number 920455929]

Publisher Taylor & Francis

Informa Ltd Registered in England and Wales Registered Number: 1072954 Registered office: Mortimer House, 37-41 Mortimer Street, London W1T 3JH, UK



Molecular Crystals and Liquid Crystals

Publication details, including instructions for authors and subscription information:

<http://www.informaworld.com/smpp/title~content=t713644168>

Effect of Lateral Substitution on Mesogenic Properties of Fluoro Aniline Derivatives

Jayrang S. Dave^a; C. B. Upasani^b; Purvang D. Patel^b

^a Applied Chemistry Department, Faculty of Technology and Engineering, The M.S. University of Baroda, Gujarat, India ^b Jyoti Om Chemical Research Centre Pvt. Ltd., Gujarat, India

First published on: 14 December 2010

To cite this Article Dave, Jayrang S. , Upasani, C. B. and Patel, Purvang D.(2010) 'Effect of Lateral Substitution on Mesogenic Properties of Fluoro Aniline Derivatives', *Molecular Crystals and Liquid Crystals*, 533: 1, 73 – 81

To link to this Article: DOI: 10.1080/15421406.2010.526455

URL: <http://dx.doi.org/10.1080/15421406.2010.526455>

PLEASE SCROLL DOWN FOR ARTICLE

Full terms and conditions of use: <http://www.informaworld.com/terms-and-conditions-of-access.pdf>

This article may be used for research, teaching and private study purposes. Any substantial or systematic reproduction, re-distribution, re-selling, loan or sub-licensing, systematic supply or distribution in any form to anyone is expressly forbidden.

The publisher does not give any warranty express or implied or make any representation that the contents will be complete or accurate or up to date. The accuracy of any instructions, formulae and drug doses should be independently verified with primary sources. The publisher shall not be liable for any loss, actions, claims, proceedings, demand or costs or damages whatsoever or howsoever caused arising directly or indirectly in connection with or arising out of the use of this material.

Effect of Lateral Substitution on Mesogenic Properties of Fluoro Aniline Derivatives

JAYRANG S. DAVE,¹ C. B. UPASANI,² AND
PURVANG D. PATEL²

¹Applied Chemistry Department, Faculty of Technology and Engineering, The M.S. University of Baroda, Gujarat, India

²Jyoti Om Chemical Research Centre Pvt. Ltd., Gujarat, India

Three new homologous series of liquid crystals with terminal fluoro group and central linkages such as ester and azo groups were synthesized and their mesomorphic properties were studied. All three series are similar in molecular structure with the difference in their lateral substitutions: series I has no lateral substitution, series II has a chloro group as lateral substitution, and series III has a methyl group as lateral substitution. All 12 homologues of each of the series are mesogenic in nature. The nematic phase of the series shows a marble texture and the smectic phase shows a Schlieren texture of the smectic C variety. The mesomorphic characteristics of the series are compared with each other.

Keywords Azo ester; chloro and methyl groups; homologues; lateral substituents; mesophase range; smectic C and nematic mesophase

Introduction

Generally, liquid-crystalline compounds are rod-like molecules with stable central linkages [1–6]. Lateral substitution makes molecules broad; lateral substituents play an effective role in mesogenic properties of a mesogenic compound. Studies on the effect of lateral substitution have been carried out by several researchers. A survey of the literature indicates that generally the mesophase range of mesogens with lateral substituent is less than that for laterally unsubstituted mesogens [7–18]. Thus, in order to study the correlation between chemical constitution and mesomorphism, three new homologous series with ester and azo central linkages, a fluoro terminal group, and chloro and methyl lateral groups were synthesized and their mesomorphic properties were studied.

Experimental

4-Hydroxy benzoic acid, the appropriate n-alkyl halides, p-fluoro aniline, phenol, o-chloro phenol, and o-cresol were used as received. Solvents were dried and distilled

Address correspondence to Jayrang S. Dave, Applied Chemistry Department, Faculty of Technology and Engineering, The M.S. University of Baroda, Vadodara 390 001, Gujarat, India. E-mail: jayrangdave@yahoo.com

prior to use. Microanalyses of some of the representative compounds were performed on a Perkin Elmer Series II 2400-CHN analyzer; infrared (IR) spectra were recorded on a Perkin Elmer GX-FTIR, and nuclear magnetic resonance (NMR) spectra were measured on a Bruker Avance II-500 spectrometer. Liquid-crystalline properties were investigated on a Leitz Laborlux 12 POL polarizing microscope provided with a Kofler heating stage. Differential scanning calorimetry (DSC) was performed on a Mettler Toledo Star SW 7.01.

1. 4-n-Alkoxy benzoic acids and 4-n-alkoxy benzoyl chlorides were synthesized by the modified method of Dave and Vora [19].
2. 4-Hydroxyphenylazo-4'-fluoro benzene, 3-chloro-4-hydroxyphenylazo-4'-fluoro benzene, and 3-methyl-4-hydroxyphenylazo-4'-fluoro benzene were prepared by a known method [20].
3. The series, namely 4-(4'-n-alkoxybenzoyloxy)-phenylazo-4''-fluorobenzenes, 4-(4'-n-alkoxybenzoyloxy)-3-chlorophenylazo-4''-fluorobenzenes, and 4-(4'-n-alkoxybenzoyloxy)-3-methylphenylazo-4''-fluorobenzenes were synthesized by adding dropwise a cold solution of 4-hydroxy phenylazo-4'-fluorobenzene (for series I), 3-chloro-4-hydroxyphenylazo-4'-fluorobenzene (for series II), and 3-methyl-4-hydroxyphenylazo-4'-fluoro benzene (for series III), respectively, in dry pyridine to a cold solution of 4-n-alkoxy benzoyl chloride. The mixture was allowed to stand overnight at room temperature. It was acidified with 1:1 cold HCl and the separated solid was filtered and recrystallized from ethanol until constant transition temperatures were obtained. These are recorded in Table 1. The elemental analysis of all the compounds was found to be satisfactory (Table 2). The synthetic route of the series is shown in Scheme 1.

Fourier Transform Infrared (Nujol, KBr Pellets, Cm^{-1})

Series I: 4-(4'-n-butyloxybenzoyloxy)phenylazo-4''-fluorobenzenes: 2,937, 1,729 (-COO-), 1,073 (-C-F), 1,597 (-N=N-), 1,496, 1,389, 1,258, 1,169, 1,073, 969, 843, 761, 692.

$^1\text{H NMR}$: (CDCl_3 , 200 MHz, δ , ppm, Standard Trimethyl Sulfoxane)

Series I: 4-(4'-n-butyloxybenzoyloxy)phenylazo-4''-fluorobenzenes: δ 1.0 (3H, t, -CH₃), 1.4–1.79 (m, alkyl chain), 4.05 (2H, t, -OCH₂-CH₂), 6.98 (2H, d, H⁵), 7.02 (2H, d, H⁴), 7.36 (2H, d, H²), 7.9 (2H, d, H⁶), 8.0 (2H, d, H¹), 8.1 (2H, d, H³).

Fourier Transform, Infrared (Nujol, KBr Pellets, Cm^{-1})

Series II: 4-(4'-n-octyloxybenzoyloxy)3-chlorophenylazo-4''-fluorobenzenes: 2,944, 1,731 (-COO-), 1,066 (-C-F), 1,606 (-N=N-), 850 (-C-Cl), 1,504, 1,420, 1,319, 1,264, 1,041, 953, 839, 755, 689.

$^1\text{H NMR}$: (CDCl_3 , 200 MHz, δ , ppm, Standard Trimethyl Sulfoxane)

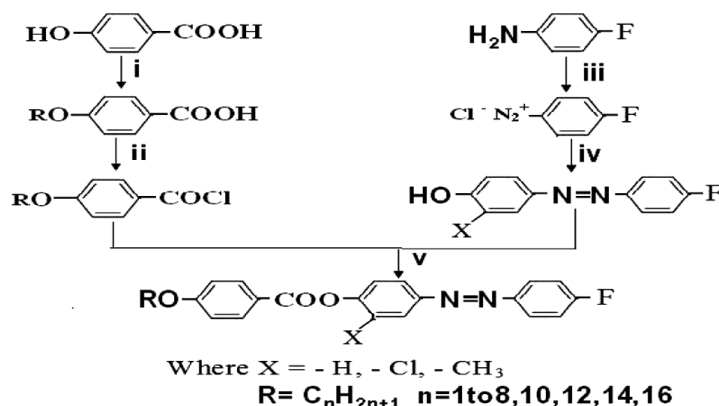
Series II: 4-(4'-n-octyloxybenzoyloxy)3-chlorophenylazo-4''-fluorobenzenes : δ 0.9 (3H, t, -CH₃), 1.4–1.79 (m, alkyl chain), 4.05 (2H, t, -OCH₂-CH₂), 6.98 (2H, d, H⁴), 7.0 (2H, d, H⁵), 7.36 (2H, d, H²), 7.9 (2H, d, H⁶), 8.0 (2H, d, H¹), 8.1 (2H, d, H³).

Table 1. Transition Temperature °C of the Present Series I, II, and III

R=n-alkyl group	Transition temperatures °C		
	Smectic C	Nematic	Isotropic
(Series I) 4-(4'-n-alkoxybenzoyloxy)-phenylazo-4''- fluorobenzenes			
Methyl	—	130	206
Ethyl	—	122	208
Propyl	—	115	205
Butyl	—	110	209
Pentyl	—	100	198
Hexyl	—	91	194
Heptyl	—	83	182
Octyl	85	93	164
Decyl	89	110	142
Dodecyl	93	—	131
Tetradecyl	04	—	126
Hexadecyl	109	—	124
(Series II) 4-(4'-n-alkoxybenzoyloxy)-3-chlorophenylazo-4''-fluorobenzenes			
Methyl	—	121	159
Ethyl	—	113	167
Propyl	—	105	163
Butyl	—	95	156
Pentyl	—	89	150
Hexyl	—	85	146
Heptyl	—	80	139
Octyl	—	77	126
Decyl	—	75	119
Dodecyl	83	93	113
Tetradecyl	92	—	110
Hexadecyl	96	—	108
(Series III) 4-(4'-n-alkoxybenzoyloxy)-3-methylphenylazo-4''-fluorobenzenes			
Methyl	—	113	148
Ethyl	—	109	139
Propyl	—	100	133
Butyl	—	90	128
Pentyl	—	84	125
Hexyl	—	78	116
Heptyl	—	73	109
Octyl	—	69	103
Decyl	—	72	98
Dodecyl	—	78	96
Tetradecyl	81	85	93
Hexadecyl	86	—	91

Table 2. Elemental Analysis

Series	Homologue	Calculated			Found		
		C (%)	H (%)	N (%)	C (%)	H (%)	N (%)
I	C4	70.40	5.35	7.14	70.24	5.29	7.18
II	C8	67.15	5.80	5.80	67.02	5.66	5.72
III	C6	71.88	6.22	6.45	71.60	5.46	6.31



- (i) Alcohol, KOH, R-Br (ii) SOCl₂ (iii) HCl, NaNO₂, 0^o-5^oC
(iv) Phenol or 2-chloro phenol or o-cresol, aq. NaOH, 0^o-10^oC
(v) Dry pyridine, 1:1 HCl

Scheme 1. Synthetic route for series I, II and III.

Fourier Transform Infrared (Nujol, KBr Pellets, Cm⁻¹)

Series III: 4-(4'-n-hexyloxybenzoyloxy)3-methylphenylazo-4''-fluorobenzenes: 2,946, 1,729 (-COO-), 1,065 (-C-F), 1,603 (-N=N-), 1,317 (-C-CH₃), 1,498, 1,317, 1,260, 1,096, 842, 724, 689, 615.

¹H NMR: (CDCl₃, 200 MHz, δ, ppm, Standard Trimethyl Sulfoxane)

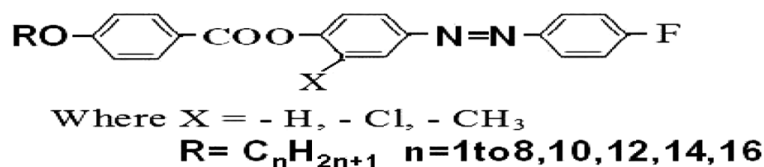
Series III: 4-(4'-n-hexyloxybenzoyloxy)3-methylphenylazo-4''-fluorobenzenes : δ 0.9 (3H, t, -CH₃), 1.3–1.8 (m, alkyl chain), 4.0 (2H, t, -OCH₂-CH₂), 6.98 (2H, d, H⁴), 7.0 (2H, d, H⁵), 7.30 (2H, d, H²), 7.9 (2H, d, H⁶), 8.1 (2H, d, H¹), 8.2 (2H, d, H³).

Results and Discussion

In the present study, 12 homologues from each of the three series, 4-(4'-n-alkoxy benzoyloxy)-phenylazo-4''-fluorobenzenes (series I), 4-(4'-n-alkoxy benzoyloxy)-3-chlorophenylazo-4''-fluorobenzenes (series II), and 4-(4'-n-alkoxy benzoyloxy)-3-methylphenylazo-4''-fluorobenzenes (series III), were synthesized and their mesomorphic properties were studied.

The general molecular structure of the series is shown in Scheme 2.

All 12 homologues of series I are mesogens; the nematic phase commences from the first derivative and remains up to the decyl derivative, whereas the smectic C



Scheme 2. General molecular structure of series I, II and III.

phase commences from the octyl derivative and remains to be exhibited up to the last hexadecyl derivative synthesized. Figure 1 shows the plot of transition temperatures against number of carbon atoms in the alkoxy chain; it indicates that N-I curve shows overall falling tendency with a slight increase at the fourth derivative and merges with the falling S-I curve as the series is ascended. No odd-even effect is observed in the N-I curves or S-I curves. The Cr-M transitions show a falling tendency from the methyl to heptyl derivative and then a rising tendency from the octyl derivative to hexadecyl derivative. The nematic phase of the series shows a marble texture and the smectic phase shows a Schlieren texture of the smectic C variety.

All 12 homologues of series II are mesogens; the nematic phase commences from the first derivative and remains up to the dodecyl derivative, whereas the smectic C phase commences from the dodecyl derivative and remains to be exhibited up to the last hexadecyl derivative synthesized. Figure 2, that is, the plot of transition temperatures against number of carbon atoms in the alkoxy chain, indicates that the N-I curve shows an overall falling tendency with a slight increase at the second derivative and merges with the falling S-I curve as the series is ascended.

Here no odd-even effect is observed in the N-I curves or S-I curves. The Cr-M transitions show a falling tendency from the methyl to decyl derivative and a rising tendency from the dodecyl derivative to hexadecyl derivative. Here, too, the nematic phase of the series shows a marble texture and the smectic phase shows a Schlieren texture of the smectic C variety.

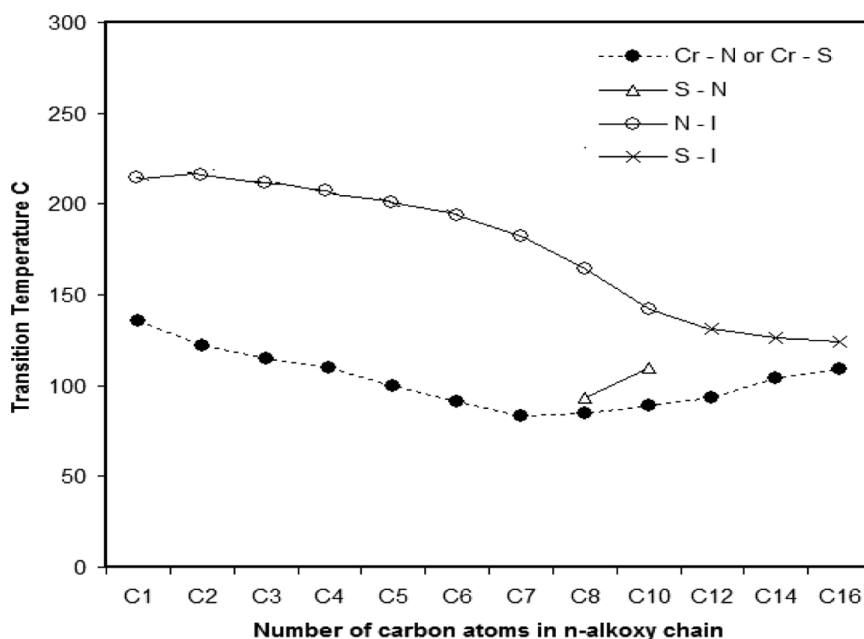


Figure 1. 4-(4'-n-Alkoxybenzoyloxy) phenylazo-4''-fluorobenzenes (series I).

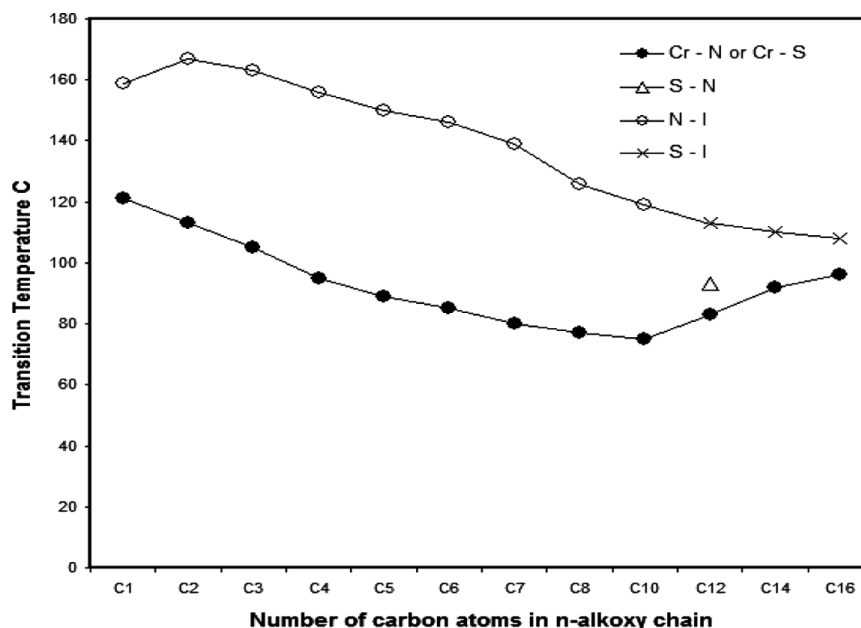


Figure 2. 4-(4'-n-Alkoxybenzoyloxy)-3chloro phenylazo-4''-fluorobenzenes (series II).

All 12 homologues of series III are mesogens; the nematic phase commences from the first derivative and remains up to the tetradecyl derivative, whereas the smectic C phase commences from the tetradecyl derivative and remains to be exhibited up to the last hexadecyl derivative synthesized. Figure 3, that is, the plot of transition temperatures against number of carbon atoms in the alkoxy chain, indicates that the N-I curve shows an overall falling tendency with a slight increase at the fifth derivative and merges with a falling S-I curve as the series is ascended.

No odd-even effect is observed in the N-I curve or S-I curves. The Cr-M transitions show a falling tendency from the methyl to dodecyl derivative and a rising

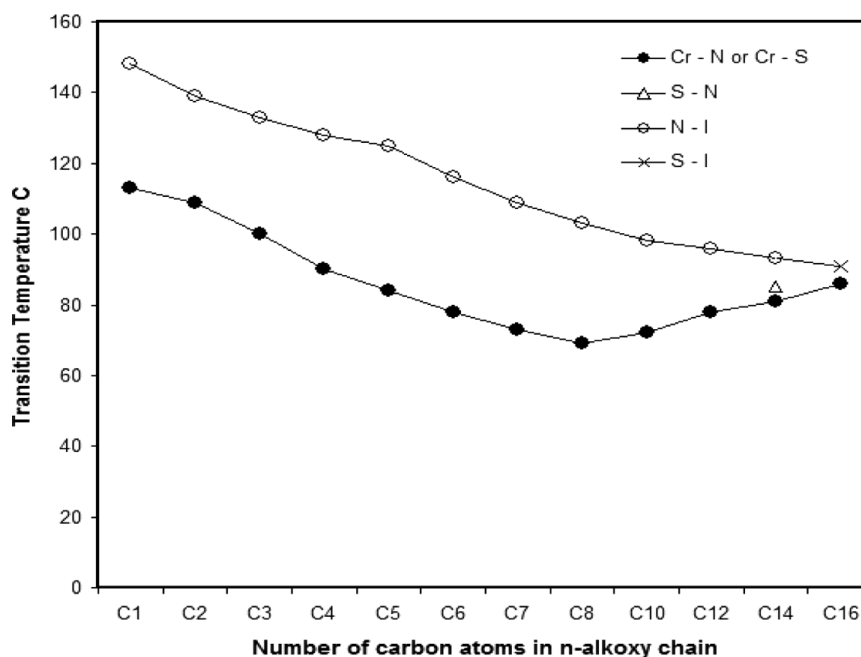


Figure 3. 4-(4-n-Alkoxybenzoyloxy)-3methyl phenylazo-4''-fluorobenzenes (series III).

Table 3. Average Mesophase Range °C

Series	Nematic	Smectic	Commencement of smectic mesophase
I	189.7 (C ₁ to C ₁₀)	116.8 (C ₈ to C ₁₆)	C ₈
II	143.8 (C ₁ to C ₁₂)	103.66 (C ₁₂ to C ₁₆)	C ₁₂
III	117.09 (C ₁ to C ₁₄)	88 (C ₁₄ to C ₁₆)	C ₁₄

tendency from the dectyl derivative to hexadecyl derivative. Like the other two series, here also the nematic phase of the series shows a marble texture and the smectic phase shows a schlieren texture of smectic C variety.

The average nematic mesophase range of series I is 189.7°C, series II is 143.8°C, and series III is 117.09 °C, similarly the average smectic mesophase range of series I is 116.8°C, that of series II is 103.6°C, and series III is 88°C. Comparison of average mesophase range of all three series (Table 3) shows that both the nematic and smectic mesophase range of series II and series III are lower than those of series I. Here, the nature of lateral substituents has important implications on phase transition temperatures and average mesophase range. The effect of the lateral group in the central benzene ring causes disruption in the molecular packing, which reduces the transition temperatures and melting points as well as the mesophase range compared to the laterally unsubstituted analogues. The introduction of a chloro group (series II) and a methyl group (series III) in the ortho position of the ester linkage of series I effectively reduced both the clearing and melting points compared to those of the parent compound (series I). The commencement of the smectic mesophase is late in series II and series III compared to series I, which is due to the non-coplanarity caused by the molecules. Series II and series III both are laterally substituted in comparison with series I; the breadth of the molecules of series II and III is increased due to the presence of a lateral group on the central benzene ring, which decreases both smectic and nematic thermal stabilities [21]. The difference in commencement of mesophase type is only because of the different nature of the lateral substitution. The smectic tendency of the molecule is less effected by the chloro group than the methyl group [21]. The enthalpies of the butyl derivative of series I, octyl derivative of series II, and hexyl derivative of series III were measured by DSC. The data are shown in Table 4 and Fig. 4 shows the DSC curves of the C4 homologue of series I, the C8 homologue of series II, and the C6 homologue of series III.

Table 4. DSC Data

Series	Member	Heating rate (°C min ⁻¹)	Transition temperature	Δ (H/Jg ⁻¹)	Δ (S/Jg ⁻¹ K ⁻¹)
I	Butyl	5	Cr-N 110	61.49	0.160
			N-I 211	2.73	0.0066
II	Octyl	5	Cr-N 77	83.00	0.237
			N-I 126	1.65	0.0041
III	Hexyl	5	Cr-N 78	72.77	0.207
			N-I 116	0.92	0.0023

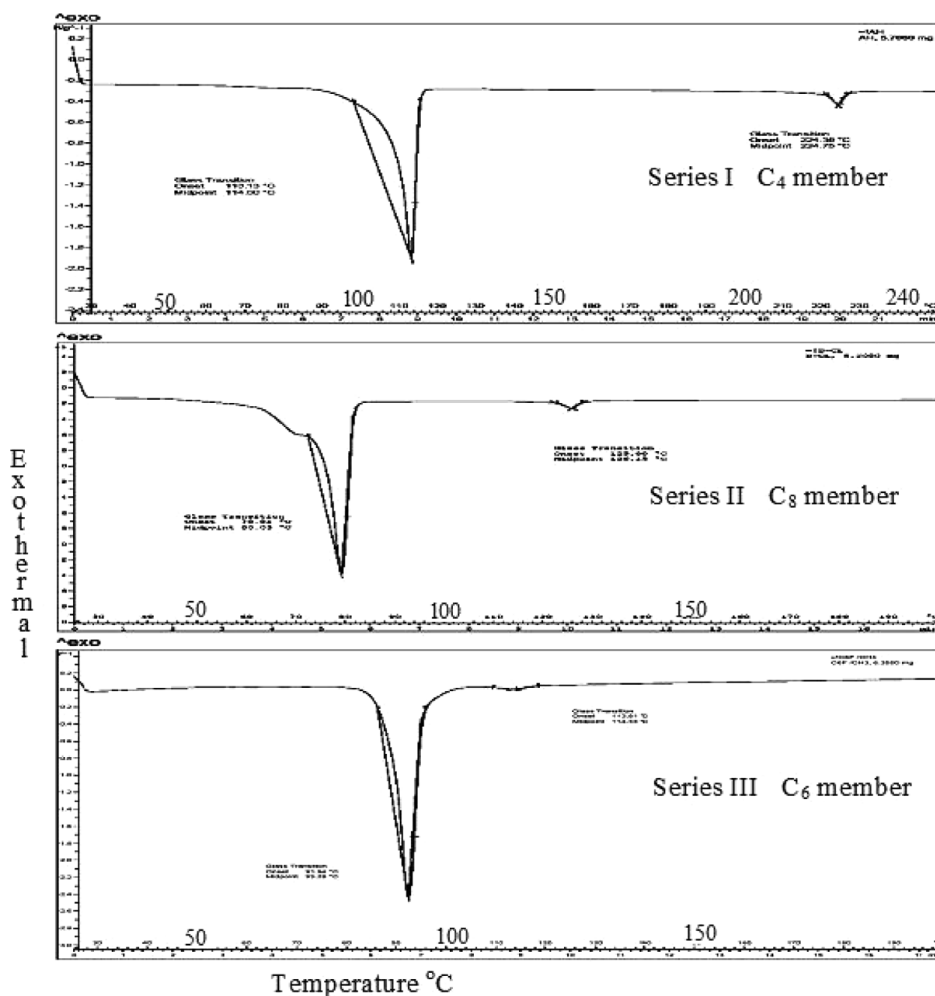


Figure 4. DSC curves.

Conclusion

The effect of $-Cl$ and $-CH_3$ lateral substituents on phase behavior, and phase transition temperatures was studied. These lateral substituents depress both melting point and clearing points of the liquid crystals. Mesogens with an ortho lateral substitution have a reduced smectic and nematic mesophase range compared to the corresponding unsubstituted homologues.

Acknowledgment

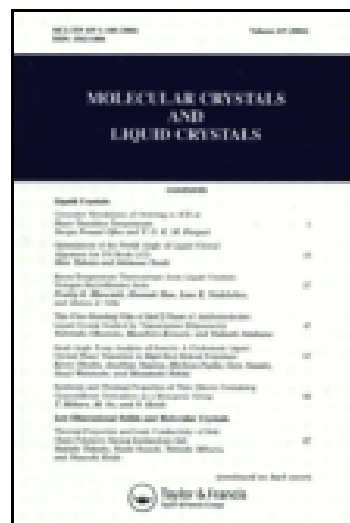
The authors thank the Head of Applied Chemistry Department, Faculty of Technology and Engineering, the M.S. University of Baroda, Vadodara, for providing us with the use of a polarizing optical microscope. We also thank Jyoti Om Chemical Research Centre Pvt. Ltd., Ankleshwar, for providing laboratory facilities.

References

- [1] Gray, G. W. (1962) *Molecular Structure and the Properties of Liquid Crystals*, Academic Press: London and New York.

- [2] Patel, P. R., & Dave, J. S. (2006). *Liq. Cryst.*, 33(9), 1065–1076.
- [3] Dave, J. S., Menon, M. R., & Patel, P. R. (2002). *Mol. Cryst. Liq. Cryst.*, 378, 1–11.
- [4] Dave, J. S., Menon, M. R., & Patel, P. R. (2001). *Mol. Cryst. Liq. Cryst.*, 364, 575–587.
- [5] Dave, J. S., & Dhake, K. P. (1992). *Bull. Chem. Soc. Jpn.*, 65, 559–561.
- [6] Gray, G. W. (1974). *Liquid Crystals and Plastic Crystals*, Gray, G. W. & Winsor, P. A. (Eds.), Ellis Horwood: Chichester, 125–129
- [7] Prajapati, A. K., & Pandya, H. M., (2003). *Mol. Cryst. Liq. Cryst.*, 393, 31–39.
- [8] Hasegawa, H., Masuda, T., Matsunaga, Y., Seo, S., & Yasuhara, K. (1989). *Bull. Chem. Soc. Jpn.*, 62, 2875–2879.
- [9] Patel, D. H., & Doshi, A. V. (2007). *Acta Ciencia Indica*, 33, 053.
- [10] Patel, D. H., & Doshi, A. V. (2007). *Acta Ciencia Indica*, 33, 187.
- [11] Gisse, P., & Cluzeau, P., Ravaine, V., Nguyen, H. T. (2002) *Liquid Crystals*, 29(1), 91–98.
- [12] Kasipar, M., Hamplovaa, V., Pakhomov, S. A., Stibor, I., Sverenyaa, H., Bubnov, A. M., Glogarovaa, M., & Vaneik, P. (1997). *Liq. Cryst.*, 22(5), 557–561.
- [13] Karahaliou, P. K., Kouwer, P. H. J., Meyer, T., Mehl, G. H., & Photinos, D. J. (2008). *Phys. Chem. B*, 112, 6550–6556.
- [14] Bezborodov, V. S., & Perrov, V. F. (1997). *Liq. Cryst.*, 23(6), 771–788.
- [15] Bristol, D. W., & Schroeder, J. P. (1974). *J. Org. Chem.*, 39(21), 3138–3141.
- [16] Sun, S., Cheung, W. S., & Fung, B. M. (2000). *Liq. Cryst.*, 27(11), 1473–1479.
- [17] Patel, D. H., & Doshi, A. V. (2006). *Acta Ciencia Indica*, 32, 413.
- [18] Bhoya, U. C., & Doshi, A. V. (2005). *J. Indian Chem. Soc.*, 82, 143–145.
- [19] Dave, J. S., & Vora, R. A. *Liquid Crystals and Ordered Fluids*, Johnson, J. F. & Porter, R. S. (Eds.), Plenum Press: New York, 477.
- [20] *Vogel's Textbook of Practical Organic Chemistry*, 4th ed. (1989). Longman Singapore Publishers.
- [21] Gray, G. W. (1974). *Liquid Crystals and Plastic Crystals*, Ellis Horwood Limited: England.

This article was downloaded by: [The Maharaja Sayajirao University of Baroda]
On: 31 July 2012, At: 00:19
Publisher: Taylor & Francis
Informa Ltd Registered in England and Wales Registered Number: 1072954 Registered office: Mortimer House, 37-41 Mortimer Street, London W1T 3JH, UK



Molecular Crystals and Liquid Crystals

Publication details, including instructions for authors and subscription information:

<http://www.tandfonline.com/loi/gmcl20>

Synthesis and Mesomorphic Characteristics of Fluoroaniline Derivatives with Different Lateral Groups

Jayrang S. Dave ^a, Purvang D. Patel ^a & Himanshu Bhatt ^a

^a Department of Applied Chemistry, Faculty of Technology and Engineering, The M.S. University of Baroda, Vadodara, India

Version of record first published: 30 Jul 2012

To cite this article: Jayrang S. Dave, Purvang D. Patel & Himanshu Bhatt (2012): Synthesis and Mesomorphic Characteristics of Fluoroaniline Derivatives with Different Lateral Groups, Molecular Crystals and Liquid Crystals, 562:1, 76-84

To link to this article: <http://dx.doi.org/10.1080/10426507.2012.669678>

PLEASE SCROLL DOWN FOR ARTICLE

Full terms and conditions of use: <http://www.tandfonline.com/page/terms-and-conditions>

This article may be used for research, teaching, and private study purposes. Any substantial or systematic reproduction, redistribution, reselling, loan, sub-licensing, systematic supply, or distribution in any form to anyone is expressly forbidden.

The publisher does not give any warranty express or implied or make any representation that the contents will be complete or accurate or up to date. The accuracy of any instructions, formulae, and drug doses should be independently verified with primary sources. The publisher shall not be liable for any loss, actions, claims, proceedings, demand, or costs or damages whatsoever or howsoever caused arising directly or indirectly in connection with or arising out of the use of this material.

Synthesis and Mesomorphic Characteristics of Fluoroaniline Derivatives with Different Lateral Groups

JAYRANG S. DAVE, PURVANG D. PATEL,*
AND HIMANSHU BHATT

Department of Applied Chemistry, Faculty of Technology and Engineering,
The M.S. University of Baroda, Vadodara, India

Two new homologous series of liquid crystals viz. 4-(4'-n-alkoxybenzoyloxy)-2-chlorophenylazo-4''-fluorobenzenes(I) and 4-(4'-n-alkoxybenzoyloxy)-2-methylphenyl azo-4''-fluorobenzenes(II) with terminal fluoro, lateral chloro(I) and methyl(II) group and central ester and azo linkages are synthesized and their mesomorphic properties are studied. Both the series are similar in molecular structure with the difference in their lateral substitutions; series I has chloro group and series II has methyl group as laterally substituted groups. All the twelve homologues of each of the series are mesogenic in nature. Series I shows nematic mesophase from the first C₁ to the last C₁₆ derivative synthesized; smectic mesophase is exhibited by last two viz. C₁₄ and C₁₆ derivative, where as all the members from C₁ to C₁₆ of series II only show nematic mesophase. The nematic mesophase shows marble texture and the smectic mesophase shows Schliere texture of the Smectic C variety. Both the series are compared with structurally related series.

Keywords Azo and ester central linkage; chloro and methyl lateral groups; homologues series; mesophase thermal stability; smectic C and nematic mesophase

Introduction

A number of homologous series with ester and azo central linkages have been synthesized having different terminal and lateral groups [1–8]. Lateral substituent in central ring system effects mesomorphic properties and play a vital role in imparting liquid crystallinity to a potentially mesogenic compound. Central phenyl ring having lateral substitution makes molecules broad; which play an effective role in mesogenic property of a mesogenic compound. Studies on the effect of lateral substitution have been comparatively less explored than terminal substitution. A survey of the literature indicates that generally the mesophase range of the mesogens having lateral substituent is less than laterally unsubstituted mesogens [9–15]. In order to establish the co-relation between chemical constitution and mesomorphism, two new homologous series with ester and azo central linkages, fluoro

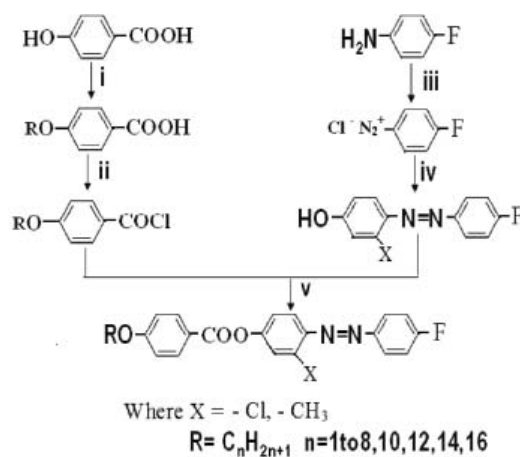
*Address correspondence to Purvang D. Patel, Department of Applied Chemistry, Faculty of Technology and Engineering, The M.S. University of Baroda, Vadodara, India. Tel.: +919825355636. E-mail: pdzpatel1983@yahoo.com

terminal group and lateral chloro (Series I) and lateral methyl (Series II) groups on central ring are synthesized and their mesomorphic properties are studied.

Experimental

4-Hydroxy benzoic acid, the appropriate n-alkyl halides, p-fluoro aniline, m-chloro phenol, and m-cresol are of Merck grade and used as received. Solvents are dried and distilled prior to use. Microanalyses of some of the representative compounds are performed on Perkin Elmer Series II 2400-CHN analyzer; IR spectra are recorded on a Perkin Elmer GX-FTIR, NMR spectra are measured on a Bruker Avance II-500 spectrometer. Liquid crystalline properties are investigated on Leitz Laborlux 12 POL polarizing microscope provided with a Kofler heating stage. DSC are performed on a Mettler Toledo Star SW 7.01.

1. 4-n-Alkoxy benzoic acids and 4-n-alkoxy benzoyl chlorides are synthesized by known methods [16].
2. 2-Chloro-4-hydroxyphenylazo-4'-fluorobenzene, 2-methyl-4-hydroxyphenylazo-4'-fluoro benzene are prepared by known method [17].
3. The series, namely 4-(4'-n-alkoxybenzoyloxy)-2-chlorophenylazo-4''-fluorobenzenes, and 4-(4'-n-alkoxybenzoyloxy)-2-methylphenylazo-4''-fluoro benzenes are synthesized by adding dropwise a cold solution of 2-chloro-4-hydroxyphenylazo-4'-fluoro benzene (for series I), 2-methyl-4-hydroxyphenylazo-4'-fluoro benzene (for series II), respectively, in dry pyridine to a cold solution of 4-n-alkoxy benzoyl chloride. The mixture is allowed to stand overnight at room temperature. It is acidified with 1:1 cold HCl and the separated solid is filtered and recrystallized from ethanol until constant transition temperatures are obtained. The elemental analysis of some of the representative compounds are found to be satisfactory. The synthetic route of the series is shown in Scheme 1.



- (i) Alcohol, KOH, R-Br (ii) SOCl₂ (iii) HCl, NaNO₂, 0^o-5^oC
(iv) m-chloro phenol or m-cresol, aq. NaOH, 0^o-10^oC
(v) Dry pyridine, 1:1 HCl

Scheme 1. Synthetic route for series I and II.

FTIR (Nujol, KBr pellets, cm⁻¹) :

Series I: 4-(4'-n-pentyloxybenzoyloxy)2-chlorophenylazo-4''-fluorobenzenes:
2930, 1740 (-COO-), 1610(-N=N-), 1516, 1360, 1250, 890, 755, 692.

Series I: 4-(4'-n-decyloxybenzoyloxy)2-chlorophenylazo-4''-fluorobenzenes:
2944, 1731 (–COO–), 1606(–N=N–), 1504, 1319, 1264, 1041, 850, 755, 689.

¹H NMR : (CDCl₃, 500 MHz, δ, ppm, standard TMS)

Series I: 4-(4'-n-pentyloxybenzoyloxy)2-chlorophenylazo-4''-fluorobenzenes :
δ 0.98 (3H, t, –CH₃), 1.45–1.82 (m, alkyl chain),

4.06 (2H, t, –OCH₂–CH₂), 6.95 (1H, s, H⁴), 7.0 (2H, d, H⁵),

7.38 (2H, d, H²), 7.9 (2H, d, H¹), 7.95 (2H, d, H⁶), 8.15 (2H, d, H³)

Series I: 4-(4'-n-decyloxybenzoyloxy)2-chlorophenylazo-4''-fluorobenzenes:

δ 0.9 (3H, t, –CH₃), 1.4–1.79 (m, alkyl chain),

4.05 (2H, t, –OCH₂–CH₂), 6.98 (1H, s, H⁴), 7.0 (2H, d, H⁵),

7.48 (2H, d, H²), 7.9 (2H, d, H¹), 8.0 (2H, d, H⁶), 8.1 (2H, d, H³)

FTIR (Nujol, KBr pellets, cm^{–1}):

Series II: 4-(4'-n-butyloxybenzoyloxy)2-methylphenylazo-4''-fluorobenzenes:
2946, 1735 (–COO–), 1603(–N=N–), 1490, 1317, 1260, 842, 724, 689.

Series II: 4-(4'-n-heptyloxybenzoyloxy)2-methylphenylazo-4''-fluorobenzenes:
2946, 1731 (–COO–), 1606(–N=N–), 1530, 1353, 1264, 890, 728, 681.

¹H NMR: (CDCl₃, 500 MHz, δ, ppm, standard TMS)

Series II: 4-(4'-n-butyloxybenzoyloxy)2-methylphenylazo-4''-fluorobenzenes:

δ 0.9 (3H, t, –CH₃), 1.5–1.8 (m, alkyl chain), 2.33 (3H, s, Ar–CH₃)

4.0 (2H, t, –OCH₂–CH₂), 6.98 (2H, d, H⁴), 7.0 (2H, d, H⁵),

7.30 (2H, d, H²), 7.9 (2H, d, H⁶), 8.1 (2H, d, H¹), 8.2 (2H, d, H³)

Series II: 4-(4'-n-heptyloxybenzoyloxy)2-methylphenylazo-4''-fluorobenzenes:

δ 0.96 (3H, t, –CH₃), 1.40–1.85 (m, alkyl chain), 2.30 (3H, s, Ar–CH₃)

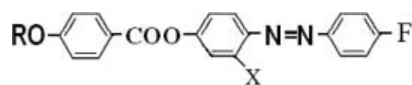
4.0 (2H, t, –OCH₂–CH₂), 6.98 (1H, s, H⁴), 7.1 (2H, d, H⁵),

7.26 (2H, d, H²), 7.93 (2H, d, H¹), 7.95 (2H, d, H⁶), 8.1 (2H, d, H³)

Results and Discussion

In the present study, 12 homologues from each of the two homologues series viz. 4-(4'-n-alkoxy benzoyloxy)-2-chlorophenylazo-4''-fluorobenzenes (series I) and 4-(4'-n-alkoxy benzoyloxy)-2-methylphenylazo-4''-fluorobenzenes (series II) are synthesized and their mesomorphic properties are studied.

The general molecular structure of the series is;



Where X = - Cl, - CH₃

R = C_nH_{2n+1} n=1 to 8, 10, 12, 14, 16

All the twelve homologues of the series I are mesogens (Table 1); the nematic phase commences from the very first derivative and remains up to the last hexadecyl derivative synthesized while Smectic C phase commences from the tetradecyl derivative and remains to be exhibited up to the last hexadecyl derivative synthesized. Figure 1, i.e., the plot of transition temperatures against number of carbon atoms in alkoxy chain indicates that N–I curve shows overall falling tendency and merges as the series is ascended; no odd–even effect is observed in N–I curves. The Cr–M transitions show overall falling tendency with a rising jump at decyl derivative. The nematic phase of the series shows marble texture and the smectic phase shows schlieren texture of smectic C variety.

Table 1. Transition temperature °C of the series I. Series I: 4-(4'-n-alkoxybenzoyloxy)-2-chlorophenylazo-4''-fluorobenzenes

R = n-alkyl group	Transition temperatures (°C)		
	Smectic C	Nematic	Isotropic
Methyl	—	114	182
Ethyl	—	104	170
Propyl	—	102	163
Butyl	—	90	158
Pentyl	—	78	160
Hexyl	—	71	157
Heptyl	—	65	149
Octyl	—	62	144
Decyl	—	85	138
Dodecyl	—	79	129
Tetradecyl	70	86	114
Hexadecyl	68	92	111

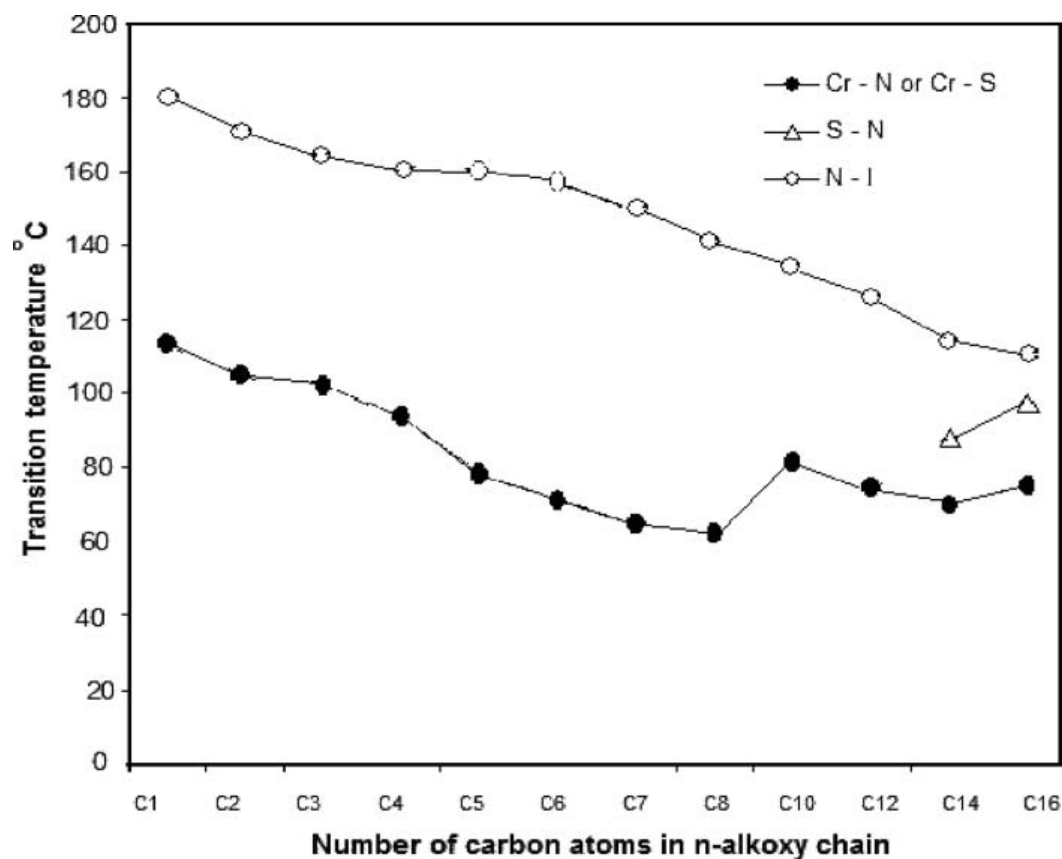
**Figure 1.** 4-(4'-n-alkoxybenzoyloxy)-2-chloro phenylazo-4''-fluorobenzenes (series I).

Table 2. Transition temperature °C of the series II. Series II: 4-(4'-n-alkoxybenzoyloxy)-2-methylphenylazo-4''-fluorobenzenes

R = n-alkyl group	Transition temperatures °C		
	Smectic	Nematic	Isotropic
Methyl	—	120	165
Ethyl	—	122	158
Propyl	—	110	138
Butyl	—	92	140
Pentyl	—	84	135
Hexyl	—	78	131
Heptyl	—	63	129
Octyl	—	67	128
Decyl	—	61	122
Dodecyl	—	72	117
Tetradecyl	—	76	112
Hexadecyl	—	68	98

All the 12 homologues of the series II are mesogens (Table 2); the nematic phase commences from the very first derivative and remains upto the last hexadecyl derivative synthesised. Figure 2, i.e., the plot of transition temperatures against number of carbon atoms in alkoxy chain indicates that N-I curve shows overall falling tendency as the series is ascended. Here also no odd-even effect is observed in N-I curve. The Cr-M transitions

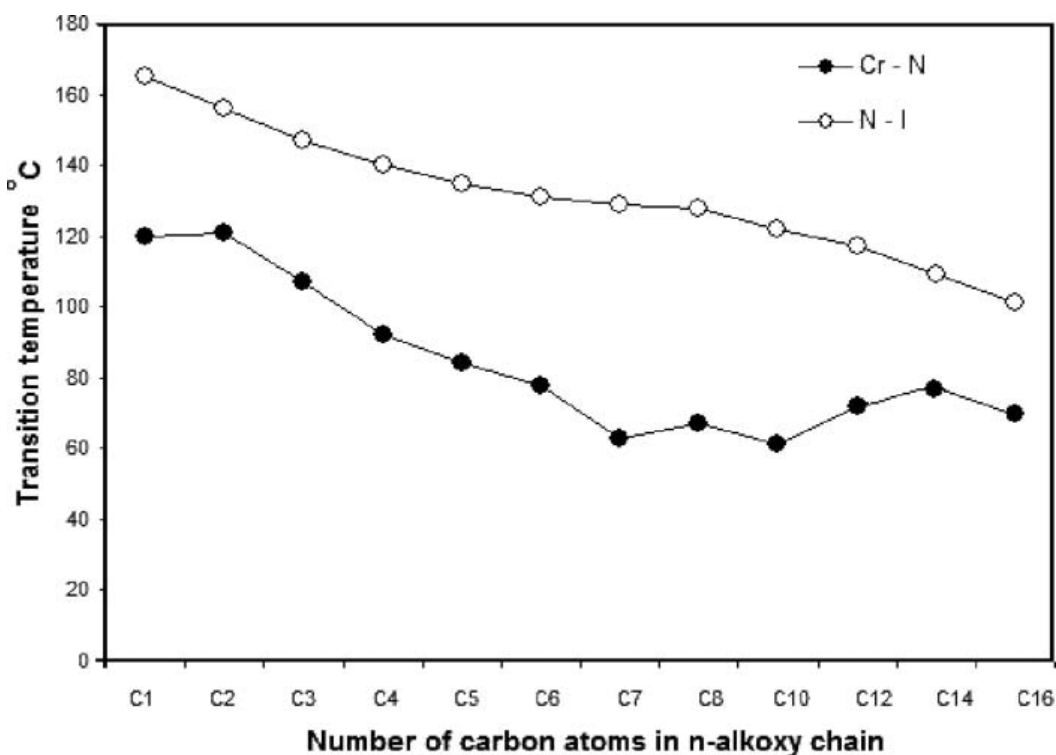
**Figure 2.** 4-(4'-n-alkoxybenzoyloxy)-2-methyl phenylazo-4''-fluorobenzenes (Series II).

Table 3. Average thermal stability °C

Series	Nematic	Smectic	Commencement of smectic mesophase
I	147.19 (C ₁ to C ₁₆)	89.00 (C ₁₂ to C ₁₆)	C ₁₄
II	131.08 (C ₁ to C ₁₆)	–	–
A	189.70 (C ₁ to C ₁₀)	116.80 (C ₈ to C ₁₆)	C ₈
B	143.80 (C ₁ to C ₁₂)	103.66 (C ₁₂ to C ₁₆)	C ₁₂
C	117.09 (C ₁ to C ₁₄)	88.00 (C ₁₄ to C ₁₀)	C ₁₄

show overall falling tendency from methyl to hexadecyl derivative with slight rise at ethyl, octyl, and tetradecyl derivative. Here also nematic phase of the series shows marble texture and the smectic phase shows schlieren texture of smectic C variety.

The average thermal stabilities of series I and II are compared with structurally related other homologous series; table 3 gives the average thermal stabilities and figure 3 gives the molecular structures of the series in comparison. The average nematic mesophase thermal stability of series I is 147.91°C and series (II) is 131.08°C similarly the average smectic mesophase thermal stability of the series (I) is 89.0°C; where as Series II shows only nematic mesophase. Comparison of average mesophase thermal stability of both the series (Table 3) shows that the nematic mesophase thermal stability of series II is lower than that of series I. Here, the nature of lateral substituents has important implications on phase transition temperatures and average mesophase thermal stability; series I has lateral chloro group where as series II has lateral methyl group. Gray has also reported a system where in lateral methyl substituent has lower thermal stability than lateral chloro substituent [18].

Comparison of series I and II with structurally related homologous series shows that all the series in comparison are structurally more or less similar, consisting of three aromatic cores, azo and ester central linkages. The difference between molecules of series I, II, and A [19] is only the lateral substitution; series I has chloro group, series II has methyl group as lateral substituent, while series A is laterally unsubstituted. The effect of the lateral group in the central benzene ring causes disruption in the molecular packing, which reduces the transition temperatures and melting points as well as the mesophase thermal

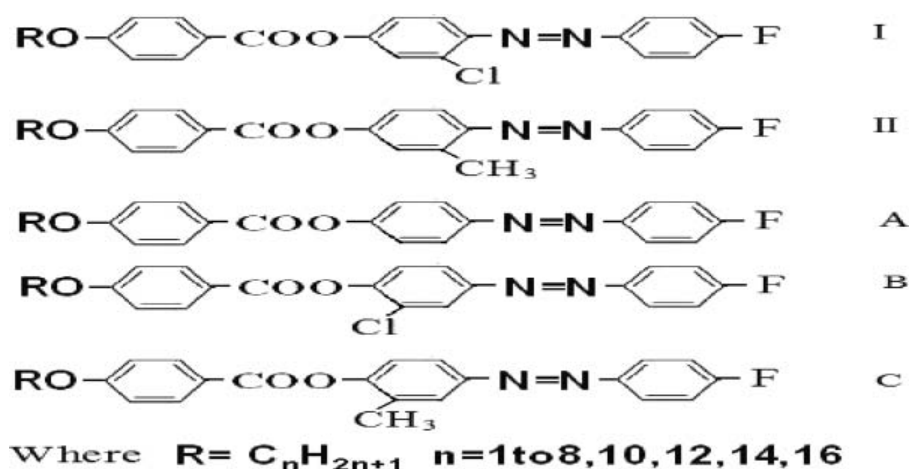
**Figure 3.** Selected homologous series for comparison.

Table 4. Elemental analysis

Series	Homologue	Calculated			Found		
		C%	H%	N%	C%	H%	N%
I	C ₅	69.81	5.33	6.78	70.53	5.86	6.11
I	C ₁₀	72.12	6.63	5.80	73.88	6.70	5.27
II	C ₄	70.93	5.66	6.89	71.57	5.91	7.05
II	C ₇	72.32	6.47	6.25	73.00	6.81	6.56

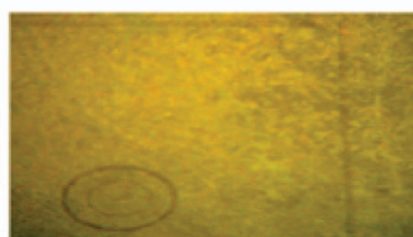
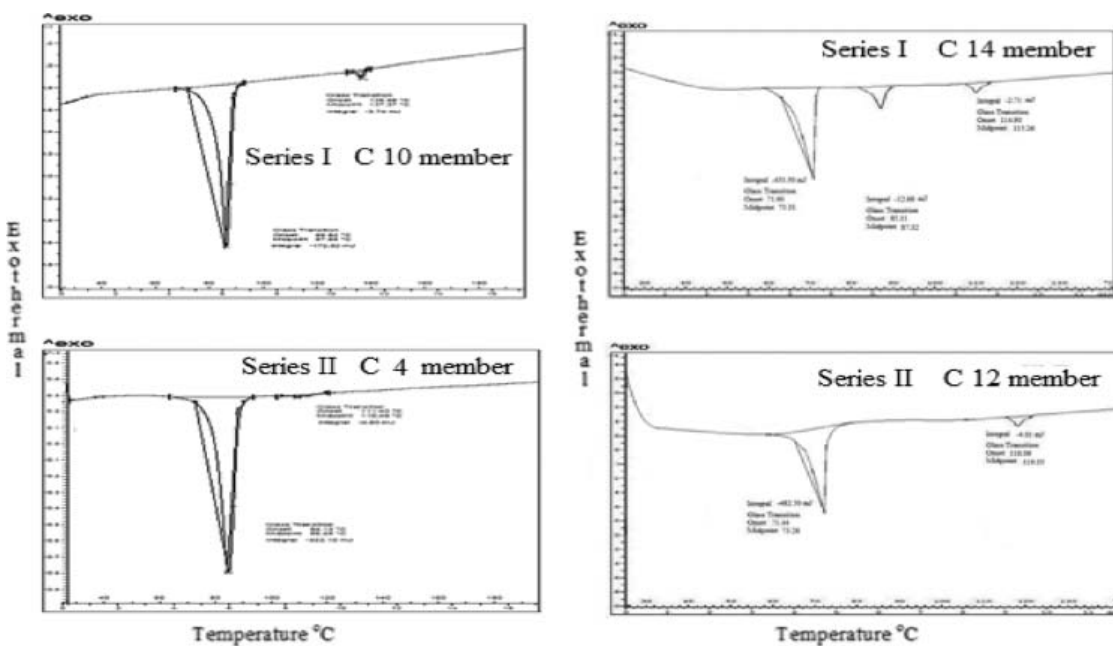
(a) Marble texture of nematic mesophase
Series I C16 member(b) Schliere texture of smectic mesophase
Series I C16 member(c) Marble texture of nematic mesophase
Series II C2 member(d) Marble texture of nematic mesophase
Series II C6 member**Figure 4.** Photomicrographs of the textures of representative derivatives.**Figure 5.** DSC curves.

Table 5. DSC data

Series	Member	Heating rate/ $^{\circ}\text{C min}^{-1}$	Transition temperature/ $^{\circ}\text{C}$	$\Delta H/\text{J g}^{-1}$	$\Delta S/\text{J g}^{-1} \text{K}^{-1}$
I	Decyl	5	Cr–N 87	48.00	0.1330
			N–I 138	1.038	0.0025
I	Tetradecyl	5	Cr–Sm 70	80.85	0.2343
			Sm–N 86	2.26	0.0063
			N–I 114	0.483	0.0012
II	Butyl	5	Cr–N 92	41.29	0.1133
			N–I 140	0.62	0.0015
II	Dodecyl	5	Cr–N 72	80.08	0.2323
			N–I 117	0.79	0.0020

stability compared to the laterally unsubstituted analogues. Thus, introduction of chloro group (Series I) and methyl group (Series II) in the ortho position of the azo linkage effectively reduce both the clearing and melting points compared to those of the parent compound (Series A). It is seen that the breadth of the molecules of the series I and II are increased due to the presence of lateral group on the central benzene ring which decreases both smectic and nematic thermal stabilities [20].

Series I and series B [19] has lateral chloro group on ortho position and meta position to the azo central linkage respectively. The average nematic mesophase thermal stability of series I is 147.91°C and that of series B is 143.8°C which is not marked different in series I. However, the average smectic mesophase thermal stability of series I is 89.0°C while that of series B is 103.66°C . Thus, the average smectic mesophase thermal stability of series I is less than series B, which can be due to the difference in position of lateral chloro group. Series I is having chloro group in the ortho position to the azo linkage whereas series B is having chloro group in the ortho position to the ester linkage.

Similarly, Series II and series C [19] has lateral methyl group on ortho position and meta position to the azo central linkage respectively. The average nematic mesophase thermal stability of series II is 131.08°C and that of series C is 117.09°C . Thus, the average nematic mesophase thermal stability of series II is higher than series C, which can be due to the difference in position of lateral methyl group. Series II is having methyl group in the ortho position to the azo linkage whereas series C is having methyl group in the ortho position to the ester linkage.

Figure 4 shows the photomicrographs of some of the representative compounds. The enthalpies of decyl and tetradecyl derivative of series I and butyl and dodecyl derivative of series II are measured by DSC. The DSC data are recorded in Table 5. Figure 5 shows the DSC curves.

Conclusion

Two new homologous series with lateral chloro(I) and lateral methyl(II) groups are synthesized. The positional effect of $-\text{Cl}$ and $-\text{CH}_3$ lateral substituent on phase behaviour, phase transition temperatures with respect to azo central linkage are studied. These lateral substituents depress both melting point and clearing points of the liquid crystals. Mesogens

with lateral substitution have reduced smectic and nematic mesophase thermal stability than the corresponding unsubstituted homologues.

Acknowledgment

The authors thank the Head of Applied Chemistry Department, Faculty of Technology and Engineering, The M.S. University of Baroda, Vadodara for providing research facilities.

References

- [1] Demus, D., & Zashcke, H. (1984). *Flussige Kristalle in Tabellen II*, VEB Deutscher Verlag für Grundstoffindustrie: Leipzig.
- [2] Dave, J. S., & Menon, M. R. (1998). *Mol. Cryst. Liq. Cryst.*, 319, 51.
- [3] Dave, J. S., & Menon, M. R. (2000). *Bulletin of Material Science*, 23(3), 237.
- [4] Patel, P. R., & Dave, J. S. (2006). *Liq. Cryst.*, 33(9), 1065.
- [5] Dave, J. S., Menon, M. R., & Patel, P. R. (2002). *Mol. Cryst. Liq. Cryst.*, 378, 1.
- [6] Dave, J. S., Menon, M. R., & Patel, P. R. (2001). *Mol. Cryst. Liq. Cryst.*, 364, 575.
- [7] Dave, J. S., & Dhake, K. P. (1992). *Bull. Chem. Soc. Jpn.*, 65, 559.
- [8] Shah, N. H., Vora, R. A., & Jadav, N. D. (1991). *Mol. Cryst. Liq. Cryst.*, 209, 291.
- [9] Prajapati, A. K., & Pandya, H. M. (2003). *Mol. Cryst. Liq. Cryst.*, 393, 31.
- [10] Hasegawa, H., Masuda, T., Matsunaga, Y., Seo S., & Yasuhara, K. (1989). *Bull. Chem. Soc. Jpn.*, 62, 2875.
- [11] Gisse, P., Cluzeau, P., Ravaine, V., & Nguyen, H. T. (2002). *Liquid Crystals*, 29(1), 91.
- [12] Kasipar, M., Hamplova, V., Pakhomov, S. A., Stibor, I., Sverenyak, H., Bubnov, A. M., Glogarova, M., & Vaneik, P. (1997). *Liquid Crystals*, 22(5), 557.
- [13] Bezborodov, V. S., & Perrov, V. F. (1997). *Liquid Crystals*, 23(6), 771.
- [14] Bristol, D. W., & Schroeder, J. P. (1974). *J. Org. Chem.*, 39(21), 3138.
- [15] Sun, H., Cheung, W. S., & Fung, B. M. (2000). *Liquid Crystals*, 27(11), 1473.
- [16] Dave, J. S., & Vora, R. A. (1970). In: J. F. Johnson & R. S. Porter, (Eds.), (*Liquid Crystals and Ordered Fluids*, Plenum Press: New York, p. 477.
- [17] Furniss, B. S., Hannford, A. J., Smith, P. W. G., & Tatchell, A. R. (Revisors). (1989). *Vogel's Textbook of Practical Organic Chemistry* (4th Edn.), Longman Singapore Publishers Pvt. Ltd.: Singapore, pp. 563–649.
- [18] G. W. Gray. (1974). In: G. W. Gray & P. A. Winsor (Eds.), *Liquid Crystals and Plastic Crystals*, Chapter 4. Ellis Horwood: Chichester, pp. 125–129.
- [19] Dave, J. S., Upasani, C. B., & Patel, P. D. (2010). *Mol. Cryst. Liq. Cryst.*, 533, 73.
- [20] Gray, G. W. (1974). In G. W. Gray & P. A. Winsor (Eds). *Liquid Crystals and Plastic Crystals*, Ellis Horwood Limited: Chichester, England, 1, pp. 130–131.